

STABLE ISOTOPE STUDIES
OF SOME
ACTIVE HYDROTHERMAL SYSTEMS

Thesis by

Steven Judson Lambert

In Partial Fulfillment of the Requirements
for the Degree of
Doctor of Philosophy

California Institute of Technology
Pasadena, California 91125

1976

(Submitted August 29, 1975)

Copyright © by

STEVEN JUDSON LAMBERT

1975

"In so many places, and with so many fires,
does Nature burn the Earth."

Pliny the Elder (A. D. 77)
in NATURAL HISTORY

to Ruth Mildred (McQueen) Lambert,

*accomplished homemaker, patient counsellor,
and -- most importantly -- my loving Mother.*

ACKNOWLEDGMENT

My greatest debt of gratitude is to the two surviving members of my immediate family, my mother and my brother, without whose constant patience, understanding and, on occasion, self sacrifice, I would never have prospered as a graduate student.

I am grateful to Dr. Samuel Epstein, my scientific advisor and friend, who has maintained such close communication with me throughout the past five years. His enthusiastic and careful guidance in this project has been indispensable, ever since the idea for this project was conceived one evening while we dined together ("Let's get crackin'!"). He has farsightedly forced me to learn the technology, design, and construction of vacuum systems, he has guided me through the thrills and spills of two national scientific meetings, and he has helped me to appreciate the lore and significance of stable isotope studies. He has freely made available to me all of the facilities of his laboratory. His many helpful discussions have added greatly to the quality of both the investigative phases of this project and the communication of scientific information in this report.

I wish also to thank Dr. Hugh P. Taylor for discussions which played no small part in the conception of the idea for this work.

Throughout the course of this investigation, I have had many valuable discussions with Crayton Yapp, Mike DeNiro, Dr. Mokhtar Hamza, and Dr. Yehoshua Kolodny. Input in the form of stimulating ideas was also received from Drs. Tom McGetchin, Ray Siever, Wilfred Elders and Tyler Coplen.

I owe my heartfelt thanks to the late Curtis Bauman, who was in large part responsible for the construction of my metal vacuum system. Victor Nenow and Armand Postma were of great assistance in matters electrical. Paul Yanigasawa and Jane Young taught me many of the finer points of various kinds of isotopic analyses, and Sam Lee performed some silicate analyses while I was engrossed in writing. Joop Goris performed the mass spectrometry on virtually all of my carbon dioxide samples.

I am indebted to Dr. Carel Otte, Richard F. Dondanville, John Kilkenny and Courtney Isselhardt of the Geothermal Division of the Union Oil Company of California for providing well-documented samples from geothermal wells at The Geysers, Valles Caldera, and the Philippines. I wish to thank Dr. John Martin, Roger Allmendinger and Mike Lane of the Standard Oil Company of California for making available to me the samples from Heber. Fondly do I hope that the information exchange between academic and industrial institutions which has taken place during this project will in the future inspire other such cooperative efforts to be made.

Although in some respects my tenure at Caltech has not been as pleasant as it might have been, a number of people have provided encouragement when I have needed it most. Principal among these are Sam and Diane Epstein. I have been fortunate to have had a cordial office-mate for four years, Todd Hinkley. No less important has been the moral support from some of my friends who almost convinced me that

I really did belong at Caltech. These include Richard Squires, Robert Miller, Dorothy Coy, Susan McCurdy, Bridget Coughran, and Hortense Reece. The last two helped me with the rough draft manuscript typing of my thesis. I have been very fortunate to have been able to engage Enid Bell to perform the final preparation of the typed text of this thesis. In the last spasmodic throes of this herculean task she has been like a second mother to me. Janet Boike has assisted her with the final preparations. Jan Scott has lent a sympathetic ear and has been a valuable source of help with the illustrations.

In the first three years of my tenure as a graduate student I was supported by a National Science Foundation Fellowship. During my last year I held a National Science Foundation Energy-Related Traineeship. This research was supported by a grant from the National Science Foundation, Contract Number DES71-0558A3.

I am grateful to my aunts, uncles and cousins in Iowa, whose constant encouragement has motivated me to complete this thesis with dispatch ("Is that kid still going to school?").

Finally, some mention should be made of my ultimate benefactors. I wish to thank John Colter, William Elliott and Kendall Bumpass. If these gentlemen had not become dissatisfied with civilization, and had actually known where they were going, it is likely that the great hot springs of America would have remained undiscovered a few years longer, thus delaying the production of this thesis.

Steven Judson Lambert
Riverside, California

ABSTRACT

Measurements of $^{18}\text{O}/^{16}\text{O}$, $^{13}\text{C}/^{12}\text{C}$ and D/H ratios have been made on rocks and minerals from wells drilled in active hydrothermal systems as an aid to the understanding of various factors which govern the ongoing natural interactions between rocks and fluids, leading to a more thorough understanding of rock-fluid interactions that have taken place in the geologic past in such processes as diagenesis, metamorphism, and hydrothermal alteration. Samples from four active hydrothermal systems have been analyzed: The Geysers, western Mayacmas Mountains, California; Valles Caldera, northern Jemez Mountains, New Mexico; Heber Geothermal Anomaly, Imperial Valley, California; the Tiwi area, Luzon, Philippines.

The Geysers, a vapor-dominated hydrothermal system, is developed in Franciscan host rock which contains veins of quartz and calcite whose $\delta^{18}\text{O}$ values record the temperatures and isotopic compositions of fluids which prevailed during at least two different episodes of rock-fluid interaction. The first episode took place at about 200°C , during which marine silica and carbonate apparently interacted with ocean water entrapped in the sediments to form veins of quartz and calcite whose $\delta^{18}\text{O}$ values were around 19‰ and 16‰, respectively. The calculated water/mineral ratios were less than unity. The water may have profoundly influenced the $\delta^{18}\text{O}$ values of spilitic basalts during their metamorphism to greenstones. The formation and emplacement of serpentine bodies were isotopically unrelated to this episode, which was essentially a low-grade burial metamorphism (post-Cretaceous?) of rocks

of the Franciscan Group. The second episode, in part recorded by cogenetic vein quartz and calcite $\delta^{18}\text{O}$ values 4 to 6‰ and 1 to 3‰, respectively, began with large quantities of meteoric water circulating in fractures in the rock at temperatures of 160 to 180°C in response to the Pliocene Clear Lake magmatism. Isotopic alteration of host rocks was most profound near fractures which carried the hot water. The temperature rose, and with the restricted circulation of fluids the ancestral hot-water system evolved into the presently-active vapor-dominated system, which, according to the cogenetic vein quartz and calcite $\delta^{18}\text{O}$ values, involved temperatures as high as 320°C and fluid/mineral ratios near unity. The change in the isotopic composition of the host rock during this activity was negligible. The $\delta^{13}\text{C}$ values of vein calcite at The Geysers reflect both a marine carbonate and organic component of carbon.

The other three areas contain hot-water systems, noteworthy of which is the Valles Caldera, an accumulation of previously hydrothermally unaltered porous sediments and pumiceous volcanic tuffs. Large volumes of meteoric water have interacted with the rock at various temperatures (100 to 280°C), indicated by changes in calcite, quartz and whole-rock $\delta^{18}\text{O}$ values in the Caldera. The shallower, little-altered rocks in the Caldera contain calcite and dolomite whose $\delta^{18}\text{O}$ values suggest they were deposited in a fresh-water lake.

Poorly-consolidated Pleistocene sand beds, whose highly variable hydrothermal carbonate $\delta^{18}\text{O}$ values indicate that they are isolated from one another by impermeable clay beds, form a series of hot-water

reservoirs at Heber in the Imperial Valley. The degree of isotopic alteration indicated by the sand and its component quartz is very minor, indicating that this system is very young.

The few data from the Philippines indicate that significant hydrothermal alteration has taken place in the Tiwi hot-water system, also. The isotopic changes, however, are less profound than those observed at other areas because the $\delta^{18}\text{O}$ of Philippines meteoric water is much closer to the initial $\delta^{18}\text{O}$ value of the local host rock than is the case elsewhere.

Measurements of D/H ratios do not seem to be conclusive in characterizing degrees of rock-fluid interaction in active hydrothermal systems.

Preface: A Guide for the Reader

For the benefit of those readers who examine this report for any specific purpose(s) in search of any specific result(s), I have included herewith an overview of this thesis, with certain passages recommended to those with specific interests.

Inasmuch as geology is an interdisciplinary science, many of its concepts are drawn heavily from other sciences. This is particularly true of studies of active hydrothermal (geothermal) systems. Such studies are potentially of interest to persons of widely-varied backgrounds, including sedimentologists, stratigraphers, low-temperature geochemists, petrologists, geophysicists and geochemists devoted to various aspects of their field: theoretical, ore deposits, organic, mineralogical, and stable isotope. This study is primarily devoted to the last-mentioned type of geochemistry, but the consequences of the study should be of interest to all the above-named disciplines. This report will be of particular significance to those interested in geothermal energy.

All are advised to read Chapter 1, the introduction to this work, for therein lies the theme, the "nuts and bolts," so to speak, which bind this dissertation together. The theme, the isotopic characterization of various types of rock-water interactions, is woven into the fabric of past work in the later part of the introductory chapter. The importance and potential consequences of studies of rock-water interactions actively taking place are unfolded in the context of their value as a guide to the interpretation of rock-water

interactions which have taken place in the geologic past -- in processes such as metamorphism, metasomatism, diagenesis, ore deposition, and hydrothermal phenomena in general. (For the less-geologically inclined, brief résumés of the scopes of some of these terms appear in Appendix I).

The thread of continuity, which wends its way through the succeeding chapters, incorporates studies of the rock-water interactions taking place (or having taken place) at a variety of localities: The Geysers, California; Valles Caldera, New Mexico; Imperial Valley, California; and Luzon, Philippines. The highlights of results of investigations are summarized in Sections 3.8, 4.6, 5.5 and in Chapter 7, which are recommended reading for those wishing to obtain a slightly more detailed overview of this thesis than is given in the Abstract.

The Prologue, which immediately follows this Preface, is entirely historical. It appears as a tribute to that special breed, the explorers, who have always been the first to travel new roads, to report their findings, and, alas, to sometimes brave the ridicule of their fellow humans. The prologue is recommended to those who appreciate the adventuresome nature of all science.

The analytical mind may take an interest in Chapter 2 and its accessory, Appendix III. To the brave, I commend Appendix II -- a thermodynamic, statistical-mechanical, quantum-mechanical review of the basic principles of the theoretical aspects of the prediction of equilibrium fractionation of trace isotopes among coexisting phases. The student, for example, who wishes to delve into the calculation of isotopic fractionation factors, may find Appendix II of some use.

Those who search for specific results of the studies of any of the systems considered in this thesis should consult the entire chapter devoted to the locality of interest. Chapter 3 details the isotopic investigations of past and present hydrothermal activity at The Geysers, a vapor-dominated system, while Chapters 4, 5 and 6 report the preliminary results and conclusions of studies focused on hot-water systems at Valles Caldera, Imperial Valley and Luzon. While the studies of hot-water systems in this thesis are more preliminary than studies of The Geysers, they have allowed some very important comparisons to be made between vapor-dominated and hot-water systems.

All of the hydrothermal systems treated in this thesis have had a different geological history. At The Geysers are found the Mesozoic rocks of the Franciscan Group, which may have experienced a variety of rock-water interactions since the accumulation of these marine deposits (Chapter 3). Valles Caldera rocks are dominated by Pleistocene Volcanics (Chapter 4). Imperial Valley is filled with poorly-consolidated detritus (Chapter 5). The Philippines are a volcanic island arc (Chapter 6). The changes, subtle and conspicuous, which occur when such different rock types react with water might be of interest to geologists devoted to the specialized study of one or more of these rock types.

In this thesis, there is something for everyone.

Table of Contents

	<u>Page</u>
Epigram	ii
Dedication	iii
Acknowledgment	iv
Abstract	vii
Preface: A Guide for the Reader	x
Table of Contents	xiii
List of Tables	xviii
List of Figures	xx
List of Photomicrographic Plates	xxiii
0. Prologue: A Brief History of Hot Spring Investigations	1
1. INTRODUCTION	8
1.1 The Aims of the Present Investigation	8
1.2 Geothermal Areas Investigated in This Work	11
1.3 Previous Work Closely Related to This Work	12
1.4 Economic Significance of the Work	14
1.5 Previous Work, Peripherally Related to This Work	17
2. ANALYTICAL PROCEDURES	26
2.1 Sample Collection	26
2.2 Estimation of Depths of Origin of Samples	27
2.3 Preparations of Samples for Analyses	28
2.3.1 Sample Selection	28
2.3.2 Separation and Purification of Minerals and Rocks	29
2.3.3 Preparation of Gas for Isotopic Analysis	35
2.3.3.1 Carbonates	35
2.3.3.2 Waters	35
2.3.3.3 D/H Analyses	36
2.3.3.4 Extraction of Oxygen from Silicates	36
2.4 Measurements	37
2.5 Analytical Precision	38
2.6 Tests of Reproducibility of Silicate $\delta^{18}\text{O}$ Values	38

	<u>Page</u>
3. STUDIES AT THE GEYSERS, SONOMA COUNTY, CALIFORNIA	45
3.1 History of Development	45
3.2 The Geysers as a Vapor-Dominated Hydrothermal System	51
3.3 Geological Overview	53
3.4 The Rocks and Minerals	54
3.4.1 The Franciscan Group in General	54
3.4.2 Graywacke	55
3.4.3 Basalt	55
3.4.4 Serpentinite	55
3.4.5 Chert ("Red Rock")	56
3.4.6 Metamorphic Rocks	56
3.5 The Wells	56
3.6 Thermal No. 7	57
3.6.1 General Statements	57
3.6.2 Isotopic Temperatures from Thermal 7	62
3.6.3 Possible Variations in Steam Reservoir Temperature in Response to the Drilling of Thermal 7	66
3.6.4 Hydrothermal Alteration of Host Rock in Thermal 7	71
3.7 The Lakoma Fame Tract	72
3.7.1 General Features	72
3.7.2 Occurrence and Distribution of Vein Minerals in Lakoma Fame Wells	75
3.7.3 Lakoma Fame No. 19	75
3.7.3.1 The Isotopic Record in Lakoma Fame No. 19 Vein Minerals	88
3.7.3.2 The Significance of Upper Zone Vein Mineral $\delta^{18}\text{O}$ Values	91
3.7.3.3 Sources of the Vein Minerals	103
3.7.3.4 Variations in $\delta^{18}\text{O}$ Values of Vein Minerals in the Lower Zone (Steam Zone)	104
3.7.3.4.1 Quartz	104
3.7.3.4.2 The Relative Resistance of Vein Quartz and Calcite to Hydrothermal Alteration	107
3.7.3.5 The Significance of the Barren Zone	108
3.7.3.6 Quartz-Calcite Oxygen Isotope Geothermometry in the Lower Zone	108
3.7.3.7 The Source of Hydrothermal Fluid in the Active Steam (Lower) Zone	112
3.7.3.8 Water/Mineral Ratios in the Active Steam Zone	118
3.7.4 Lakoma Fame No. 13	121
3.7.5 Lakoma Fame No. 15	129
3.7.5.1 General Features	129
3.7.5.2 The Upper Zone	129
3.7.5.3 The Active Steam Zone and Oxygen Isotope Geother- mometry in Lakoma Fame No. 15	134
3.7.6 $\delta^{18}\text{O}$ Values of Vein Material from Lakoma Fame Numbers 8 and 9	137
3.7.7 The Thermal History of the Steam Zone	141

	<u>Page</u>	
3.7.8	Implication of Carbonate $\delta^{13}\text{C}$ Values in Lakoma Fame Wells	145
3.7.8.1	Overview	145
3.7.8.2	Upper Zone	158
3.7.8.3	$\delta^{13}\text{C}$ variations in Lower Zone Calcites	163
3.7.9	Hydrothermal Alteration of Franciscan Host Rock	165
3.7.9.1	General Statements	165
3.7.9.2	Isotopic Compositions of Host Rocks	168
3.7.9.2.1	Graywacke in the Upper Zone	169
3.7.9.2.2	Implications of $\delta^{18}\text{O}$ Values of Graywacke Quartz	174
3.7.9.2.3	δD of Upper Zone Vein Water, Indicated by δD of Graywacke	185
3.7.9.2.4	Upper Zone Greenstones	189
3.7.9.2.5	Serpentinities	192
3.7.9.2.5.1	General Features	192
3.7.9.2.5.2	Upper Zone Serpentine	193
3.7.9.2.5.3	Hydrothermal Alteration of Serpentine in the Steam Zone	194
3.7.9.2.6	Greenstone, Graywacke and "Red Rock" in the Steam Zone	198
3.7.9.2.7	"Metamorphic Rock"	202
3.8	Summary of Hydrothermal Alteration of Host Rock at the Lakoma Fame Tract of The Geysers	202
4.	STUDIES AT VALLES CALDERA, JEMEZ MOUNTAINS, NEW MEXICO	208
4.1	A Hydrothermal System in a Volcano	208
4.2	Geological Overview	209
4.3	Rock Types Encountered in Cuttings from the Wells	211
4.3.1	The Sources of Samples	211
4.3.2	Quaternary Rocks	211
4.3.3	Pre-Volcanic (Tertiary and Older) Rocks	216
4.4	Estimation of Isotopic Composition of Local Meteoric Water	217
4.5	The Wells	217
4.5.1	General Statements	217
4.5.2	Isotopic Analyses of Materials from Baca No. 7	221
4.5.2.1	General Statements	221
4.5.2.2	Unaltered or Little-Altered Rock in Baca No. 7 (surface to 500 meters depth)	221
4.5.2.2.1	Redondo Creek Member, Valles Rhyolite	221
4.5.2.2.2	Caldera Fill	229
4.5.2.2.3	Determination of the Upper Boundary of the Hot-Water Zone in Baca No. 7	229
4.5.2.3	Physical Evidence for Hydrothermal Alteration of Host Rock in Baca No. 7	230
4.5.2.3.1	Authigenic Minerals	230
4.5.2.3.2	Changes in Rock Textures	231

	<u>Page</u>	
4.5.2.4	Isotopic Changes Accompanying Hydrothermal Alteration of Rock	231
4.5.2.5	Isotopic Changes in Individual Minerals in the Hot-Water Zone of Baca No. 7 (depth greater than 700 meters)	236
4.5.2.5.1	$\delta^{18}\text{O}$ Values of Carbonates	236
4.5.2.5.2	Quartz $\delta^{18}\text{O}$ Values	238
4.5.2.5.3	Feldspar	241
4.5.2.5.4	Hydrous Minerals (Clays and Micas)	242
4.5.2.5.5	δD Variations in Rocks of Baca No. 7	245
4.5.2.5.6	$\delta^{13}\text{C}$ Variations in Carbonates	246
4.5.3	Isotopic Data from Baca No. 4	246
4.5.3.1	Introduction	246
4.5.3.2	Results	247
4.6	Summary: Rock-Fluid Interactions at Valles Caldera	252
5.	STUDIES AT THE HEBER GEOTHERMAL ANOMALY, IMPERIAL VALLEY CALIFORNIA	256
5.1	General Statements Concerning the Imperial Valley and Heber Samples	256
5.2	Variations in Carbonate $\delta^{18}\text{O}$ and $\delta^{13}\text{C}$	257
5.3	Variations in $\delta^{18}\text{O}$ Values of Sandstones and Quartz	264
5.4	Relationships between Results from J.D. Jackson No. 1 and Studies of Other Imperial Valley Wells	268
5.5	Summary of Hydrothermal Activity at Heber	271
6.	A BRIEF INVESTIGATION OF A SAMPLE FROM NAGLABONG WELL NO. 3, PHILIPPINE ISLANDS	273
7.	CONCLUSION: ISOTOPIC RECORDS IN VAPOR-DOMINATED HYDROTHERMAL SYSTEMS AND HOT-WATER SYSTEMS	277
 <u>APPENDICES</u>		
Appendix I:	Terminology	284
Appendix II:	The Theoretical Basis for Isotopic Equilibrium Fractionation	288
II.1	Introduction	288
II.2	The Thermodynamic Consideration	288
II.3	The Statistical Mechanical Free Energy	290
II.4	The Canonical Partition Function, Q	291
II.5	The Molecular Partition Function, q	293

Appendix II		<u>Page</u>
II.6	The One-Dimensional Harmonic Oscillator	294
II.7	A Free Particle in a Three-Dimensional Box	296
II.8	The Cubic-Quartic Anharmonic Oscillator	297
II.8.1	The Morse Potential	297
II.8.2	The Perturbation Theory Solution	298
II.8.3	Application of Ladder Operators	302
II.8.4	The Relationship between Energy Level Spacings and the Anharmonic Potential	308
II.8.5	The Precision of Approximations to the Morse Potential	311
II.9	Q Ratio for a Perfect Gas	323
II.10	The Effects of Anharmonicity on Perfect Gas Q's	326
II.11	Q Ratios for Crystals	330
II.12	Sources of Data for Calculations	336
II.13	Liquids	338
II.14	Sample Calculation: Calcite-Water Oxygen Isotope Fractionation at 0°C (273°K) and 527°C (800°K)	338
Appendix III: Corrections and Conversions to Mass Spectro- metric Results		346
III.1	Introduction	346
III.2	Background and Port Leakage	346
III.3	Corrections for CO ₂ Analyses	346
III.4	Conversion of $\delta^{18}\text{O}$ and $\delta^{13}\text{C}$ to the PDB Standard	347
III.5	Conversion of δD to the SMOW Standard	348
III.6	Measurement of $^{18}\text{O}/^{16}\text{O}$ Ratios of Total Oxygen in Carbonates	348
III.7	Conversion of $\delta^{18}\text{O}$ (PDB) Measurements to $\delta^{18}\text{O}$ (SMOW)	348
III.8	Correction for $\delta^{18}\text{O}$ Analyses of Water Samples	349
III.9	Correction for Contaminant Oxygen in the Fluorine	349
III.10	Conversion of Silicate $\delta^{18}\text{O}$ Values to the SMOW Scale Using a Reference Sample of Known Isotopic Composition	350
BIBLIOGRAPHY		352

List of TablesText Tables

	<u>Page</u>
Table 1. Chemical Analyses (ppm) of Spring Water at The Geysers.	52
Table 2. Descriptions and Isotopic Analyses of Minerals from Thermal No. 7, The Geysers.	63
Table 3. Descriptions and Isotopic Analyses of Rocks and Minerals from Lakoma Fame No. 19, The Geysers.	78
Table 4. Isotopic Compositions of Non-Thermal Water Samples from The Geysers and the Surrounding Area.	116
Table 5. Descriptions and Isotopic Analyses of Rocks and Minerals from Lakoma Fame No. 13, The Geysers.	122
Table 6. Descriptions and Isotopic Analyses of Rocks and Minerals from Lakoma Fame No. 15, The Geysers.	132
Table 7. Descriptions and Isotopic Analyses of Rocks and Minerals from Lakoma Fame Nos. 8 and 9, The Geysers.	138
Table 8. Surface Water Samples from the Jemez Mountains, New Mexico.	218
Table 9. Descriptions and Isotopic Compositions of Rocks and Minerals from Baca No. 7, Valles Caldera, New Mexico.	222
Table 10. Isotopic Composition of Surface Samples of Bandelier Tuff, Los Alamos, New Mexico.	235
Table 11. Descriptions and Isotopic Analyses of Rocks and Minerals from Baca No. 4, Valles Caldera, New Mexico.	250
Table 12. Descriptions and Isotopic Analyses of Rocks and Minerals from J.D. Jackson No. 1, Heber, California.	258

Appendix Tables

Table II-1 Deviation from Morse Potential of Harmonic, Cubic-Anharmonic and Cubic-Quartic-Anharmonic Potentials.	318
--	-----

Appendix Tables (cont'd)

	<u>Page</u>
Table II-2 Vibrational Frequency Data for Calcite.	340
Table II-3 Values of the Debye Energy Function.	342
Table II-4 Contributions to Calcite Partition Function Ratios for $^{18}\text{O}/^{16}\text{O}$.	343

List of Figures

*(The first page cited contains the caption;
the following page contains the actual figure.)*

Text Figures

	<u>Page</u>
FIGURE 1. Effects of HF and HCl treatments on $\delta^{18}\text{O}$ values and oxygen yields of Franciscan graywacke.	31-32
FIGURE 2. X-ray powder diffractograms of Franciscan graywacke before and after treatment with HF and HCl.	33-34
FIGURE 3. δ^{18} values (relative to Harding Iceland Spar working reference) from 98 analyses of Ramona Rose Quartz, plotted against % yield).	39-40
FIGURE 4. Histogram of $\delta^{18}\text{O}$ values of 69 Ramona Rose Quartz analyses.	42-43
FIGURE 5. Map showing The Geysers and vicinity, Mayacmas Mountains, California.	46-47
FIGURE 6. Location map of wells at The Geysers whose samples were studied.	48-49
FIGURE 7. Temperature records at various depths in Thermal Well No. 7, The Geysers.	60-61
FIGURE 8. Temperatures in wells drilled between 1957 and 1962, The Geysers.	68-69
FIGURE 9. $\delta^{18}\text{O}$ values of vein minerals from various depths, Lakoma Fame No. 19, The Geysers.	89-90
FIGURE 10. Calculated extrapolation to lower temperatures of $\delta^{18}\text{O}$ values of quartz, calcite and water from upper zone veins, Lakoma Fame No. 19, The Geysers.	101-102
FIGURE 11. Variations in $\delta^{18}\text{O}$ and δD values of near-neutral chloride-type thermal waters and geothermal steam from geothermal areas.	113-114
FIGURE 12. $\delta^{18}\text{O}$ values of minerals and a rock from various depths, Lakoma Fame No. 13, The Geysers.	125-126

	<u>Page</u>
FIGURE 13. $\delta^{18}\text{O}$ values of rocks and minerals from various depths, Lakoma Fame No. 15, The Geysers.	130-131
FIGURE 14. $\delta^{13}\text{C}$ values of vein calcite from various depths Lakoma Fame No. 19, The Geysers.	146-147
FIGURE 15. $\delta^{13}\text{C}$ values <i>versus</i> $\delta^{18}\text{O}$ values for calcites from Lakoma Fame No. 19, The Geysers.	148-149
FIGURE 16. $\delta^{13}\text{C}$ values of vein calcite from various depths Lakoma Fame No. 15, The Geysers.	150-151
FIGURE 17. $\delta^{13}\text{C}$ values <i>versus</i> $\delta^{18}\text{O}$ values for calcites from Lakoma Fame No. 15, The Geysers.	152-153
FIGURE 18. $\delta^{13}\text{C}$ values of vein calcite from various depths, Lakoma Fame No. 13, The Geysers.	154-155
FIGURE 19. $\delta^{13}\text{C}$ values <i>versus</i> $\delta^{18}\text{O}$ values for calcites from from Lakoma Fame No. 13, The Geysers.	156-157
FIGURE 20. $\delta^{13}\text{C}$ values of vein calcite and other carbon-bearing matter from The Geysers.	160-161
FIGURE 21. $\delta^{18}\text{O}$ values of host rocks and non-vein minerals from various depths, Lakoma Fame No. 19, The Geysers.	166-167
FIGURE 22. $\delta^{18}\text{O}$ values of upper-zone graywacke quartz from various depths, Lakoma Fame No. 19, The Geysers.	172-173
FIGURE 23. $\delta^{18}\text{O}$ values of upper zone graywacke quartz plotted against the values of graywacke from which they came, Lakoma Fame No. 19, The Geysers.	183-184
FIGURE 24. δD <i>versus</i> $\delta^{18}\text{O}$ for rocks, minerals and waters from The Geysers.	186-187
FIGURE 25. Superimposed variations with depth of $\delta^{18}\text{O}$ and $\delta^{13}\text{C}$ values of vein calcite and $\delta^{18}\text{O}$ of serpentine host rock in the lower 800 meters of Lakoma Fame No. 19, The Geysers.	196-197
FIGURE 26. Schematic thermal and fluid history of hydrothermal activity at The Geysers.	203-204
FIGURE 27. Map of Valles Caldera and vicinity, New Mexico.	212-213
FIGURE 28. $\delta^{18}\text{O}$ values of calcite and whole-rocks from various depths, Baca No. 7, Valles Caldera.	225-226

	<u>Page</u>
FIGURE 29. $\delta^{18}\text{O}$ values of minerals from various depths in the hot-water zone, Baca No. 7, Valles Caldera.	227-228
FIGURE 30. δD values of hydrothermally-altered volcanic rocks plotted against water content in weight percent, Baca No. 7, Valles Caldera.	243-244
FIGURE 31. $\delta^{18}\text{O}$ values of calcite, sandstone quartz and whole rocks from various depths, J.D. Jackson No. 1, Imperial Valley.	260-261
FIGURE 32. $\delta^{13}\text{C}$ values plotted against $\delta^{18}\text{O}$ values of calcite, J.D. Jackson No. 1, Imperial Valley.	265-266
FIGURE 33. $\delta^{18}\text{C}$ values plotted against $\delta^{18}\text{O}$ values of calcite from various hot-water systems.	269-270
FIGURE 34. $\delta^{13}\text{C}$ values <i>versus</i> $\delta^{18}\text{O}$ values of all hydrothermal calcites analyzed in this study.	281-282

Appendix Figures

FIGURE II-1 The Morse potential.	299-300
FIGURE II-2 The harmonic potential.	312-313
FIGURE II-3 The cubic-anharmonic potential.	314-315
FIGURE II-4 The cubic-quartic anharmonic potential.	316-317
FIGURE II-5 Deviations from the Morse potential of the harmonic, cubic-anharmonic, and cubic-quartic anharmonic potentials.	319-320

List of Photomicrographic Plates

*(The first page cited contains the caption;
the following page contains the actual plate.)*

	<u>Page</u>
PLATE 1. Hydrothermally-altered graywacke with veins Thermal No. 7, The Geysers.	58-59
PLATE 2. Hydrothermally-altered graywacke with quartz vein, Thermal No. 7, The Geysers.	58-59
PLATE 3. Massive quartz vein in graywacke, Lakoma Fame No. 19, The Geysers.	76-77
PLATE 4. Massive quartz and calcite veins in greenstone, Lakoma Fame No. 19, The Geysers.	76-77
PLATE 5. "Red Rock," aggregate of hematite and quartz, Lakoma Fame No. 15, The Geysers.	139-140
PLATE 6. "Metamorphic Rock," with calcite vein, Lakoma Fame No. 8, The Geysers.	139-140
PLATE 7. Lithic graywacke, containing greenstone fragment, Lakoma Fame No. 19, The Geysers.	170-171
PLATE 8. Feldspathic graywacke, Lakoma Fame No. 19, The Geysers.	170-171
PLATE 9. Cataclastic graywacke, showing sericitization of plagioclase clast, Lakoma Fame No. 19, The Geysers.	175-176
PLATE 10. Typical graywacke, Franciscan Group, Lakoma Fame No. 19, The Geysers.	175-176
PLATE 11. Greenstone (spilitic basalt) with sericitized plagioclase pseudomorph, Lakoma Fame No. 19, The Geysers.	178-179
PLATE 12. Greenstone (spilitic basalt) with fresh phenocrysts of augite, Lakoma Fame No. 19, The Geysers.	178-179
PLATE 13. Groundmass of greenstone (spilitic basalt) from Franciscan Group, Lakoma Fame No. 19, The Geysers.	180-181

	<u>Page</u>
PLATE 14. Amygdule of quartz and chlorite in greenstone, Lakoma Fame No. 19, The Geysers.	180-181
PLATE 15. Mesh-structure antigorite, from serpentinite body, Lakoma Fame No. 19, The Geysers.	200-201
PLATE 16. Hydrothermally-altered graywacke from steam zone, Lakoma Fame No. 19, The Geysers.	200-201
PLATE 17. Fresh Bandelier Tuff, Los Alamos, New Mexico.	232-233
PLATE 18. Hydrothermally-altered Bandelier Tuff, Baca No. 7, Valles Caldera.	232-233
PLATE 19. Hydrothermally-altered Bandelier Tuff, with sanidine phenocryst, Baca No. 7, Valles Caldera.	248-249
PLATE 20. Hydrothermally-altered Bandelier Tuff, Baca No. 4, Valles Caldera.	248-249
PLATE 21. Hydrothermally-altered volcanic rock, Naglabong No. 3, Philippines.	274-275

0. Prologue: A Brief History of Hot-Spring Investigations

While this report is not about hot springs per se, it is doubtful that it would have been written had they never existed.

"Hot springs have long been regarded as the latest phase of volcanism, and it is in this role that they have made their widest appeal. Geologists, however, with few exceptions, have focused their attention on the more spectacular phases of igneous activity (active volcanoes) or on phases of economic importance (ore deposits), regarding thermal springs as of incidental interest only."

(Allen and Day, 1935)

Geologists are not the only segment of society in which the above-expressed attitude is manifest. Certainly, the geological phenomena which attract the most attention from humans are those which potentially either endanger life and property (active volcanoes, earthquakes, etc.), or yield a source of monetary income (ore deposits, hot mineral springs, caves, tourist traps, etc.). The origins of interest in the latter are lost in antiquity. Because of their cataclysmic nature, the former appear periodically in the literature of historic times: Etna, 476 B.C., Vesuvius, A.D. 79, Monte Nuovo, 1538, Tambora, 1815, Krakatoa, 1883, Pelée, 1902, Katmai, 1912, Lassen, 1914, Pericutin, 1943, Kilauea, 1960. These, of course, are some of the most famous volcanic eruptions, all of which, except the last, came as a surprise to the local inhabitants. True, some eruptions, for example, Sunset Crater, A.D. 1064, yielded immediate benefits, such as rich ash-mulch creating an Indian land-rush in Arizona in 1065 which rivaled that in Oklahoma many centuries later. Most eruptions, however, served only to temporarily frighten away the inhabitants,

who, when the underlying fires died down and the infernal emissions subsided, returned to rebuild new lives on the ruins of the old.

With very few of these eruptive incidents are there associated reports of hot spring activity: the display of the volcano would naturally overshadow any other thermal features. It had not occurred to many people to look for hot springs, aside from those obviously spectacular features such as the Valley of Ten Thousand Smokes. That area of fumarolic emissions displayed an activity which persisted for some years following the eruption of Katmai (Alaska).

Not even Georg Bauer (Georgius Agricola) in his classic work "De Re Metallica" (1556) recognized the connection between volcanism and ore deposition, but treated some elements of the former in an earlier work "De Ortu et Causis Subterraneorum" (1546). Agricola was obviously a product of his neighborhood (Europe); although virtually all of the world's known cinnabar deposits are known to be associated with thermal activity, two of the largest, Idria and Almadén, have no apparent association with hot springs or volcanic surface flows (Lindgren, 1933).

It is not known how long hot springs and geysers (the name comes from the Icelandic word, "geysir", to gush forth) have been a source of amusement to people in those lands where such features abound, Iceland and New Zealand. It is safe to say that delight in their usefulness as objects of curiosity and/or sources of hot water (for bathing, laundering, etc.) has persisted since the discovery of thermal springs (Hague, 1892b). For a time, superstitions inspired by such

works as Virgil's Aeneid and Dante Alighieri's Divine Comedy evidently remained a deterrent to the close approach of some of the more gassy features, which were thought to be earthly protrusions of the nether regions.

Even in the United States, nature's "all-healing" mineral waters had not become big business before the beginning of the 19th century, but that time was a turning point. It remains somewhat an enigma just how the Lewis and Clark expedition managed to avoid completely the area now known as Yellowstone National Park in Wyoming, but they did. The thermal wonders of that region might have gone unnoticed for several more years if one of the members of that expedition had not become restless at the thought of returning to civilization. In August of 1806, John Colter asked to be "relieved from further service" that he might go up the (Missouri) river to trap beaver. Having established an auspicious relationship with the celebrated trader, Manuel Lisa, and having distinguished himself in battle in the eyes of the Crow Indians, he was evidently completely enraptured by the country. Thus, in 1807, John Colter is believed to have been the first white man to enter the Yellowstone area. After some adventures with the hostile Blackfeet, Colter returned to St. Louis in 1810 and talked about his exploits of the previous four years. So incredible were his descriptions of the Yellowstone region, that this obviously non-existent wild mountain-man's mythical kingdom was christened "Colter's Hell". (Chittenden, 1895).

Warren Angus Ferris, who visited what is now Upper Geyser Basin in 1834, is the next to describe thermal activity in the northern Rocky Mountains. As early as 1811, this activity was thought to be associated with "evident traces of extinguished volcanoes". His descriptions are largely free from the storyteller-exaggerations of John Colter, Jim Bridger and the like. (Chittenden, 1895). In spite of public disbelief in the existence of the thermal features, there were recognizable signs of volcanism in the nearby Absoroka Range.

In the meantime, most of the rest of the world speculated. Evidently, everyone else knew about geysers and knew exactly how they worked. The first geyser theory was published in 1811 by Sir George Mackensie, who visited Iceland. (Note that this post-dated John Colter's escapades.) Next came Krug von Nidda's theory published in 1836, based on his visit to Iceland three years earlier. The first important work on hot springs was that of Robert Bunsen in 1847, based also on a visit to Iceland; he was a good experimentalist as well as a trained observer (he invented the Bunsen electric cell and the Bunsen gas burner, co-discovered the principle of spectrum analysis and investigated geyser action). Unfortunately, his theory of geysers (which are simply hot springs that discharge water intermittently) was intended only for application to Great Geyser in Iceland. Other investigators/theorists/experimenters followed: the model-builders Hague (1892a,b), Hallock (1884), Thoroddsen (1925); later, Hills and Warthin (1942), Forrester and Thune (1942), Allen and Day (1935), Benseman (1965), and White (1967).

Parallel with the development of hydrothermal system theory stemming from the work of Bunsen was the view of Élie de Beaumont (1847). His view was that both hot springs and mineral veins were related to volcanic emanations containing the more volatile components (sulfur, arsenic, mercury, halogens, etc.) which had escaped from hot rocks at depth. Sainte-Claire Deville (1855) was the first to collect and analyze volcanic gases and so added substance to the theories of de Beaumont regarding the distribution and concentration of some chemical elements in the earth's crust. It is interesting to note here that the hypothesis of meteoric origin of thermal waters was held in high esteem as early as 1883: A. C. Peale's model for hydrothermal fluid origin is extremely close to the ideas held today, and in all due respect, had its birth without benefit of isotopic data!

Let us return to Yellowstone. Stories persisted, but not until 1869 was an expedition organized to test the veracity of the tales; this was the famous Folsom-Cook party. Unfortunately, the accounts of this trip were not immediately publicized, due to a fire in the office of the Western Monthly, the publication which carried Folsom's article; all but a few copies were destroyed (Allen and Day, 1935). When Cook submitted his timid report to Lippincott's Magazine, the polite rejection slip said, "Thank you but we do not print fiction."

Doubtless such men as Lieutenant Gunnison, Father De Smet, Captain Charles Reynolds and Walter DeLacy either visited or heard of the land of the Rock-Yellow River from traders and trappers such as

Jim Bridger even before 1850. Alas, a skeptical world awaited an official report. (Tilden, 1956). That report came in the form of the accounts of the Washburn expedition of 1870, published by some of its members: Langford, Trumbull, Everts and Doane. No longer was this land unknown. The Hayden Survey, begun in 1871 and extending into 1878, included not only a geological reconnaissance, but also careful measurements of temperatures of springs and geyser eruption heights. On March 1, 1872, Yellowstone became the first national park, and hot spring studies were underway, in Wyoming at least.

No one knows who was the first to report the thermal activity in the Cascade Range of the Northwest. Captain John Charles Frémont doubtless saw Mount Baker and Mount St. Helens in eruption in 1843. The southernmost peak in this chain of volcanoes was largely ignored until a pioneer by the name of Peter Lassen began conducting parties from Humboldt, Nevada to the Sacramento Valley of California during the time of the gold rush, 1848. It is said that as a guide, Lassen left much to be desired, using Mt. Lassen as a landmark one day, and Mt. Shasta the next, never really knowing the difference. The legend goes on to say that since the Lassen Trail was neither direct nor reproducible, one day Peter became lost. The group he was guiding forced him at gunpoint to climb his peak in order to find his way. (Yeager, 1959). The nearby Cinder Cone erupted in 1851. In 1864 Kendall V. Bumpass discovered the thermal area in the caldera of the now-collapsed Mount Tehama near Lassen Peak. The following year he returned with a newspaper editor from Red Bluff. After cautioning the

editor to take care of the thin crust which may hide boiling pools below, Bumpass himself managed to break through the crust, scalding his leg. The place is now known as Bumpass Hell. (Matthews, 1968, Tilden, 1956).

On May 30, 1914 at 5:00 A.M., Mount Lassen asserted itself as an active volcano. The subsequent dacite flow, mud flow and Great Hot Blast aroused the interest not only of the local inhabitants but also of science. Here was an opportunity to investigate the relationships of active volcanism to hot springs. Investigate they did (Day and Allen, 1925), and Elie de Beaumont's ideas had come into full fruition.

1. INTRODUCTION

1.1 The Aims of the Present Investigation

Although great interest has been expressed in hot springs and geysers over the years, the effects of surface outpourings of water and steam are of small consequence to the geologic record. Thermal springs are merely superficial expressions of volumetrically more important processes taking place at depth. Furthermore, hot springs are not always present to indicate that there is subsurface thermal activity. Some known geothermal fields have no hot springs, but their existence is indicated by abnormally high geothermal gradients. Evidence of previous, large-scale subsurface interactions between rocks and fluids (water and/or carbon dioxide, usually) are quite abundant. Some common examples of the results of such interactions are regional and contact metamorphism, diagenesis, some kinds of ore deposits, and non-economic hydrothermal alteration.

Studies of the light stable isotopes (those having atomic numbers below 16) have been shown to be indicators of rock-fluid interaction. Particularly significant in such studies have been the variations in the D/H, $^{13}\text{C}/^{12}\text{C}$, $^{18}\text{O}/^{16}\text{O}$, and $^{34}\text{S}/^{32}\text{S}$ ratios. These elements are nearly ubiquitous in the earth's crust. Deviations from "expected" ratios for various materials indicate perturbations in minerals which might not otherwise be readily detected. Historically, one of the first problems to be encountered in these studies was to determine those "expected" values. In this work, only hydrogen, carbon and oxygen were considered, not to imply the scarcity

of sulfur-bearing matter.

Active hydrothermal systems are natural laboratories, carrying out rock-fluid interactions at temperatures as high as 350°C in time periods of over 10,000 years (Averiev, 1967). In the laboratories of mankind, many hydrothermal experiments involving minerals proceed at rates which are simply too slow to obtain complete or even partial equilibrium within the span of a human lifetime. Furthermore, it is difficult to design laboratory experiments which take into account many naturally-controlled factors, such as catalysis by trace constituents, surface adsorption, the effects of having a large open system, etc.

The temperature range encountered in natural hydrothermal systems is also commonly encountered in diagenesis (Yeh and Savin, 1974), low-grade burial metamorphism (Eslinger and Savin, 1973a), and ore deposition (Taylor, 1974). Chemical changes occur during these processes. Also, isotopic changes occur in minerals, reflecting changes in temperature and changes in characteristics of the fluid reservoir. The processes taking place in the temperature range of active hydrothermal systems are geologically very important, but are incompletely understood.

The present work is directed toward a study of reactions between minerals and fluids from a diversity of hydrothermal systems, some of which are associated with surface hot springs, and some not.

The specific objectives of this work are:

1. To deduce the natures of the fluids which have been responsible for various episodes of deposition and/or alteration.
2. To characterize the original isotopic compositions of unaltered rocks and fluids (water and carbon dioxide) that interacted with rocks.
3. To characterize the isotopic differences between original and altered host rocks and minerals.
4. To determine the nature and degree of alteration in host rocks of different lithology, and the factors that control the alteration.
5. To characterize the essential isotopic differences between systems dominated by steam and those dominated by liquid water.

Consequences of the results of the above-outlined avenues of study are:

1. Determinations of the degree and spatial extent of isotopic equilibrium between host rock and fluid in hydrothermal systems.
2. Measurements of the temperatures of deposition and/or alteration, using stable isotope partitioning between coexisting phases.
3. Calculations of fluid/rock ratios involved in various episodes of hydrothermal activity.

4. Possible extensions or confirmations of low-temperature extrapolations of some isotopic geothermometers.
5. Comparison of isotopically-determined temperatures in hydrothermal systems with directly-measured temperatures.
6. Determinations of paragenetic relationships of minerals from their isotopic records.
7. Derivations of the thermal histories of the systems that were isotopically studied.

1.2 Geothermal Areas Investigated in This Work

Due in large part to extensive drilling and sampling of geothermal systems conducted by private corporations in the exploration for geothermal energy resources, a number of samples from a variety of hydrothermal systems are available for study. The systems whose samples were studied in this investigation are briefly described as follows:

1. The Geysers, western Mayacmas Mountains, Sonoma County, California. The Geysers is one of the largest known vapor-dominated hydrothermal systems. Its host rocks are of the Franciscan Group and its associated serpentinites, all of which are of low inherent permeability, but are fractured. This geothermal area is associated with quaternary volcanism and the surrounding region was formerly a quicksilver mining district.
2. Valles Caldera, northern Jemez Mountains, New Mexico. Valles Caldera was the site of quaternary volcanism on the

edge of the Rio Grande Trough. The hot water system developed at the Caldera has intersected a large variety of rocks, including granite, limestone, and arkosic sandstone as well as pumiceous tuffs.

3. Heber Geothermal Anomaly, southern Imperial Valley, California. The Imperial Valley contains a number of geothermal anomalies, some of which have associated with brines containing high concentrations (up to 30 weight %) of dissolved solids, with temperatures as high as 350°C. The Heber anomaly contains a hot-water system of low dissolved solids content, whose host rocks are poorly-consolidated sands and muds derived from the surrounding mountains and the nearby Colorado River delta.
4. The Tiwi area, Philippine Islands. The host rocks for this hot-water system are volcanics associated with the Philippines Island Arc, located in a tropical region.

The results of studies at each of these locations will be described in detail in separate sections. A synthesis of the conclusions will follow the separate sections. The hydrothermal systems chosen provide a wide spectrum in host rock lithology, permeability, meteoric water, isotopic composition, temperature, and amount of water available.

1.3 Previous Work Closely Related to this Work

Very few isotopic investigations of the kind proposed here have been made in active hydrothermal systems. The only previous work

directly related to isotopic studies of minerals in active hydrothermal systems was that of Clayton, Muffler and White (1968) and Eslinger and Savin (1973a).

The investigations of Clayton, Muffler and White were made on cuttings materials from one thermal brine well in the Salton Geothermal Field. The materials studied isotopically were mostly bulk carbonates in the cuttings and the silicate residues remaining after the extraction of CO₂ from the cuttings. From a knowledge of the change in ¹⁸O/¹⁶O of the minerals and the change in this ratio of the water, the relative amounts of rock and water that had isotopically exchanged with each other were determined. It was also found that the observed calcite-water fractionations indicated temperatures very close to those measured in the well. The few but important results of Clayton et al. (1968) will be discussed in detail in subsequent text.

The isotopic studies of materials from two holes in the Ohaki-Broadlands in New Zealand by Eslinger and Savin were performed principally to calibrate a quartz-illite geothermometer in an active hydrothermal system. This thermometer was used to study the progressive burial metamorphism in sedimentary rocks of the Belt Supergroup, Montana. (Eslinger and Savin, 1973b). Their work also will be utilized in a discussion appearing in the body of this work.

The preliminary work of Clayton et al. (1968) and Eslinger and Savin (1973a) showed that some rock alteration took place and that temperature determinations were possible, using the partitioning of

stable isotopes between coexisting phases. One obvious exploitation of these important hydrothermal system samples was not made: the study of rock alteration in active systems. Another feature of previous studies is that they have been concerned entirely with hot-water systems. The much less common, but more economically important vapor-dominated hydrothermal systems have been neglected in terms of geochemical and even petrologic study. Examples of such systems are Larderello (Italy), the Mud Volcano area of Yellowstone (Wyoming), the Silica Pit area of Steamboat Springs (Nevada), and of course The Geysers (California). Two of the primary objectives of this work is to exploit in detail the available samples for the purposes of evaluating (1) the alteration of host rocks by hydrothermal fluids, and (2) the nature and degree of hydrothermal alteration in vapor-dominated systems.

1.4 Economic Significance of the Work

The isotopic study of active hydrothermal systems is fundamental to the study of paleo-hydrothermal systems, which may in turn lead to an understanding of the processes of magmatic-hydrothermal deposition of ores, and to determinations of locations of ore bodies for economic exploitation. For example, stable isotopes are potentially a prospecting tool for finding the most probable locations of the host rocks richest in ores, which was illustrated by Engel et al. (1958). As a result of isotopic investigations, circulation of meteoric ground waters driven into convection by a cooling

epizonal pluton has been proposed as a potential ore-depositing process (Taylor, 1974). Isotopic investigations of active hydrothermal systems should allow for detailed studies of some veining processes as to whether they may be episodic, or result from a single depositional event. The ore deposition at Butte, Montana is thought to be episodic. It is anticipated that the isotopic record should confirm the presence or absence of periodicity in the thermal history of recently-active systems.

Geothermal steam from active hydrothermal systems is now being used to generate electricity. In Iceland and Pagosa Springs, Colorado natural hot water is also used for space heating. In the course of the development of this energy resource, it is obviously important to determine the past thermal history and the future of a system so used. Some economically-relevant problems connected with a study of this type are: change with time in temperature of the heat reservoir, whether the usefulness of the steam field is on the rise or is playing out, whether or not it will be necessary to add water to prolong the life of the field, the effects of water injection, location of formerly hottest surface activity, and the best place to drill the next hole (based on isotopic results from previous holes). Isotopic studies might provide some insight toward solving some of the above-mentioned problems.

Although active hydrothermal systems are potentially economically important, a major factor in determining their economic potential is the nature of the fluid involved in these systems. Economically, a

vapor-dominated hydrothermal system is inherently more usable than a hot-brine-dominated system. A vapor-dominated hydrothermal system (White et al., 1971) is characterized by:

1. Host rocks of low initial permeability, which will limit the amount of water admitted to the system.
2. Low rates of fluid discharge from surface manifestations (springs and fumaroles) if any, which are indicative of small amounts of fluid in the system.
3. Surface and subsurface thermal waters that are low in chloride (<20 ppm). Low concentrations of solutes are important considerations in the engineering and design of fluid-handling equipment, since the fluid is relatively non-corrosive.
4. The presence of dry or slightly superheated steam, indicating high steam-reservoir temperatures.

Hot-water systems display the following features:

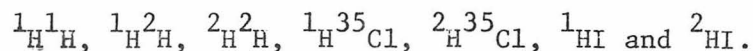
1. Permeable or competent fractured host rocks.
2. Moderate to high fluid discharge at the surface, if any surface features are present.
3. High concentrations of solutes (alkali chlorides, SiO_2 , boron, arsenic, etc.), up to 300,000 ppm for the Salton-Imperial Valley system.
4. Sub- or near-boiling water.

Isotopic analyses of rocks and minerals which are sensitive to the H_2O /rock ratio and temperature offer the opportunity to investigate

a hydrothermal system as to its evolution as either of the two above-defined systems.

1.5 Previous Work, Peripherally Related to this Work

The earliest recognition that isotopic species of a molecule will have different thermodynamic properties was in 1933. Urey and Rittenberg investigated, by theoretical calculations, the differences in Gibbs' free energy in a few hydrogen-containing molecules:



These differences were derived by calculating the partition functions for the various species. (A detailed consideration of this subject appears in Appendix II of this work.) An augmented treatment of the situation was given by Urey in 1947, in which partition function (Q) ratios were calculated for molecules formed from H, Li, B, C, N, O, Cl, Br and I and their isotopic species.

Work by Bigeleisen and Mayer (1947) was a simplification of the above treatment. Their calculations of free energy changes and equilibrium constants were made using only the spectroscopic vibrational frequency shifts arising from isotopic substitutions. The approach involved the harmonic oscillator approximation, and hence is invalid for hydrogen-bearing molecules which vibrate with considerable anharmonicity.

In the same year, instrumentation became available so that small differences in the isotopic compositions of gases could be measured. The instrument was the now-familiar mass spectrometer of A. O. Nier (1947). His work described the details of construction of the machine,

complete with electronic circuit schematic diagrams. Reproducibility of the measurements of differences in isotopic ratios was on the order of 0.003 (3‰).

Improvements to the Nier mass spectrometer were made by McKinney, McCrea, Epstein, Allen and Urey (1950). These improvements involved the use of advanced electronics to construct a regulated power supply for the magnet current and ion accelerating voltage, and a better regulator for the emission of the ionizing electrons streaming off the filament. A commercial vibrating reed electrometer for the ion beam detector, and rapid alternate admission to the machine of the two gas samples being compared were also significant improvements. The reproducibility of the $^{18}\text{O}/^{16}\text{O}$ and $^{13}\text{C}/^{12}\text{C}$ improved to 0.0001 (0.1‰) of the ratio and to 1‰ for the D/H ratio.

The improvements in the mass spectrometer were made for the purpose of measuring the temperature at which CaCO_3 -bearing invertebrate animals precipitated the material for their shells, thus measuring the temperatures of the oceans of the past. If a carbonate sample is well preserved, its $^{18}\text{O}/^{16}\text{O}$ ratio is established in isotopic equilibrium with its surrounding water, and the isotopic composition of both the carbonate and the ocean water are known, the temperature of carbonate deposition should be obtainable from the difference between $^{18}\text{O}/^{16}\text{O}$ ratios of the carbonate and the water. Experiments were done to find the best way of extracting CO_2 for machine analysis from carbonates. The laboratory equilibrium growth of inorganic (McCrea, 1950) and biogenic carbonates in waters of

various temperatures and isotopic compositions were successful. These results established a carbonate oxygen isotope paleo-temperature scale (Urey, Lowenstam, Epstein and McKinney, 1951; Epstein, Buchsbaum, Lowenstam and Urey, 1951). A slight revision of the scale was made by Epstein, Buchsbaum, Lowenstam and Urey (1953). The paleotemperature work also established typical values for the carbon and oxygen isotopic compositions of marine carbonates.

Mass spectrometry was used to determine $^{13}\text{C}/^{12}\text{C}$ ratios in natural materials by Nier and Gulbransen in 1939. The reservoir of carbon isotopic data was expanded by Craig (1953), who analyzed ocean bicarbonate, the atmosphere, flora, fauna, coal and petroleum as well as marine carbonates.

Analyses of natural waters were developed along two approaches: the deuterium content (Friedman, 1953) and the ^{18}O content (Epstein and Mayeda, 1953). Both works revealed the significance of isotopic fractionation in the hydrologic cycle. Both established that the ocean water was among the heaviest, and that meteoric waters were lighter, having been "distilled" from the oceans. The variations of the $^{18}\text{O}/^{16}\text{O}$ ratio with latitude could be very profound.

Although the above studies of waters included some samples from Yellowstone and Parícutín, one of the first discussions of isotopic variations in an active hydrothermal environment was that of Craig, Boato and White (1956). Again Professor Peale's concept of the meteoric origin of thermal waters was considered (although not specifically cited by Craig *et al.*), and it was recognized that

stable isotopes might well resolve the question of what proportions of thermal waters could be magmatic. The problem was investigated in greater detail by Craig (1963).

Meanwhile, techniques had been developed with which to prepare CO_2 from minerals. Clayton and Epstein (1958) established some fundamental isotopic relationships among coexisting minerals. It was found that in certain kinds of geological environments, coexisting minerals tended to be in isotopic equilibrium with each other and with a (fluid?) reservoir. It was recognized that mineralogical equilibrium (based on textural evidence) commonly implied isotopic equilibrium. Qualitatively as the temperature increased, the fractionations became smaller. By extrapolating the isotopic relationships among the minerals to infinite temperature, the isotopic composition of the large reservoir could be inferred (Epstein, 1959).

The new perspective introduced by Clayton and Epstein was applied to the study of the effects of an ancient hydrothermal system by Engel, Clayton and Epstein (1958). Again, the temperature effect was found, and the highest apparent isotopic temperatures corresponded to the most intense hydrothermal alteration. This result was of great potential economic importance, for the areas of greatest hydrothermal temperatures commonly held the highest concentrations of ores. The far greater, general geological significance of this study was manifest in its consideration of the effects of the interactions between preexisting rock and hot water. A depletion in ^{18}O of host

rock as large as 10‰ indicated that the water might have been meteoric, but the water had lost its meteoric character by exchange with rock.

After many more water analyses, Craig (1961a) published the least squares fit to meteoric water analyses which is the familiar straight line described by the equation

$$\delta D = 8 \delta^{18}O + 10$$

changed to $\delta D = 8 \delta^{18}O + 5$ by the later work of Epstein, Sharp and Gow (1965, 1970).

The earliest attempts to extract oxygen from silicates for isotopic analysis were those of Baertschi and Silverman in 1951, and involved the use of fluorine, hydrogen fluoride and chlorine trifluoride. The work of Clayton and Epstein in 1958, involving the preparation of CO₂ from silicates, relied on carbon reduction, and conversion of CO to CO₂ was necessary. Studies by Taylor and Epstein (1962 a,b) again proved the usefulness of extracting oxygen by gaseous fluorine treatment and converting the O₂ to CO₂. More importantly, this work served to demonstrate the applicability of stable isotope studies to the solution of petrologic problems. Also, some typical values of oxygen isotope compositions for igneous and metamorphic rocks were established. The results suggested that in many cases the isotopic composition of an igneous mineral could be predicted a priori. An outgrowth of this finding was that many igneous and metamorphic minerals seemed to have exchanged oxygen with a large reservoir, giving rise to the uniform isotopic compositions of certain minerals

and rocks, regardless of locality. Both of these results are of importance to the present work. This large reservoir has the isotopic composition of the mantle of the earth, as suggested by the similarities in $^{18}\text{O}/^{16}\text{O}$ and $^{30}\text{Si}/^{28}\text{Si}$ of mantle-derived terrestrial rocks and lunar basalts and gabbros. The moon, the earth and chondritic meteorites all appear to be genetically related somehow, based on their isotopic compositions; the reservoir of isotopically homogeneous material from which they all formed seems to have been very large indeed.

Isotopic studies were made on neutral, chloride-type water discharged from thermal springs, and on meteoric water at Steamboat Springs, Lassen, Niland (Imperial Valley), Iceland, The Geysers, Lardarello and Wairakei by Craig (1963). It was found that hot spring and fumarolic waters had the same hydrogen isotopic composition as local meteoric water, but the oxygen could be substantially ^{18}O -richer in hot water than in meteoric. Similar studies of acid-type ($\text{pH}<7$) hot springs at Yellowstone, Lassen and The Geysers indicated an enrichment in hot spring water in both deuterium and ^{18}O , with respect to local meteoric values, due in large part to evaporation-fractionation. Thus it was shown that hot spring water originates from local meteoric water.

Similarly, Craig (1966) illustrated that geothermal brines at Niland and in the Red Sea were predominantly meteoric in origin, further illustrating the power of stable isotopic identifications of waters. In the same year, Garlick and Epstein investigated the

hydrothermal ore deposit at Butte, Montana. Many samples of vein and wall-rock alteration minerals showed an oxygen isotope shift towards low $\delta^{18}\text{O}$ values with respect to typical unaltered quartz monzonite host rock. The only way to lower $\delta^{18}\text{O}$ of igneous material was for it to interact with fresh water which is the only known source of low $\delta^{18}\text{O}$ material.

Garlick and Epstein (1967) conducted an isotopic survey of regionally metamorphized rocks. The temperature effects on fractionation between minerals in zones of different grades were evaluated. It was found that fractionations between minerals apparently decrease fairly regularly with increasing grade. These observations also served to test the sequences of first appearances of index minerals conceived by Barrow (1893). The isotopic analyses were also a test of geographic extent of equilibrium within a given mineral assemblage. Furthermore it was possible in principle to characterize the isotopic composition of the metamorphic pore fluid. Finally, it was shown that minerals could be ranked in the tendency to concentrate ^{18}O .

Sedimentation potentially involves mineral-water interactions at very low temperatures (0 to 25°C). The studies of Savin and Epstein (1969 a, b, c) considered the isotopic systematics of some sedimentary processes. They examined the effects of chemical composition and grain size on the isotopic equilibria (or approach thereto) in sedimentary materials. Those materials included clays, ocean sediments and coarse-grained elastics. Savin and Epstein also established

typical isotopic compositions for authigenic minerals and various sediments. Their work could be thought of as a general treatment of low temperature mineral-water interactions.

The measurements of $^{18}\text{O}/^{16}\text{O}$ ratios in igneous rocks and minerals by Taylor and Epstein (1962a, 1962b) were followed soon afterwards by their isotopic investigations of a well-understood example of magmatic crystallization, the Skaergaard intrusion of East Greenland. Pronounced lowering in ^{18}O in later-formed minerals relative to early-formed minerals was found (Taylor and Epstein, 1963). The conclusion of that preliminary study was that the magma had become more depleted in ^{18}O as higher- ^{18}O minerals crystallized and settled to the bottom of the magma chamber without isotopically reequilibrating with the magma. Mineralogical and isotopic evidence indicated that the chilled marginal gabbros had exchanged oxygen with meteoric ground water, resulting in hydrous minerals and lower $^{18}\text{O}/^{16}\text{O}$ ratios near the contact.

Large scale interactions between epizonal plutons and meteoric ground waters were recognized in the tertiary volcanic centers in western Scotland at Skye, Mull and Ardnamurchan (Taylor, 1968; Taylor and Forester, 1971). The $\delta^{18}\text{O}$ values of virtually all of the intrusive rocks at these localities were anomalously low, implying that the rocks had exchanged oxygen with some low- ^{18}O material. The only material low enough in ^{18}O to account for the low $\delta^{18}\text{O}$ values of the rocks was meteoric water. These plutons were situated in country rocks which were highly-jointed plateau lavas.

A more detailed sampling of the Skaergaard intrusion and its country rocks, some of which are jointed plateau basalts, established that the portions of the intrusion adjacent to the more porous basalts had undergone oxygen exchange with meteoric water after solidification of the magma, but at temperatures high enough to preclude pervasive formation of hydrous minerals (Taylor and Forester, 1973; Taylor, 1974). The model which was developed to explain the large-scale interaction between cooling magmas and meteoric water involved the magma as a source of heat to drive local ground water into convection. Some deeply-eroded plutons and country rocks low in ^{18}O are thought to be remnants of fossil hydrothermal systems, some of which were able to concentrate certain minerals in quantities large enough to be economically important. Some additional examples of sites of fossil hydrothermal systems are the Tonopah, Comstock Lode and Goldfield mining districts of Nevada (Taylor, 1973). Other examples are given by Taylor (1974). One section of the present investigation will discuss rock-water interactions in a recently-active volcanic center in New Mexico: an active geothermal system at Valles Caldera. This system is a modern analogue of the fossil systems cited above.

Fluid inclusions have been studied as samples of mineral-forming fluids. Whereas the above-described investigations have deduced the nature and origin of the hydrothermal fluids from isotopic records in minerals, isotopic studies of fluid inclusions have in some cases been used to characterize fluids. Examples of such studies are investigations of Rye and O'Neil (1968) and Landis and Rye (1974).

2. ANALYTICAL PROCEDURES

2.1 Sample Collection

All rock materials studied were provided by the Geothermal Divisions of the Union Oil Company and the Standard Oil Company of California. These samples are in three forms: (1) plugs cut from well core sections from exploration holes, (2) cuttings fragments recovered from holes during the drilling process, (3) rock fragments "blown out" from zones of high fluid pressure as the drill bit penetrated those zones. Chips were simply broken off from the cores and from the blown-out fragments to obtain material for analysis. Cuttings, by far the most common sample type available for this research, presented some unique problems. They consisted of material disaggregated to various degrees, but for the most part were free of drilling mud. Typically in any one cuttings fraction the cuttings grain size is between 1/4 mm and 10 mm. Each sample of cuttings consists of 50 to 100 grams of rock fragments in an envelope marked with the nominal depth of origin. These cuttings had been washed and dried, but some lumps of fragments were found which were still held together with dried mud. Many cuttings fractions contained more than one rock type.

Surface water samples were collected in glass bottles whose caps were fitted with conical polyethylene liners. Such containers have been shown to preserve the isotopic composition of the water for periods of years.

2.2 Estimation of Depths of Origin of Samples

Some reasonably precise knowledge of depth of origin of the samples to be analyzed is important to any isotopic study pertaining to active hydrothermal systems.

The best documented samples are cores. Well drilling and logging in geothermal areas are difficult, and coring is exceedingly expensive. As a result, very few cores are taken during the drilling of any well. Some cores originate from depths "known" within 3 cm, but such samples are rare.

The next-best documented samples are blown-out fragments. The blowing-out action results in little contamination by rocks which originate nearer the surface provided the well is cased down to a level near the blow-out. Consequently the depth of the drill bit at blow-out is recorded as the depth of origin of the blown-out fragments. If the blown-out rock formation is porous, explosive action of steam may be initiated deeper than the level of the drill bit, bringing quantities of deeper rock up to the surface as well.

The depths of origin are known least precisely for cuttings, which are fragments brought up during the drilling of a well. The depth of origin for each cuttings fraction is expressed as a range covering 3 to 20 meters of well section. The depth of origin for cuttings is the depth of the drill bit at the time a cuttings sample was scooped from the mud screen. The "lag time" (time required for rock dis-aggregated at the bottom of the hole to reach the mud screen) is "very short" at The Geysers, according to Courtney Isselhardt, the Union Oil

geologist in charge of the drilling. Thus, the uncertainty of depth of origin imparted by lag time is estimated to be well within the uncertainty described by the range in depth of origin assigned to each cuttings fraction.

A greater probability of contamination by shallower rocks is possible during the recovery of cuttings; however, a knowledge of local stratigraphy and comparisons of cuttings with descriptions of formations in the section allow the elimination of suspected contaminants that are known not to be associated with certain depths.

2.3 Preparations of Samples for Analyses

2.3.1 Sample Selection

All cuttings fractions were examined under a binocular microscope. At least half the material of every cuttings fraction and core fragment was preserved intact for future studies.

Steam-well samples chosen for analysis were hand-picked either from cuttings or disaggregated core material. This procedure was used to obtain both monomineralic and mineralogically complex grains in reasonable quantity of desired purity for analysis. Some muddy fragments had to be rinsed in distilled water and dried before further processing.

Twenty-nine thin sections and six polished grain-mounts were made from samples collected for this study. Many samples of poorly-consolidated material had to be embedded and/or impregnated before sectioning and polishing.

Sufficiently large fragments were found in most cuttings fractions which were representative of the whole rock.

2.3.2 Separation and Purification of Minerals and Rocks

Aside from the removal of residual drilling mud, whole rock samples were used directly, without further processing. Some carbonate-rich rock fragments were soaked in cold 2 N formic acid, prior to extraction of silicate oxygen, to avoid the contribution of carbonate oxygen. Formic acid was used because it is strong enough to decompose carbonates, but not strong enough to attack silicates.

Due to the limited quantity of any one cuttings fraction, only in few cases was there enough material to allow for the preparation of more than one or two pure mineral separates. A technique for the purification of quartz from rocks was developed particularly for Franciscan graywackes, but works well for any rock. This process is gentle, avoids even the etching of the quartz, but removes most other minerals.

The quartz preparation procedure consists of four steps, designed to dissolve feldspar and free even fine-grained quartz from other minerals which may be attached to quartz:

1. The sample is crushed to between 32 and 100 mesh, and is washed in water to remove the very fine dust. It is then soaked in cold 25% hydrofluoric acid solution for not longer than 10 minutes.
2. The resulting muddy suspension, which is due to partially

disintegrated HF-soluble material is decanted and the rock is rinsed free of HF. The sample is then cleaned ultrasonically for 30 seconds.

3. The sample is soaked in hot 2N HCl for 2 hours. The solution usually turns green which indicates that fresh HCl solution should be added. The residue is then rinsed and dried at 100°C.
4. The residue is inspected under the microscope. The residue contains some impurities, including large composite grains containing feldspar that dissolved incompletely, and a few grains of minerals resistant to the treatment, such as epidote and magnetite, and some paper fragments, all of which can easily be picked out of the quartz.

The sequence of steps 1, 2 and 3 were repeated at least twice. Both visual inspection and measurement of oxygen yield are sensitive to non-quartz materials, and both these measurements and x-ray analyses provided the criteria that the quartz resulting from this treatment was 98% pure. Figure 1 shows the effects of the various steps on both oxygen yield and $\delta^{18}\text{O}$. Figure 2 shows x-ray diffraction patterns of powders of Franciscan graywacke before and after the treatment. As a reference an aliquot of rose quartz sample was also subjected to the quartz purification treatment. The sample was not affected in any way by this treatment, as shown by no loss or gain of weight, and by no change in its $^{18}\text{O}/^{16}\text{O}$.

FIGURE 1

Effects of HF and HCl treatments on $\delta^{18}\text{O}$ values and oxygen yields of Franciscan graywacke.

Oxygen yield in $\mu\text{moles/mg}$ is plotted against $\delta^{18}\text{O}$ (SMOW) in ‰ of products of various steps in the procedure to isolate quartz from graywacke. Values of $\delta^{18}\text{O}$ and yield are indicated for whole-rock (wr), and rock after treatment with cold 25% HF, after subsequent treatment with hot 2NHCl, and after further combinations of HF and HCl treatments. Points marked "Q" are pure quartz, as indicated by visual inspection, x-ray analysis, and by their yields, with values near 16.67 $\mu\text{moles/mg}$.

EFFECTS OF HF AND HCl
TREATMENTS ON $\delta^{18}\text{O}$ VALUES
AND OXYGEN YIELDS
OF FRANCISCAN GRAYWACKE

YIELD
 $\mu\text{moles/mg}$

wr: whole rock

Q: quartz isolated from rock

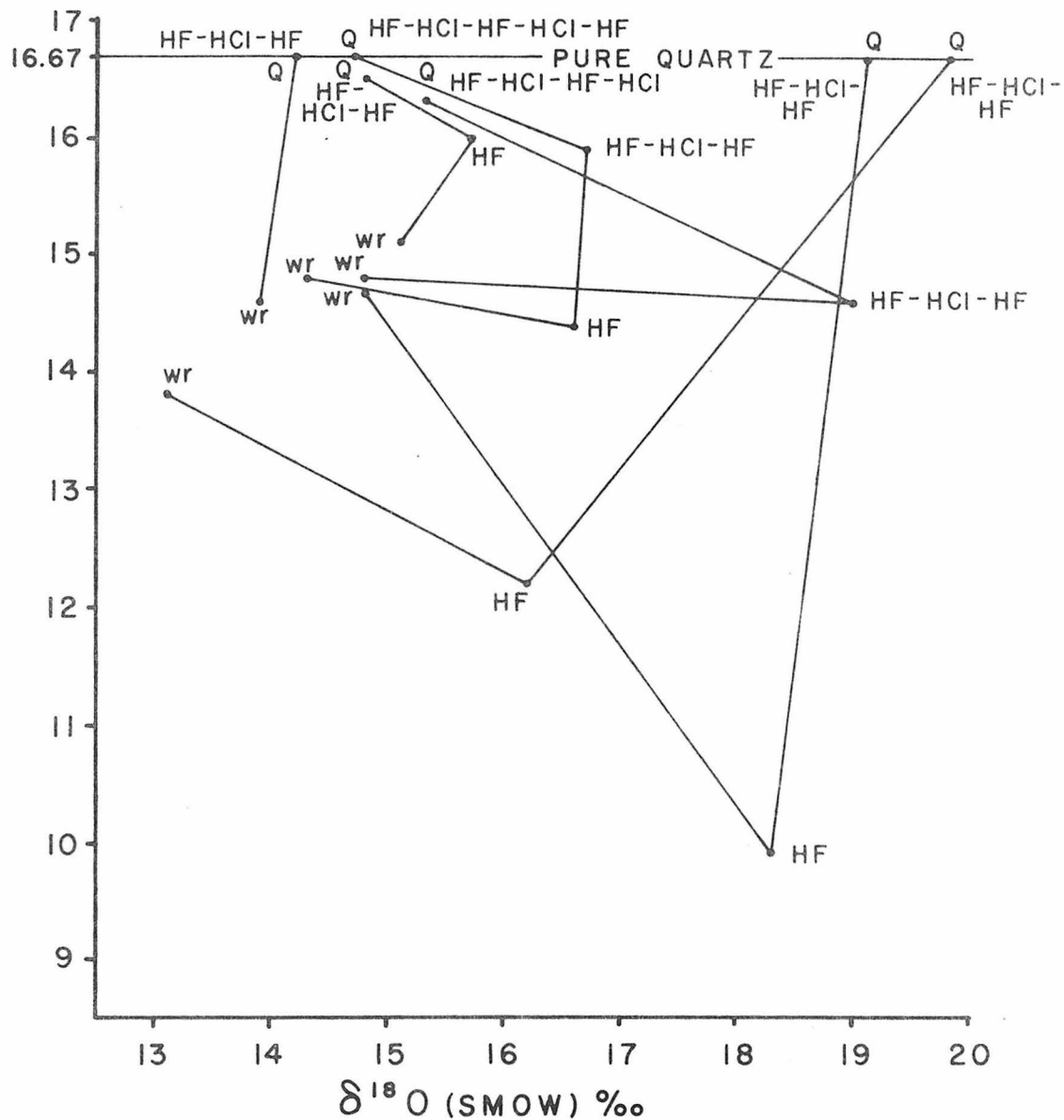


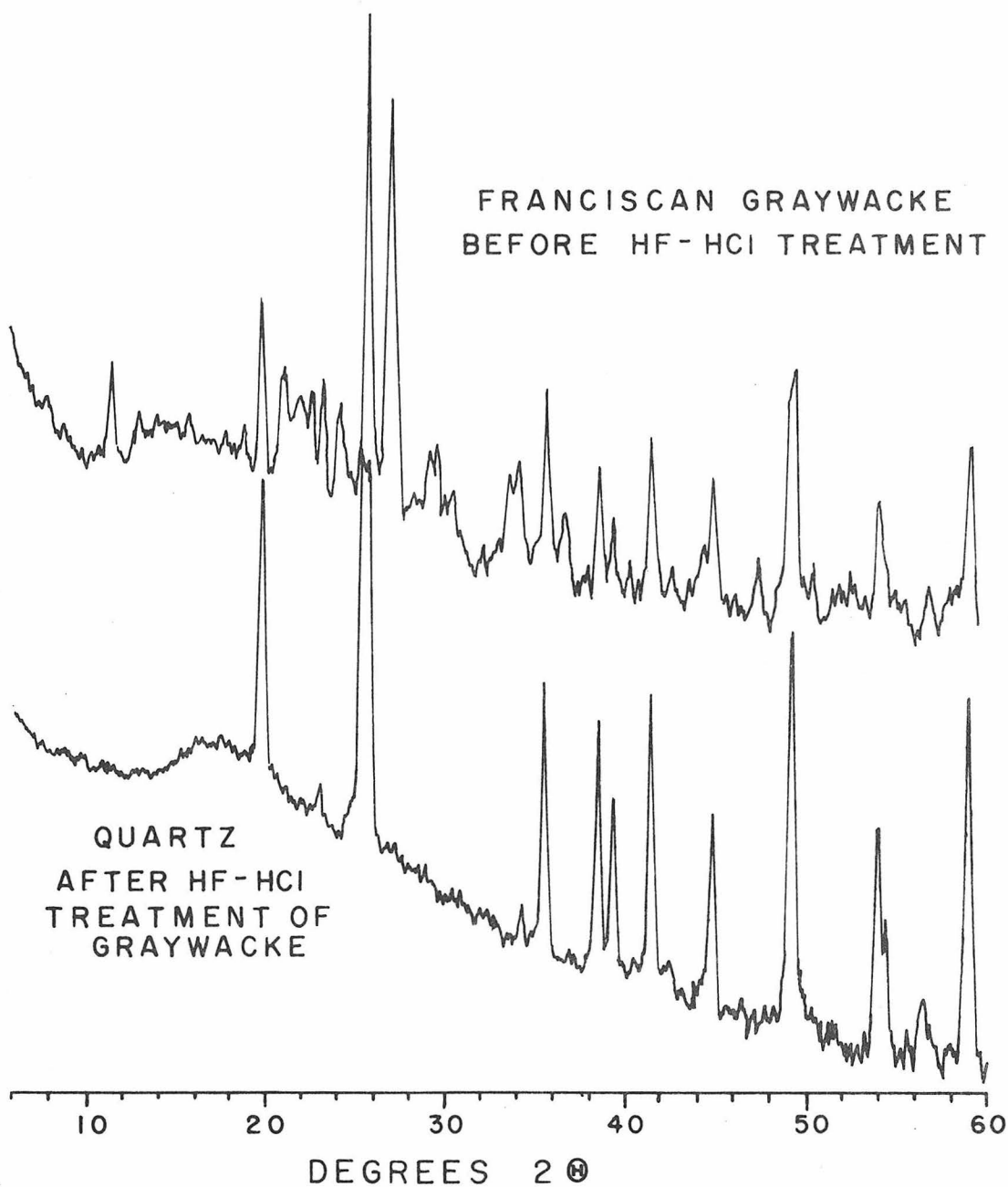
FIGURE 2

X-ray powder diffractograms of Franciscan graywacke before and after treatment with HF and HCl.

These analyses were made with $\text{CuK}\alpha$ radiation, and the traces were recorded using a logarithmic ratemeter response. The upper trace is the diffractogram of untreated graywacke and consists of diffraction peaks characteristic of quartz, plagioclase, chlorite and muscovite. The lower trace was obtained for an aliquot of the same rock sample, which had been subjected to two cycles of the cold 25% HF and hot 2N HCl treatments. The only diffraction peaks remaining in the lower trace are those of quartz. Note that the principal feldspar peak, to the right of the second quartz peak from the left, has been eliminated, as has the chlorite peak at about $11^\circ 2\theta$.

X-RAY POWDER DIFFRACTOGRAMS
OF FRANCISCAN GRAYWACKE
BEFORE AND AFTER TREATMENT
WITH HF AND HCl

Cu K α Radiation Log Intensity Scale



Actinolite, hornblende and antigorite were isolated successfully by a combination of gravimetric (using tetrabromoethane) and magnetic techniques for only one sample, LF 19-45. The other cuttings fractions contained fine-grained intimately-intergrown composite grains. Some fractions contained high percentages of high-purity antigorite that could be easily hand-picked.

Chlorite could be separated from graywackes only if the graywacke initially contained more than 30% chlorite. The technique was based on differential settling rates in water, and final purification was done magnetically. Purity of minerals was always checked by x-ray diffraction. The purity of mineral separates prepared by gravimetric and magnetic means is not better than about 95%.

2.3.3 Preparation of Gas for Isotopic Analysis

Gas for mass spectrometry was extracted from samples by standard methods. Procedures followed for various substances will be briefly reviewed.

2.3.3.1 Carbonates

CO₂ was liberated from carbonate-bearing materials with 100% H₃PO₄ (McCrea, 1950). In some cases up to 200 mg of crushed rock was required in order to obtain convenient ($\geq 30 \mu$ moles) amounts of CO₂ from carbonate-poor rocks.

2.3.3.2 Waters

Water was analyzed for oxygen by the equilibration of CO₂ with H₂O at 25.4°C (Epstein and Mayeda, 1953).

2.3.3.3 D/H Analyses

Water was extracted from hydrous rocks and minerals in a procedure like that of Friedman and Smith (1958) and Godfrey (1962). A powdered sample was heated in a platinum crucible with an induction furnace. For small samples, likely to yield less than about 75 μ moles, the necessary precautions were taken in order to minimize contamination by atmospheric water adsorbed on the sample powder, the platinum crucible, and the inner walls of the glass pyrolysis vessel. These precautions included preheating under vacuum the platinum crucible to a temperature higher than that achieved during the extraction of water, and loading the sample in a drybox (Epstein and Taylor, 1970). For large samples, such precautions were unnecessary, and the samples were loaded in air. Care was taken that no plasma-discharge was initiated by the high-frequency induction furnace, since this profoundly affects the D/H ratio of the gas.

Hydrogen was extracted from water by passing the water over hot uranium (Bigeleisen, Perlman and Prosser, 1952).

2.3.3.4 Extraction of Oxygen from Silicates

Silicate rock and mineral samples were reacted with F_2 gas in nickel vessels at 480°C in order to liberate oxygen (Taylor and Epstein, 1962a). The reaction vessels were loaded in a drybox after the samples and vessels had been allowed to dry for at least 20 hours, so as to minimize contamination by atmospheric water. Conversion of oxygen to carbon dioxide was carried out quantitatively with hot spectrographic-grade graphite, at temperatures low enough to preclude

the formation of carbon monoxide.

One out of every six samples fluorinated was an aliquot of rose quartz from the Ramona pegmatite, California (abbreviated RRQ), whose $^{18}\text{O}/^{16}\text{O}$ is known. The frequent analysis of this working reference helps to minimize effects of systematic errors in the extraction procedure and secular variations in the mass spectrometer system.

2.4 Measurements

Analyses of CO_2 for carbon and oxygen isotopes and H_2 for hydrogen isotopes were done on 60-degree sector, single focus, double-collecting, dual gas-fed mass spectrometers of the type described by Nier (1947), with modifications by McKinney, McCrea, Epstein, Allen and Urey (1950). Corrections and conversions performed on mass spectrometric numerical results are discussed in Appendix III. Measurements are reported in the usual " δ " notation, in parts per thousand ("per mille")

$$\delta_x \text{ (in } \text{‰}) = \frac{R_x - R_{\text{std}}}{R_{\text{std}}} \times 1000$$

in which $R = ^{18}\text{O}/^{16}\text{O}$, D/H or $^{13}\text{C}/^{12}\text{C}$. For oxygen and hydrogen "std" is Standard Mean Ocean Water (SMOW), as defined by Epstein and Mayeda (1953) and Craig (1961b). The standard for carbon is the Chicago Peedee Belemnite (Craig, 1957). The difference between two δ values, $\Delta_{\text{AB}} = \delta_{\text{A}} - \delta_{\text{B}}$. The fractionation factor, α_{AB} between A and B rigorously defined as $\frac{R_{\text{A}}}{R_{\text{B}}}$, can be approximated

$$\alpha_{\text{AB}} \cong 1 + \frac{\Delta_{\text{AB}}}{1000}$$

within 0.2 ‰ if $\Delta_{\text{AB}} \leq 20 \text{ ‰}$.

2.5 Analytical precision

Since the reproducibility of mass spectrometric measurements is $\pm 1 \text{ ‰}$ for hydrogen, the greatest source of error is in the extraction and/or preparation. Reproducibility in carbonate analyses for both carbon and oxygen is ± 0.2 to 0.25 ‰ .

2.6 Tests of Reproducibility of Silicate $\delta^{18}\text{O}$ Values

It is noteworthy to consider the apparent variation in Ramona Rose Quartz (RRQ) $\delta^{18}\text{O}$ values, as measured against the mass spectrometer reference sample. During the course of this work, the reference sample was a quantity of CO_2 prepared from a sample of Iceland spar found 100 yards south of Harding Pegmatite, Taos County, New Mexico.

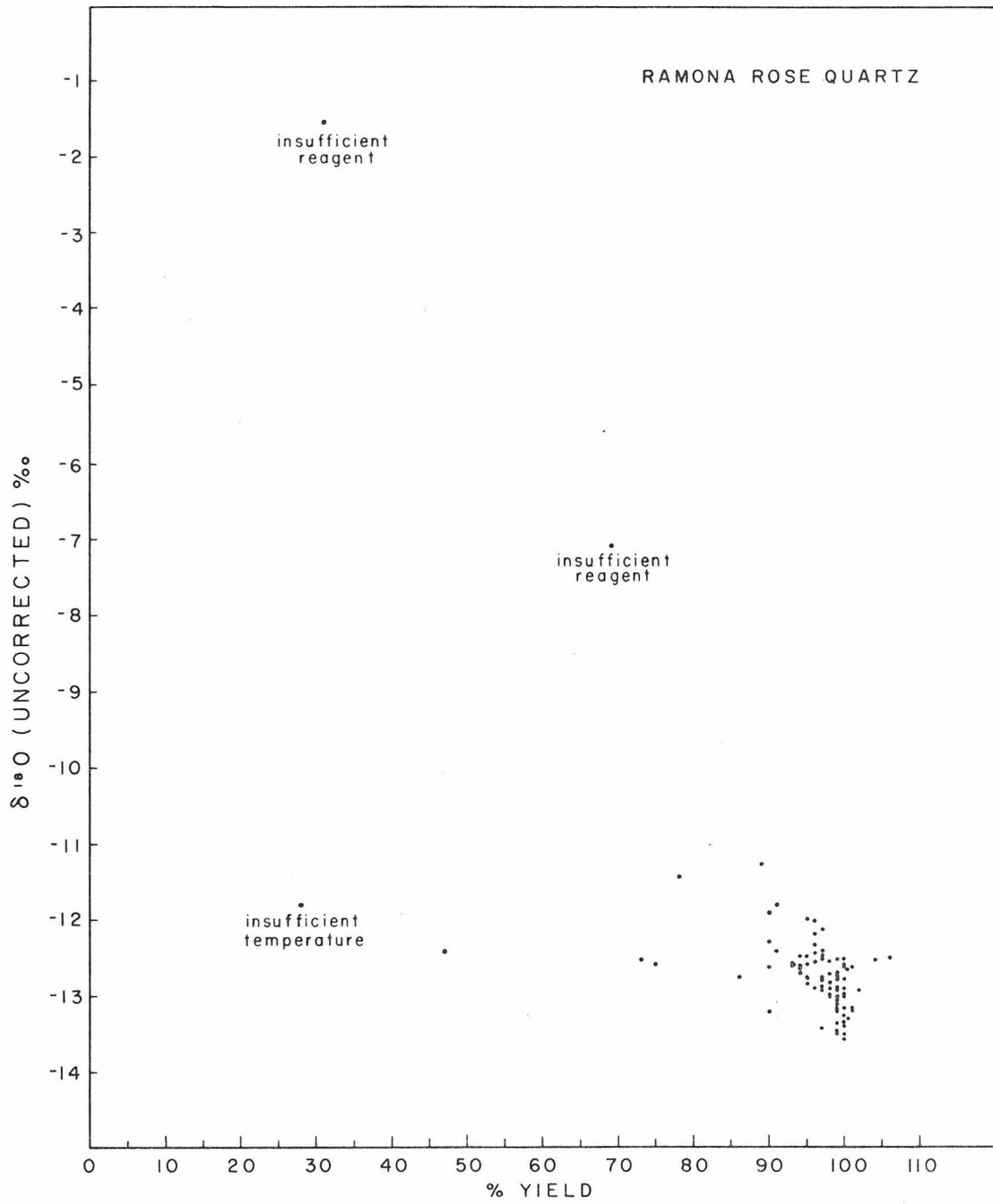
Figure 3 shows 98 $\delta^{18}\text{O}$ values of RRQ (with respect to Harding Iceland Spar) versus yield in percent. For those analyses which did not produce 100% yield, there is a variation of 12 ‰ .

The two numbers -1.5 ‰ and -7 ‰ , and many others greater than about -12.5 ‰ , illustrate the effect of insufficient fluorination. The two high $\delta^{18}\text{O}$ values resulted when stainless steel ferrules from Swagelok fittings were introduced into nickel vessels along with rose quartz. The fluorine reacted with the stainless steel at 480°C , leaving a large portion of RRQ untouched. The oxygen recovered had a $\delta^{18}\text{O}$ higher than that measured on 100% yields. In the first several analyses of RRQ in each nickel vessel, yields as low as 78% (without the ferrules) gave $\delta^{18}\text{O}$ values as much as 1.5 ‰ higher than 100% yields. The structure of the reaction vessel assembly was such that a stainless

FIGURE 3

$\delta^{18}\text{O}$ values (relative to Harding Iceland Spar working reference) from 98 analyses of an aliquot of Ramona Rose Quartz, plotted against % yield.

Yields greater than 97% resulted in the most reproducible $\delta^{18}\text{O}$ values. The effect of insufficient amounts of fluorine on both $\delta^{18}\text{O}$ and yield is illustrated, and the $\delta^{18}\text{O}$ value is much less sensitive to the lowering of the reaction temperature by 100°C (the point marked "insufficient temperature") than it is to amounts of reagent insufficient to completely liberate all of the silicate oxygen (the points marked "insufficient reagent"). The data were gathered over two years' time.



steel fitting was exposed to heated fluorine. Thus, the incomplete yields and the abnormally high $\delta^{18}\text{O}$ values are attributable to incomplete reaction due to the fact that some of the fluorine reacted with the stainless steel instead of the quartz. After several analyses the stainless steel apparently had built up a fluoride armor coating that inhibited any further reaction of stainless with fluorine. The above experiments illustrate the undesirability of stainless steel in any part of the reaction vessel. These results also emphasize the importance of pre-fluorinating all stainless steel parts thoroughly before analyses begin in earnest.

The effect of lowering the reaction temperature to 380°C is illustrated by the point labeled "insufficient temperature" in Figure 3. The effect of a 30% yield on the $\delta^{18}\text{O}$ values due to insufficient temperature is much less detrimental than that of a 30% yield due to insufficient reagent.

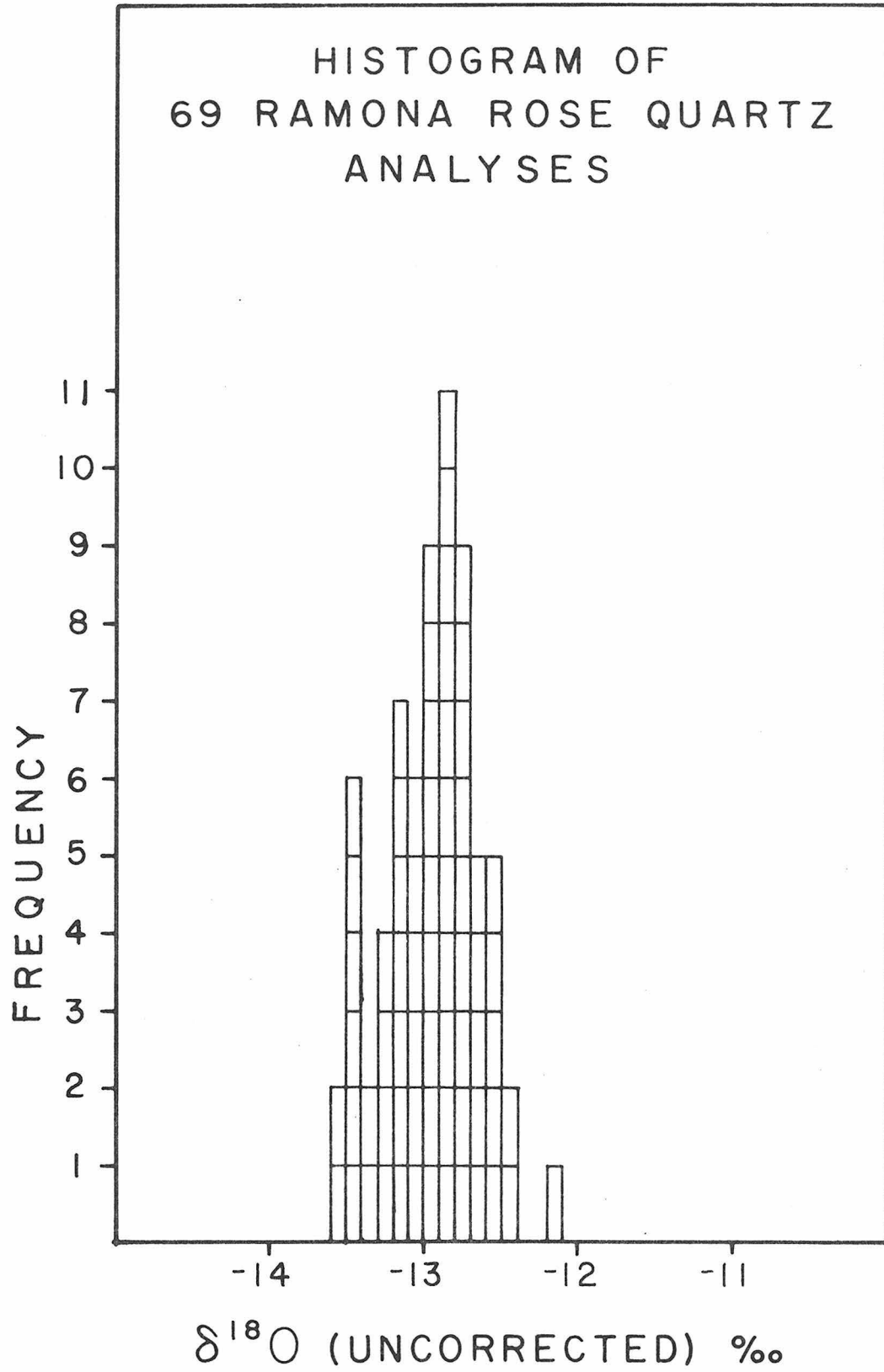
In general, the reproducibility of $\delta^{18}\text{O}$ values of RRQ, at least, does not seem to be seriously hampered when yields are as low as 97%. The apparent variations in $\delta^{18}\text{O}$ values of RRQ when the yield is 97% or more are illustrated more clearly in Figure 4 which is a histogram of RRQ $\delta^{18}\text{O}$ values from extractions which proceeded without mishap.

The apparent variation in $\delta^{18}\text{O}$ of RRQ measured against Harding Iceland Spar is probably due to a number of factors, but is chiefly due to (1) variations induced by systematic errors in the extraction procedure; (2) small variations in the $^{18}\text{O}/^{16}\text{O}$ ratio of Harding Iceland Spar, introduced in the preparation of CO_2 . Systematic errors in

FIGURE 4

Histogram of $\delta^{18}\text{O}$ values of 69 Ramona Rose Quartz analyses.

The number of times $\delta^{18}\text{O}$ values of Ramona Rose Quartz relative to Harding Iceland Spar working reference is given for 0.1‰ intervals of $\delta^{18}\text{O}$. Data were collected in a two-year interval. Those reported in the figure had oxygen yields of 97% or greater. Intervals lie between 0.00 and 0.09‰ below the nearest 0.1‰, for example, -13.30 to -13.39‰. Frequency maxima, such as -12.80 to -12.89, -13.10 to -13.19, and -13.40 to -13.49‰ probably represent different $^{18}\text{O}/^{16}\text{O}$ ratios in different aliquots of the Iceland Spar reference CO_2 , several of which were consumed during the two years covered by the study. The width of each "peak" may represent the precision of the fluorination technique, which is at worst 0.25‰.



the extraction might include residual amounts of water vapor which might have entered the reaction vessels, "memory" effects in the extraction system, and barely-perceptible leaks or outgassing in the extraction system. Variations in the $^{18}\text{O}/^{16}\text{O}$ ratio of the mass spectrometer working standard can result from incomplete reproducibility of one batch with respect to another (the working standard must be replenished periodically). A third factor which can contribute a random error in the $\delta^{18}\text{O}$ measurements is the incompletely-reproducible technique used by the analyst who operates the mass spectrometer.

In Figure 4, there are three distinct frequency maxima: -12.6 to -12.8 ‰, -13.1 to -13.2 ‰, -13.4 to -13.5 ‰. There is even a hint of a fourth maximum at -12.5 to -12.7 ‰. Each peak has associated with it a distribution which is suggestive of a Gaussian, but each peak is separated by 0.2 ‰. Each "peak" has a width of 0.3 ‰, corresponding to an uncertainty of ± 0.15 ‰. The peak width corresponds to the uncertainty in the extraction procedure. Each peak probably reflects a different $^{18}\text{O}/^{16}\text{O}$ ratio of the reference CO_2 sample. The total variation illustrated in the histogram of Figure 4 took place over a period of two years, during which time 6 to 7 different batches of CO_2 prepared from Harding Iceland Spar were used as working standards. Each batch is routinely measured against a secondary standard, whose $\delta^{18}\text{O}$ value with respect to PDB is known, so that carbonate $\delta^{18}\text{O}$ values versus reference sample can be converted to the PDB standard. The reproducibility of silicate $\delta^{18}\text{O}$ values with respect to SMOW, however, was not adversely affected.

3. STUDIES AT THE GEYSERS, SONOMA COUNTY, CALIFORNIA

3.1 History of Development

Thermal activity in the western part of the Mayacmas Mountains was first discovered in 1847 about 150 kilometers north of San Francisco (McNitt, 1963). In the next 50 years, the area became the site of a nationally-known health spa. The place was called "The Geysers," because steam spouting from enthusiastic fumaroles reminded the early exploiters of similar phenomena in Iceland. "The Geysers" is an unfortunate misnomer, for no true geysers occur there. The name properly refers to the area covered by sections 13 and 14, T. 11 N., R. 9 W. (with respect to Mount Diablo) in Sonoma County, California on the U. S. Geological Survey topographic map, The Geysers quadrangle, 7.5 minute series. The area of greatest fumarolic activity is on the north side of Big Sulphur Creek (in the early days called "Pluton Creek") in what was named Geyser Canyon (Figures 5 and 6). Fanciful names were given to more spectacular features in The Geysers area, such as Steamboat Spring, Witches' Cauldron, Devil's Teakettle, etc. (none were as spectacular as Yellowstone features, not yet explored at that time).

In 1921 a resident of Healdsburg, J. D. Grant, formed a company and drilled a well on the east side of Geyser Canyon. The plan was to use the steam to generate electricity, which has been done at Larderello, Italy, since 1904. The newly formed "Geysers Development Company" had as one of its investors Luther Burbank of Santa Rosa, the noted horticulturalist. In 1925 the drilling continued under the auspices of the Diamond Drill Contracting Company, which completed 8 wells and a number

FIGURE 5

Map showing The Geysers and vicinity, Mayacmas Mountains, California.

Information was taken from geologic maps of the Kelseyville 15' quadrangle (McNitt, 1968) and the Lower Lake 15' quadrangle (Brice, 1953). Prominent landmarks are shown, such as Geyser Peak, Big Sulphur Creek, and the peaks formed from the extrusive Clear Lake volcanics: Cobb Mountain, Boggs Mountain, Seigler Mountain and Mount Hannah. Fumarolic areas are indicated at Sulphur Banks, The Geysers, The Little Geysers, Castle Rock Springs and Anderson Springs, showing their geographic relationships to the volcanics. The rectangular area enclosing The Geysers and Burned Mountain is magnified in Figure 6.

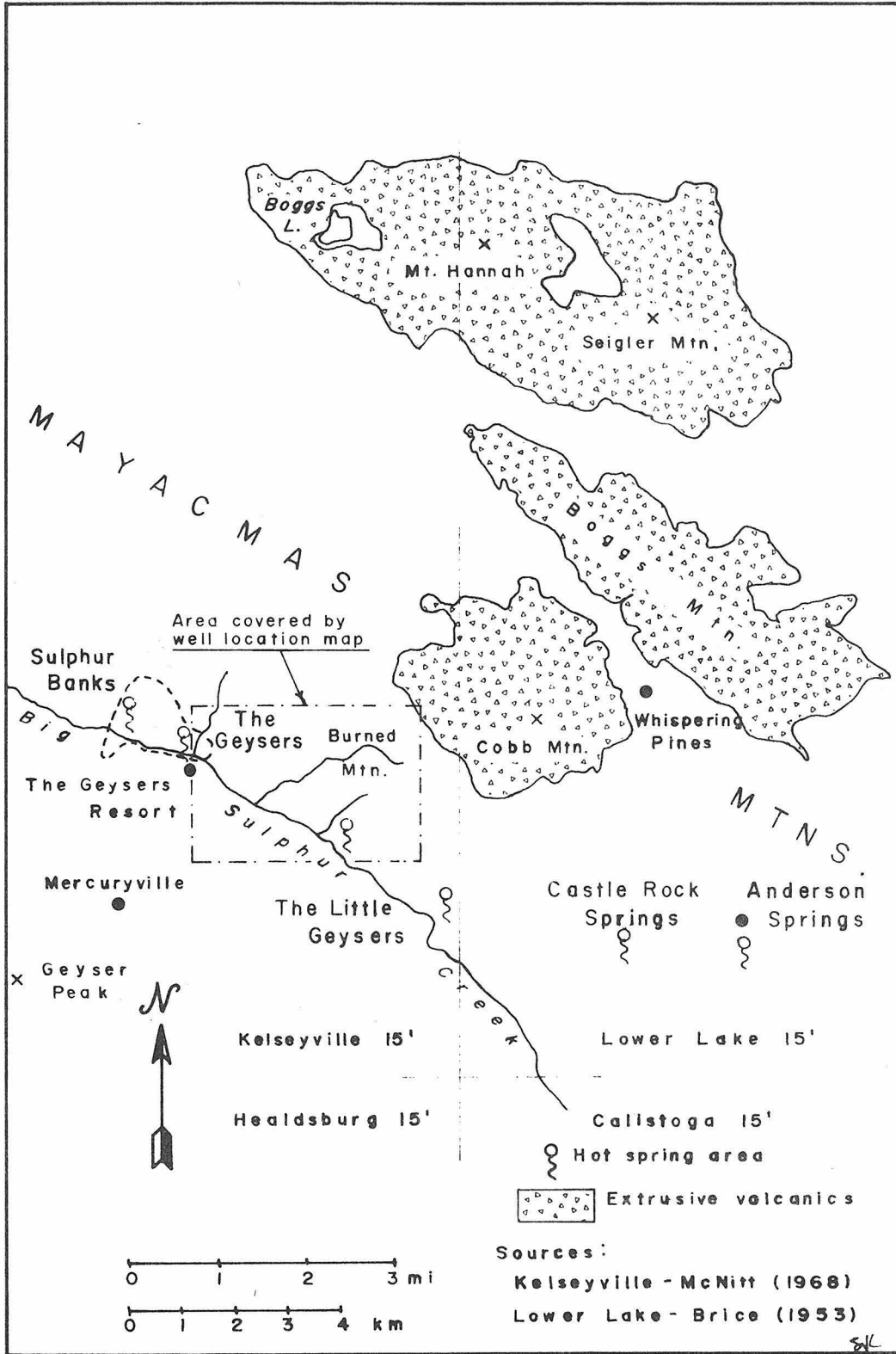
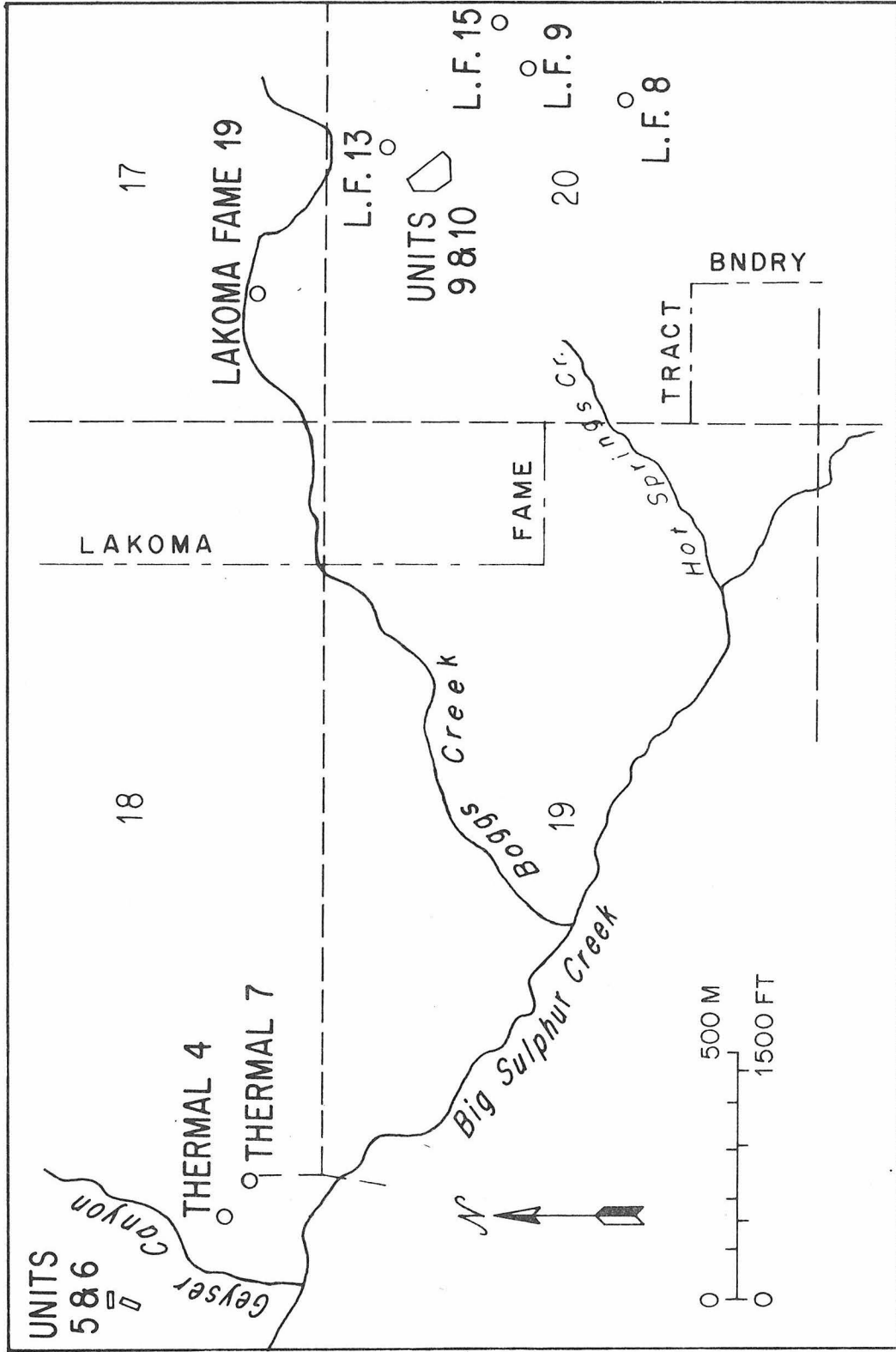


FIGURE 6

Location map of wells at The Geysers whose samples were studied.

This figure is a more detailed map of the area outlined by the small rectangle in Figure 5. Electrical generating facilities in the earliest-exploited part of The Geysers (near Geysers Canyon) are represented by Units 5 and 6. Steam is escaping uncontrollably from Thermal No. 4, shown for reference. The most thoroughly-studied samples came from wells from the Lakoma Fame Tract, which covers most of sections 17 and 20, and whose western boundary is shown, as well as the recently-built power plant, Units 9 and 10.



of tests that year. There was found to be no market for the superheated steam. Allen and Day made a number of studies of the steam and its reservoir and published their findings in 1927. Unfortunately, all this drilling put an end to the fumarolic activity of those fancifully-named scenic features.

Thirty years later, Magma and Thermal Power Companies took a 99-year lease on the hot-spring area north of Big Sulphur Creek, mostly private land. Pacific Gas and Electric contracted to build a steam-electric power plant. As of 1961, 14 wells had been drilled (in addition to those of 1921 to 1925) and the power capacity was 28,000 kw (McNitt, 1963). The greatest depth of drilling was 640 meters, and the highest measured temperature was 300°C.

The region has been the site of mercury mining activity for almost as long as it has been the site of a health resort. Fumarolic activity and mineralization in a linear northwest-southeast trend passing through The Geysers inspired exploratory drilling along that trend. These developments to the northwest are at Sulphur Banks (not to be confused with the Sulphur Bank mercury mining district north of Clear Lake), and those to the southeast are at the Little Geysers, Castle and Anderson Springs (Figure 5). These explorations on federal, state and private lands have resulted in leases by the Union Oil Company of California, Signal Oil and Gas Company, Geothermal Resources International, and others (Otte and Dondanville, 1968). Today, there are 92 wells at The Geysers (exclusive of exploratory and dry holes). The average depth is 1.5 km, and the total cost as of 1972 was $\$23 \times 10^6$. The power output

capability of the facilities is almost 500 megawatts (Garrison, 1972).

3.2 The Geysers as a Vapor-Dominated Hydrothermal System

A vapor-dominated hydrothermal system (White, Muffler and Truesdell, 1971) is characterized by host rocks of low initial permeability, surface manifestations producing low fluid discharge, surface and subsurface thermal waters of low (<20 ppm) chloride content and dry or slightly superheated steam. Additionally some low-chloride waters may contain considerable amounts of sulfate resulting from the atmospheric oxidation of H_2S , a common volatile constituent of the steam. The fluid may also be rich in CO_2 .

The western part of the Mayacmas Mountains is dominated by graywacke interbedded with shale and conglomerate, spilitic basalts (commonly called "greenstones"), serpentinites and amphibole-rich metamorphic rocks, thus presenting host rocks of low initial permeability (McNitt, 1968). Steam is conducted through the graywacke by series of dipping fracture systems, which in many places account for the total permeability of the system (McNitt, 1963; C. Isselhardt, private communication). During the summer of 1925, before the onset of extensive drilling, the total hot-spring discharge rates along Geyser Creek (the area of largest concentration of surface thermal features in the vicinity) were between 100 and 200 liters per minute (Allen and Day, 1927). The water analyses, reproduced in Table 1, indicate that two waters from The Geysers contain 0.5 and 1.5 ppm chloride and 766 and 5710 ppm sulfate.

It has long been recognized that dry steam, in abundance at The

TABLE 1

CHEMICAL ANALYSES (PPM) OF SPRING WATER AT THE GEYSERS

	Witches' Cauldron bicarbonate-sulfate water	Devil's Kitchen acid-sulfate water
SiO ₂	66	225
Al		14
Fe		63
Mn		1.4
Ca	58	47
Mg	108	281
Na	18	12
K	6	5
NH ₄	111	1400
H		9.5
HCO ₃	176	0
CO ₃	-	-
SO ₄	766	5710
Cl	1.5	0.5
B	15	3.1
H ₂ S	0	-
total reported	1330	7770
pH	neutral	1.8±
T°C	100	Boiling?

from White et al. (1963) as cited in
 White et al. (1971) modified from
 Allen and Day (1927).

Geysers, is suitable for the generation of electrical power, as indicated by the extensive utilization of this resource by Magma, Thermal and Union Oil. The Geysers thus represents a unique opportunity for the study of a vapor-dominated hydrothermal system because it is a commercially-important dry-steam field.

3.3 Geological Overview

The Geysers area is included in the Kelseyville 15 minute geologic map sheet (McNitt, 1968). The most widespread rocks are the Mesozoic Franciscan and Great Valley Groups. Serpentinites occur in association with the Franciscan Group. Swe and Dickinson (1970) showed that rocks in the Clear Lake region, similar to those at The Geysers, were Franciscan, although these same rocks are called "upper unit, Jurassic-Cretaceous" by McNitt (1968). The Pliocene to Pleistocene Clear Lake Volcanic Series also abound in the area (Figure 5).

The geologic history of the Clear Lake region has been summarized by Garrison (1972), who used the nomenclature and descriptions of Franciscan and related rocks, which were discussed by Bailey et al., 1964. Detailed mapping was done by McNitt (1968) and by Swe and Dickinson (1970). The latter work was concerned primarily with sedimentation and tectonics in the Clear Lake area, northeast of The Geysers.

Prominent landforms in the area are expressions of volcanism responsible for the Clear Lake Series: Mt. Konocti (dacite), Mt. Hannah, Seigler Mountain (dacite and andesite), Boggs Mountain (andesite) and Cobb Mountain (rhyolite and rhyolite tuff). Koenig (1969) gives previously unpublished radiometric ages of 3,000,000 to 50,000

years for the Clear Lake volcanics. Tuff and basalt intercalated with the Cache Formation indicated that the volcanics are at least as old as early Pleistocene, the age of fossil diatoms in the Cache (Brice, 1953).

The volcanics in the active thermal area are only surficial and are not the steam-reservoir rocks. Most of the volcanics are northeast of the thermal area. It is generally recognized that a cooling magma chamber is nearby and is the heat source. There is a large circular Bouguer gravity anomaly of about -50 milligals centered underneath Mt. Hannah. An arcuate fault pattern around Mt. Hannah is interpreted as an indication of volcano-tectonic uplift associated with the emplacement of this magma (Garrison, 1972).

Prevolcanic structure is dominated by a fossil Benioff zone. The Soda Creek Thrust, northeast of the Mayacmas Mountains, is the lowest member of a series of imbricate thrusts. The Soda Creek Thrust, not serpentinite bodies (as in other areas where both Franciscan and Great Valley rocks occur) separates the Franciscan from the overthrust Great Valley Group. The Clear Lake region is seismically active (Garrison, 1972).

3.4 The Rocks and Minerals

3.4.1 The Franciscan Group in General

The reservoir at the Mayacmas Mountains steam field is mostly what McNitt calls the "lower unit, Jurassic-Cretaceous" (part of the Franciscan Group, by later work). In the Clear Lake area to the north the unit has been dated as late Jurassic, no older than Tithonian (Swe and Dickinson, 1970). The minimum thickness computed from structural

cross-sections is about 4000 meters. Individual rock type descriptions follow those of McNitt (1968).

3.4.2 Graywacke

The graywackes are massive, well-indurated gray to greenish-gray sandstones with about 40% fine-grained matrix. Cataclastic texture is developed locally. The rock contains ubiquitous quartz veins, but calcite veins occur only in association with some sort of hydrothermal alteration. Clastic constituents include quartz, plagioclase, and fragments of chert, schists, volcanics and carbonaceous material. Feldspar accounts for less than 30% of the clastics.

3.4.3 Basalt

Gray to greenish-gray spilitic meta-basalt is called "greenstone" in this area. The aggregate thickness is as much as 2100 meters, distributed throughout the section as flows less than 100 meters thick. Amygdaloidal texture is common. The rock is porphyritic, with euhedral crystals of plagioclase and augite in a fine-grained groundmass of plagioclase laths, chlorite and magnetite.

3.4.4 Serpentinite

Concordant masses of serpentinite, up to several hundred meters thick, occur commonly with the Franciscan. It is mostly a sheared mesh-structure antigorite, with traces of opaques (similar to sheared serpentinite described by Bailey et al., 1964). There is no relict diopside, and the bodies are probably dunite derivatives. The serpentinite contains chlorite and pyrite in the steam zone.

3.4.5 Chert ("Red Rock")

Red, thinly-bedded, fine-grained aggregates of hematite and quartz, which are commonly veined with quartz, occur sporadically in the cuttings. They are inferred to be a derivative of red chert.

3.4.6 Metamorphic rocks

"Metamorphic rocks" occur in thin bands adjacent to serpentinite bodies. They are blue-green hornblende albite schist, as encountered in the well cuttings. They are chloritized, and contain sericite. Calcite veins up to 2 cm across were found in this rock type in the steam zone.

Individual rock types will be illustrated and discussed as they occur in specific environments of hydrothermal alteration.

3.5 The Wells

A location map of wells discussed in this part of the study is in Figure 6. Historically, the west part of the area (near Geyser Canyon) was the first to be drilled. It contains the group of wells belonging to Magma and Thermal Power Companies who drilled the wells between 1955 and 1961. Steam is escaping uncontrollably from Thermal Well No. 4. All efforts to seal it since 1957 have failed. A lesser-known area, the Lakoma Fame tract of private land, is located 2 km east of Geyser Canyon (Figure 5) at the heads of Cobb and Hot Springs Creeks. The tract is now leased by the Union Oil Company of California. Lakoma Fame (abbreviated "LF") wells were drilled between 1969 and 1972.

3.6 Thermal No. 7

3.6.1 General Statements

Only two well-documented core fragments from Thermal 7 were available: T7-450 (137 meters depth) and T7-636 (194 meters depth). These two samples were significant in this study because they come from a well drilled near the center of the most intense fumarolic activity at The Geysers.

Both of the core fragments are dense graywacke, containing veins of calcite, quartz and traces of muscovite, all of which are cogenetic according to their textural relationships (Plate 1). The calcite in the veining is well developed in T7-450, but poorly developed in T7-636 (Plate 2). In addition, the graywacke itself is highly silicified. In 1960, temperatures were measured at various depths in 8 wells, including Thermal 7, by Magma and Thermal Power Companies.

In Thermal 7 temperatures were measured as a function of depth after the well had been sealed at the well head for two months, longer than for any of the other seven wells. Since drilling a hole in steam-producing rocks lowers the rock temperature in the immediate vicinity of the hole, a long sealed-off period should allow the pre-drilling temperatures to be approached more closely than if the sealed-off period were short. Complete reestablishment of original rock temperatures is probably never obtained.

The directly-measured temperature-depth profile of Thermal 7 is given in Figure 7. The profile is characterized by a constant temperature of 180°C in the upper 130 meters, below which the temperature

PLATE 1.

Hydrothermally-altered graywacke with veins, Thermal No. 7, The Geysers.
137 meters depth, steam zone.

Area of view: 1.6 × 1.2 mm. X-nicols.

Silicified fine-grained graywacke (dark areas) of Franciscan Group
containing intersecting veins of cogenetic quartz (white), calcite
(mottled gray) and muscovite (tabular laths).

PLATE 2.

Hydrothermally-altered graywacke with quartz vein, Thermal No. 7, The
Geysers. 194 meters depth, steam zone.

Area of view: 1.6 × 1.2 mm. X-nicols.

Silicified graywacke of Franciscan Group, with 0.5 mm wide quartz vein,
in center of view. Note finer-grained quartz at vein margin than in
center.

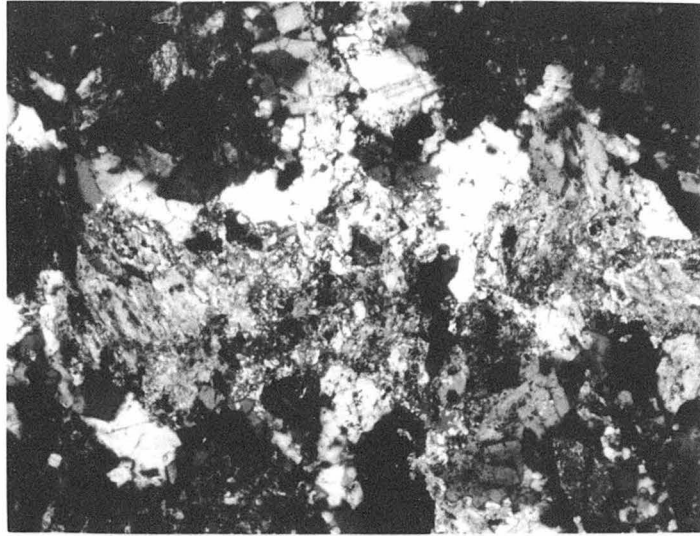


PLATE 1

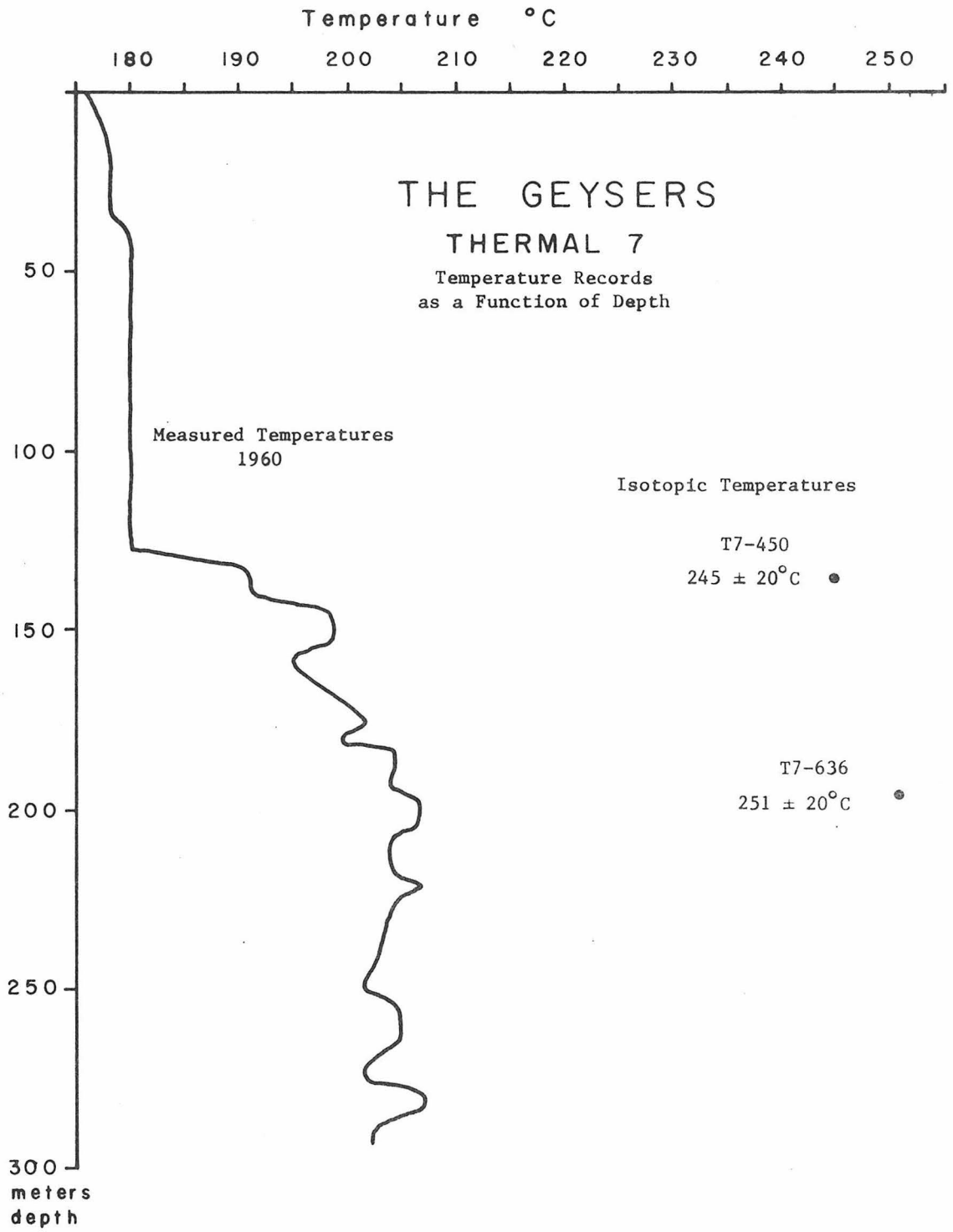


PLATE 2

FIGURE 7

Temperature records at various depths in Thermal Well No. 7, The Geysers.

The rock temperature profile in the left part of the diagram was determined by thermocouple measurements made in 1960 after the well had been sealed for two months (McNitt, 1963). Oxygen isotope temperatures obtained from cogenetic vein quartz and calcite from two Thermal 7 core fragments appear at the right. The isotopically-determined temperatures are about 50° higher than logged rock temperatures, indicating that the temperatures in Thermal 7 between 130 and 200 meters depth may have at one time been higher than those presently observed.



increases to about 210°C at 200 meters depth (profile taken from McNitt, 1963).

3.6.2 Isotopic Temperatures from Thermal 7

Table 2 contains descriptions of samples from Thermal 7 (abbreviated T7), depths of origin, and the isotopic compositions for some of the samples. The isotopic data allow for the calculation of two isotopic temperatures of formation of the vein minerals in the T7 samples. Even aside from such calculations of temperature that might be made, the apparent coexistence of calcite and quartz and muscovite indicates that low temperatures, less than about 400°C, prevailed during the formation of these minerals. At higher temperatures, under low pressures, products of decarbonation of calcite and dehydration of muscovite would form. Specifically, the calcite and quartz might combine to form wollastonite or other calcium silicates, and the muscovite might decompose to form andalusite.

An isotopic equilibrium temperature was calculated using the $\delta^{18}\text{O}$ values of quartz and calcite from T7-450 and the quartz-calcite temperature-dependent oxygen isotope fractionation:

$$1000 \ln \alpha_{\text{QC}} = 0.60 (10^6 T^{-2}) \quad (\text{G-1})$$

Equation (G-1) results from a combination of the quartz-water fractionation between 200°C and 500°C:

$$1000 \ln \alpha_{\text{QW}} = 3.38 (10^6 T^{-2}) - 3.40 \quad (\text{G-2})$$

(Clayton, O'Neil and Mayeda, 1972) and the calcite-water fractionation:

TABLE 2

DESCRIPTIONS AND ISOTOPIC ANALYSES OF MINERALS
FROM THERMAL NO. 7, THE GEYSERS

See "General Remarks", Table 3

<u>Well and Number</u>	<u>Depth, meters</u>	<u>Sample Description</u>	$\delta^{18}\text{O}$ ‰	$\delta^{13}\text{C}$ ‰	δD ‰	<u>Remarks</u>
T7 - 450	137	calcite, vein	+ 9.65	-12.27		} 9.74 ± 0.12
		calcite, vein	+ 9.82	-11.83		
		quartz, vein	+12.06			} cleaned with HF 11.94 ± 0.12
		quartz, vein	+11.93			
		quartz, vein	+11.82			
		graywacke, altered	+ 9.67		-59.4	
		unaltered Franciscan graywacke	+13 to +15		-30 to -60	See Table 3
I7 - 636	194	quartz, from rock	+12.00			HF-HCl treated
		quartz, from rock	+11.52			HF-HCl treated

$$1000 \ln \alpha_{CW} = 2.78 (10^6 T^{-2}) - 3.39 \quad (G-3)$$

O'Neil, Clayton and Mayeda, 1969). In T7-450, $1000 \ln \alpha_{QC}$ is 2.18 (Table 2) and the temperature calculated from (G-1) is $245 \pm 20^\circ\text{C}$. The 20° uncertainty arises from the 0.2% total uncertainty in Δ_{QC} , which is approximately $1000 \ln \alpha_{QC}$. This assumes that $\delta^{18}\text{O}$ values for calcite and quartz have an uncertainty of 0.1% . In the neighborhood of 240°C , a change in Δ_{QC} of 0.2% corresponds to a change in temperature of 20° . The uncertainties in the experimental work undertaken to derive Equations (G-2) and (G-3) were not taken into consideration.

Using Equation (G-3) and the $\delta^{18}\text{O}$ of T7-450 calcite, the calculated $1000 \ln \alpha_{CW}$ at 245°C is 7.0, leading to $\delta^{18}\text{O}$ of $+2.8\%$ for water equilibrium with vein quartz and calcite of T7-450. This calculated water value can be used in conjunction with the $\delta^{18}\text{O}$ of graywacke quartz from T7-636 to calculate a temperature of formation for quartz from the deeper sample. $1000 \ln \alpha_{QW}$ in T7-636 is 8.9% , which corresponds to a temperature of $251 \pm 20^\circ\text{C}$. Within the given uncertainty, the temperatures indicated by the isotopic compositions of minerals in T7-450 and T7-636 (245°C and 251°C , respectively), are virtually the same. These non-independent isotopic equilibrium temperatures, based on quartz-calcite and quartz-water, are plotted at their appropriate depths in Figure 7, so that isotopic equilibrium temperatures might be compared with measured temperatures.

Even the little isotopic data obtained from samples from T7 provide some very interesting information. The "water" which might have been in equilibrium with quartz and calcite in the veins intersected by T7 has a $\delta^{18}\text{O}$ value $+2.8\%$ which is unlike any known normal meteoric

water. The isotopic value indicates that even if the thermal water entered the steam system as meteoric water, it has lost its meteoric $\delta^{18}\text{O}$ value by oxygen exchange with rocks and minerals. A high $\delta^{18}\text{O}$ value for hydrothermal water usually indicates a low water/mineral ratio in the hydrothermal system. Of course, if the fluids reacting with the rocks were entrapped ocean water, then the value of 2.8‰ for the calculated $\delta^{18}\text{O}$ of "hydrothermal water" would indicate that the water/rock ratio would be large in the part of the hydrothermal system in which isotopic exchange took place.

A low $\text{H}_2\text{O}/\text{rock}$ ratio suggests a dry system. Low rates of mass transport of water are to be expected if the water in the hydrothermal system is steam. Several implications from the conclusions inferred from the $\delta^{18}\text{O}$ of water which reacted with T7 vein minerals will be discussed in the light of other data from samples from The Geysers.

The $\delta^{13}\text{C}$ value of the carbonate in T7-450 veins, -12‰ is unusual. This value is unlike that of marine carbonates, which is approximately 0‰. Nor does this value seem to be characteristic of those of limestones that have undergone fresh-water diagenesis. The $\delta^{13}\text{C}$ value of the vein calcite in Thermal 7 is similar to $\delta^{13}\text{C}$ values of calcite in rock samples from the steam zone in other wells at The Geysers, and also to the $\delta^{13}\text{C}$ value of CO_2 at The Geysers, -11 to -12‰ according to Craig (1963). The implication of these similarities is that the $\delta^{13}\text{C}$ of steam-zone carbonates is controlled by CO_2 in the steam-rich fluid. A more detailed discussion of all of the carbon isotopic data from The

Geysers will appear in a subsequent section.

3.6.3 Possible Variations in Steam Reservoir Temperature in Response to the Drilling of Thermal 7

The two isotopic temperatures recorded by the $\delta^{18}\text{O}$ values of the minerals in Thermal No. 7 are significantly higher than the corresponding temperatures measured directly at the same depths (Figure 7). The isotopic temperatures are higher by about 45 to 50°C. Either The Geysers heat source has diminished in intensity since the time the isotopic records of the vein minerals were established, or the isotopic record gives true pre-drilling reservoir temperatures and the drilling caused the establishment of a different temperature distribution in the well.

It was already mentioned that drilling a well seriously disrupts the heat balance in the immediately adjacent steam reservoir. Allen and Day (1927) pointed out that there is a ground water body perched upon the superheated steam zone at The Geysers. A well provides a direct conduit between superheated steam and the upper walls of the well, cooled by groundwater. Pressure in a shut-in well is nearly constant. The local heat balance shifts to a new "equilibrium" (actually, steady-state) resulting in a new temperature distribution after drilling. Steam condenses on the cooler walls of the casing in contact with ground water, heating the ground water. Steam temperature will decrease where it is losing heat to ground water. At a given pressure, the sub-critical temperature at which steam condenses is fixed. Steady-state conditions result in which just enough heat from the superheated

zone balances the heat lost to ground water at the condensation point. These are called "saturation conditions" by McNitt (1963). These conditions account for the 180°C constant temperature zone in T7. Below that zone, superheat is observed, but not to the same extent as before drilling.

Another example of the effect of temperature decrease in response to drilling is illustrated by Magma Well No. 1. The highest temperature ever measured during drilling at The Geysers was 300°C at 183 meters in Magma No. 1, 1957. In the 1960 logging project the temperature at 183 meters was around 195°C, illustrating the effect of removing steam (and therefore heat) from the reservoir (McNitt, 1963).

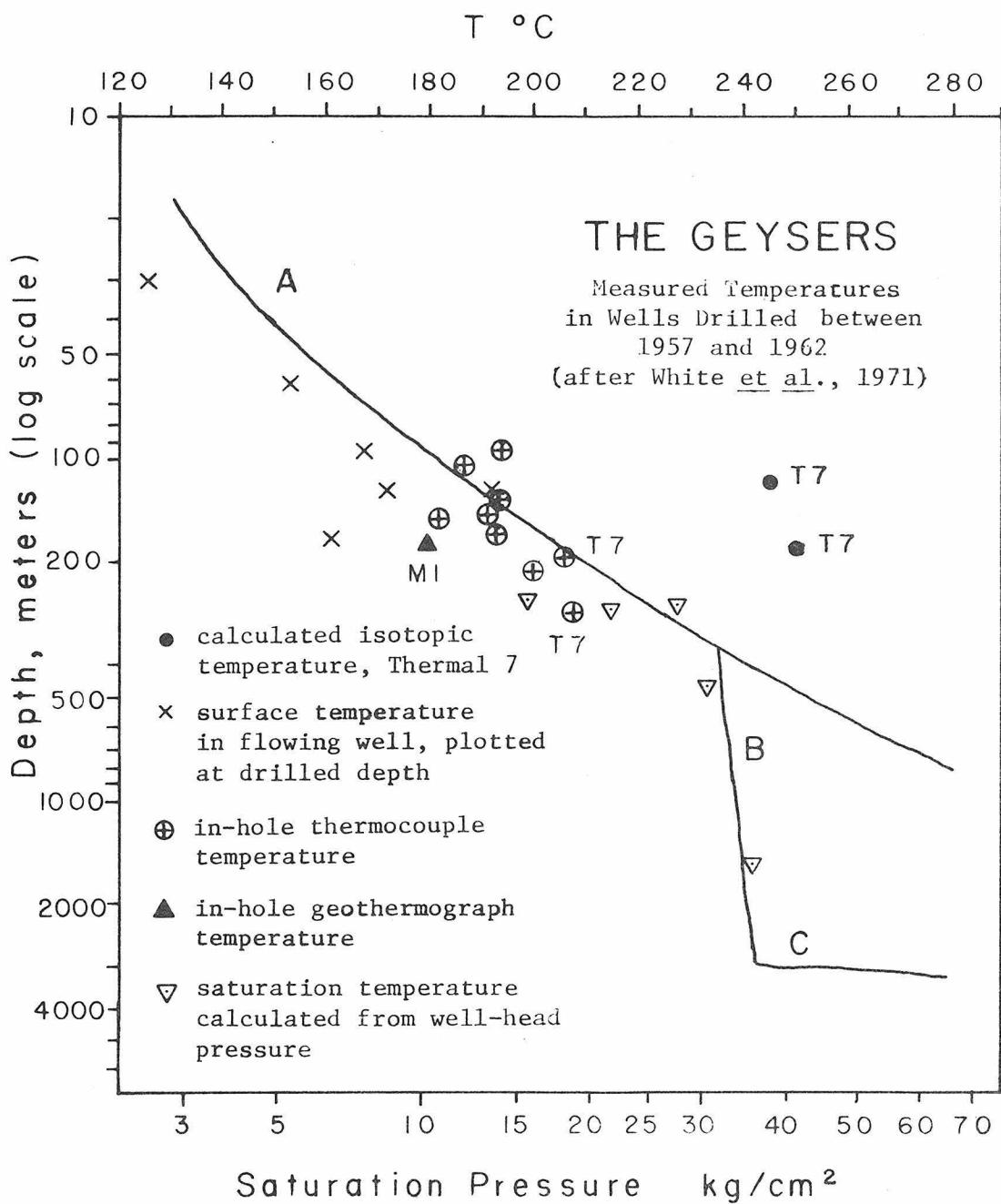
Some results of the 1960 temperature-logging project are plotted in Figure 8, modified from White, Muffler and Truesdell (1971). The curve marked "A" is the locus of points corresponding to conditions of temperature and hydrostatic pressure at which pure water boils. The depth parameter corresponds to the hydrostatic pressure imposed by a ground water zone perched on the steam zone. Curve "A," the boiling-point curve for pure water, indicates the temperatures and pressures which would be found in the near-surface ground-water zone. The fact that most well temperatures plotted in Figure 8 fall near curve "A" indicates that these wells do not penetrate the steam zone, whose temperature-pressure regime is indicated by curve "B."

Temperatures measured in Magma 1 (M1) and Thermal 7 (T7) after sealing are indicated in Figure 8. The two isotopically determined temperatures obtained for T7 are also marked at their respective depths

FIGURE 8

Temperatures in wells drilled between 1957 and 1962, The Geysers (after White et al., 1971).

Temperatures are given for various wells near Geyser Canyon at various depths. The techniques used to determine or deduce the temperatures are quite diverse: surface measurement, thermocouple, geothermograph, calculation saturation temperature at given pressure, and oxygen isotopes. Most measurements lie near the boiling-point curve of pure water (curve "A"), for which depth is a measurement of hydrostatic pressure. Curve "B" indicates the combinations of temperatures and pressures expected to occur in the steam-water mixture in the steam zone of a vapor-dominated hydrothermal system (cf. White et al.). Curve "C" indicates the temperatures and pressures in a postulated deep-seated geothermal brine water table. Isotopic equilibrium temperatures from Thermal 7 indicate superheat with respect to curve "A," and may have been established in an active steam zone which is presently deeper than 130 to 200 meters below the surface. "M1" denotes Magma No. 1 while "T7" stands for Thermal No. 7.



in Figure 8. The isotopic temperatures demonstrate 45 to 50° of superheat with respect to the boiling point curve at the indicated depths. The temperature of M1 during drilling at 183 meters (300°C) indicated 120° superheat with respect to the temperature logged at 183 meters in 1960 (180°C). Thus it is probable that steam reservoir temperatures in Thermal 7 were lowered from about 250°C (in the interval 130 to 200 meters depth) to around 200°C by the drilling which allowed fluid to escape when lithostatic pressure was lowered by the drilling operation, so that boiling at the steam-groundwater interface could take place, generating more steam which escaped from the system through the hole. The loss of material from the system is equivalent to a heat loss, which lowers the steam reservoir temperature.

The fact that the isotopic temperatures in T7 were $250^{\circ}\text{C} \pm 20^{\circ}\text{C}$ is in itself a significant fact. The temperature 240°C is important in the theory of vapor-dominated systems, according to White, Muffler and Truesdell (1971). This is the temperature at which a mixture of water and steam has its maximum enthalpy, and this temperature should prevail throughout the active steam zone. The temperatures predicted for the active steam zone by the model of White et al. are indicated by curve "B" in Figure 13. The fact that T7 isotopic temperatures are found at depths less than those predicted by the intersection of curves "A" and "B" (the depth of the steam-groundwater interface) suggests that at one time the active steam zone extended up to the 130 meter level in T7. If the isotopic temperatures were locked into the vein minerals of T7 in the active steam zone at about 240°C, an effect of

drilling is the lowering of the depth of the top of the active steam zone.

According to the model of White et al. temperatures greater than 240°C should occur only below the postulated hot brine water table at 3000 meters depth, whose temperatures are indicated by curve "C" in Figure 13. This and other points of the White et al. model will be discussed after more data from The Geysers have been presented and discussed.

3.6.4 Hydrothermal Alteration of Host Rock in Thermal 7

Although host rock alteration at The Geysers is to be discussed in detail in a subsequent section, it is important to note here that the $\delta^{18}\text{O}$ of whole rock graywacke of T7-450 is +9.7‰, and the δD of its total hydrogen is -59.4‰ (Table 2). This $\delta^{18}\text{O}$ value is 3‰ lower than the lowest $\delta^{18}\text{O}$ of graywacke outside the active steam zone, while there is no distinct difference in δD between altered and unaltered graywacke. The $\delta^{18}\text{O}$ of the "unaltered" graywacke is +13 to +15‰, and the δD of its total hydrogen is -30 to -60‰.

In order to test the plausibility of the $\delta^{18}\text{O}$ value of hydrothermally-altered graywacke in Thermal No. 7, 9.7‰, the isotopic composition was calculated by taking reasonable proportions of minerals typically found in graywacke, all of which are assumed to be in isotopic equilibrium. If the quartz in the graywacke has the same $\delta^{18}\text{O}$ as the vein quartz (+12‰) and the other graywacke constituents are in isotopic equilibrium with the quartz (and with water whose $\delta^{18}\text{O}$ is +2.8‰) at 250°C, the $\delta^{18}\text{O}$ of whole rock graywacke, +9.7‰ is quite reasonable.

Chlorite, sericite and calcite are the other constituents, and at 250°C in equilibrium with water whose $\delta^{18}\text{O}$ is +3‰, their respective $\delta^{18}\text{O}$ values would be 4‰, 8‰, and 10‰. If the respective proportions of total rock oxygen in quartz, sericite, calcite and chlorite are 50%, 15%, 20% and 15%, the graywacke $\delta^{18}\text{O}$ would be 9.8‰, very close to the observed graywacke $\delta^{18}\text{O}$ value. ^{16}O must have been added to the graywacke to lower its $\delta^{18}\text{O}$ value from 13 or 15‰ to about 10‰. Conversely ^{18}O must have been added to meteoric water to cause its $\delta^{18}\text{O}$ value to be as high as 3‰, if meteoric water is the source of hydrothermal fluid.

If the water was originally meteoric (whose local $\delta^{18}\text{O}$ value is -8‰, as will be seen), the water $\delta^{18}\text{O}$ was raised 11‰, and the Thermal 7 graywacke $\delta^{18}\text{O}$ was lowered at least 3‰. The large change in water $\delta^{18}\text{O}$ and the small change in rock $\delta^{18}\text{O}$ suggests that the circulation of water through the reservoir rock has been restricted giving rise to a water/rock oxygen atom ratio 0.27 and a mass ratio of 0.15. Implications of steam zone water/rock ratios inferred from isotopic data and the significance of apparently negligible changes in δD of rocks during hydrothermal alteration will be discussed in the context of more data from other wells.

3.7 The Lakoma Fame Tract

3.7.1 General Features

A parcel of land named the Lakoma Fame Tract covers most of sections 17 and 20 in Figure 6. The steam field underlying the Lakoma Fame Tract is the most recently drilled and exploited part of the

hydrothermal system at The Geysers. It is the site of the two most recently built electrical generating units at The Geysers, Units 9 and 10. Until the value of the steam resource under Lakoma Fame Tract was proven by Union Oil by drilling in the late 1960's, the subsurface geology of the tract was entirely speculative. The distribution of holes on the tract describes a band that follows the general trend of the regional structural grain, west-northwest.

Wells from which rock samples were obtained are located on Figure 6. which includes the landmarks Boggs and Hot Springs Creeks, Units 9 and 10, Geyser Canyon (the site of the discovery of The Geysers), Thermal No. 4 (the blown-out well), Thermal No. 7 (previously discussed), Units 5 and 6 and Big Sulphur Creek. The Lakoma Fame wells (henceforth referred to as "LF" wells) are 1500 to 2000 meters east of the main activity at The Geysers. Samples from the wells Lakoma Fame Numbers 19, 15, 13, 9, and 8 were analyzed.

According to Garrison (1972), steam reservoirs are isolated laterally and vertically by cooler, impermeable bodies of rock. Impermeability is ascribed either to inherent rock impermeability or to self-sealing of fractures, a process by which a hydrothermal system forms its own cap by depositing minerals in its upper, cooler reaches. The Lakoma Fame Tract is effectively isolated from the main activity at The Geysers, as will be seen.

An important feature of the LF samples is their spatial isolation from the main activity (and area of most thorough drilling) of The Geysers. Samples from LF wells should not have been affected

isotopically by post-drilling phenomena which was discussed in section 3.6.3, dealing with Thermal No. 7, because (1) LF wells are far away from Geyser Canyon, where the extensive drilling took place; 2) LF wells are far from each other, so that drilling one is unlikely to create a thermal anomaly in the reservoir rock which might affect an adjacent well a few hundred meters away.

The chief disadvantage posed by the LF samples is the unavailability of temperature data for the LF wells. The most complete sets of cuttings came from the LF 19 and 15 exploratory holes. Only the shallow portion of LF 13, another exploratory well, was made available. Only one core fragment each was available from steam-producing wells LF 9 and LF 8; no other samples from these two wells were available for study.

The rock types of the Lakoma Fame tract are those which have been described in the early part of this chapter.

The succession with depth of rock types penetrated by LF wells is: (1) a complex colluvial surface layer of mixed rock types, generated by frequent landsliding in the area (≤ 150 meters thick); (2) graywacke (≤ 200 meters); (3) greenstone (≤ 200 meters); (4) metamorphic rock (< 50 meters); (5) sheared serpentinite (≤ 800 meters); (6) metamorphic rock (< 10 meters); (7) graywacke intercalated with greenstones (most wells reach total depth in this zone). Most of these bodies of rock dip about 40° northeast, accounting for an apparent thickness greater than stratigraphic thickness (McNitt, 1968).

3.7.2 Occurrence and Distribution of Vein Minerals in Lakoma Fame Wells

Calcite and quartz are the dominant vein minerals found in the samples examined. Wells are very markedly zoned with respect to the abundance and contents of veins. In LF 19 and LF 15 shallow zone veins are dominated by calcite, with small amounts of massive milky quartz, at depths less than 900 meters below the surface. Below the shallow zone there is a zone devoid of veining, spanning 180 to 200 m. Deep zone veins are mostly massive quartz, but small amounts of euhedral quartz and calcite are found in open fractures. Textural features in many samples indicate that calcite and quartz, where they occur together, formed contemporaneously, forming veins by filling open fractures (Plates 3, 4). Cuttings from only the uppermost 660 meters of LF 13 were available, and the vein minerals in the LF 13 samples are characteristic of the upper zone.

It is appropriate to work with vein minerals because they are the materials most sensitive to changes in the chemical nature and amount of fluids confined to fractures in host rocks of low inherent permeability. As will be seen, the host rock experiences only slight isotopic alteration. The isotopic compositions of vein minerals are the likeliest to preserve records of temperature and isotopic composition of the fluid from which the vein minerals are deposited.

3.7.3 Lakoma Fame No. 19

The excellent collection of samples from this well resulted in LF 19 being the most thoroughly investigated well. Isotopic analyses of materials from Lakoma Fame 19 cuttings are reported in Table 3.

PLATE 3.

Massive quartz vein in graywacke, Lakoma Fame No. 19, The Geysers.
152 to 159 meters depth, upper zone.

Area of view: 1.6 × 1.2 mm. X-nicols.

Fracture in slightly-altered graywacke of Franciscan Group, filled with
massive quartz. 640 meters above steam zone.

PLATE 4.

Massive quartz and calcite veins in greenstone, Lakoma Fame No. 19,
The Geysers. 622 to 628 meters depth, upper zone.

Area of view: 1.6 × 1.2 mm. X-nicols.

Fractures in metamorphosed basalt (greenstone) of Franciscan Group,
filled with cogenetic quartz (white) and calcite (mottled gray).

Note "splintering" veins above and below largest vein. 175 meters
above steam zone.

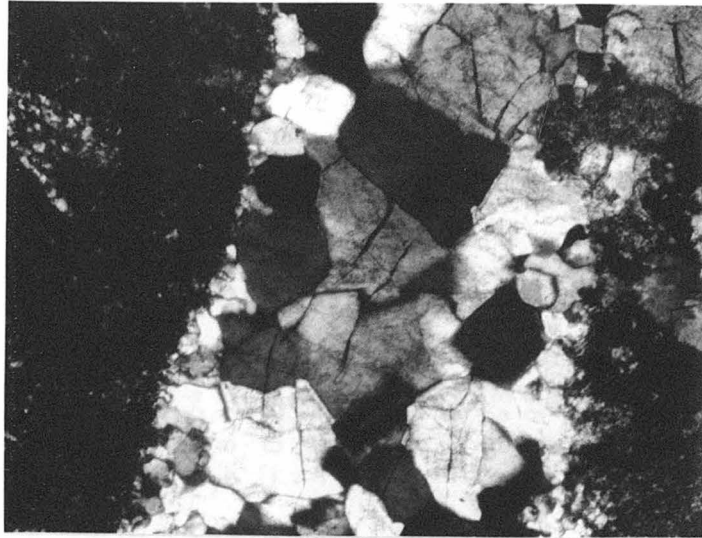


PLATE 3

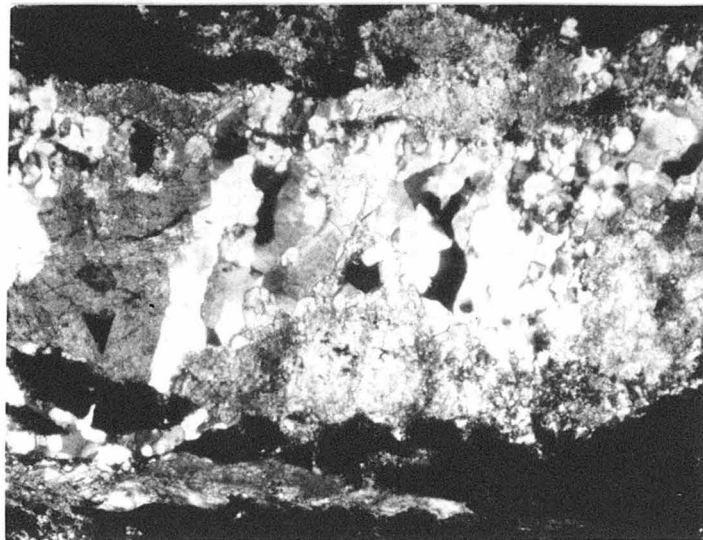


PLATE 4

TABLE 3

DESCRIPTIONS AND ISOTOPIC ANALYSES OF ROCKS AND MINERALS
FROM LAKOMA FAME NO. 19, THE GEYSERS

Surface: 777 meters above sea level

Well and Number	Depth, meters	Sample Description	$\delta^{18}\text{O}$ ‰	$\delta^{13}\text{C}$ ‰	δD ‰	Remarks
LF 19 - 4 a	61 - 67	calcite, vein	+16.45	- 8.54		
b		calcite, vein	+16.21	- 8.58		
LF 19 - 5	73 - 79	calcite, vein	+17.40	- 0.27		
LF 19 - 6	91 - 98	calcite, vein	+18.89	- 1.74		
			+16.70	- 2.34		
LF 19 - 7	104 - 110	calcite, vein	+17.21	- 3.40		
LF 19 - 9	134 - 140	calcite, vein	+16.30	- 7.92		
LF 19 - 10 a	152 - 159	calcite, vein	+16.14	- 8.43		} 16.06 ± 0.16
b		calcite, vein	+15.97	- 8.90		
c		quartz, vein	+19.56			
d		quartz, from graywacke	+15.11			HF-HCl treated } 15.00 ± 0.16
e		quartz, from graywacke	+14.88			HF-HCl treated }
f		graywacke	+15.19			HCl treated
g		graywacke	+14.40			-40.9 untreated; 2.7 wt. % H ₂ O
h		graywacke				-45.8 untreated
i		carbon in graywacke				CO ₂ from combustion
LF 19 - 11	165 - 171	calcite, vein	+15.94	-14.53		

General Remarks:

- Standard for reporting $\delta^{18}\text{O}$ and δD is SMOW. Standard for reporting $\delta^{13}\text{C}$ is PDB.
- Unless otherwise designated, all analyses were done on individually-prepared samples. Analyses joined by brackets indicate multiple analyses of one sample; mean $\delta^{18}\text{O}$ and standard deviation are reported.

TABLE 3: LAKOMA FAME NO. 19 - CONTINUED

<u>Well and Number</u>	<u>Depth, meters</u>	<u>Sample Description</u>	$\delta^{18}\text{O} \text{ ‰}$	$\delta^{13}\text{C} \text{ ‰}$	$\delta\text{D} \text{ ‰}$	<u>Remarks</u>
LF 19 - 12	183 - 189	a calcite, vein	+17.50	- 7.71	}	17.48 ± 0.01
		b calcite, vein	+17.46	- 7.79		
		c quartz, vein	+19.56			
		d quartz, from graywacke	+14.72			HF-HCl treated
		e graywacke	+14.61			HCl treated
		f graywacke	+14.04			-42.6 untreated; 3.2 wt. % H ₂ O
LF 19 - 15	226 - 232	a calcite, vein	+15.52	- 6.41		
		b quartz, from graywacke	+14.80			HF-HCl treated
		c graywacke	+14.61		-51.9	} 2.6 wt. % H ₂ O
		d graywacke	+14.70			
		e graywacke	+14.71			
		f chlorite-rich fraction	+ 9.29			-58.2
LF 19 - 16	244 - 250	calcite, vein	+15.61	-10.36		
		LF 19 - 17	256 - 262	calcite, vein	+16.01	- 6.41
LF 19 - 18	274 - 280	a calcite, vein	+14.44	-10.59		
		b quartz, from graywacke	+14.20			HF-HCl treated
		c graywacke	+13.89		-33.9	} 3.2 wt. % H ₂ O
		d graywacke	+13.94			
		e graywacke	+13.67			
LF 19 - 19	287 - 293	a calcite, vein	+15.64	- 9.25		
		b calcite, vein	+15.92	- 8.81		15.78 ± 0.20
		c quartz, vein	+19.92			} 19.75 ± 0.24
		d quartz, vein	+19.58			

TABLE 3: LAKOMA FAME NO. 19 - CONTINUED

Well and Number	Depth, meters	Sample Description	$\delta^{18}\text{O} \text{ ‰}$	$\delta^{13}\text{C} \text{ ‰}$	$\delta\text{D} \text{ ‰}$	Remarks
LF 19 - 20	305 - 311	a calcite, vein	+17.69	+ 0.56	} 17.53 ± 0.23	HF-HCl treated -58.0 3.1 wt. % H ₂ O -55.6
		b calcite, vein	+17.37	+ 1.06		
		c quartz, vein	+19.58			
		d quartz, from graywacke	+19.75			
		e graywacke	+13.38			
		f chlorite-rich fraction	+11.74			
LF 19 - 21	317 - 323	a calcite, vein	+16.85	- 6.96	} 15.19 ± 0.23	
		b graywacke	+15.02			
		c graywacke	+15.35			
		d graywacke	+14.70			
LF 19 - 22	335 - 341	a calcite, vein	+17.28	- 2.33	} 17.27 ± 0.01	HF-HCl treated -58.3 5.5 wt. % H ₂ O -57.3
		b calcite, vein	+17.26	- 2.26		
		c quartz, vein	+18.53			
		d quartz, from graywacke	+19.17			
		e graywacke	+14.99			
		f graywacke	+14.76			
		g chlorite-rich fraction	+11.62			
LF 19 - 23	366 - 372	a calcite, vein	+15.40	- 1.37		
		b calcite, vein	+14.91	- 1.16		
		c quartz, vein	+18.87			
		d greenstone	+10.13			
LF 19 - 24	378 - 384	calcite, vein	+16.75	- 2.47		
LF 19 - 25	396 - 402	a calcite, vein	+16.22	- 4.90	} 10.94±0.15; 4.1 wt. H ₂ O	
		b greenstone	+11.04			
		c greenstone	+10.83			

TABLE 3: LAKOMA FAME NO. 19 - CONTINUED

Well and Number	Depth, meters	Sample Description	$\delta^{18}\text{O} \text{ ‰}$	$\delta^{13}\text{C} \text{ ‰}$	$\delta\text{D} \text{ ‰}$	Remarks
LF 19 - 27	427 - 433	quartz, from graywacke	+15.30			HF-HCl treated
		graywacke	+15.05			
		graywacke	+14.62			
		chlorite-rich fraction	+10.77		-57.3	} 10.65 ± 0.18
		chlorite-rich fraction	+10.52			
LF 19 - 28	439 - 455	calcite, vein	+16.12	- 9.23		
LF 19 - 30	470 - 476	greenstone	+ 9.71			HCl treated
		greenstone	+ 9.58		-68.4	untreated; 5.2 wt. % H ₂ O
LF 19 - 31	488 - 494	calcite, vein	+16.37	+ 1.20		
LF 19 - 32	500 - 506	greenstone	+11.21			} 11.16 ± 0.07
		greenstone	+11.11			
LF 19 - 35	549 - 555	calcite, vein	+14.92	- 6.60		
		greenstone	+11.22		-66.4	3.9 wt. % H ₂ O
		greenstone	+10.63		-68.2	4.2 wt. % H ₂ O
LF 19 - 38	591 - 598	greenstone	+11.18			
			+10.53			
LF 19 - 39	610 - 616	calcite, vein	+16.10	- 1.82		
LF 19 - 40	622 - 628	quartz, vein	+18.69			
		quartz, vein	+19.16			
		greenstone	+ 9.97		-65.1	4.6 wt. % H ₂ O
		greenstone	+ 9.48			
LF 19 - 43	671 - 677	calcite, vein	+16.07	- 3.34		

TABLE 3: LAKOMA FAME NO. 19 - CONTINUED

Well and Number	Depth, meters	Sample Description	$\delta^{18}\text{O} \%$	$\delta^{13}\text{C} \%$	$\delta\text{D} \%$	Remarks
LF 19 - 45	701 - 707	a	+ 6.63		-85.3	
		b	+ 7.37		-70.3	
		c			-75.9	
		d	+ 7.37		-80.8	
		e	+ 7.37		-78.2	
		f	+ 6.35			
			+ 6.15			
		g	+ 9.07			
LF 19 - 48	744 - 750	actinolite-hornblende mix	+ 9.07		-60.8	Originally pyritic; formic acid treated.
		actinolite-hornblende mix	+ 9.07			
LF 19 - 50	774 - 780	a	+16.81	- 3.50		
		b	+ 6.58			chloritic, pyritic; formic acid treated.
LF 19 - 53	823 - 829	a	+ 6.59			chloritic, pyritic; formic acid treated.
		b	+ 6.93			
		c	+ 7.00			
LF 19 - 55	866 - 872	a	+ 5.63		-86.4	pyritic; formic acid treated.
		b	+ 5.66		-87.6	
		c	+ 5.63			
LF 19 - 58	915 - 921	a	+ 5.82			chloritic, pyritic; formic acid treated.
		b				

TABLE 3: LAKOMA FAME NO. 19 - CONTINUED

<u>Well and Number</u>	<u>Depth, meters</u>	<u>Sample Description</u>	$\delta^{18}\text{O} \text{ ‰}$	$\delta^{13}\text{C} \text{ ‰}$	$\delta\text{D} \text{ ‰}$	<u>Remarks</u>
LF 19 - 59 a	927 - 933	calcite, vein	+ 1.83	-13.00		chloritic, pyritic, untreated
b		serpentinite	+ 6.03			
c		serpentinite	+ 5.49			
d		serpentinite	+ 5.09			
LF 19 - 60	945 - 951	calcite, vein	+ 3.45	-10.52		same, formic acid treated
LF 19 - 62 a	976 - 982	calcite, vein	+ 2.58	-11.16		
b		serpentinite	+ 4.51			
LF 19 - 65 a	1018 - 1024	serpentinite	+ 4.62			chlorite, pyritic, formic acid treated
c		serpentinite	+ 4.76			
LF 19 - 66	1037 - 1043	serpentinite	+ 5.23			chloritic, pyritic, formic acid treated
LF 19 - 68 a	1067 - 1073	calcite, vein	+ 5.19	- 8.69		
b		antigorite	+ 5.52			
c		antigorite	+ 5.54			
LF 19 - 71 a	1110 - 1116	antigorite	+ 5.62		-88.0	} 5.56 ± 0.05
b		serpentinite	+ 5.41			
LF 19 - 72 a	1128 - 1134	serpentinite	+ 5.05			chloritic, pyritic, formic acid treated
b		calcite, vein	+ 0.94	-10.20		
LF 19 - 73 a	1140 - 1146	quartz, massive vein	+17.92			chloritic, pyritic, formic acid treated
		quartz, massive vein	+17.77			

TABLE 3: LAKOMA FAME NO. 19 - CONTINUED

<u>Well and Number</u>	<u>Depth, meters</u>	<u>Sample Description</u>	$\delta^{18}\text{O} \text{ ‰}$	$\delta^{13}\text{C} \text{ ‰}$	$\delta\text{D} \text{ ‰}$	<u>Remarks</u>
LF 19 - 73	b	quartz, massive vein	+17.37			chloritic, pyritic, formic acid treated
	c	serpentinite	+ 6.64			
	d	serpentinite	+ 6.73			
LF 19 - 74	a	calcite, vein	+12.21	- 9.75	} 12.17 ± 0.06	chloritic, pyritic, formic acid treated
	b	calcite, vein	+12.13	- 9.61		
	c	quartz, massive vein	+17.43			
	d	serpentinite	+ 7.45			
	e	serpentinite	+ 7.43			
LF 19 - 75	a	calcite, vein	+ 9.38	-11.09	} 18.25 ± 0.17	chloritic, pyritic, formic acid treated
	b	quartz, massive vein	+18.37			
	c	quartz, massive vein	+18.13			
LF 19 - 77	a	calcite, vein	+ 5.39	-13.07	} 5.53 ± 0.06	quartz crystals on calcite platelet
	b	calcite, vein	+ 5.30	-13.28		
	c	quartz, massive vein	+17.19			
	d	quartz, euhedral crystals	+ 7.29			
	e	quartz, euhedral crystals	+ 6.85			
f	serpentinite	+ 7.00		chloritic, pyritic, formic acid treated		
g	serpentinite	+ 6.52				

TABLE 3: LAKOMA FAME NO. 19 - CONTINUED

<u>Well and Number</u>	<u>Depth, meters</u>	<u>Sample Description</u>	$\delta^{18}\text{O} \text{ ‰}$	$\delta^{13}\text{C} \text{ ‰}$	$\delta\text{D} \text{ ‰}$	<u>Remarks</u>
LF 19 - 78 a	1220 -1226	quartz, massive vein	+17.30			} 17.34 ± 0.05
b		quartz, massive vein	+17.37			
c		quartz, euhedral crystals	+ 7.31			
LF 19 - 79	1232 -1238	calcite, vein	+ 6.28	-13.30		
LF 19 - 80	1250 -1256	calcite, vein	+ 7.24	-10.58		
LF 19 - 81	1262 -1268	quartz, euhedral crystals	+ 7.65			
LF 19 - 82 a	1280 -1287	serpentinite	+ 7.48			chlorite, no pyrite
b		serpentinite	+ 6.83			
LF 19 - 84	1311 -1317	serpentinite	+ 4.47			chloritic, pyritic; formic acid treated
			+ 3.94			
LF 19 - 89 a	1384 -1390	serpentinite	+ 5.39			chloritic, pyritic; formic acid treated
b		serpentinite	+ 4.97			} 4.71 ± 0.03
c		quartz	+11.77			
			+ 1.09	-15.28		
LF 19 - 90 a	1402 -1409	calcite, vein	+ 1.84	-15.02		} 4.71 ± 0.03
b		calcite, vein	+ 4.69			
c		quartz, euhedral crystals	+ 4.73			
d		quartz, euhedral crystals				

TABLE 3: LAKOMA FAME NO. 19 - CONTINUED

<u>Well and Number</u>	<u>Depth, meters</u>	<u>Sample Description</u>	$\delta^{18}\text{O} \text{ ‰}$	$\delta^{13}\text{C} \text{ ‰}$	$\delta\text{D} \text{ ‰}$	<u>Remarks</u>
LF 19 - 91 a	1415 -1421	quartz, massive vein	+15.59			with drusy quartz overgrowths
b		quartz, massive vein	+15.40			with drusy quartz overgrowths
c		serpentinite	+ 6.22			chloritic, pyritic; formic acid treated
d		serpentinite	+ 6.32			chloritic, pyritic; formic acid treated
e		"red rock"	+ 4.62			quartz-hematite mixture
f		graywacke	+ 6.09		-71.4	3.6 wt. % H ₂ O
g		quartz, from graywacke	+14.95			HF-HCl treated
LF 19 -93 a	1445 -1451	antigorite	+ 3.67		-84.2	Note the variations in $\delta^{18}\text{O}$
b		antigorite	+ 4.20			of antigorite in the same
c		antigorite	+ 4.87			cuttings fraction. All five
d		antigorite	+ 5.38			samples were hand-picked
e		antigorite	+ 4.11			independently.
LF 19 - 96 a	1494 -1500	quartz, massive vein	+18.60			associated with "red rock"
b		quartz, massive vein	+19.01			
LF 19 - 97	1506 -1512	quartz, massive vein	+19.93			associated with "red rock"
LF 19 -98 a	1524 -1530	serpentinite	+ 5.73			chloritic, pyritic; formic acid treated
b		serpentinite	+ 5.19			

TABLE 3: LAKOMA FAME NO. 19 - CONTINUED

<u>Well and Number</u>	<u>Depth, meters</u>	<u>Sample Description</u>	$\delta^{18}\text{O} \text{ ‰}$	$\delta^{13}\text{C} \text{ ‰}$	$\delta\text{D} \text{ ‰}$	<u>Remarks</u>
LF 19 - 100 a	1555 -1561	quartz, massive vein	+15.32			Fragments have varying degrees of overgrowth by drusy quartz
b		quartz, massive vein	+15.42			
c		quartz, massive vein	+16.15			
d		quartz, massive vein	+17.00			
LF 19 - 101 a	1567 -1573	quartz, massive vein	+17.75			} 7.41 ± 0.01
b		quartz, euhedral crystals	+ 7.42			
c		quartz, euhedral crystals	+ 7.40			
d		greenstone	+ 3.22		-69.4	
LF 19 - 102	1585 -1591	quartz, massive vein	+17.42			
LF 19 - 104	1616 -1622	quartz, massive vein	+17.19			
LF 19 - 105	1628 -1634	quartz, massive vein	+16.24			

Other relevant information, such as depth of origin, modes of occurrence of some minerals and special treatments given to some samples are also noted in this table.

3.7.3.1 The Isotopic Record in Lakoma Fame No. 19 Vein Minerals

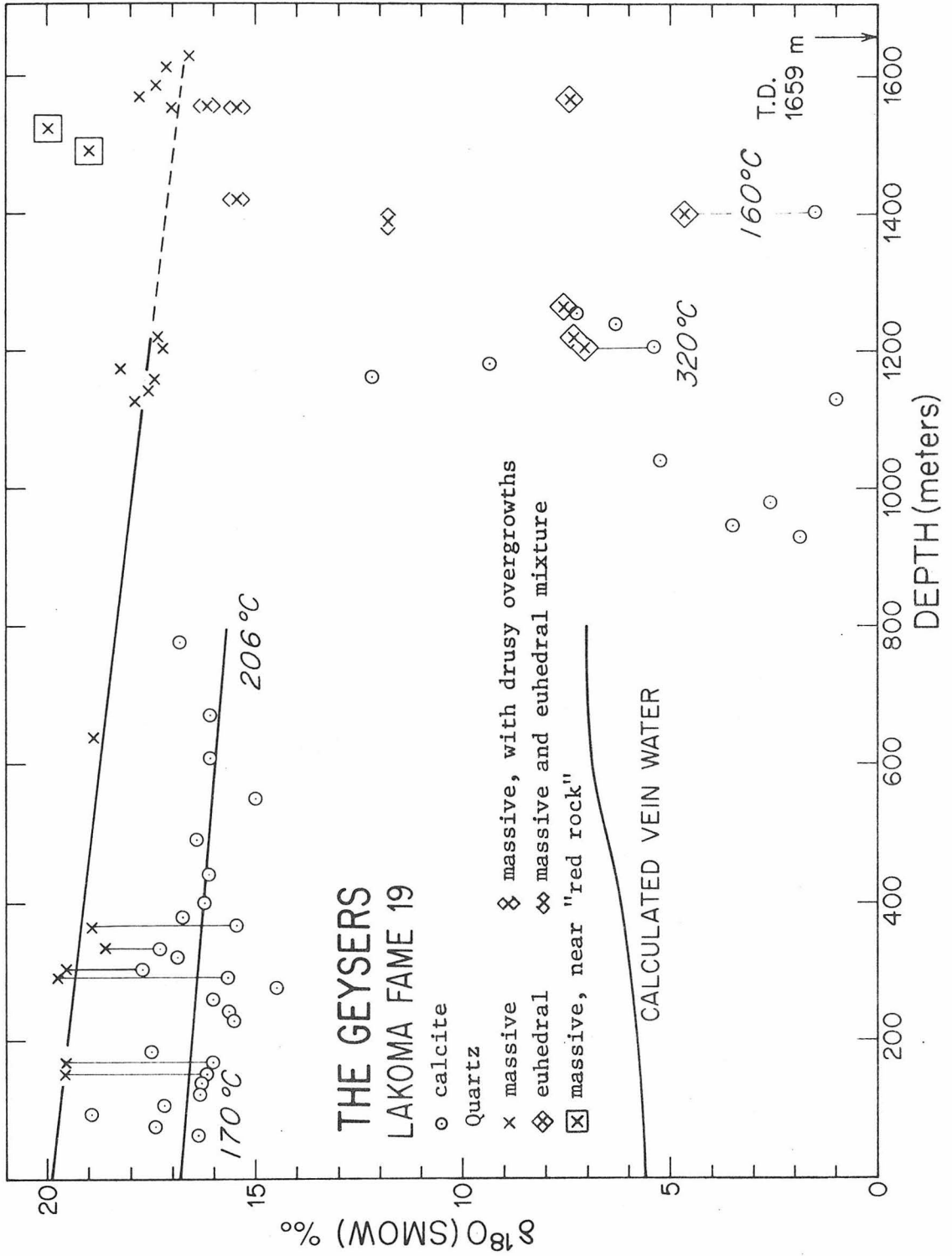
$\delta^{18}\text{O}$ values of vein minerals of LF 19 from various depths are plotted in Figure 9. The figure shows a large variation in calcite $\delta^{18}\text{O}$ values, from 1‰ to 19‰, and a similarly large variation in quartz $\delta^{18}\text{O}$ values, from 5‰ to 20‰. One of the most significant features of the $\delta^{18}\text{O}$ -depth profile is the discontinuity in carbonate $\delta^{18}\text{O}$ values in the interval 750 to 950 meters deep. In this zone the $\delta^{18}\text{O}$ of the carbonate varies from +17‰ to +2‰. At depths greater than 900 meters all the calcite values are less than 12‰, and most are less than 7‰ as compared to 16 to 20‰ at depths less than 800 meters. These data indicate that the environment of calcite-fluid interaction was quite distinct in the "upper zone" above the discontinuity, as compared to that of the "lower zone" below the discontinuity. Visually, in most cases, the calcites from the upper and lower zones are indistinguishable. The interval 800 to 900 meters deep is devoid of vein minerals (the "barren" zone). 800 meters below the surface in LF 19 corresponds to 23 meters below sea level; the level of occurrence of the carbonate discontinuity in a number of wells will be compared and therefore should be referred to a common reference plane, sea level.

$\delta^{18}\text{O}$ values of massive milky vein quartz decrease slightly with increasing depth, without discontinuity. Nowhere is massive quartz $\delta^{18}\text{O}$ less than 16‰, but all $\delta^{18}\text{O}$ values of the euhedral quartz, which

FIGURE 9

$\delta^{18}\text{O}$ values of vein minerals from various depths, Lakoma Fame No. 19, The Geysers.

$\delta^{18}\text{O}$ values of various types of calcite and quartz are plotted at the depths of origin of the samples. Lines connect $\delta^{18}\text{O}$ values of quartz and calcite which were found in the same cuttings fraction. A discontinuity in vein calcite $\delta^{18}\text{O}$ values at about 800 meters depth is conspicuous. Least-squares lines are drawn through massive calcite points down to 800 meters and through massive quartz points down to 1200 meters. Isotopic temperatures obtained from $1000 \ln \alpha$ values defined by the distance between the least squares lines (Δ_{QC}) are given for the surface (170°C) and 800 meters depth (206°C). The locus of points whose $\delta^{18}\text{O}$ values are those of water calculated to be in equilibrium with quartz and calcite (having $\delta^{18}\text{O}$ values taken from the least squares lines at any given depth) is the curve marked "calculated vein water." Isotopic equilibrium temperatures are given for the two calcite-euhedral quartz pairs at 1200 and 1400 meters depth. The $\delta^{18}\text{O}$ values of other varieties of quartz are also given. Note that the linear relationship of decreasing massive quartz $\delta^{18}\text{O}$ values with depth appears to continue to the bottom of the well, as indicated by the broken extension of the quartz least-squares line.



begins to appear at 1200 meters depth, are less than 8‰ quartz in the lower zone, below 1400 meters, also exhibits some values different from those of the massive and euhedral quartz. Values between 15‰ and 16.5‰ in the interval 1400 to 1550 meters depth are obtained from massive quartz fragments which have overgrowths of drusy quartz. Values between 19‰ and 20‰ in the neighborhood of 1500 meters deep came from quartz which was closely associated with "red rock," a hematite-quartz mixture which is inferred to be a recrystallized red chert.

Now that the distribution of vein mineral $\delta^{18}\text{O}$ values with depth has been described, together with modes of occurrence of the minerals, the significance of the observed patterns may be discussed. The patterns of $\delta^{18}\text{O}$ -depth profiles in the upper zone will be dealt with first.

3.7.3.2 The Significance of Upper Zone Vein Mineral $\delta^{18}\text{O}$ Values

The $\delta^{18}\text{O}$ values of upper zone vein quartz (17 to 20‰) are unusual compared to $\delta^{18}\text{O}$ values of quartz found in other well-described geological environments. They are higher than typical values of igneous quartz, (8 to 10‰; Taylor, 1968) higher than most values of quartz in regionally-metamorphosed rocks (13 to 16‰; Garlick and Epstein, 1967), and lower than most cherts (28 to 38‰; Knauth and Epstein, 1974). Calcite in the upper zone (14 to 19‰) is more depleted in ^{18}O than most marine limestones (20 to 30‰; Engel, Clayton and Epstein, 1958), but contain more ^{18}O than does calcite in many high-temperature contact-metamorphic skarns and marbles (10 to 17‰; Shieh and Taylor, 1969).

The $\delta^{18}\text{O}$ of upper zone vein quartz appears to decrease

continuously with depth. The same relationship seems to be valid for massive vein quartz to depths as great as 1200 meters, and for calcite in the upper zone, to 800 meters depth. Since upper zone quartz and calcite appear to be cogenetic, an attempt was made at calculating temperatures of formation and isotopic compositions of fluids with which the vein minerals had been in equilibrium from the oxygen isotopic fractionation factors between quartz and calcite. Unfortunately, coexisting quartz and calcite did not occur in amounts large enough to be analyzed in every cuttings fraction. The resulting values of $1000 \ln \alpha_{QC}$ are derived (Table 3) for samples from each of the following depths: 156 meters ($1000 \ln \alpha_{QC} = 3.44$), 186 meters (2.04), 290 meters (3.90), 308 meters (2.01), 338 meters (1.24) and 369 meters (3.65). According to Equation (G-1), the corresponding isotopic equilibrium temperatures are 145°C, 269°C, 119°C, 273°C, 423°C, and 132°C. This variation in temperature over 200 meters of stratigraphic section is not reasonable. The erratic temperature distribution is probably due entirely to the erratic distribution of calcite $\delta^{18}O$ values. The calcite had suffered post-depositional oxygen isotope exchange, while the quartz has in large part preserved its $\delta^{18}O$ -depth linear relationship. Because the calcite-water oxygen isotope equilibrium fractionation (Equation G-3) increases with decreasing temperature, a retrograde exchange between vein water and calcite would push $\delta^{18}O$ of calcite to higher values, effectively lowering α_{QC} , giving a higher apparent temperature. Quartz seems to be less sensitive to these retrograde effects, once it is formed.

The calcite and quartz upper zone $\delta^{18}\text{O}$ values appear to decrease with depth in such a manner that their $\delta^{18}\text{O}$ -depth relationships can be estimated by fitting straight lines to the data with least-squares analyses. The least-squares lines were drawn through calcite points down to 800 meters depth, and through quartz points down to 1200 meters. The quartz line is described by the equation:

$$\delta^{18}\text{O}(\text{Q}) = 19.92 - 0.00197d \quad (\text{G-4})$$

in which d is the depth in meters. The correlation coefficient, r , is -0.93. The equation for the calcite line is:

$$\delta^{18}\text{O}(\text{C}) = 16.81 - 0.00140d \quad (\text{G-5})$$

for which $r = -0.27$. The linear correlation of quartz values with depth is very good, as indicated by the absolute value of r near unity, but the scatter in calcite values leads to a poor, yet definite correlation, indicated by the lower value of the absolute value of r , 0.27. The primary purpose for calculating least-squares lines is to allow for the determination of an approximate temperature profile with depth. The resulting α_{QC} values from Equations (G-4) and (G-5) can be used to calculate isotopic temperatures anywhere in the upper zone.

It should be noted that the quartz-water isotopic fractionation represented by Equation (G-2) is based on experimental work at temperatures above 195°C (Clayton, O'Neil and Mayeda, 1972). For lower temperatures, Equation (G-2) is an extrapolation of the high-temperature

curve. Consequently, when Equation (G-1), which is in part derived from (G-2), is used to obtain temperatures lower than 195°C, some caution is warranted. Nevertheless, because the extrapolation is made to only 170°C, the expression

$$1000 \ln \alpha_{\text{QC}} = 0.60(10^6 T^{-2})$$

should be a fair approximation to the quartz-calcite fractionation below 200°C.

Isotopic temperatures calculated from the least squares $\delta^{18}\text{O}$ values of quartz and calcite in Figure 9 are 170°C at the surface and 206°C at 800 meters, giving an apparent geothermal gradient of 45°C per kilometer. Equation (G-3) allows the calculation of the $\delta^{18}\text{O}$ value of water at any depth. The locus of points corresponding to $\delta^{18}\text{O}$ values of water in isotopic equilibrium with the vein minerals describes the smooth curve labeled "calculated vein water" in Figure 9. $\delta^{18}\text{O}$ of calculated vein water is +5.5‰ at the surface and 7‰ at 800 meters. The vein water curve and the quartz and calcite curves all converge to a point at about 5460 meters depth, where the temperatures are such that no isotopic fractionation exists. This hypothetical depth is very approximate, because the quartz-water fractionation has not been determined for temperatures greater than 700°C; besides, α is probably not linear with $10^6 T^{-2}$ at very high temperatures. Nevertheless, the possibility that magmatic temperatures existed at depths of about 5 kilometers below the present surface is not unreasonable.

There is no evidence of recent thermal activity at the surface

on Burned Mountain, at the head of Hot Springs Creek, around Units 9 and 10 or anywhere else on the Lakoma Fame Tract. Therefore the calculated isotopic surface temperature, 170°C, cannot represent a recent episode of hot spring activity. The paleo-thermal gradient preserved in the upper zone of LF 19 is probably indicative of a now deeply eroded fossil hydrothermal system.

Neither the mineral nor the water $\delta^{18}\text{O}$ values of the upper zone are characteristic of those known from previous work in geothermal systems, or most other geological environments for that matter. Where the "upper zone" high $\delta^{18}\text{O}$ quartz is preserved in the lower zone, its value approaches that of some quartz in regionally-metamorphosed rocks, +15‰ (Garlick and Epstein, 1967). The quartz as high in $\delta^{18}\text{O}$ as +19‰ is characteristic neither of cherts (> +30‰; Knauth and Epstein, 1974) nor igneous quartz (+8 to +10‰; Taylor, 1968). Similarly the calcite (14 to 18‰) is similar neither to marine limestones (> +20‰; Engel et al., 1958) nor to geothermal system calcites, which are lighter than 14‰ (Clayton et al., 1968; Eslinger and Savin, 1973a; this work).

The $\delta^{18}\text{O}$ values of the minerals reflect conditions of restricted circulation of water, in which the bulk isotopic composition of the minerals plus water system is controlled to a large degree by the minerals. If the water was meteoric in origin, the fluid/minerals oxygen atomic ratio was small. Otherwise, a vein water with a $\delta^{18}\text{O}$ as high as 5.5 to 7‰ would not have resulted. Examples of such environments previously reported are: hydrothermally altered and contact-metamorphosed siliceous limestones, such as those at Gilman, Colorado

(Engel et al., 1958); low-temperature veins in regionally-metamorphosed rocks (Garlick and Epstein, 1967); metasedimentary rocks near the borders of a pluton (Turi and Taylor, 1971); low-grade burial metamorphism (high-grade diagenesis) of sediments, such as those of the Belt Supergroup, Montana (Eslinger and Savin, 1973b). The gradient here (45°C/km) is slightly larger than that given by Eslinger and Savin (36°C/km), and the highest temperature here (206°C) is near the lowest temperature reported by Eslinger and Savin (~ 225°C). Assuming a uniform gradient over several kilometers, the present topographic surface of Burned Mountain must have been buried 3.8 kilometers at the time this veining took place. It is important to note that the high-pressure phase assemblages characteristic of some Franciscan rocks -- glaucophane, lawsonite, jadeite, aragonite -- occur rarely in the Mayacmas Mountains, and thus a shallow burial (4 kilometers) is not unreasonable for the Franciscan sedimentary rocks of the Lakoma Fame tract.

It is assumed that an oxygen-rich fluid provided a reservoir for the precipitation of quartz and calcite in the upper veins. Even the small variation in $\delta^{18}\text{O}$ of the vein minerals with depth is quite striking, for a straight line can be drawn through the quartz points down to 1200 meters in Figure 9 almost without benefit of the least-squares treatment. The calcite $\delta^{18}\text{O}$ values are more scattered, probably because calcite oxygen is exchangeable. All quartz values fall on the high $\delta^{18}\text{O}$ side of the calcite line, and all calcite values fall on the low $\delta^{18}\text{O}$ side of the quartz line, so some isotopic equilibrium between quartz and calcite is indicated. The upper-zone veins contain no open

spaces. With no open space, the permeability to fluids which might cause further complications in the $\delta^{18}\text{O}$ records of the vein minerals is negligible. Quartz, once formed, is resistant to isotopic exchange.

The quartz and calcite are found in textural intergrowths, a further indication of some isotopic equilibrium (Plates 3, 4). In hand-picked vein samples, the H_3PO_4 reaction always left a quartz residue. Similarly, quartz had to be formic acid-treated to eliminate the calcite.

Water/mineral ratios for the upper zone can be determined from the following relationship, derived from an expression for material balance:

$$\frac{\text{number of O atoms in water}}{\text{number of O atoms in mineral}} = \frac{\text{change in } \delta^{18}\text{O} \text{ (mineral)}}{\text{change in } \delta^{18}\text{O} \text{ (water)}} \quad (\text{G-4})$$

Using the differences in $\delta^{18}\text{O}$ in quartz, and water shown in Figure 9 down to a depth of 800 meters, the value for the oxygen atom ratio is 1.14. The water/calcite oxygen atom ratio is 0.79. The corresponding weight ratio values are 0.68 for water/quartz and 0.43 for water/calcite, or, 21 weight % water, 31 weight % quartz and 49 weight % calcite. These results are indicative of how much water participated in oxygen isotope exchange relative to the vein minerals. The actual amount of water circulating through the vein system could have been greater than 21 weight % of the total water-calcite-quartz system, but a mineral/ H_2O ratio whose value is 4 to 1 indicates that the total amount of water in the fractures was small.

Because the circulation of water in the upper-zone fractures was restricted, material transport into or out of the upper zone rocks probably did not take place. In order to account for the unusual $\delta^{18}\text{O}$ values of calcite and quartz in the upper zone veins, some combination of $\delta^{18}\text{O}$ values for minerals and water must be found (in the temperature range 170 to 200°C) which could result in the $\delta^{18}\text{O}$ values for calcite, quartz and vein water given by the curves in Figure 9. Since the $\delta^{18}\text{O}$ values of calcite, quartz and water in the upper zone veins are changing with depth (and with temperature), the $\delta^{18}\text{O}$ values can be extrapolated in order to determine what $\delta^{18}\text{O}$ values these components would have at temperatures lower than the calculated isotopic temperatures in the upper zone.

From a previous calculation, the oxygen-atom ratios quartz/water and calcite/water are known:

$$\frac{n_Q}{n_W} = 0.88$$

$$\frac{n_C}{n_W} = 1.27$$

in which n is the number of oxygen atoms in the species quartz (Q), calcite (C) and water (W). The atom fractions of oxygen in the three components quartz, calcite, and water are:

$$X_Q = \frac{n_Q}{n_Q + n_C + n_W} = 0.28$$

$$X_C = \frac{n_C}{n_Q + n_C + n_W} = 0.40$$

$$X_W = \frac{n_W}{n_Q + n_C + n_W} = 0.32$$

At any temperature, the quartz-water and calcite-water oxygen isotope fractionation factors are known:

$$\alpha_{QW} = \frac{1 + \frac{\delta_Q}{1000}}{1 + \frac{\delta_W}{1000}} \quad (G-5)$$

$$\alpha_{CW} = \frac{1 + \frac{\delta_C}{1000}}{1 + \frac{\delta_W}{1000}} \quad (G-6)$$

whose values can be obtained from the evaluation of Equations (G-2) and (G-3) at any temperature. The material balance equation is

$$X_W \cdot \delta_W + X_C \cdot \delta_C + X_Q \cdot \delta_Q = K \quad (G-7)$$

in which K is a constant for the system. According to the data, taken from the curves in Figure 9, for $\delta_Q = 18.4\%$, $\delta_C = 15.7\%$, and $\delta_W = 7.0\%$ (800 meters depth) the value of K is 14.08. Using $\delta_Q = 19.9\%$,

$\delta_C = 16.8\text{‰}$, and $\delta_W = 5.6\text{‰}$ (at the present-day surface), K is 13.67. The two agree within 0.4, so the mean, 13.88, will be used in subsequent calculations.

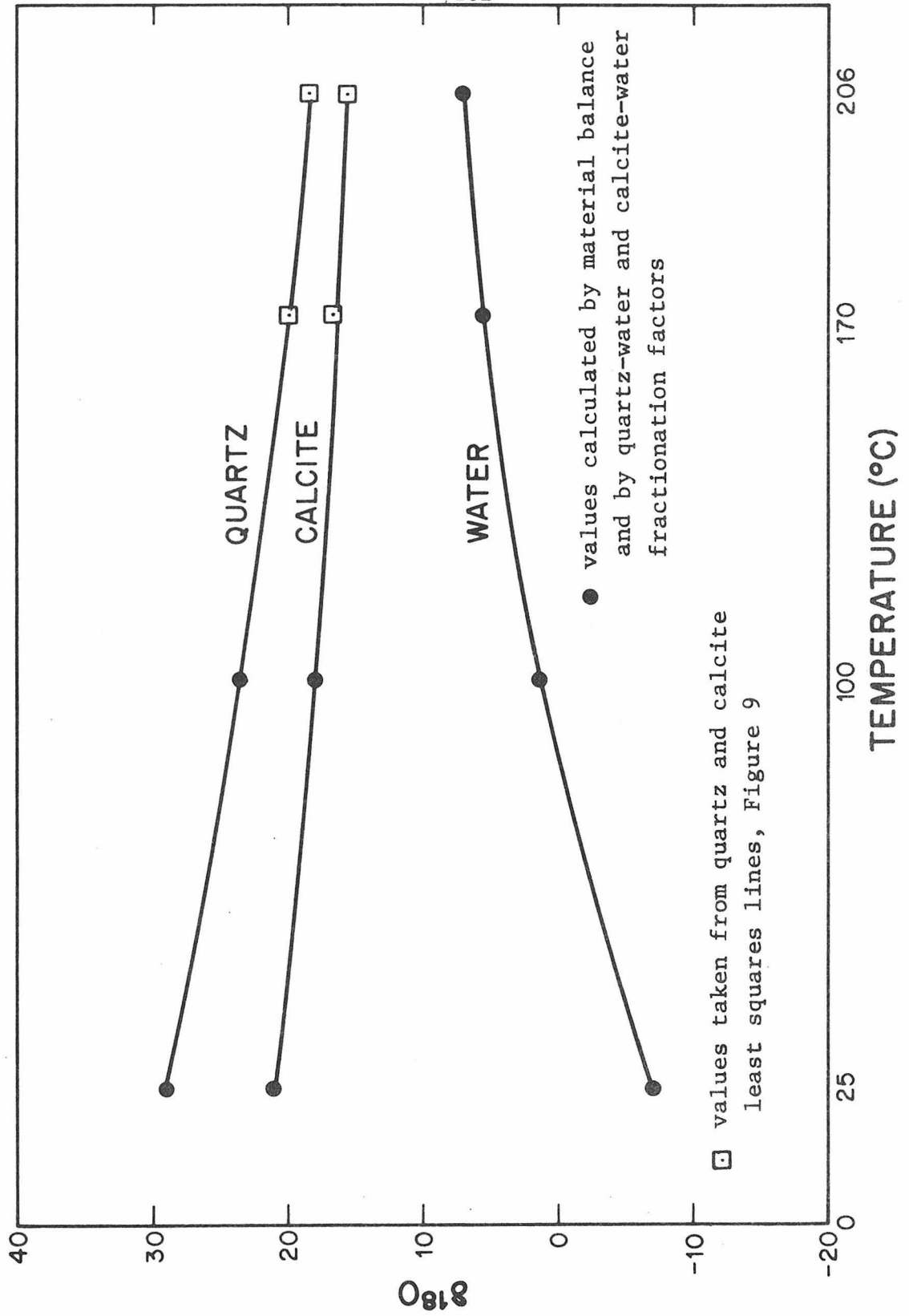
When Equations (G-5), (G-6), and (G-7) are solved simultaneously at 100°C , given that $\alpha_{CW} = 1.0166$ and $\alpha_{QW} = 1.0212$, $\delta_W = 1.3\text{‰}$, $\delta_C = 17.9\text{‰}$ and $\delta_Q = 22.5\text{‰}$. Similarly, at 25°C , at which $\alpha_{CW} = 1.0283$ and $\alpha_{QW} = 1.0283$, the calculated $\delta^{18}\text{O}$ values are $\delta_W = -7.2\text{‰}$, $\delta_C = 20.9\text{‰}$ and $\delta_Q = 27.8\text{‰}$. These results are plotted in Figure 10. The most important consequence of these results is that the $\delta^{18}\text{O}$ values of calcite and quartz extrapolated to low temperature (25°C) are very similar to $\delta^{18}\text{O}$ values of marine sediments. A $\delta^{18}\text{O}$ value of 21‰ for calcite corresponds closely to a marine limestone that has undergone some diagenesis, and a $\delta^{18}\text{O}$ value of 28‰ for quartz is reasonable for a chert from a similar environment. (Compare these values with those obtained by Engel, Clayton and Epstein, 1958, for carbonates, 21‰ to 24‰ , and cherts, 28‰ to 30‰ , from "inferred [hydrothermally] unaltered or little altered" Leadville Formation, a Mississippian marine limestone in Colorado.)

It is important to note that because the amount of water, indicated by previous calculations, that has exchanged isotopically with the minerals is small (one-fourth the mass of the minerals), the $\delta^{18}\text{O}$ of the water in the above low-temperature extrapolation is very sensitive to the exact amount of water relative to the amount of minerals. The relative amounts of water and vein minerals calculated are very approximate, since the water/mineral ratios are based upon

FIGURE 10

Calculated extrapolation to lower temperatures of $\delta^{18}\text{O}$ values of quartz, calcite and water from upper zone veins, Lakoma Fame No. 19, The Geysers.

Open squares denote $\delta^{18}\text{O}$ values of vein quartz and calcite taken from the least squares lines of Figure 9 at 0 and 800 meters depth. Those data, together with the values of α_{QW} and α_{CW} at various temperatures, and water/mineral ratios given in the text were used to obtain the $\delta^{18}\text{O}$ values denoted by solid dots. The water/mineral ratios are about 1:1, so $\delta^{18}\text{O}$ of water is very sensitive to the values of the ratios. The extrapolation to low temperature points out the possibility that the vein quartz and calcite might have been derived from marine silica and carbonate.



small changes taking place with depth in the $\delta^{18}\text{O}$ values of quartz, calcite, and vein water, which were taken from the curves in Figure 9. If the change in $\delta^{18}\text{O}$ for calcite, quartz or water were incorrect by 0.2‰, the weight percent of water would be incorrect by 2%. If both the calcite and quartz values taken from the curves are incorrect by $\pm 0.2\text{‰}$, the range in calculated weight % water would be 17% to 25%.

If, for example, the vein system were composed of 24 weight % water, 29 weight % quartz and 47 weight % calcite, the low-temperature extrapolation calculation above would give about the same $\delta^{18}\text{O}$ values for quartz and calcite at 25°C, but the $\delta^{18}\text{O}$ of water would be 0‰, the same as that of ocean water. Thus it is likely that the $\delta^{18}\text{O}$ values of the quartz and calcite in the upper-zone veins have resulted from the interaction of marine limestone and chert at 170° to 200°C with ocean water entrapped in the Franciscan sediments.

3.7.3.3 Sources of the Vein Minerals

The calculations in Section 3.7.3.2 have shown that the isotopic compositions of the quartz and calcite in upper zone veins could have originated by isotopic exchange between materials found in marine sediments and ocean water. There is no scarcity of marine sediments in the rocks penetrated by wells at The Geysers, for the rocks are the Franciscan graywackes and spilitic basalts (greenstones), indicative of geosynclinal marine deposition. Although McNitt (1968) has found no mappable limestone bodies anywhere in the Franciscan rocks in the Mayacmas Mountains, a certain amount of marine carbonate could be expected to be incorporated into these muddy sediments and pillow-lavas.

McNitt also reported the occurrence of small lenses of thin-bedded red cherts a few meters thick in the vicinity of The Geysers. "Red rock" fragments, thought to be chert relics, are found in the upper zone of LF 15 and LF 13, but consist largely of hematite, and contain veins of quartz (Plate 5). The source of the vein minerals would be the most soluble and consequently the most easily transported material available, specifically calcite and hydrous silica (chert). The preferential removal of silica from the chert by dissolution would leave a residue rich in the less-soluble hematite, which is observed in most samples of "red rock."

3.7.3.4 Variations in $\delta^{18}\text{O}$ Values of Vein Minerals in the Lower Zone (Steam Zone)

It was indicated previously that calcite samples from depths greater than 900 meters in Lakoma Fame No. 19 had $\delta^{18}\text{O}$ values lower than those of the upper zone vein calcite. Furthermore, crystals of euhedral quartz in the lower zone were found to be of lower ^{18}O content than fragments of massive quartz from the lower zone. The significance of this difference will be discussed below, but first the variations in $\delta^{18}\text{O}$ and modes of occurrence of each mineral will be described in more detail.

3.7.3.4.1 Quartz

Quartz is the principal vein mineral in the lower zone of LF 19. A number of cuttings fractions in LF 19 contained both milky-massive and euhedral quartz. Massive quartz is invariably richer in ^{18}O than the euhedral variety. The euhedral quartz $\delta^{18}\text{O}$ values are always less

than 8‰, one value being as low as 4.7‰. Clusters of euhedral crystals, less than 3 mm across were found adhering to host rock fragments in lower zone cuttings. Two cuttings fractions contained such clusters attached to the crystal faces of rhombohedral platelets of calcite about 2 mm across. The presence of these well-defined crystal faces indicates that these crystals grew in open fractures. The dominant host rock type in the steam zone is serpentinite. One serpentinite core kept by Union Oil shows open fractures lined with rhombs of calcite and prisms of quartz.

The fact that mineral deposition occurs in open fractures in serpentinite, indicated by Union's core and the crystals from LF 19 cuttings, is somewhat unusual. Serpentinite "flows" under pressure, and does not possess the mechanical rigidity necessary to maintain open fractures. The Clear Lake area is seismically active (Garrison, 1972; Lange and Westphal, 1969). Evidently this seismic activity is sufficient to continuously form open fractures, counteracting the tendency of serpentinite to mechanically self-seal. Open fractures are essential to allow for the passage of steam through a hydrothermal system, if the permeability of host rock is low, as is the case in most vapor-dominated hydrothermal systems.

In the depth interval 1418 meters to the bottom of LF 19 (1659 meters), massive quartz fragments commonly exhibit overgrowths in the form of drusy coatings. If these coatings were generated by the same episode of deposition which was responsible for the euhedral quartz, whose $\delta^{18}\text{O}$ is 8‰ or less, the overgrowths would change the $\delta^{18}\text{O}$ of

massive quartz fragments, whose $\delta^{18}\text{O}$ values initially lay near the quartz least-squares line in Figure 9. The isotopic effect would be to lower the $\delta^{18}\text{O}$ of the total quartz.

The contribution of lower- $\delta^{18}\text{O}$ quartz to some fragments of massive quartz seems minor, because the $\delta^{18}\text{O}$ values of massive quartz seem to be still genetically related to those of upper zone massive quartz. Many of the lower zone massive quartz $\delta^{18}\text{O}$ values lie near the extension of the least-squares line defined by the $\delta^{18}\text{O}$ values of the upper zone massive vein quartz.

In the neighborhood of 1509 meters depth some quartz fragments have $\delta^{18}\text{O}$ values higher than most other massive quartz values in the lower zone. Their values are 19 and 20‰. These particular fragments were found in cuttings fractions that also contained appreciable amounts of "red rock," which was inferred to be a recrystallized derivative of chert. Cherts typically have $\delta^{18}\text{O}$ values as high as 38‰ (Knauth and Epstein, 1974). The chert in the Franciscan sequence could have served as a local source of silica rich in ^{18}O , and the quartz samples whose $\delta^{18}\text{O}$ values are 19 to 20‰ could conceivably preserve in their isotopic records indications of their derivation from ^{18}O -rich materials such as cherts.

All euhedral quartz samples have $\delta^{18}\text{O}$ values between 4.7 and 7.7‰. One quartz sample, from 1387 m in LF 19 had a $\delta^{18}\text{O}$ of +11.8. Visual inspection showed it to be a nonseparable aggregate of euhedral and massive quartz. The intermediate $\delta^{18}\text{O}$ value is the expected result of the mixing of the two types of quartz. The 4.7 to 7.7‰ range in

ehedral quartz values from LF 19 also covers the range of authigenic quartz values encountered in the Salton Sea Geothermal Field (7.25‰; Clayton, Muffler, and White, 1968) and in the Ohaki-Broadlands are in the lower 500 meters of hole Br-16 (6.04 to 7.43; Eslinger and Savin, 1973). The 4.71‰ value from 1406 meters depth in LF 19 is one of the lowest yet found for quartz in an active hydrothermal system, but is not as low in $\delta^{18}\text{O}$ as quartz from a sericite vein at Butte, which has a $\delta^{18}\text{O}$ near 0‰ as reported by Garlick and Epstein (1966).

3.7.3.4.2 The Relative Resistance of Vein Quartz and Calcite to Hydrothermal Alteration

The fact that upper-zone type $\delta^{18}\text{O}$ values are preserved in massive quartz of the lower zone pays tribute to the resistance of quartz to oxygen isotope exchange, once the quartz is formed. Calcite $\delta^{18}\text{O}$ seems to be less resistant to change in the lower zone environment, for all lower zone calcite $\delta^{18}\text{O}$ values are less than 12‰ and most are less than 10‰. The lowest $\delta^{18}\text{O}$ value for calcite in the upper zone is 14.5‰ by comparison.

The total stratigraphic section seems to be poor in limestone and the lower zone host rock (mostly serpentinite) is poor in free silica. Consequently, vein minerals now preserved mostly in the upper zone probably provided silica and carbonate to be dissolved and redeposited by the fluid active in the lower zone fractures. The isotopic compositions of the newly-deposited minerals will reflect the temperature and isotopic composition of the fluid with which they were most recently in isotopic (and chemical) equilibrium.

3.7.3.5 The Significance of the Barren Zone

It is not known precisely at what depth dry steam was encountered in LF 19. The precise depth of the carbonate discontinuity is similarly unknown, aside from the fact that it occurs somewhere between 784 and 930 meters depth. The dominant rock type deeper than about 600 meters is chloritic serpentinite, probably not sufficiently competent to maintain open fractures for very long. Absence of open fractures implies no vein-system development. Serpentine tends to "flow" under pressure, and probably seals fractures by mechanical deformation. Serpentine is not a good reservoir rock for this reason. This probably explains why LF 19 was not considered economical by Union Oil. The unveined zone is perhaps a mechanically-produced analogue of self-sealing by fracture filling, described by Facca and Tonani (1967).

3.7.3.6 Quartz-Calcite Oxygen Isotope Geothermometry in the Lower Zone

It is difficult to determine quartz-calcite oxygen isotope temperatures from $\delta^{18}\text{O}$ values of minerals in the lower zone. First, there are few lower zone cuttings fractions which contain both quartz and calcite. Secondly, in the cases of cuttings fractions which do contain both quartz and calcite there is a question of whether or not the original equilibrium α_{QC} has been preserved. The first complication is irreparable and inescapable, in the light of the haphazard sampling of cuttings on the mud screen during the drilling of exploratory wells. The second complication arises from the fact that quartz, once formed, does not exchange its oxygen with fluids as readily as can calcite.

The latter difficulty is assuaged in part through an examination

of the modes of occurrence of lower zone quartz and calcite. When calcite and euhedral quartz were found in the same cuttings fraction, only then were their $\delta^{18}\text{O}$ values used to calculate an isotopic temperature. Also, only those quartz-calcite pairs were considered which came from cuttings fractions containing quartz crystal clusters attached to faces of calcite rhombs. Such a relationship is surely indicative of chemical and isotopic equilibrium between the minerals. Some calcite rhombs occur singly, without attached quartz. None of the calcite rhombs are etched or corroded; all are bounded by reflective crystal faces.

Since no limestone bodies have been found anywhere in the Franciscan stratigraphic section in the Mayacmas Mountains, the largest accumulation of carbonate originally nearest to the lower zone is the type of calcite that is now preserved only in the upper zone. Massive quartz occurs throughout the section penetrated by LF 19, and it was shown above that all the massive quartz belongs to the same veining episode. It is likely that vein calcite was similarly distributed through the entire stratigraphic section. In Figure 9 the trend of calcite $\delta^{18}\text{O}$ values through which the least-squares line was drawn stops abruptly at 800 meters, but the trend probably at one time extended through the entire stratigraphic section penetrated by LF 19.

The original calcite of higher $\delta^{18}\text{O}$ (about 15‰) in lower zone veins was probably dissolved by some fluid. The present day $\delta^{18}\text{O}$ values of lower zone calcite, most of which are less than 10‰, resulted when the calcite was precipitated from a fluid whose $\delta^{18}\text{O}$ was lower than

that from which upper-zone-type calcite ($\delta^{18}\text{O}$ greater than 14‰) formed. The only euhedral calcite found in LF 19 occurred in association with euhedral quartz. The other samples of lower zone calcite are massive and are visually indistinguishable from upper zone vein calcite. At some horizons in LF 19 the dissolution-reprecipitation process appears to be incomplete. In LF 19-74 (Table 3) the calcite $\delta^{18}\text{O}$ was +12.2, a value intermediate between upper zone values (15 to 16‰) and most lower-zone values (6‰ and less). It is clear that this calcite is not in isotopic equilibrium with the other lower zone calcites. The anomalous intermediate $\delta^{18}\text{O}$ value (+12.2‰) could be the result of mixing of some incompletely dissolved higher- $\delta^{18}\text{O}$ calcite and some lower- $\delta^{18}\text{O}$ calcite that was precipitated later, both varieties of which were found in the same cuttings fraction. There are no apparent overgrowths of calcite on calcite in that cuttings fraction, but some fragments of higher and lower $\delta^{18}\text{O}$ calcite were probably mixed together in the hand-picked calcite sample, since the two varieties are visually indistinguishable.

The details of the calculation of temperatures from quartz and calcite $\delta^{18}\text{O}$ values are the same as those described in the Thermal 7 discussion. In LF 19-77, 1204 meters depth, two analyses of calcite gave a mean $\delta^{18}\text{O}$ of 5.35‰ with a standard deviation of 0.06‰. The mean $\delta^{18}\text{O}$ of two different hand-picked batches of euhedral quartz was 7.07‰ with a standard deviation of 0.31‰. The mean $1000 \ln \alpha_{\text{QC}}$ for this pair is 1.71, giving a mean isotopic temperature of 320°C. Using the maximum α_{QC} allowed by the individual quartz and calcite analysis,

$\alpha_{\text{QC}} = 1.00729/1.00530 = 1.00198$, the calculated temperature is 278°C. Using the minimum $\alpha_{\text{QC}} = 1.00685/1.00539 = 1.00145$, the temperature is 370°C. This temperature range may have a real significance in terms of the thermal history of the lower zone, but it should be realized that the quartz-calcite geothermometer in the region of 300°C is highly sensitive: a change in $1000 \ln \alpha_{\text{QC}}$ of 0.1‰ changes the indicated isotopic equilibrium temperature by 20°C. In spite of the possibility that the temperature may have varied between 278°C and 370°C during the deposition of quartz and calcite in this cuttings fraction, the mean value of 320°C will be used in subsequent discussions.

Another coexisting quartz-calcite pair from LF 19, 1405 meters depth, had a mean quartz $\delta^{18}\text{O}$ of 4.71‰, standard deviation 0.03‰, and a mean calcite $\delta^{18}\text{O}$ of 1.47‰, standard deviation 0.53‰. $1000 \ln \alpha_{\text{QC}}$ obtained from the mean values, 3.23, indicates an oxygen isotope temperature of 158°C. The extremes, obtained as above, are 134°C and 187°C. Again, the temperature variation, indicated by variation in $\delta^{18}\text{O}$ values of this quartz-calcite pair, may have physical significance, but in subsequent discussions, an intermediate temperature, 160°C, will be cited.

When the extremes in the above temperatures are taken into consideration, together with the extremes of calcite $\delta^{18}\text{O}$ variations, waters calculated to be in equilibrium with the above-mentioned calcites have mean $\delta^{18}\text{O}$ values of -1‰ (S.D. 1‰) for the "320°C" quartz-calcite pair, and -10‰ (S.D. 3‰) for the "160°C" pair.

These calculated $\delta^{18}\text{O}$ values for water differ greatly from those

calculated for the upper zone veins (5.5 to 7‰), indicated by the water curve in Figure 9. The fact that the $\delta^{18}\text{O}$ values for water in the lower zone are much lower than those in the upper zone indicates that the regimes of hydrothermal alteration in the two zones were quite distinct. The fact that the lower zone waters have $\delta^{18}\text{O}$ values less than zero suggests that their origins may be traced to meteoric waters, whereas it was shown in section 3.7.3.2 that the upper zone vein water was probably derived from ocean water. The calculated $\delta^{18}\text{O}$ values of lower zone waters will next be compared with the $\delta^{18}\text{O}$ values of waters which might serve as a predominant source of fluid in the lower zone. It will be shown that the isotopic temperatures and $\delta^{18}\text{O}$ values of fluids in the lower zone are those which would be expected in an active hydrothermal system containing hot water and/or steam; therefore, the lower zone will hereafter be called the "active steam zone."

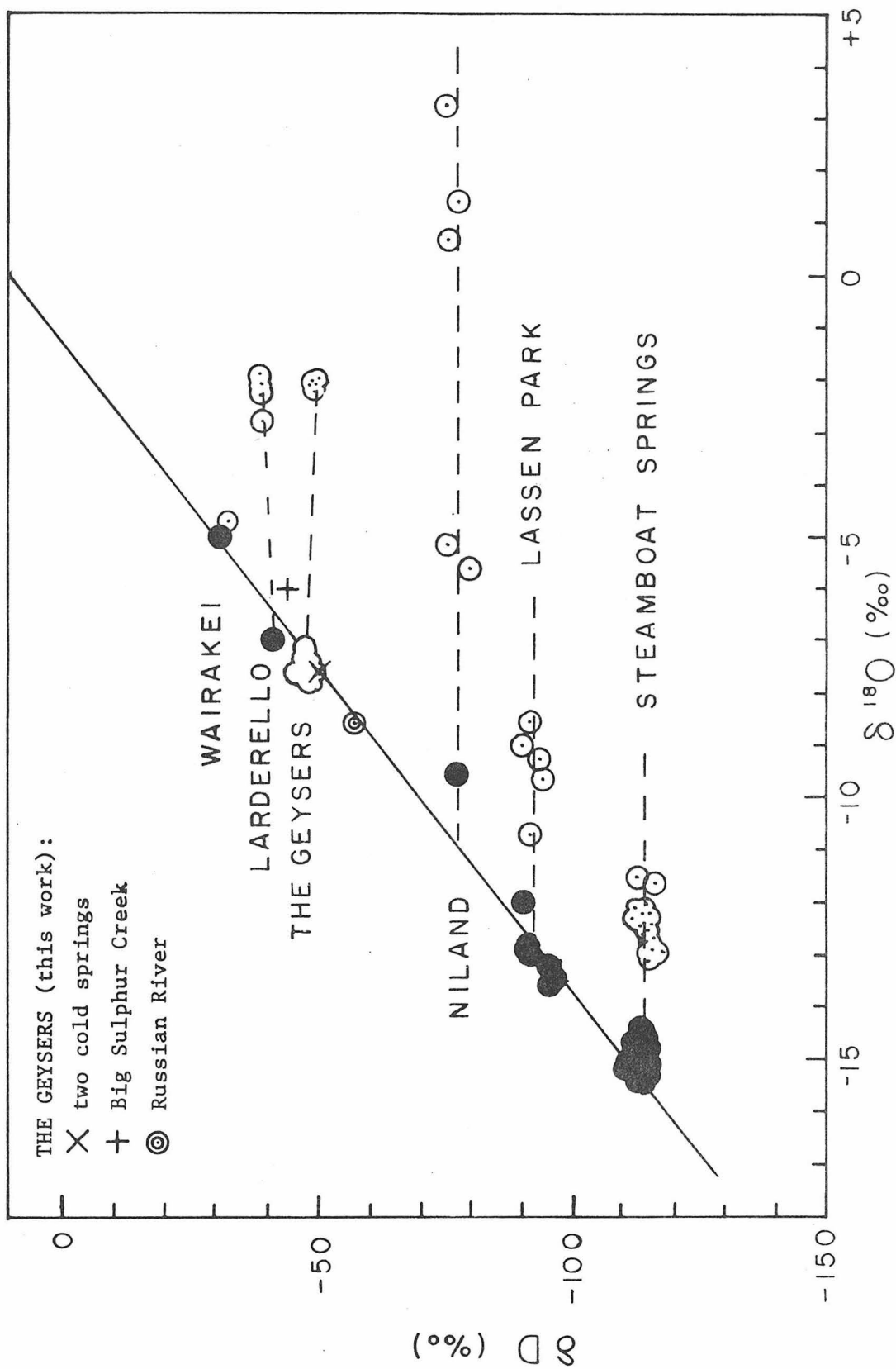
3.7.3.7 The Source of Hydrothermal Fluid in the Active Steam (Lower) Zone

Virtually all hot-spring waters have been shown to have been derived from local meteoric waters, regardless of locality. Relationships between $\delta^{18}\text{O}$ and δD values of waters from various thermal areas and the corresponding values of local meteoric waters in those areas are shown in Figure 11, which is modified from Craig (1963). All the thermal waters in Figure 11 are of the near-neutral, chloride type. Thermal waters have about the same deuterium content as local meteoric waters, but they commonly have higher $\delta^{18}\text{O}$ values than local meteoric waters.

FIGURE 11

Variations in $\delta^{18}\text{O}$ and δD values of near-neutral chloride-type thermal waters and geothermal steam from geothermal areas (after Craig, 1963).

Solid circles (except for The Geysers) are local meteoric waters. open circles with dots are geothermal waters (except for Larderello and The Geysers, which are steam). $\delta^{18}\text{O}$ and δD values of waters from The Geysers are given. Surface cold-spring water values fall inside the open figure which outlines Craig's meteoric water values from The Geysers. The "oxygen isotope shift" of thermal waters with respect to local meteoric waters is illustrated.



The apparent enrichment in ^{18}O in thermal water with respect to meteoric water, with little or no difference in δD values, has sometimes been called the "oxygen isotope shift"; this term will be used to refer to this phenomenon in following discussions.

The enrichment in ^{18}O of originally-meteoric water is said to come about through the interaction of heated water with the host rock of a hydrothermal system. The action of the hot water commonly hydrothermally alters the host rock, adding ^{16}O to the rock and forming authigenic minerals. Conversely the rock adds ^{18}O to the water when part of the rock dissolves in the hot water. Thus, important aspects of hydrothermal alteration are not only the isotopic changes in the minerals of the host rock, but also isotopic changes in the hydrothermal fluid. Because a change in host rock isotopic composition during hydrothermal alteration must be accompanied by a change in the isotopic composition of the water, and because the hot water is commonly considered to be the altering agent, water might be said to experience "auto-hydrothermal alteration." In a common example of products of hydrothermal alteration, veined ore deposits, the fluid has long since vanished in most cases. In active hydrothermal systems, both the rock and the water are potentially available for study, so that isotopic changes in both may be measured.

Table 4 gives some $\delta^{18}\text{O}$ and δD values of some surface meteoric water samples collected from the region around The Geysers. Local ground water from the springs, collected in July of 1973, have $\delta^{18}\text{O}$ and δD values close to those reported for meteoric waters at The Geysers

TABLE 4
ISOTOPIC COMPOSITIONS OF NON-THERMAL WATER SAMPLES
FROM THE GEYSERS AND THE SURROUNDING AREA

<u>Source</u>	$\delta^{18}\text{O} \text{ ‰}$	$\delta\text{D} \text{ ‰}$	<u>Location</u>
Cold Spring 1 (hillside)	-7.70	-51.0	behind Union Oil Co. field office, The Geysers
Cold Spring 2 (muddy hole)	-7.70	-51.4	behind Union Oil Co. field office, The Geysers
Big Sulfur Creek	-6.04	-44.8	above bridge upstream from power plant, Units Nos. 1 and 2
Russian River	-8.47	-57.6	Alexander Valley Campground, Healdsburg - Geysers Road

by Craig (1963). The spring waters plot within the open figure which outlines a number of Craig's analyses for meteoric waters at The Geysers. The average $\delta^{18}\text{O}$ of The Geysers meteoric water is -8% , and the δD is -51% . Big Sulphur Creek Water, whose $\delta^{18}\text{O}$ and δD values are also indicated in Figure 11, contains higher ^{18}O and D concentrations than meteoric water. This is probably because Big Sulphur Creek drains the entire area of The Geysers and some of its water comes from fumaroles, whose aqueous emissions include water which experienced some evaporation, introducing a kinetic fractionation of oxygen and hydrogen with loss of some ^{16}O and H-rich steam, leaving the water slightly enriched in ^{18}O and D. Russian River water is depleted in ^{18}O and D with respect to The Geysers cold spring water. It drains a large area, including parts of the California Coast Ranges further inland, where the $\delta^{18}\text{O}$ and δD values of the precipitation are likely to be lower than those of the precipitation at The Geysers. Both the spring waters and the Russian River have $\delta^{18}\text{O}$ and δD values whose combinations plot in Figure 11 near the meteoric water line described by the equation of Craig (1961):

$$\delta\text{D} = 8\delta^{18}\text{O} + 10$$

which was later modified to

$$\delta\text{D} = 8\delta^{18}\text{O} + 5$$

by the work of Epstein et al. (1965, 1970).

3.7.3.8 Water/Mineral Ratios in the Active Steam Zone

It will be recalled (section 3.7.3.6) that the $\delta^{18}\text{O}$ value of water in equilibrium with calcite of the 160°C quartz-calcite pair in LF 19 was variable. The extremes in $\delta^{18}\text{O}$ values of water, calculated from the maximum and minimum isotopic temperatures (134°C to 187°C) and the maximum and minimum calcite $\delta^{18}\text{O}$ values, (using G-3) were actually -12.30‰ and -8.66‰, which have a mean of -10.48‰ and a standard deviation of 2.57, which was rounded off to $-10 \pm 3\%$. The extreme $\delta^{18}\text{O}$ values of water, calculated from the maximum and minimum $\delta^{18}\text{O}$ values of quartz and the maximum and minimum isotopic temperatures were -12.30‰ and -7.84‰, by virtue of Equation (G-2). These results have a mean of -10.08‰ and a standard deviation of 3.16‰ ($-10 \pm 3\%$). Both of these sets of results encompass in their ranges the $\delta^{18}\text{O}$ of meteoric water. $\delta^{18}\text{O}$ of meteoric water is about -8‰. As a result it can be concluded that, for all practical purposes, the water which deposited the quartz and calcite at 160°C in Lakoma Fame 19 was meteoric. The $\delta^{18}\text{O}$ of water was not altered markedly by its interaction with the host rock. This implies that during this hydrothermal deposition of quartz and calcite the amount of water was very much larger than the amount of the minerals; tersely stated, the water/mineral ratio was very large.

The same sort of material balance treatment can be applied to the maxima and minima of $\delta^{18}\text{O}$ values of quartz and calcite and isotopic temperatures of the "320°C" pair at 1200 meters. The corresponding extremes for $\delta^{18}\text{O}$ of water based on the extremes of calcite $\delta^{18}\text{O}$ are

-0.47‰ and -2.06‰ (at isotopic temperatures of 278°C and 370°C, respectively) and -0.88‰ and -2.51‰ based on extremes of quartz $\delta^{18}\text{O}$. The first pair of numbers has a mean $\delta^{18}\text{O}$ of water of -1.27‰ (S.D. 1.12‰) and the second pair has a mean $\delta^{18}\text{O}$ of water of -1.7‰ (S.D. 1.15‰). These calculated $\delta^{18}\text{O}$ values of water, more properly stated as $-1\text{‰} \pm 1\text{‰}$, are not characteristic of meteoric water in the area. Either this water is marine or meteoric water from an earlier time, during which the climate in the area of The Geysers was warmer (almost tropical), or possibly the water has acquired some ^{18}O during its interaction with rock in the hydrothermal system. $\delta^{18}\text{O}$ values for near-neutral chloride-type water from The Geysers were as high as -2‰ (Figure 11; Craig, 1963). The $\delta^{18}\text{O}$ of the water calculated from the 320°C quartz-calcite pair to LF 19 is probably the result of oxygen isotope shift, in which the water $\delta^{18}\text{O}$ was changed from its meteoric value -8‰ to -1‰ by the interaction of the hot water with country rock and/or vein minerals during dissolution/precipitation. Waters having $\delta^{18}\text{O}$ values as high as +8‰ have been reported from The Geysers by Craig (1963). However, these waters are from near-surface springs, and their high $\delta^{18}\text{O}$ values are thought to arise from non-equilibrium evaporation at the surface at 80° to 90°C (section 3.7.3.7). The oxygen shift is not as great as that which has apparently occurred in Thermal 7 in which the water might have changed its $\delta^{18}\text{O}$ from -8‰ to +3‰. If the inferred Thermal 7 water actually did undergo oxygen shift to the extent indicated, the shift is one of the largest ever encountered in an active hydrothermal system, 11‰. The maximum shift ever measured

was at Niland, in the Salton Geothermal Field of Imperial Valley, California. The $\delta^{18}\text{O}$ shift was from -10‰ to +3‰ (Figure 11).

It is perhaps significant that the highest isotopic temperature calculated from coexisting minerals in LF 19 is associated with the highest $\delta^{18}\text{O}$ of water calculated in the active steam zone. This suggests that higher temperatures are associated with lesser degrees of fluid circulation in the active steam zone. A simple material balance calculation involving only the initial meteoric water and the pre-steam episode vein material (now preserved mostly in the upper zone) will serve to illustrate the approximate water/mineral ratio involved in the formation of the "320°C" quartz and calcite. The material balance expression is:

$$\begin{aligned} &(\text{amount of mineral oxygen}) \times (\text{change in } \delta^{18}\text{O} \text{ of mineral}) = \\ &(\text{amount of water oxygen}) \times (\text{change in } \delta^{18}\text{O} \text{ of water}). \end{aligned}$$

Quartz will be used as the mineral, because quartz is the dominant authigenic mineral in the fractures in the active steam zone. In this simple closed system, $\delta^{18}\text{O}$ of quartz has been changed from 17.2‰ (massive) to 7.1‰ (euhedral). The water $\delta^{18}\text{O}$ value has been changed from -8‰ (meteoric) to -1‰ (inferred hydrothermal). The atom ratio of oxygen between vein quartz and water is

$$\frac{\text{change in quartz } \delta^{18}\text{O}}{\text{change in water } \delta^{18}\text{O}} = \frac{\text{amount of water oxygen}}{\text{amount of quartz oxygen}} = \frac{10.1}{7} = 1.44$$

There was 1 to 2 times as much water as there was quartz which exchanged oxygen during the quartz dissolution/reprecipitation at 320°C. The ratio obtained in this manner is a minimum, because some of the water which flowed through the fractures might never have interacted with the quartz.

The 320°C isotopic temperature is in good agreement with the highest temperature ever measured at The Geysers in the steam zone, 300°C.

3.7.4 Lakoma Fame No. 13

Lakoma Fame No. 13 lies a distance of 400 meters southeast of Lakoma Fame No. 19. The cuttings of LF 13 were available to a depth of 655 meters (Figure 12). Since LF 19, 13 and 15 lie along the regional structural strike (northwest-southeast, according to McNitt, 1968), the same rock types appear in all the wells. Differences in the degree of intercalation of rock types and depths of first occurrence of rock types were not surprising, considering the nonuniformity of Franciscan stratigraphy.

Quartz and calcite only from the upper zone were available for analysis, and the results appear in Table 5 and Figure 12. Note that the calcite $\delta^{18}\text{O}$ -depth profile, while far from following a simple linear relationship with depth, shows considerably less scatter than in LF 19. Except for the sample at 473 m, almost all the points describe a smooth arcuate pattern, with a maximum $\delta^{18}\text{O}$ of 17.8‰ at 213 m and a minima near 13‰ at the top and bottom of the sampled interval. The absence of a sharp discontinuity may be a function of incomplete sampling.

TABLE 5

DESCRIPTIONS AND ISOTOPIC ANALYSES OF ROCKS AND MINERALS
FROM LAKOMA FAME NO. 13, THE GEYSERS

Surface: 945 meters above sea level

See "General Remarks", Table 3

<u>Well and Number</u>	<u>Depth, meters</u>	<u>Sample Description</u>	$\delta^{18}\text{O} \text{ ‰}$	$\delta^{13}\text{C} \text{ ‰}$	<u>Remarks</u>
LF 13 - 4	61 - 67	calcite, vein	+13.73	-13.16	host rock: graywacke
LF 13 - 6	104 - 110	calcite, vein	+15.64	-10.37	
LF 13 - 7	122 - 128	calcite, vein	+16.43	- 6.72	
LF 13 - 8 a	134 - 140	calcite, vein	+16.14	- 5.69	
b		quartz, massive	+17.44		HF-HCl treated, adhering to host rock
LF 13 - 9 a	152 - 159	calcite, vein	+16.23	- 7.29	} 16.28 ± 0.06
b		calcite, vein	+16.32	- 7.37	
c		quartz, vein	+18.45		
LF 13 - 10	165 - 171	calcite, vein	+16.55	- 6.94	
LF 13 - 11	183 - 189	calcite, vein	+16.39	- 7.22	
LF 13 - 12 a	195 - 201	calcite, vein	+17.07	- 8.49	
b		quartz, from graywacke	+13.35		HF-HCl treated
LF 13 - 13	213 - 220	calcite, vein	+ 7.79	- 0.47	
LF 13 - 15	244 - 250	calcite, vein	+17.57	- 0.30	Lithology change, graywacke to greenstone

TABLE 5: LAKOMA FAME NO. 13, CONTINUED

<u>Well and Number</u>	<u>Depth, meters</u>	<u>Sample Description</u>	<u>$\delta^{18}\text{O} \text{ ‰}$</u>	<u>$\delta^{13}\text{C} \text{ ‰}$</u>	<u>Remarks</u>
LF 13 - 17 a	274 - 280	calcite, vein	+17.49	- 3.55	
b		quartz, massive	+19.71		
LF 13 - 22	360 - 366	calcite, vein	+17.09	- 2.32	Lithology change, greenstone to graywacke
LF 13 - 23	366 - 372	calcite, vein	+18.89	- 3.14	
LF 13 - 24	378 - 384	calcite, vein	+16.81	- 0.40	
LF 13 - 27	427 - 433	calcite, vein	+16.16	- 0.33	
LF 13 - 29	457 - 463	calcite, vein	+16.58	-10.16	
LF 13 - 30	470 - 476	calcite, vein	+ 7.39	- 7.93	} 7.37 \pm 0.04 Lithology change, graywacke to greenstone
			+ 7.34	- 7.97	
LF 13 - 31	482 - 488	calcite, vein	+15.48	-11.98	
LF 13 - 32	500 - 506	calcite, vein	+16.25	- 2.50	
LF 13 - 33 a	518 - 524	calcite, massive	+16.93	- 5.89	
b		calcite, crumbly	+17.65	- 5.18	
LF 13 - 34	530 - 537	calcite, vein	+16.92	- 5.43	
LF 13 - 35	549 - 555	calcite, vein	+18.11	- 0.66	
LF 13 - 38	591 - 598	calcite, vein	+16.39	- 2.85	
LF 13 - 39 a	610 - 616	calcite, massive	+14.27	- 1.17	
b		calcite, crumbly	+16.75	- 0.89	

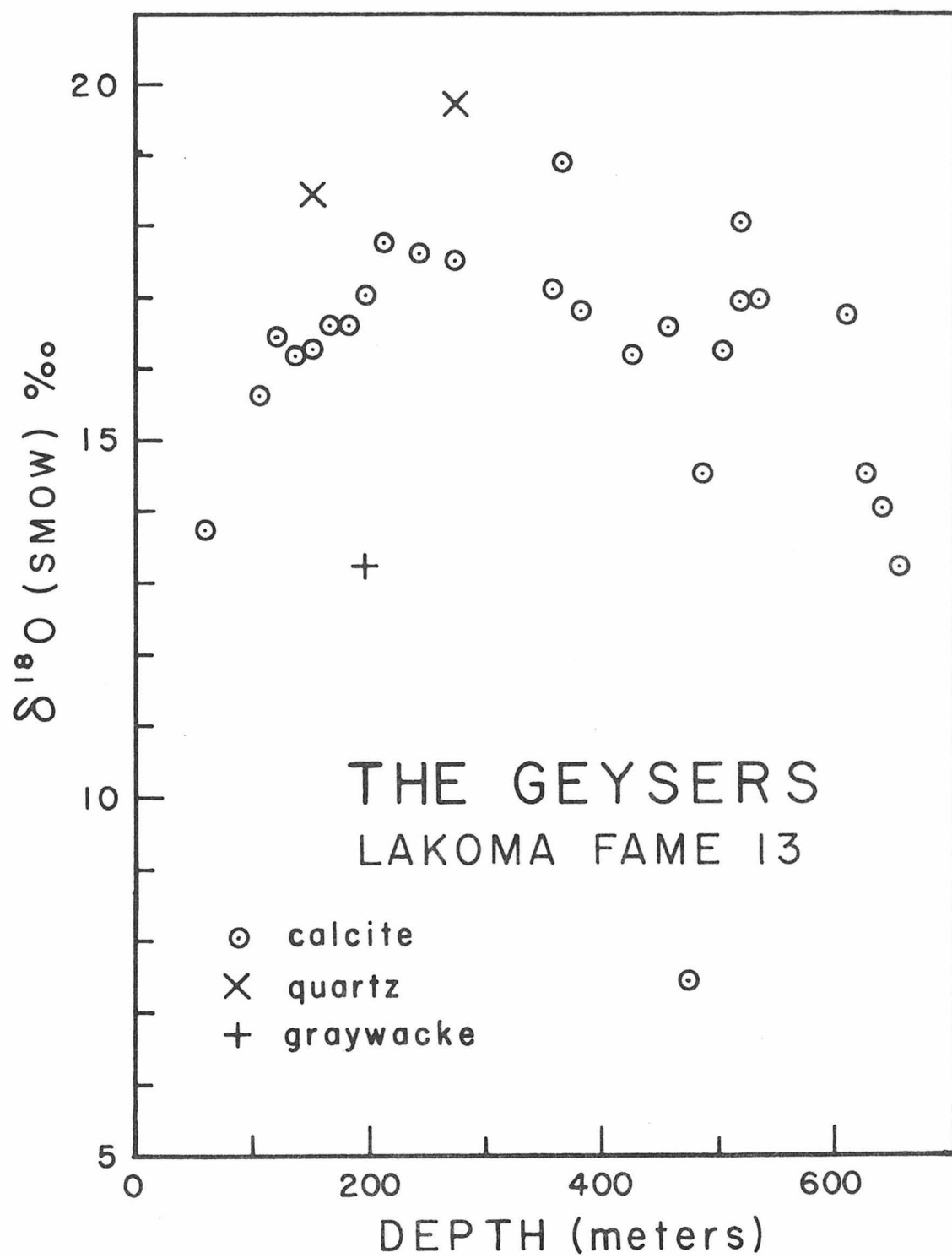
TABLE 5: LAKOMA FAME NO. 13, CONTINUED

<u>Well and Number</u>	<u>Depth, meters</u>	<u>Sample Description</u>	<u>$\delta^{18}\text{O}$ ‰</u>	<u>$\delta^{13}\text{C}$ ‰</u>	<u>Remarks</u>
LF 13 - 40	622 - 628	calcite, vein	+13.93	- 4.70	
LF 13 - 41	640 - 646	calcite, vein	+13.54	- 1.66	
LF 13 - 43	652 - 659	calcite, vein	+12.64	- 2.54	

FIGURE 12

$\delta^{18}\text{O}$ values of minerals and a rock from various depths, Lakoma Fame No. 13, The Geysers.

$\delta^{18}\text{O}$ values of vein calcite, vein quartz, and graywacke from specified depths of origin. Note the resemblance of most calcite $\delta^{18}\text{O}$ values to those from the upper zone of Lakoma Fame No. 19 (Figure 9). The two coexisting quartz-calcite pairs were used to calculate isotopic temperatures (see text).



With few exceptions, however, the range of values corresponds to that in the upper zone of LF 19.

It is probable that the sharp downward trend in the calcite $\delta^{18}\text{O}$ values near the bottom end of the sampled interval is close to the discontinuity in carbonate $\delta^{18}\text{O}$ values, which was observed in well LF 19. Some warm, low $\delta^{18}\text{O}$ fluid certainly seems to have been at work at the 473 m depth, whose calcite $\delta^{18}\text{O}$ value is 7.4‰, lower than those of many other calcites in LF 13 by 10‰.

The fact that a $\delta^{18}\text{O}$ -depth calcite profile is simpler in LF 13 than in LF 19 indicates a better state of preservation of the isotopic record of the original calcite (i.e., less post-veining reequilibration which would have produced large scatter).

Two cuttings fractions from Lakoma Fame No. 13 contained calcite of two varieties: (1) "crumbly" fragments, which disaggregated readily at the slightest pressure from forceps used in hand-picking; (2) the commonly found calcite in white massively-crystalline aggregates. In both cases the crumbly variety of calcite had the higher $\delta^{18}\text{O}$ by about 0.5‰. The "crumbly" $\delta^{13}\text{C}$ values were also higher by about 1 to 2‰. The habit and isotopic composition of the crumbly calcite suggests that it crystallized at lower temperatures than the massive variety, and may represent an ancient analog of the fine-grained calcite precipitated during quenching of a modern hydrothermal laboratory experiment (cf. O'Neil et al., 1969).

In addition to the calcite, analyses of two vein quartzes apparently coexisting with calcite are reported in Table 5 and Figure 12.

Those two quartz-calcite pairs at 152 and 274 meters give temperatures of 266° and 254°C, respectively. The calculated $\delta^{18}\text{O}$ values of vein water are 10‰ and 10.9‰, respectively. Temperatures and vein waters from the two pairs are in good agreement. A third massive quartz sample, from 137 meters depth, was a mixture of vein quartz and graywacke quartz, and had to be cleaned with the HF-HCl treatment. Because it was not purely vein quartz, its $\delta^{18}\text{O}$ value was not used to calculate an isotopic temperature.

The average upper zone vein isotopic temperature indicated by the two quartz-calcite pairs, 260°C, is significantly higher than the LF 19. The inferred horizontal gradient is around 20°C per 100 meters, between LF 19 and LF 13, normalized to the same elevation (600 meters above present sea level). The upper-zone vein fluid is not isotopically uniform over the area, but seems to be locally controlled by the temperature, which produces a mineral-fluid fractionation varying with temperature. The small fluid/rock ratio is in effect in this well also. An isotopic gradient of 3 to 5‰ in water over 400 meters is impressive. Taylor, Albee and Epstein (1963) concluded from their work that in the regional metamorphism of pelitic schists, a "widespread oxygen-bearing fluid of relatively constant $^{18}\text{O}/^{16}\text{O}$ ratio" was responsible for isotopic uniformity in mineral crystals separated as much as 200 meters. No such uniformity is indicated in the upper zone vein fluid at The Geysers, probably because less oxygen-bearing fluid was present.

3.7.5 Lakoma Fame No. 15

3.7.5.1 General Features

Lakoma Fame No. 15 lies 350 meters southeast of Lakoma Fame 13, in a straight line with LF 19 and LF 13 (Figure 6). It is the deepest of the five Lakoma Fame wells (2898 meters total depth) but was sampled only to 2200 meters. Isotopic data for various materials, depths of origin of cuttings fractions and other pertinent information are shown in Table 6, and the $\delta^{18}\text{O}$ values of materials are plotted in Figure 13. As before, most of the material analyzed comes from veins.

Although samples from Lakoma Fame 15 were not as thoroughly studied as those from LF 19 and LF 13, this well exhibits many of the features described previously in the discussions of LF 19 and LF 13. These features include (1) a discontinuity in vein carbonate $\delta^{18}\text{O}$ values, separating an upper zone from a lower zone, (2) a predominance of calcite in upper zone veins and quartz in lower zone veins, (3) the host rock types graywacke, spilitic basalt (greenstone) and serpentinite. The barren zone in LF 15 covers the depth interval 950 to 1190 meters and marks the occurrence of the carbonate $\delta^{18}\text{O}$ discontinuity. Since the surface elevation at LF 15 is 976 meters, the carbonate $\delta^{18}\text{O}$ discontinuity occurs at about 26 meters above sea level. The same feature in LF 19 (the highest occurrence of the barren zone) was observed 23 meters below sea level.

3.7.5.2 The Upper Zone

The upper zone vein carbonates in LF 15 show the $\delta^{18}\text{O}$ depth

FIGURE 13

$\delta^{18}\text{O}$ values of rocks and minerals from various depths, Lakoma Fame No. 15, The Geysers.

Many of the features depicted in Figure 9 are found in the $\delta^{18}\text{O}$ values of minerals in this figure. The ranges in $\delta^{18}\text{O}$ values in calcite in upper and lower zones correspond to the ranges found in Lakoma Fame No. 19 (Figure 9). Quartz from the upper zone is that found in gray-wacke and shows considerable deviation from massive vein quartz values (Figures 9 and 12). The one euhedral quartz and calcite pair from about 1400 meters depth shows that the $\delta^{18}\text{O}$ value of calcite is somewhat lower than the others from the lower zone (see text).

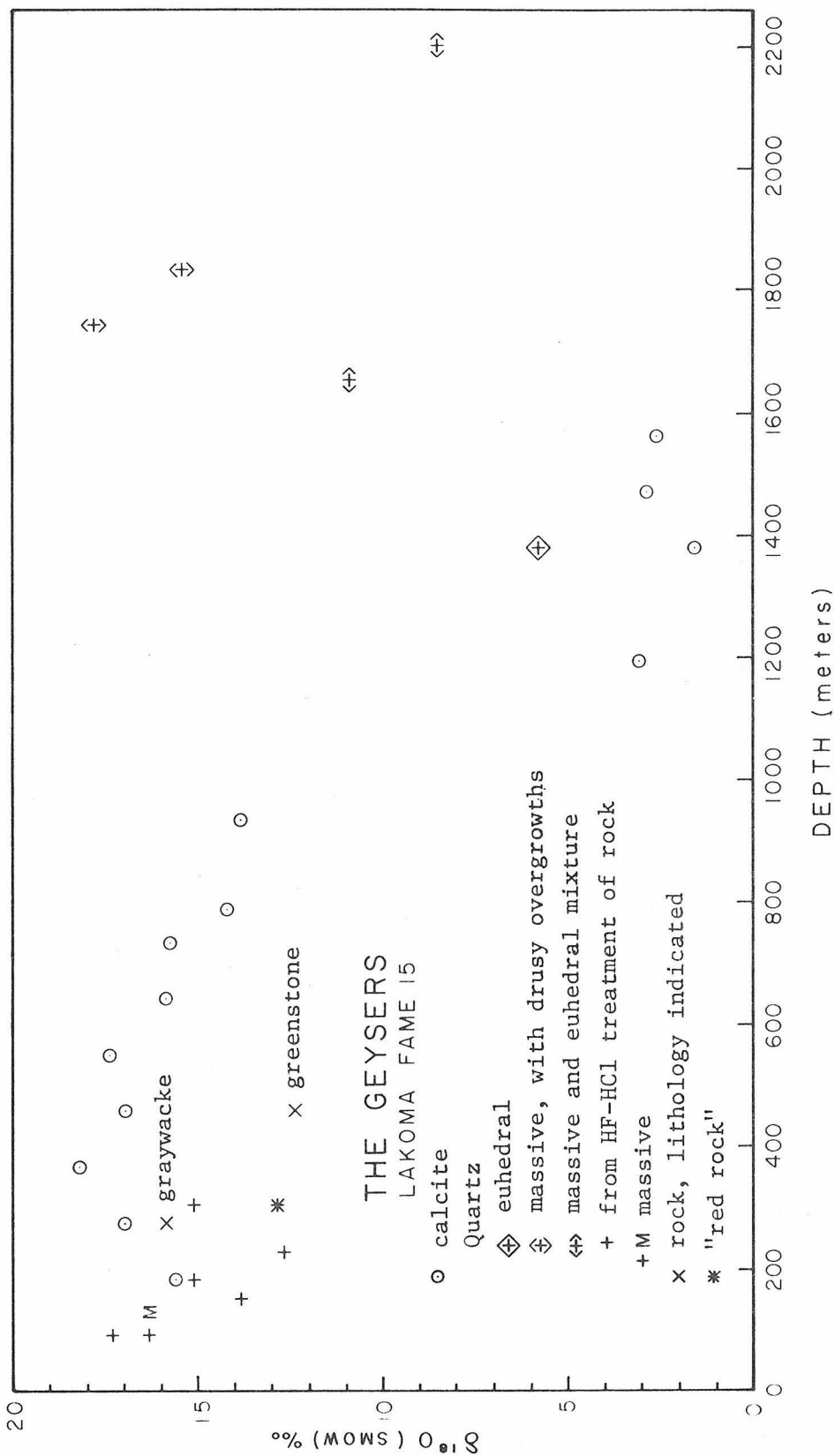


TABLE 6
 DESCRIPTIONS AND ISOTOPIC ANALYSES OF ROCKS AND MINERALS
 FROM LAKOMA FAME NO. 15, THE GEYSERS

Surface: 976 meters above sea level

See "General Remarks", Table 3

<u>Well and Number</u>	<u>Depth, meters</u>	<u>Sample Description</u>	$\delta^{18}\text{O} \text{ ‰}$	$\delta^{13}\text{C} \text{ ‰}$	<u>Remarks</u>
LF 15 - 7 a	91 - 98	calcite, vein	+17.27	-10.68	
b		quartz, massive	+16.30		
c		quartz, from graywacke	+17.30		HF-HCl treated
LF 15 - 10	152 - 159	quartz, from graywacke	+13.77		HF-HCl treated
LF 15 - 12 a	183 - 189	calcite, vein	+15.52	- 4.65	
b		quartz, from graywacke	+15.06		HF-HCl treated
LF 15 - 14	226 - 232	quartz, from graywacke	+12.63		HF-HCl treated
LF 15 - 17 a	274 - 280	calcite, vein	+16.99	- 6.74	
b		quartz, from graywacke	+17.08		HF-HCl treated
c		graywacke	+15.78		
LF 15 - 20 a	305 - 311	quartz, from graywacke	+15.06		HF-HCl treated
b		"red rock"	+12.93		
LF 15 - 24	366 - 372	calcite, vein	+18.21	- 0.37	
LF 15 - 30 a	457 - 463	calcite, vein	+16.93	- 6.14	
b		greenstone	+12.33		

TABLE 6: LAKOMA FAME NO. 15, CONTINUED

<u>Well and Number</u>	<u>Depth, meters</u>	<u>Sample Description</u>	$\delta^{18}\text{O} \text{ ‰}$	$\delta^{13}\text{C} \text{ ‰}$	<u>Remarks</u>
LF 15 - 36	549 - 555	calcite, vein	+17.40	- 1.51	
LF 15 - 43	640 - 646	calcite, vein	+15.84	- 5.18	
LF 15 - 50	732 - 738	calcite, vein	+15.73	- 1.85	
LF 15 - 54	780 - 787	calcite, vein	+14.18	- 2.63	
LF 15 - 65	927 - 933	calcite, vein	+13.86	- 7.39	
LF 15 - 82	1189 -1195	calcite, euhedral	+ 3.08	-11.84	
LF 15 - 99 a	1372 -1378	calcite, euhedral	+ 1.56	-13.15	} 6.02 ± 6.01
b		quartz, euhedral	+ 6.02		
c		quartz, euhedral	+ 6.01		
LF 15 - 103	1463 -1470	calcite, euhedral	+ 2.83	-13.50	
LF 15 - 109	1555 -1561	calcite, euhedral	+ 2.56	-14.72	
LF 15 - 115	1646 -1652	quartz, mixture	+10.88		mixture, euhedral and massive
LF 15 - 121	1738 -1744	quartz, massive	+17.82		
LF 15 - 126	1829 -1835	quartz, massive	+15.39		drusy coating
LF 15 - 150	2195 -2201	quartz, mixture	+ 8.50		mixture, euhedral and massive
	2898				bottom of well

profile characteristic of LF 19 and LF 13 upper zones, a general decline in $\delta^{18}\text{O}$ with increasing depth, similar to patterns previously described. The $\delta^{18}\text{O}$ values of carbonate are also comparable to those of upper zones in other wells. Unfortunately, no realistic quartz-calcite isotopic temperatures can be obtained for the upper zone in this well. In cuttings fractions containing both quartz and calcite the quartz does not demonstrably occur in veins; the $\delta^{18}\text{O}$ values of the two minerals either fall on top of each other, or else Δ_{QC} is less than 0, indicating non-equilibrium. Either the quartz is not wholly contemporaneous with the calcite, or the calcite has undergone post-depositional exchange with some fluid, calcite $\delta^{18}\text{O}$ values having been shifted to higher values than those originally established. The former is the more probable reason for the apparent isotopic disequilibrium because: (1) the anomalous behavior in $\delta^{18}\text{O}$ distribution is displayed in the quartz, not the calcite; (2) none of the quartz was found as free milky-white fragments but had to be chemically purified by dissolving the host rock. The resulting quartz was likely a mixture of vein and host-rock quartz, giving rise to $\delta^{18}\text{O}$ values between +12.6 and +17.3‰.

3.7.5.3 The Active Steam Zone and Oxygen Isotope Geothermometry in Lakoma Fame No. 15

Although the data presented for Lakoma Fame No. 15 in Figure 13 at first glance might appear difficult to understand, the distributions of $\delta^{18}\text{O}$ values of quartz and calcite of various varieties is virtually the same as the distribution patterns found in Lakoma Fame No. 19, depicted in Figure 9. A detailed description of $\delta^{18}\text{O}$ values of cuttings

materials from the lower zone of LF 15 will not be repeated, since the same types of features, both physical and isotopic, have been described for the lower zone of LF 19.

Only one cuttings fraction from Lakoma Fame No. 15 contained both calcite platelets and euhedral quartz: LF 15-99, at a depth of 1375 meters (Table 6). Since the quartz $\delta^{18}\text{O}$ value was 6.02‰ (a mean of two analyses; standard deviation was 0.01) and the calcite $\delta^{18}\text{O}$ value was 1.56‰, the value of $1000 \ln \alpha_{\text{QC}}$ is 4.44, which implies an equilibrium temperature of 94°C, according to Equation (G-1), and a $\delta^{18}\text{O}$ of water of -15.4‰. This temperature is much lower than any heretofore calculated from apparently cogenetic calcite and quartz at The Geysers, and the calculated $\delta^{18}\text{O}$ of water, -15.4‰ is lower even than that of local meteoric water (-8‰) which presumably supplies the hydrothermal system with fluid!

Whether or not the $\delta^{18}\text{O}$ values of quartz and calcite used in the above calculation are truly cogenetic is the critical question. The textural relationship of quartz physically attached to calcite could not be demonstrated for the LF 15 pair. Since the resistance of euhedral quartz to post-depositional isotopic alteration has been demonstrated, it is more likely that the original isotopic composition of calcite has been perturbed by recrystallization. If this recrystallization were achieved at temperatures higher than those which governed quartz deposition, the $\delta^{18}\text{O}$ would be decreased, even if the isotopic composition of the water did not change. When the quartz $\delta^{18}\text{O}$ value, 6‰, is used in conjunction with the $\delta^{18}\text{O}$ value of meteoric water, -8‰,

the calculated temperature is 167°C according to Equation (G-2). This is very close to the isotopic temperature calculated from the $\delta^{18}\text{O}$ values of quartz and calcite at 1400 meters depth in LF 19 (section 3.7.3.6), which were associated with a calculated $\delta^{18}\text{O}$ value of water close to meteoric at 160°C.

The $\delta^{18}\text{O}$ value of calcite (1.6‰) itself is anomalous with respect to the other three steam-zone calcites of Lakoma Fame No. 15, which have a mean $\delta^{18}\text{O}$ of 2.8‰ and a standard deviation 0.3‰ (Table 8; Figure 15). If this $\delta^{18}\text{O}$ value for calcite is used to recalculate the quartz-calcite isotopic equilibrium temperature and $\delta^{18}\text{O}$ of water, the temperature is 175°C and the $\delta^{18}\text{O}$ of water is -7.6‰. The calculated $\delta^{18}\text{O}$ value of the water is essentially the same as that of present-day meteoric water, -8‰. Furthermore, the temperature 175°C is in good agreement with a quartz-calcite isotopic temperature calculated from $\delta^{18}\text{O}$ values of minerals from 1400 meters depth in Lakoma Fame No. 19 (160°C). The formation of those LF 19 minerals, it will be recalled, was also associated with a water whose $\delta^{18}\text{O}$ value was around -8‰. The similarity between the calculated temperatures and the similarity between the calculated $\delta^{18}\text{O}$ values of water suggest that quartz and calcite at 1375 meters depth in LF 15 and at 1400 meters in LF 19 were deposited contemporaneously. The fact that the $\delta^{18}\text{O}$ value of water calculated for this episode of deposition is nearly meteoric indicates that the $\text{H}_2\text{O}/\text{vein mineral}$ ratio was very large. The episode of deposition described above will be called the "170°C event," in contrast to the "320°C event" inferred from the quartz and calcite $\delta^{18}\text{O}$ values

from 1200 meters depth in Lakoma Fame No. 19.

3.7.6 $\delta^{18}\text{O}$ Values of Vein Material from Lakoma Fame Numbers 8 and 9

The locations of Lakoma Fame wells 8 and 9 are indicated in Figure 6. Results of isotopic analyses of materials from the core fragments from these wells are given in Table 7, together with brief descriptions of the material.

A sample of Lakoma Fame 8 core came from 1260 meters depth. According to the descriptions of McNitt (1968) the rock type was originally a blue-green hornblende albite schist, a "metamorphic" rock. The feldspar is completely sericitized, and chlorite is extensively developed in the rock (Plate 6). Calcite veins, up to 2 cm wide, permeate the core fragment. The calcite has a $\delta^{18}\text{O}$ value of 3.4‰, characteristic of the active steam zone. The $\delta^{18}\text{O}$ of the whole rock from LF 8 (less calcite) is 5.6‰, and the δD value is -49.2‰. These values are not indicative of interaction between the metamorphic rock and meteoric water. They are more closely related to the type of hydrothermal alteration associated with minerals in the upper zone, as will be seen when host rock alteration is discussed.

The sample of core from LF 9 came from 1351 meters depth, and is an altered graywacke similar in appearance to the Thermal 7 material. It contains 1 to 2 mm wide veins, some of which are intricately crenulated, consisting primarily of calcite having a $\delta^{18}\text{O}$ of +2.5‰, characteristic of many other calcites from the steam zone. The chemically purified quartz gave a $\delta^{18}\text{O}$ value of +16.1. This $\delta^{18}\text{O}$ value of

TABLE 7

DESCRIPTIONS AND ISOTOPIC ANALYSES OF ROCKS AND MINERALS
FROM LAKOMA FAME NOS. 8 AND 9, THE GEYSERS

See "General Remarks", Table 3

Well and Number	Depth, meters	Sample Description	$\delta^{18}\text{O}$ ‰	$\delta^{13}\text{C}$ ‰	δD ‰	Remarks
LF 8 - 4133 a	1260	calcite, vein	+ 3.36	-12.62	} 3.40 ± 0.06	-49.2 LF 8-4133 is a core fragment
b			+ 3.44	-12.90		
c		chlorite-amphibole mixture	+ 5.61			
LF 9 - 4430	1351	calcite, vein quartz, from graywacke	+ 2.51 +16.12	-13.48		LF 9-4430 is a core fragment HF-HCl treated

PLATE 5.

"Red Rock," aggregate of hematite and quartz, Lakoma Fame No. 15, The Geysers. 305 to 311 meters depth, upper zone.

Area of view: 1.6×1.2 mm. X-nicols.

Intergrowth of hematite (dark) and quartz (white) inferred to be a recrystallized derivative of red chert. At least 600 meters above steam zone.

PLATE 6.

"Metamorphic Rock," with calcite vein, Lakoma Fame No. 8, The Geysers. 1260 meters depth, steam zone.

Area of view: 1.6×1.2 mm. X-nicols.

Schist composed of chlorite (dark), blue-green hornblende (bright crystals in dark field) and sericitized albite (not shown). Large white field is edge of calcite vein. Note lamellar twinning.

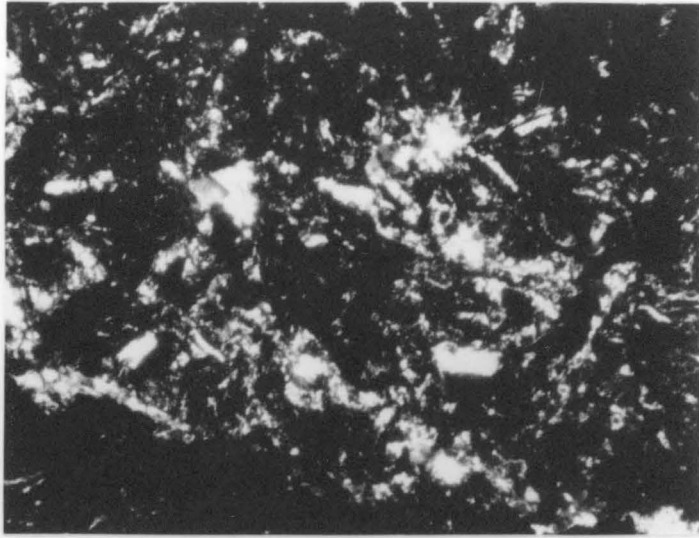


PLATE 5

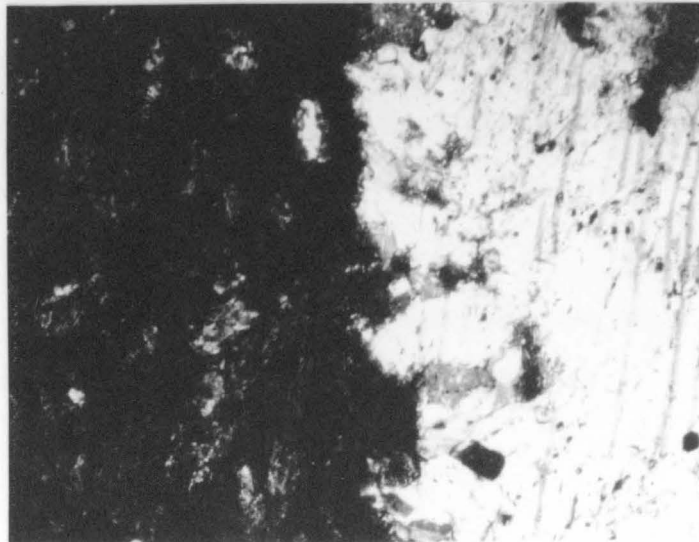


PLATE 6

quartz cannot be unambiguously interpreted as that of either detrital or hydrothermal quartz. If the quartz is detrital, it has the highest $\delta^{18}\text{O}$ value of any totally-detrital quartz yet found in The Geysers host rocks. The significance of the $\delta^{18}\text{O}$ of this quartz will be discussed under the topic of host-rock alteration in the steam zone.

Calcite samples from LF 8 and LF 9 have $\delta^{13}\text{C}$ values around -12‰ , the same as that measured in Thermal 7 calcite. The significance of the $\delta^{13}\text{C}$ values will be discussed in a section to follow.

3.7.7 The Thermal History of the Steam Zone

The isotopic analyses of quartz and calcite which have formed in fractures in the active steam zones of Lakoma Fame wells 19 and 15 indicate at least two different episodes of mineral deposition. One of these episodes was characterized by large amounts of meteoric water with respect to amounts of vein minerals. The temperature was 160 to 180°C. The other episode was associated with a higher temperature, 320°C, and comparable amounts of minerals and water. The water $\delta^{18}\text{O}$ was about -1‰ .

The first episode, involving large amounts of meteoric water in the system at 160 to 180°C is reminiscent of a hot-water system. It is conceivable that a hot-water system was a precursor to the vapor-dominated system at The Geysers. Even though there were no direct temperature measurements available from Lakoma Fame wells, there is evidence to suggest that temperatures higher than 160 to 180°C prevail in the active steam zone. First, the calculated isotopic temperature range 160° to 180°C is associated with calculated water $\delta^{18}\text{O}$ values

near that of local meteoric water, with no apparent oxygen isotope shift. All the fumarolic water from The Geysers that was analyzed by Craig (1963) had $\delta^{18}\text{O}$ values around -2% , indicating an oxygen isotope shift of $+6\%$ with respect to meteoric water (Figure 11). Those fumarolic waters originated from wells whose measured temperatures were mostly higher than 190°C (Figure 8). The isotopic results of Thermal 7 suggested that measured temperatures might be lower than pre-drilling steam reservoir temperatures. Consequently, temperatures of steam reservoirs whose fluid has an oxygen isotope shift would be substantially higher than 180°C . The most obvious indication of steam-reservoir temperatures higher than 180°C , however, is the fact that steam from wells drilled in the Lakoma Fame tract is successfully being used to generate electricity. The Pacific Gas and Electric Company steam turbines are designed to operate at temperatures of around 200°C and pressures of around 7 kg/cm^2 (McNitt, 1963). Steam is fed directly from production wells to the turbines, so the steam reservoir temperature must be substantially higher than 200°C in order for the resource to be economic, since there is heat loss (a temperature decrease) in the steam between the bottom of the well and the turbine. Thus, if there were a 160 to 180°C hydrothermal episode, as indicated by the isotopic data, it must have occurred before the episode that is now producing geothermal steam.

Isotopic records in quartz and calcite that bear testimony to a former episode of water-rock interaction at 160 to 180°C are relics which must have been partially preserved in "pockets" isolated from

fluids of higher temperature. Isotopic records of this event have not been completely preserved, as could be seen in the case of calcite from sample number LF 15-99. Note that its observed $\delta^{18}\text{O}$ value, 1.6‰, indicated a quartz-calcite oxygen isotope temperature of around 100°C, which was thought to be too low. Since three other calcite $\delta^{18}\text{O}$ values in the steam zone of LF 15 were around 3‰, it was reasoned that the LF 15-99 calcite $\delta^{18}\text{O}$ had been lowered from its original value through an interaction with a fluid at temperatures higher than those at which the LF 15-99 euhedral quartz formed. The lower $\delta^{18}\text{O}$ value for calcite (1.6‰) yielded a $1000 \ln \alpha_{\text{QC}}$ value of 4.4‰, which indicated a temperature of about 100°C and an equilibrium $\delta^{18}\text{O}$ value for water which was -15‰, 7‰ less than the local meteoric water $\delta^{18}\text{O}$, -8‰. When the LF 15-99 calcite $\delta^{18}\text{O}$ value was readjusted to be consistent with the others from the lower zone of LF 15 (2.8‰), the calculated temperature was 175°C and the equilibrium $\delta^{18}\text{O}$ value of water was around -8‰. These results were in good agreement with similarly derived results from Lakoma Fame No. 19, cuttings fraction LF 19-90. If the LF 15-99 calcite measured $\delta^{18}\text{O}$ (1.6‰) is used with the $\delta^{18}\text{O}$ of meteoric water (-8‰), the oxygen isotope temperature, according to Equation (G-3), is 260°C.

Since the likelihood of a temperature increase in the history of the steam zone has been indicated, it is logical that the 320°C event, preserved in the isotopic records of quartz and calcite at 1200 meters depth in Lakoma Fame No. 19, would follow the 260°C event. At the same time, restricted water circulation is associated with the 320°C event,

because the calculated equilibrium $\delta^{18}\text{O}$ value of water was as high as -1‰, an oxygen isotope shift of +7‰ with respect to meteoric water. A warming trend is expected, if the heat source for The Geysers hydrothermal system is a cooling magma chamber, which had earlier produced the Clear Lake volcanics. Country rocks become warmer as magma cooling progresses. Increase in temperature indicated by isotopic compositions of fracture-filling minerals is consistent with heating of host rocks by cooling magma.

History of the steam zone can be presented in terms of the processes occurring in a self-sealing geothermal field, as suggested by Facca and Tonani (1967). An episode of hot meteoric water circulated in fractures at 160 to 180°C, depositing minerals. The closest analogue of this is a hot-water system, but only fractures contributed permeability. Fractures in serpentinite seal by mechanical deformation and by mineral deposition. The temperature was raised to about 250°C; calcite filled most space that was left. Temperature increased with little water circulation. When a new fracture system formed, circulation was not as great and involved less fluid. A vapor-dominated hydrothermal system developed in which mineral deposition was slow to fill fractures, since a steam-water mixture is not an efficient solvent. The effects of interaction between steam and host rocks will be discussed in conjunction with the variations in isotopic compositions of host rocks, in a following section.

3.7.8 Implications of Carbonate $\delta^{13}\text{C}$ Values in Lakoma Fame Wells

3.7.8.1 Overview

$\delta^{13}\text{C}$ values taken from Table 3 for calcites from LF 19 are plotted in Figure 14. The 800-meter depth carbonate discontinuity is readily apparent. The distinction between upper and lower zone is made not on the basis of the absolute $\delta^{13}\text{C}$ values, but on the range in $\delta^{13}\text{C}$ values. This range is 16‰ (from +1‰ to -15‰) in the upper zone, and only 7‰ (from -8‰ to -15‰) in the lower zone. Furthermore, the two ranges overlap. Certainly there is no correlation of $\delta^{13}\text{C}$ of calcite with depth as there was in the case of upper zone carbonate $\delta^{18}\text{O}$.

The essential difference between upper and lower zone carbonate $^{13}\text{C}/^{12}\text{C}$ ratios is seen more easily in the $\delta^{18}\text{O}-\delta^{13}\text{C}$ plot in Figure 15. The upper 800 meters of the well is characterized by a wide range of $\delta^{13}\text{C}$ and a narrow range of $\delta^{18}\text{O}$, and the trend in the pattern has a very steep positive slope. A nearly-horizontal trend is indicated by the data from lower zone carbonates: the narrow range of $\delta^{13}\text{C}$ but a diversity of $\delta^{18}\text{O}$ values.

Similar features are found in the $\delta^{13}\text{C}$ data from LF 15 (Table 6) shown in Figure 16 and in Figure 17. Compared to Figure 15, Figure 17 shows more oxygen variation in the upper zone, and less in the lower zone.

Even though only the upper zone is represented in LF 13, the large $\delta^{13}\text{C}$ variation is much the same as in the other two wells (Figure 18). The nearly-vertical trend in the $\delta^{18}\text{O}-\delta^{13}\text{C}$ pattern is also found in this well (Figure 19).

FIGURE 14

$\delta^{13}\text{C}$ values of vein calcite from various depths, Lakoma Fame No. 19, The Geysers.

Note the $\delta^{13}\text{C}$ variation (-15 to +1‰) in the zone less than 800 meters deep, whereas the variation at greater depths is only -15 to -8‰. The abrupt change in $\delta^{13}\text{C}$ range occurs at a depth which corresponds to that of the calcite $\delta^{18}\text{O}$ discontinuity in Figure 9.

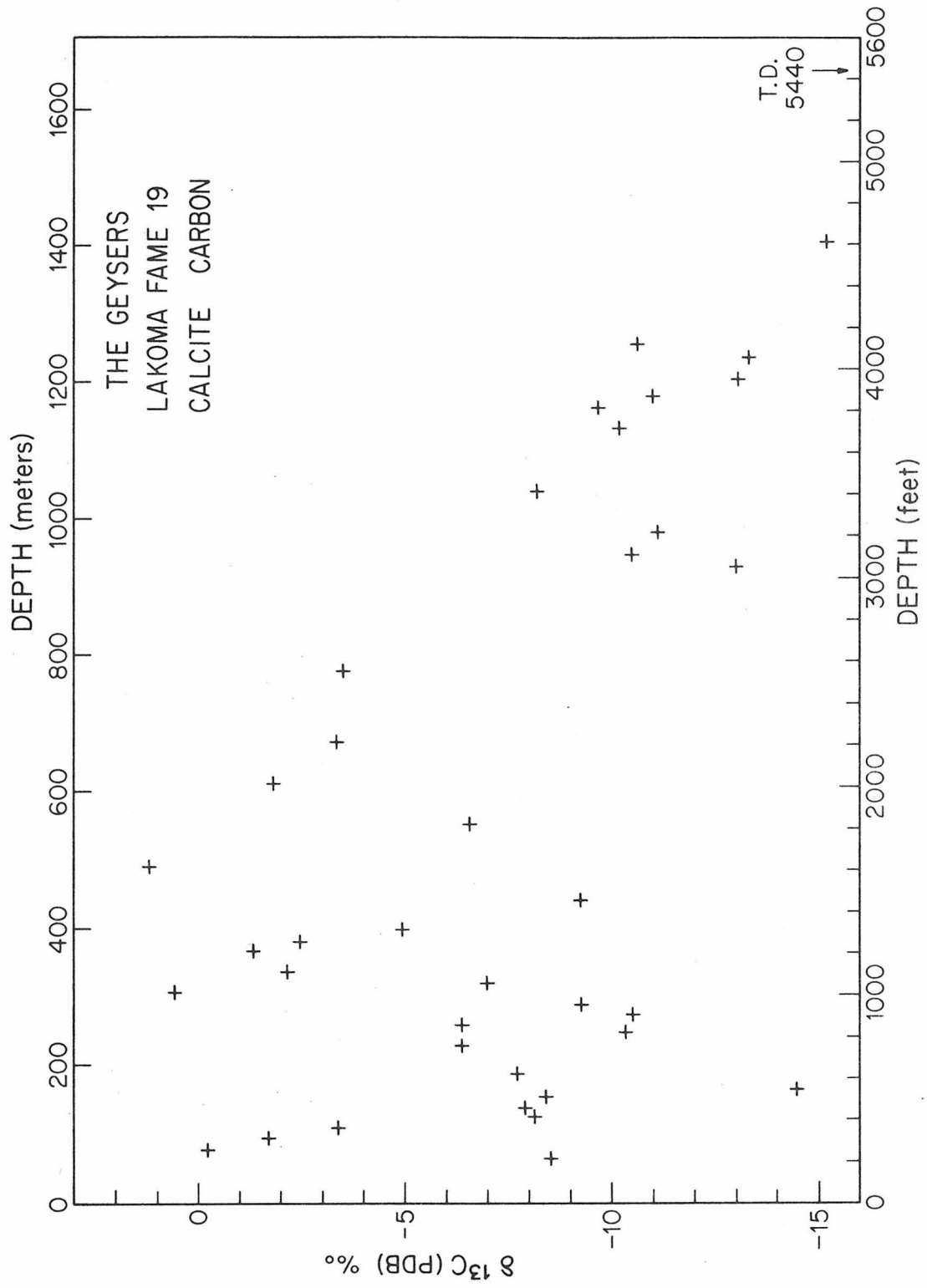


FIGURE 15

$\delta^{13}\text{C}$ values *versus* $\delta^{18}\text{O}$ values for calcites from Lakoma Fame No. 19, The Geysers.

The upper zone calcite points are discernible in the nearly-vertical trend, showing a large variation in $\delta^{13}\text{C}$ and a smaller variation in $\delta^{18}\text{O}$. The lower (active steam) zone calcite points are distributed as a nearly-horizontal trend, with considerably more variation in $\delta^{18}\text{O}$ than in $\delta^{13}\text{C}$ values. $\delta^{13}\text{C}$ and $\delta^{18}\text{O}$ values of calcite from the steam zone of Thermal No. 7 (T7-450) are also shown.

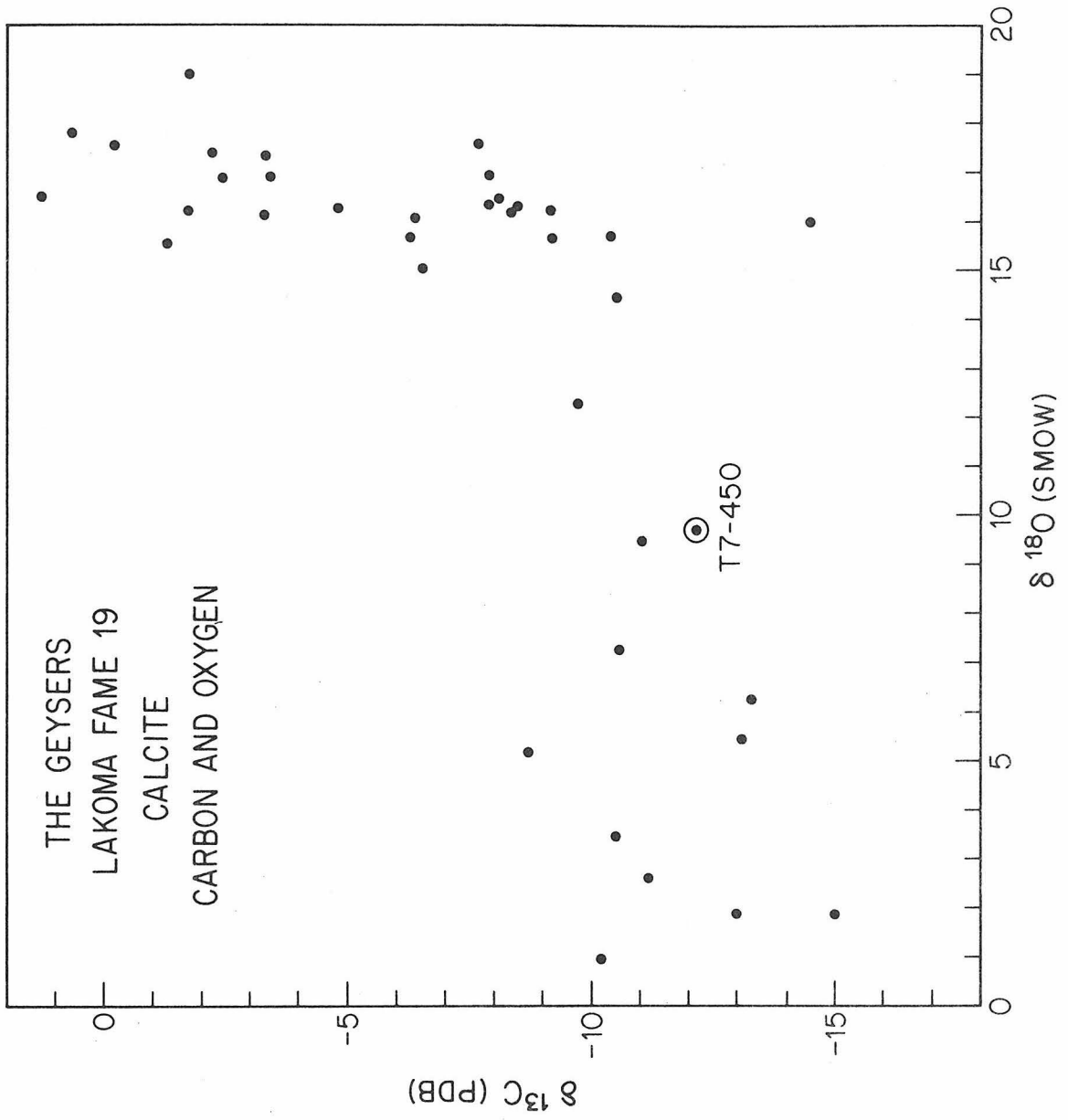


FIGURE 16

$\delta^{13}\text{C}$ values of vein calcite from various depths, Lakoma Fame No. 15, The Geysers.

This distribution of calcite $\delta^{13}\text{C}$ values with depth displays the same features as were shown in Figure 14. The calcite discontinuity occurs at about 1000 meters depth. Above that level the $\delta^{13}\text{C}$ variation is large (-11 to 0‰) and below that level the variation is much smaller (-14 to -12‰).

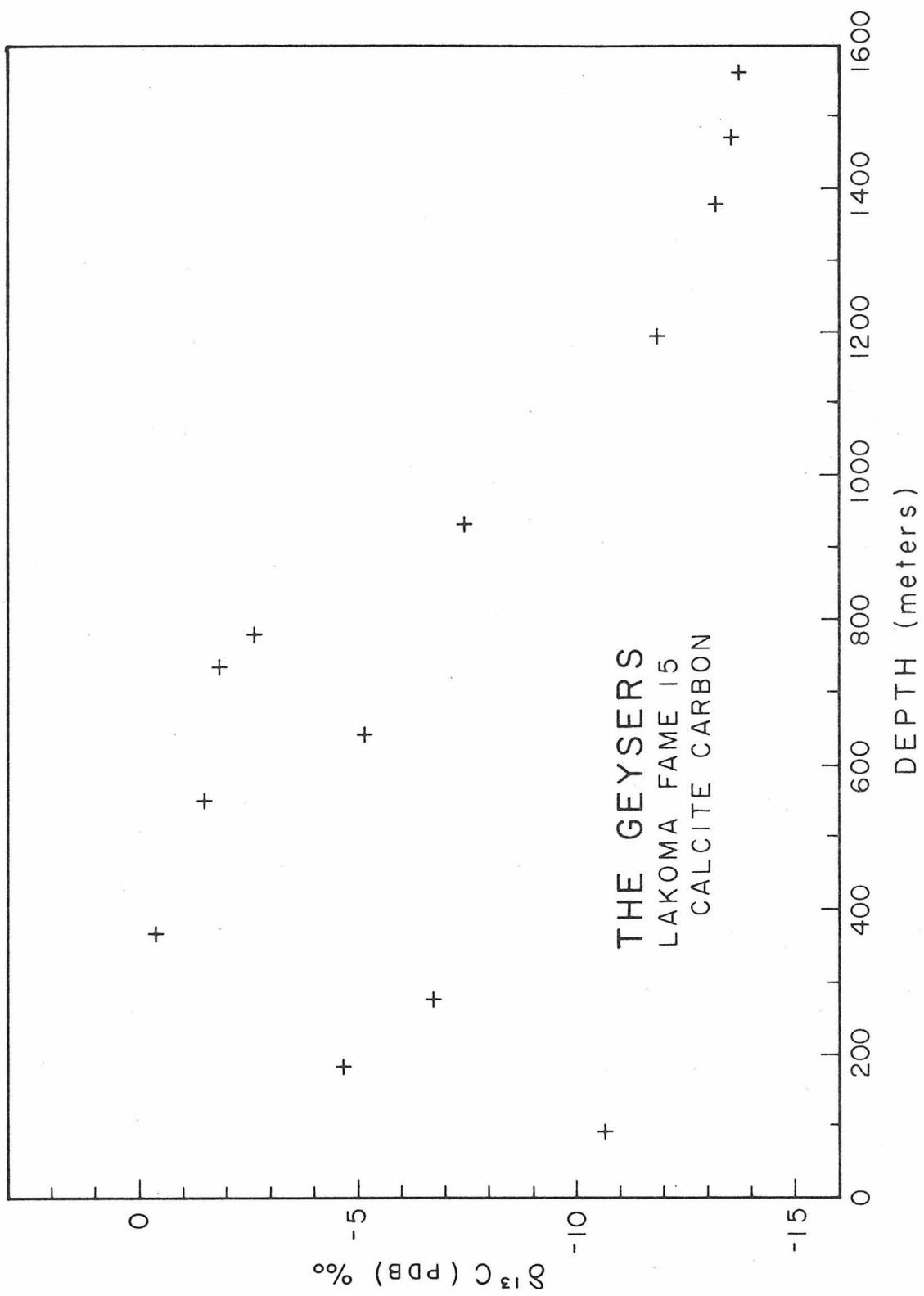


FIGURE 17

$\delta^{13}\text{C}$ values *versus* $\delta^{18}\text{O}$ values for calcites from Lakoma Fame No. 15, The Geysers.

The distribution of $\delta^{13}\text{C}$ and $\delta^{18}\text{O}$ values of calcite in Lakoma Fame No. 15 does not differ significantly from the distribution that was observed in Lakoma Fame No. 19 (Figure 15). The principal difference is attributable to the fact that there are fewer data points in this figure. The Thermal No. 7 steam zone calcite is shown for reference (T7-450).

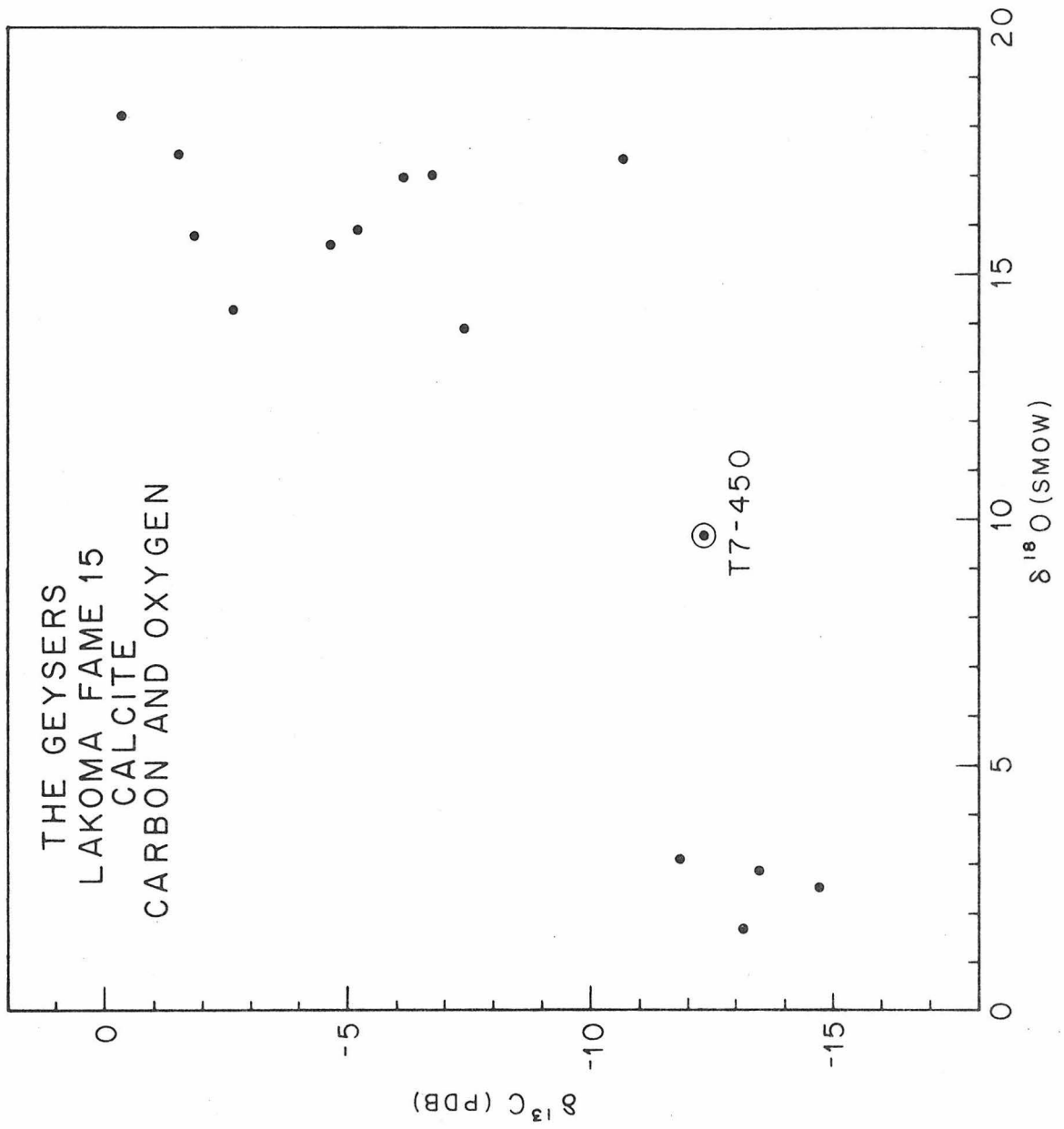


FIGURE 18

$\delta^{13}\text{C}$ values of vein calcite from various depths, Lakoma Fame No. 13, The Geysers.

The variation in $\delta^{13}\text{C}$ values of calcite from the sampled interval of Lakoma Fame No. 13 (-13 to +1‰) is much the same as the variations in upper-zone calcite $\delta^{13}\text{C}$ values observed in Lakoma Fame No. 19 (Figure 14) and Lakoma Fame No. 15 (Figure 16).

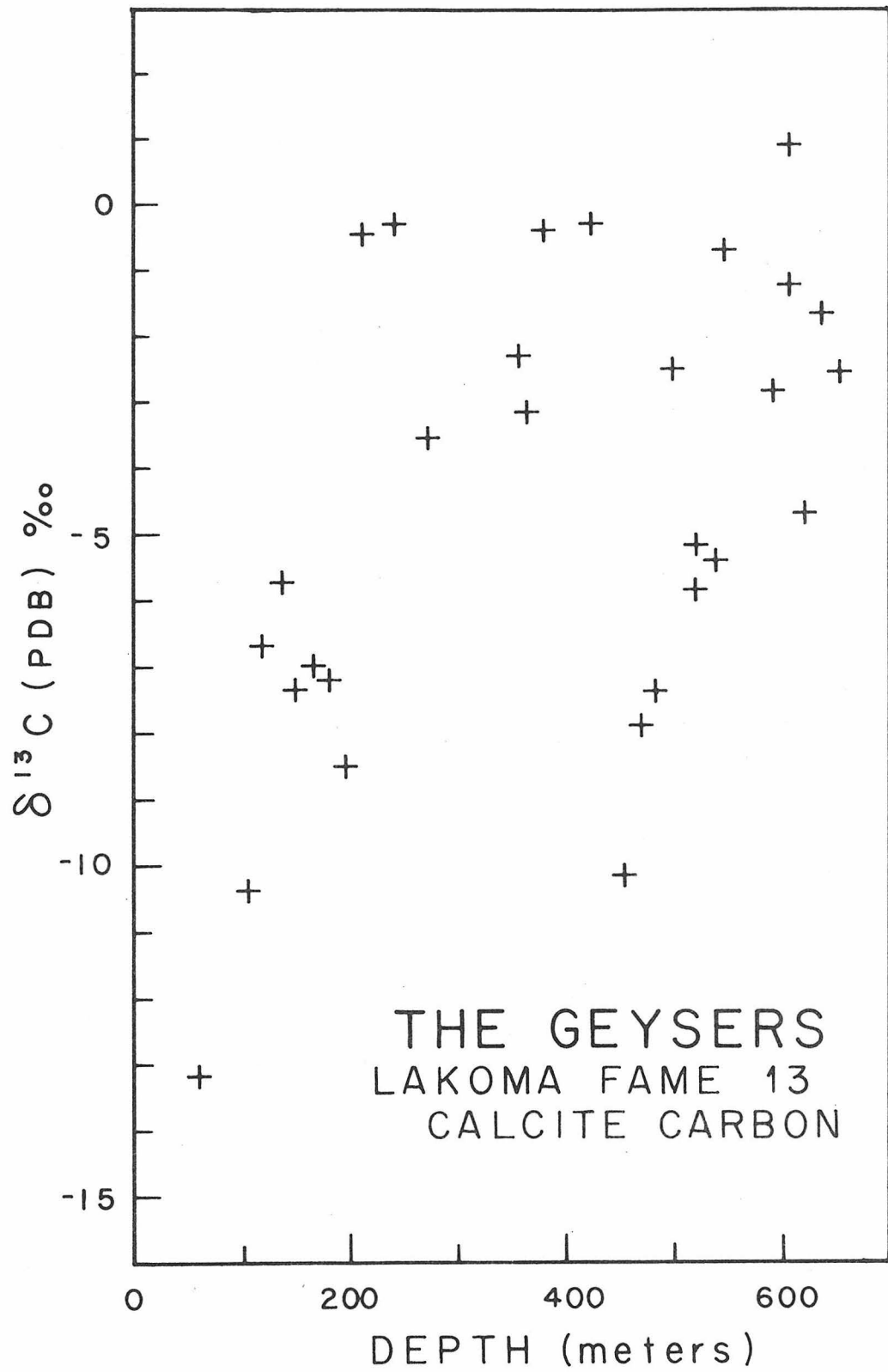
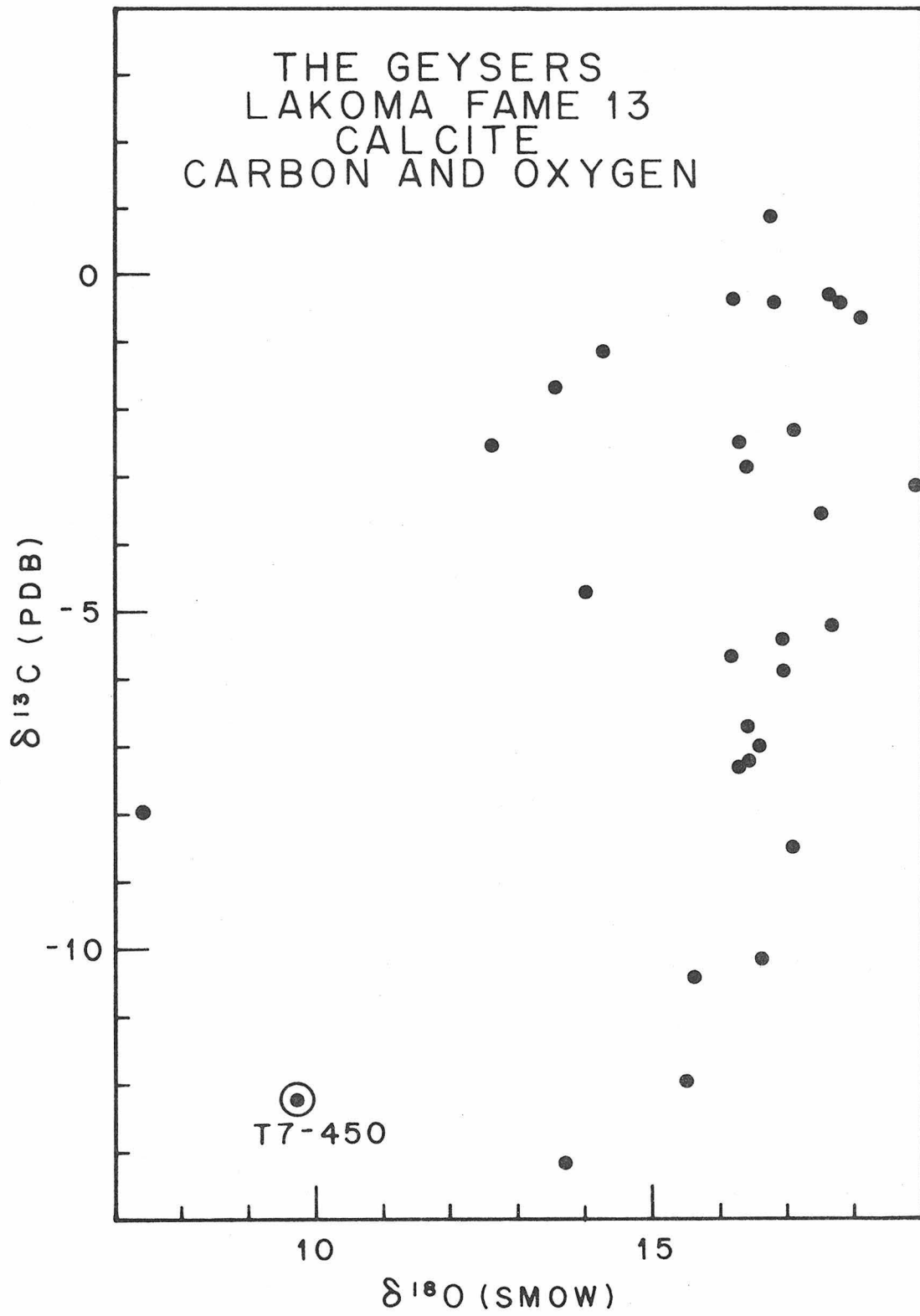


FIGURE 19

δ^{13} values *versus* δ^{18} O values for calcites from Lakoma Fame No. 13, The Geysers.

Since samples only from the upper zone were available, the nearly-vertical trend showing large δ^{13} C variation (-13 to +1‰) is not surprising (compare with Figures 15 and 17). The calcite with a δ^{18} O value of 7.4‰ (476 meters depth) may have formed in response to steam-zone type hydrothermal fluids. The Thermal 7 steam-zone calcite is included for comparison (T7-450).



3.7.8.2 Upper Zone

It was mentioned previously that some oxygen-bearing mobile component produced isotopically homogeneous (i.e., uniform $\delta^{18}\text{O}$) vein calcite over a substantially large depth interval in a hydrothermal episode prior to the active steam stage. No homogenization of calcite $^{13}\text{C}/^{12}\text{C}$ has taken place in vein material now found only in the upper zone. The vein fluid was deficient in any mobile component containing exchangeable carbon; hence, the fluid was probably CO_2 -poor.

The nonuniformity of $\delta^{13}\text{C}$ values in upper zone calcites is not an effect of decarbonation. The upper limit of $\delta^{13}\text{C}$ values is the same as the $\delta^{13}\text{C}$ of marine carbonate (Craig, 1953), near 0‰. Thermal decarbonation could conceivably lower the calcite $\delta^{13}\text{C}$ values by means of a loss of CO_2 whose $\delta^{13}\text{C}$ is higher than that of the calcite (Shieh and Taylor, 1969). A definite correlation between $\delta^{13}\text{C}$ and $\delta^{18}\text{O}$ would be expected to result from such a process because partial thermal decomposition of calcite changes $\delta^{18}\text{O}$ and $\delta^{13}\text{C}$ of remaining calcite to more negative values, but with a greater change in $\delta^{18}\text{O}$ (Shieh and Taylor, 1969). Instead, the magnitude of variation in $\delta^{13}\text{C}$ is several times larger than that of $\delta^{18}\text{O}$ in the upper zone. Also, decarbonation in a nearly uniform temperature field would be expected to produce a CO_2 reservoir which could homogenize the $\delta^{13}\text{C}$ values by isotopic exchange. There is no indication, however, of temperatures high enough to thermally decompose CaCO_3 , because no mineralogical products of decarbonation reactions were found.

The calcite veins are probably concentrations of carbonate

derived locally from host rocks (muddy sands and lavas laid down on the ocean floor). In view of the history of the Franciscan, the $\delta^{13}\text{C}$ values in the upper zone are not products of near-surface fresh water diagenesis. If this were the process that determined $\delta^{13}\text{C}$, (1) considerably less variation in $\delta^{13}\text{C}$ and (2) a minimum $\delta^{13}\text{C}$ of -8% would be observed (Hudson, 1975).

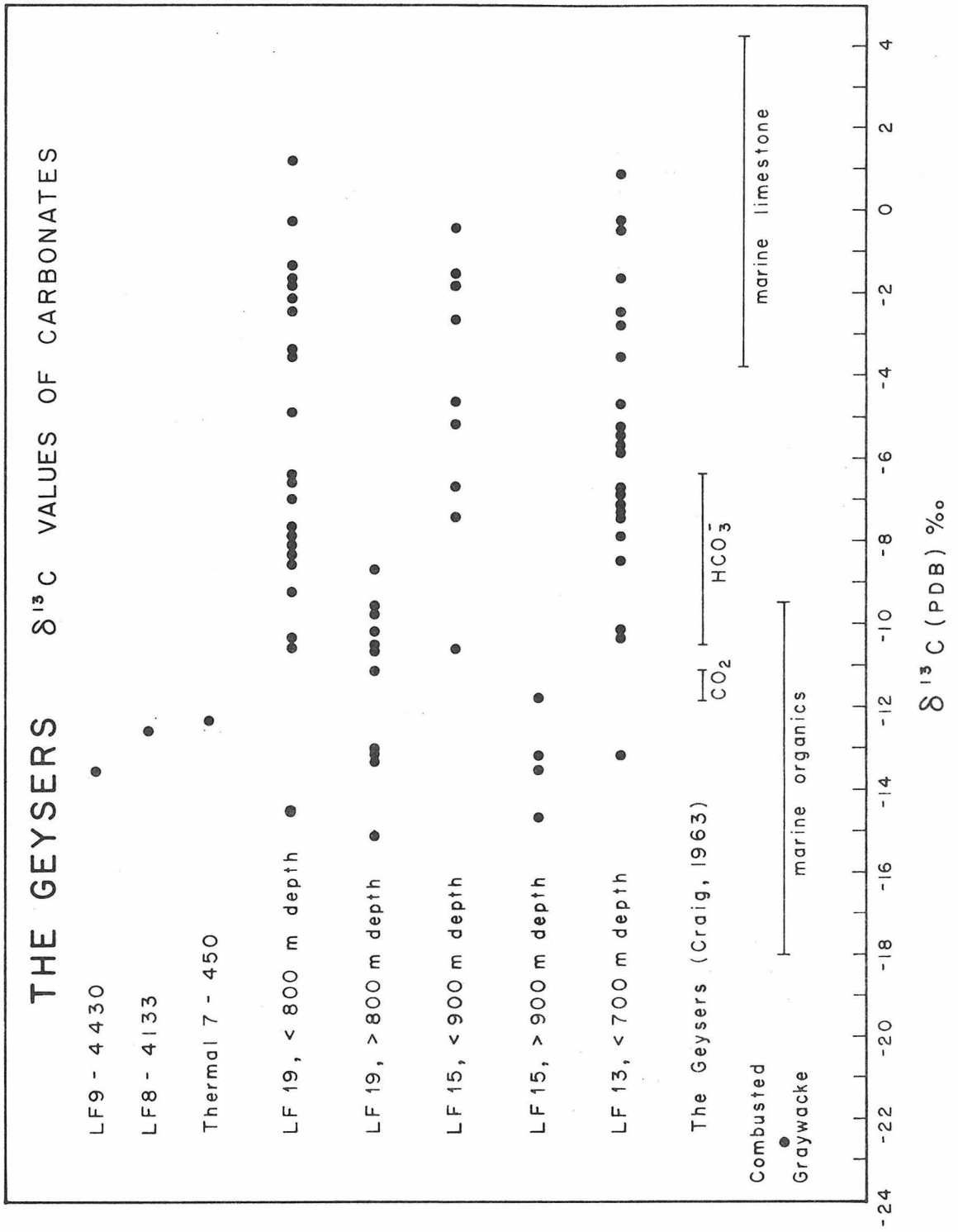
The upper limit of $\delta^{13}\text{C}$ of the upper zone calcite corresponds to values typical of marine carbonates. The lower limit of the range of $\delta^{13}\text{C}$ values (-14.5%) is one of the lowest $\delta^{13}\text{C}$ values for a hydrothermal calcite on record. The lowest values taken from other investigations include -5.4% from the Leadville Limestone, Colorado (Engel, Clayton and Epstein, 1958), -9% from Steamboat Springs, Nevada (Craig, 1963), -5.5% from the Salton geothermal field, California (Clayton, Muffler, and White, 1968), and -9.1% from Ohaki-Broadlands, New Zealand (Eslinger and Savin, 1973a). Certain processes have produced $\delta^{13}\text{C}$ values as low as -23.4% (Kolodny and Gross, 1974) in the Mottled Zone of Israel, but those processes belong more to the realm of thermal metamorphism than to that of hydrothermal alteration.

$\delta^{13}\text{C}$ values of all calcite samples from The Geysers are shown in Figure 20. Under the assumption that carbonates found in the Franciscan were originally marine, marine diagenesis would not account for the 15% depression of $\delta^{13}\text{C}$ values with respect to average marine values (Keith and Weber, 1964; Gross, 1964; Choquette, 1968). Hudson (1975) suggests that a possible source of carbon for interaction with marine carbonates is CO_2 associated with petroleum and natural gas in

FIGURE 20

$\delta^{13}\text{C}$ values of vein calcite and other carbon-bearing matter from The Geysers.

Vein calcites from Lakoma Fame (LF) Nos. 19 and 15 are divided into two groups: those from the upper zone (nearer the surface) and those from the steam zone (deeper). Thermal 7, LF 9 and LF 8 samples came from the steam zone, while samples available from LF 13 were entirely from the upper zone. Ranges of $\delta^{13}\text{C}$ values of CO_2 and bicarbonate, determined by Craig (1963) are included, as are marine organics and limestones (Craig, 1953), and the $\delta^{13}\text{C}$ value of CO_2 from combustion of Franciscan graywacke (this work). The figure shows that the vein calcite carbon may be derived in part from carbon sources that are isotopically characteristic of organic matter, and in part from marine carbonate.



sedimentary basins. Such CO_2 is strongly depleted in ^{13}C with respect to marine carbonates (Zartman, Wasserburg and Reynolds, 1961). The possibility of such interaction was also proposed by Murata, Friedman and Madsen (1969). There is no petroleum or natural gas in the Franciscan, but there is organic material in the Franciscan graywacke.

In Figure 20 is included the range of $\delta^{13}\text{C}$ for marine limestone and for marine organics (Craig, 1953). Also included is the $\delta^{13}\text{C}$ of CO_2 derived from a graywacke, LF 19-10 (Table 3), by combustion. Its value is -22.56% , and the CO_2 yield was $0.5 \mu\text{mole/mg}$. The range of $\delta^{13}\text{C}$ for vein calcite in the upper zone spans the $\delta^{13}\text{C}$ gap between marine organics and marine limestone values. Some time after sedimentation the present day $\delta^{13}\text{C}$ values of calcite came about through an interaction of carbonate with oxidized organic material. Varying proportions of carbonate and organic carbon evidently produced various $\delta^{13}\text{C}$ values between those of marine carbonate (0%) and the organically-derived material (-23%). Murata, Friedman and Madsen (1969) proposed that low $\delta^{13}\text{C}$ CO_2 is produced by nonequilibrium oxidation of organic matter. That oxygen was available is indicated by the presence of hematite throughout the stratigraphic section.

The calculated low-temperature extrapolation of the upper zone $\delta^{13}\text{O}$ values for water, calcite and the quartz in the veins (section 3.7.3.2) showed that ocean water interacting with marine sediments, given an initial mineral/water ratio 4 to 1, at 170° to 200°C produced calcite whose $\delta^{18}\text{O}$ has been lowered from 22% to about 16% , and water whose $\delta^{18}\text{O}$ had been raised from 0% to about 7% . In the case of carbon,

marine carbonate, whose $\delta^{13}\text{C}$ value was near 0‰, and organically-derived carbon, whose $\delta^{13}\text{C}$ value was -23‰, interacted to various degrees, and the resulting values of $\delta^{13}\text{C}$ observed in calcites were found to vary between 0 and -15‰. In Figure 33, near the end of this work, $\delta^{13}\text{C}$ and $\delta^{18}\text{O}$ values of all the calcite samples analyzed from The Geysers are plotted. The upper zone calcites are those whose $\delta^{18}\text{O}$ values are greater than 12‰; the rest are from the lower zone. The variation in $\delta^{13}\text{C}$ in upper zone calcites (15‰) is twice the variation in $\delta^{18}\text{O}$ (7.5‰). The fact that both variations are large (implying the absence of an isotopically-homogeneous reservoir of exchangeable carbon and oxygen) suggests that the amount of fluid in the upper zone veins was small relative to the amount of minerals. However, the larger variation in $\delta^{13}\text{C}$ than in $\delta^{18}\text{O}$ indicates that fluid/mineral oxygen atom ratio in the upper zone veins was less variable than the fluid/mineral carbon atom ratio.

3.7.8.3 $\delta^{13}\text{C}$ Variations in Lower Zone Calcites

One reason for the sparsity of calcite in the steam zone is that the dominant host rock of the steam zone in these wells is serpentinite, which is unlikely to initially contain any marine carbonate.

All $\delta^{13}\text{C}$ values of calcites in the steam zone are less than -8.5‰. The smaller range in $\delta^{13}\text{C}$ values (one-half as large as the upper zone range in $\delta^{13}\text{C}$ values of calcite) indicates that the pre-existing, highly variable $\delta^{13}\text{C}$ values of vein calcite have been homogenized during the dissolution/precipitation of calcite in the steam zone.

In Figure 20 $\delta^{13}\text{C}$ data for CO_2 and HCO_3 are given for The Geysers, as determined by Craig (1953). The $\delta^{13}\text{C}$ of CO_2 is between -11 and -12‰. According to Table 1 CO_2 (as bicarbonate) accounts for somewhat more than 1% of the total vapor in The Geysers active hydrothermal system. Even this small amount is sufficient to provide a reservoir of carbon which can exchange with calcite carbon during the dissolution/precipitation of calcite in the steam zone.

The CO_2 -calcite fractionation is given by Bottinga (1968):

$$1000 \ln \alpha_{\text{CO}_2\text{-cc}} = -2.988(10^6 T^{-2}) + 7.663(10^3 T^{-1}) - 2.4612$$

This expression (which may be in error, as pointed out in Appendix II) gives rise to the following α 's: 1 at 184°C, 1.00182 at 300°C. Calcite in equilibrium with CO_2 at these temperatures would have $\delta^{13}\text{C}$ values 0 to 2‰ less than CO_2 . This is the case for many calcite $\delta^{13}\text{C}$ values in the steam zone as seen in Figure 20. Almost all are less than -10‰, but some appear to have only partially approached carbon isotopic equilibrium with CO_2 . Calcite $\delta^{13}\text{C}$ values from the steam zones of one pair of wells differ only by 0.3‰, but geographically they are 2 kilometers apart! (Thermal 7 and Lakoma 15). Even 1% CO_2 in the steam can have a profound effect on homogenizing $\delta^{13}\text{C}$ values over a large volume. By comparison the amount of CO_2 in the upper zone fluid must have been negligible. The significance of this last statement is illuminated in a discussion of host rock alteration.

The behavior of oxygen and carbon isotopes in calcite of the lower zone seems to be the reverse of that in calcites of the upper

zone. In the upper zone, the $\delta^{18}\text{O}$ values of calcite are more homogeneous than the $\delta^{13}\text{C}$ values, which by various degrees of interaction with organic carbon were caused to vary by 15‰. In the lower zone, various degrees of interaction between calcite and a low- $\delta^{18}\text{O}$ reservoir of oxygen (meteorically-derived hydrothermal fluid) has caused the $\delta^{18}\text{O}$ values of the calcite to vary. At the same time, a pervasive reservoir of exchangeable carbon (CO_2) in the steam zone fractures has interacted with the steam zone calcite to impart a certain degree of homogeneity to the calcite $\delta^{13}\text{C}$ values. The complementary behaviors of oxygen and carbon isotopes in calcites from The Geysers leads to a characteristic "reverse-L" shaped $\delta^{18}\text{O}$ - $\delta^{13}\text{C}$ plot, depicted in Figures 15, 17 and 33.

3.7.9 Hydrothermal Alteration of Franciscan Host Rock

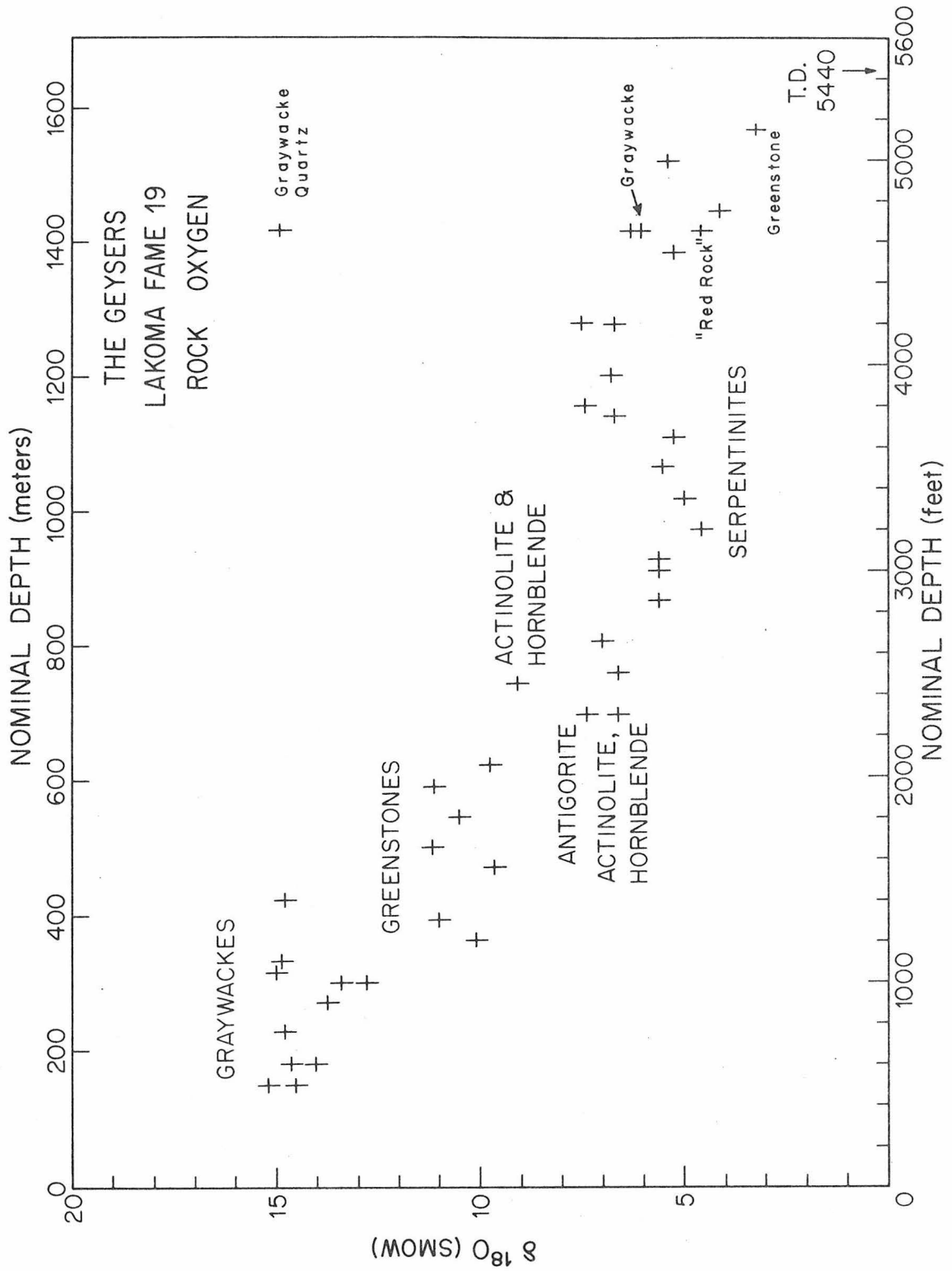
3.7.9.1 General Statements

Fluids in fractures have at one time been in contact with upper zone host rock. Fluids deposited minerals in the fractures, which became veins when they were filled. Minerals deposited from a fluid would naturally be responsive to the isotopic composition of the fluid as well as to the temperature. The present study now endeavors to examine the response of host rocks to the fluids, in both upper and lower zones now that the fluids of various episodes have been characterized. The genetic relationships between veins and host rocks are, in general, not well known, because cuttings very rarely show the original relationships between veins and rocks. In most cases it is not known how much distance separated a cuttings fragment from the nearest vein.

FIGURE 21

$\delta^{18}\text{O}$ values of host rocks and non-vein minerals from various depths, Lakoma Fame No. 19, The Geysers.

$\delta^{18}\text{O}$ values of graywacke, greenstone and serpentinite from both the upper zone and the steam zone. The carbonate $\delta^{18}\text{O}$ discontinuity which separates the zones (cf. Figure 9) occurs at 800 meters. Since samples were originally marked as to depth of origin in feet, depth scales in both feet and meters are given. "Nominal depth" refers to the depth of the drill bit at the time the cuttings were taken from the mud screen. Upper zone graywacke and greenstone $\delta^{18}\text{O}$ values have no systematic depth dependence, but serpentinite $\delta^{18}\text{O}$ values seem to "dip" from an upper zone value of about 7‰ at 1400 meters, and down again to 4‰ at 1450 meters. The serpentinite is less isotopically altered at 1200 meters, more altered at about 1000 meters and 1400 meters. Actinolite and hornblende came from a hornblende-albite schist. Note the low $\delta^{18}\text{O}$ values of graywacke, greenstone and "red rock" in the steam zone with respect to their upper zone values (cf. Figure 13 for upper zone "red rock"), while steam-zone graywacke quartz is isotopically unlike most authigenic steam zone quartz (cf. Figure 9).



In general the relative vein volume is also not known. Based on three core fragments (from Thermal 7 and Lakoma Fame 9) the vein volume is estimated to be about 3% of total rock volume in graywacke and greenstone. The vein volume might be even less in serpentinite.

The hand-picking process for selecting rock fragments ensures uniformity of rock type, especially in cuttings fractions which contain more than one type of rock fragment. In addition, more than one batch was picked from some cuttings fractions. The ranges in δ -values resulting from some of the multiple batches well exceeded the variation ascribable to analytical error alone. Those extremes from Table 3 are indicated in the plot of $\delta^{18}\text{O}$ values of whole rocks from Lakoma Fame No. 19, Figure 21.

3.7.9.2 Isotopic Compositions of Host Rocks

Figure 21 shows $\delta^{18}\text{O}$ values, for whole rocks of various types from Lakoma Fame No. 19 plotted as a function of depth. Throughout the upper zone (less than 800 meters depth) each of the rock types, graywacke, greenstone, and serpentinite, shows very little variation in $\delta^{18}\text{O}$, and what little variation exists is not related to depth.

Figure 21 depicts a systematic decrease in whole rock $\delta^{18}\text{O}$ value with depth. In actual fact the $\delta^{18}\text{O}$ is mostly a function of the bulk chemical composition and mineralogy which are distinct for each of the rock types: graywacke is simply a muddy sandstone, greenstone a hydrated spilitic basalt, and antigorite-serpentinite a hydrated olivine. While the $^{18}\text{O}/^{16}\text{O}$ ratio of rock seems to have decreased with depth, the magnesium content has also increased. There has not been

appreciable oxygen communication between veins and host rock in the upper zone, or among the major rock types in this part of the Franciscan Group. Graywacke and greenstone have, however, undergone some very profound changes in the steam zone. Each rock type will be discussed individually. Variations in mineral and whole-rock δD values will be discussed in the context of $\delta^{18}O$ variations, and these values are plotted in Figure 24.

3.7.9.2.1 Graywacke in the Upper Zone

Most of the upper zone graywackes analyzed have $\delta^{18}O$ values between +12.5 and +16.0‰ in LF 19, LF 15 and LF 13 (Tables 3, 6, and 5; Figures 21, 13, and 12). This much variation is not unreasonable, considering the heterogeneity of muddy sandstone. They consist of quartz, plagioclase, chlorite and "white micas," and some lithic fragments. A typical lithic graywacke is shown in Plate 7, and a graywacke rich in feldspar is shown in Plate 8.

The graywacke is composed of up to 40% detrital quartz (exclusive of the quartz in lithic fragments). The $\delta^{18}O$ values of this quartz, prepared from graywacke from LF 19 by the HF-HCl treatment, are reported in Table 3 and plotted at their depths of origin in Figure 22. The quartz, calcite and vein water curves (cf. Figure 9) are included for reference. The bimodal distribution of the $\delta^{18}O$ values of detrital quartz is striking. Most $\delta^{18}O$ values for detrital graywacke quartz are in the 14 to 15.5‰ range, but two, with values of about 19‰, at about 300 meters depth, fall near the quartz least-squares line! The principal difference between the rock types from which these

PLATE 7.

Lithic graywacke, containing greenstone fragment, Lakoma Fame No. 19, The Geysers. 152 to 159 meters depth, upper zone.

Area of view: 1.6×1.2 mm. X-nicols.

Slightly-altered graywacke of Franciscan Group, showing detrital quartz (white), large spilitic basalt clast (stippled with plagioclase laths), shale clasts (dark), and matrix (fine-grained, mottled pattern).

Note distinct clast boundaries. 640 meters above steam zone.

PLATE 8.

Feldspathic graywacke, Lakoma Fame No. 19, The Geysers. 152 to 159 meters depth, upper zone.

Area of view: 1.6×1.2 mm. X-nicols.

Two large plagioclase (An_{20-30}) clasts, in fine-grained matrix, with quartz (white) and lithic clasts. Note distinct grain boundaries of the feldspar clast on the right. 640 meters above steam zone.

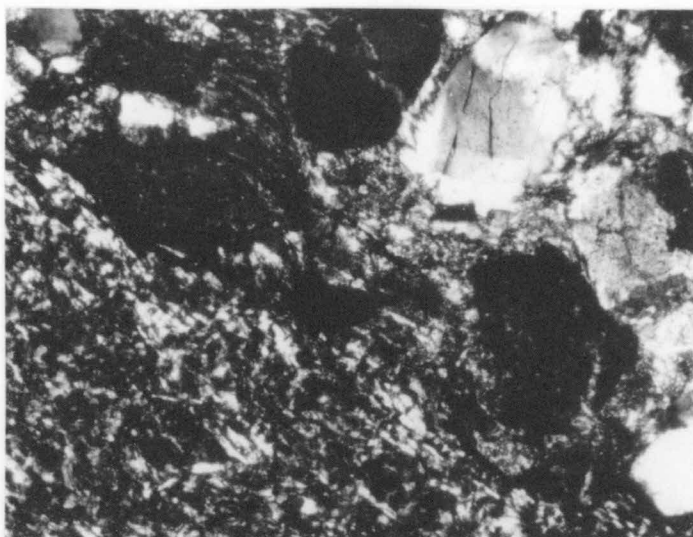


PLATE 7

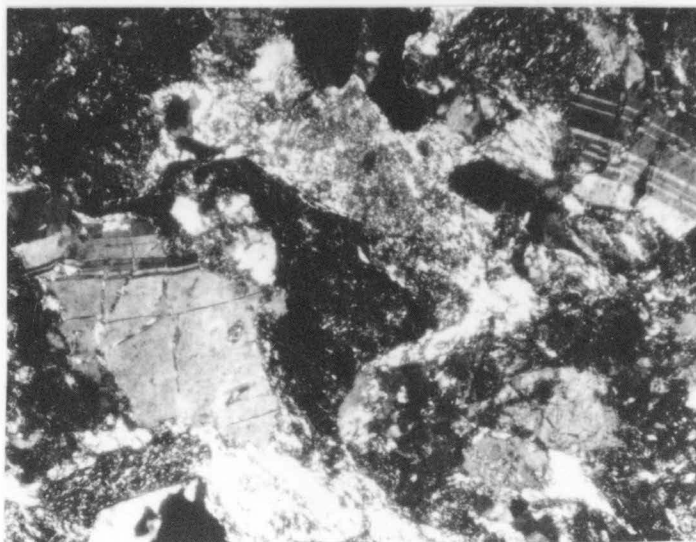
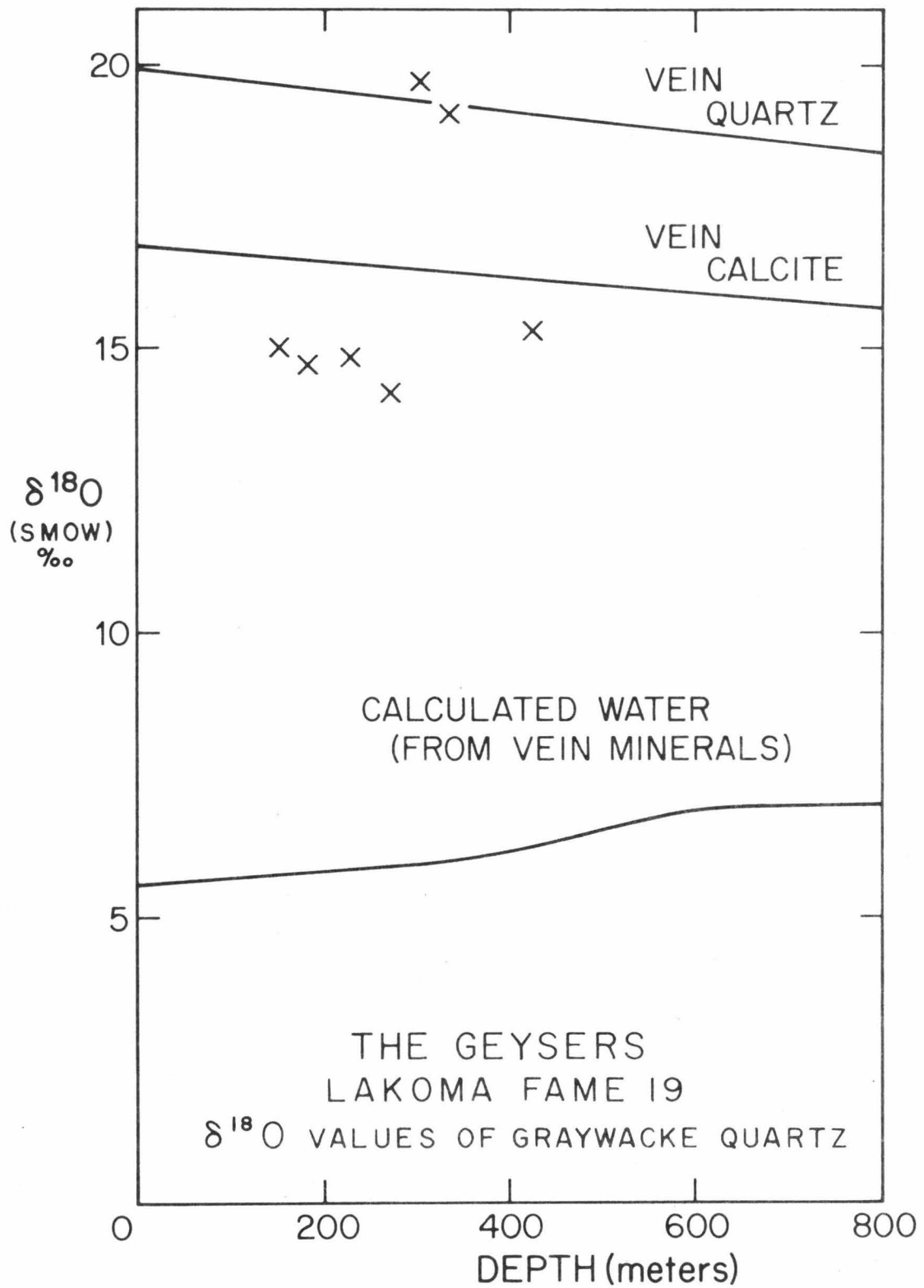


PLATE 8

FIGURE 22

$\delta^{18}\text{O}$ values of upper-zone graywacke quartz from various depths, Lakoma Fame No. 19, The Geysers.

All quartz samples whose $\delta^{18}\text{O}$ values appear in this figure were prepared from graywacke by the HF-HCl treatment. Most graywacke quartzes have $\delta^{18}\text{O}$ values characteristic of regionally-metamorphosed rocks, and are probably detritus derived from such rocks, having been incorporated into the graywacke. Two quartzes, however, from graywacke with cataclastic texture, have $\delta^{18}\text{O}$ values that fall on the least-squares line drawn through the massive quartz points in Figure 9. The quartz and calcite least-squares lines and the calculated vein water $\delta^{18}\text{O}$ values line, all from Figure 9, are included for reference. Coincidence of $\delta^{18}\text{O}$ values of quartz from cataclastic graywacke with the massive quartz least-squares line suggests that these two quartzes may have recrystallized in isotopic equilibrium with the upper zone vein water.



different sorts of quartz values came is illustrated in Plates 9 and 10. Rock containing detrital quartz whose $\delta^{18}\text{O}$ is about 19‰ has a cataclastic texture, and shows some signs of recrystallization (Plate 9); these rocks are richer in carbonate and finer-grained than typical graywacke shown in Plate 10. Presumably the fluid in the upper-zone veins has interacted completely with the material in the highly-fractured cataclastic zone at about 300 meters depth such that the graywacke quartz at about 300 meters depth has the same $\delta^{18}\text{O}$ value as vein quartz. The cataclastic zone is not megascopically veined; the fluid could have penetrated the zone through minute fractures. The granulated quartz could have been more amenable to oxygen isotope exchange with upper zone vein fluid. The alternative to isotopic exchange in the cataclastic zone is that the detrital quartz at 300 meters had an initial $\delta^{18}\text{O}$ value of +19‰. This would imply a different source area for the sediments of this part of the section. In view of the isotopic homogeneity of the whole rock graywacke above and below this horizon, this seems unlikely. Probably most of the graywacke quartz whose $\delta^{18}\text{O}$ is 15‰ did not achieve isotopic equilibrium with upper zone vein water.

3.7.9.2.2 Implications of $\delta^{18}\text{O}$ Values of Graywacke Quartz

$\delta^{18}\text{O}$ values for graywacke quartz in the range of +14 to +15.5‰ correspond closely with those values reported for quartz in regionally metamorphosed rocks by Garlick and Epstein (1967); however, these rocks are not regionally metamorphosed. Rocks in the western part of the Mayacmas Mountains exhibit characteristics of the Franciscan sequence of Bailey et al. (1964). In many places there are slight indications

PLATE 9.

Cataclastic graywacke, showing sericitization of plagioclase clast, Lakoma Fame No. 19. 335 to 341 meters depth, upper zone.

Area of view: 1.6×1.2 mm. X-nicols.

Note granulation, partial recrystallization of quartz as well as sericitization of feldspar; overall reduction in grain size. 460 meters above steam zone.

PLATE 10.

Typical graywacke, Franciscan Group, Lakoma Fame No. 19. 274 to 280 meters depth, upper zone.

Area of view: 1.6×1.2 mm. X-nicols.

Sandstone composed of clasts of quartz, plagioclase and lithic fragments in fine-grained matrix of chlorite, white mica and quartz, not conspicuously hydrothermally altered. 520 meters above steam zone.

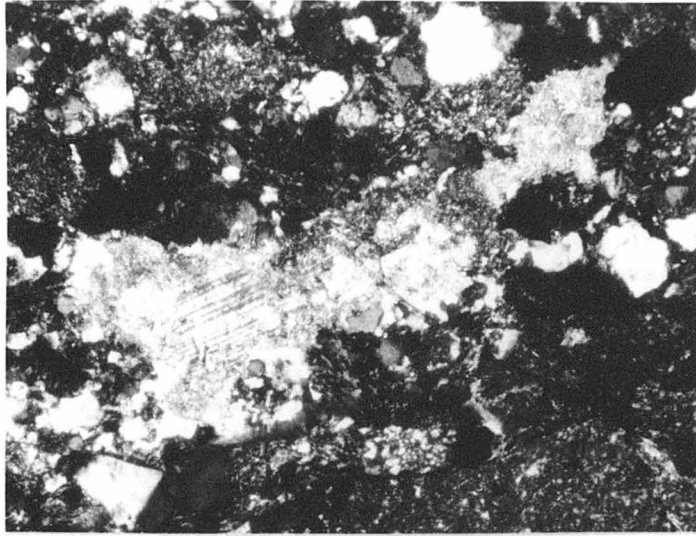


PLATE 9



PLATE 10

of a low-grade greenschist facies metamorphism of Franciscan rocks. Petrographic features of some rocks in LF 19 include some mineral assemblages characteristic of the chlorite zone of the greenschist facies, such as quartz-albite-epidote muscovite-chlorite-graphite in quartzofeldspathic rocks (graywackes) and chlorite-albite-epidote-muscovite-actinolite-sphene-magnetite in spilitic basalts. These features are confined to the fine-grained matrix of the graywacke, and the fine-grained groundmass (Plate 11) in the spilitic basalt (greenstone) (cf. Brown, 1967). Some of the minerals, such as feldspars, may occur in graywacke fortuitously, as clastic material and may have nothing to do with mineralogical equilibrium imposed by a regional metamorphism. Some basaltic glass fragments in greenstones still have sharp corners (Plate 11). Euhedral augite has remained virtually untouched (Plate 12). Lithic fragments of basalt in graywacke are virtually indistinguishable from the other basalt, and the fragments have distinct edges (Plate 7).

The sandstones and basalts have, however, been hydrothermally altered. In the basalt, plagioclase phenocrysts have been completely sericitized (Plate 7). Quartz is present in vein-like aggregates (Plate 14). The fine-grained groundmass is entirely chloritized, and epidote is found in the groundmass (Plate 13). The amygdules in the greenstone are filled with chlorite and quartz (Plate 14). In the graywacke, incipient sericitization of plagioclase feldspars has taken place, plagioclase grains are corroded only in rocks from the cataclastic zone at about 300 meters depth. The chlorite-muscovite matrix

PLATE 11.

Greenstone (spilitic basalt) with sericitized plagioclase pseudomorph, Lakoma Fame No. 19, The Geysers. 470 to 476 meters depth, upper zone.

Area of view: 1.6×1.2 mm. X-nicols.

Greenstone from Franciscan Group, showing zoned plagioclase phenocryst fragment completely sericitized. Devitrified glass shards and pocket of quartz to the left, groundmass of chlorite, epidote, actinolite and albite laths to the right. 330 meters above steam zone.

PLATE 12.

Greenstone (spilitic basalt) with fresh phenocrysts of augite, Lakoma Fame No. 19, The Geysers. 622 to 628 meters depth.

Area of view: 1.6×1.2 mm. X-nicols.

Augite phenocrysts in groundmass of chlorite, epidote, actinolite and albite laths. 175 meters above steam zone.



PLATE 11

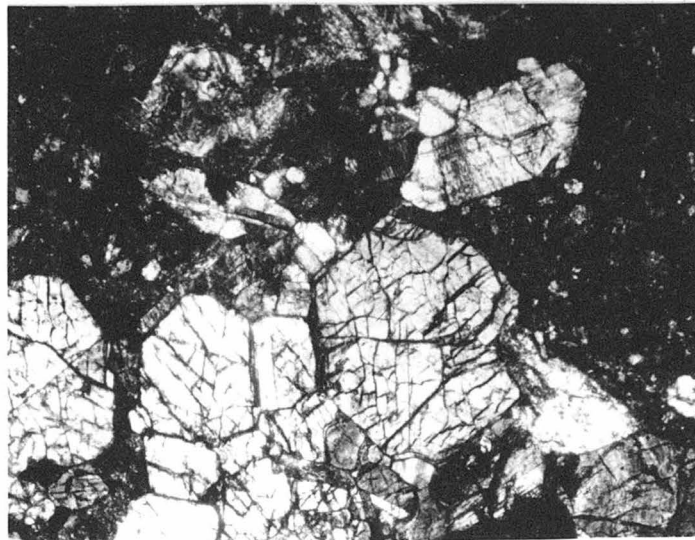


PLATE 12

PLATE 13.

Groundmass of greenstone (spilitic basalt) from Franciscan Group, Lakoma Fame No. 19, The Geysers. 622 to 628 meters depth.

Area of view: 1.6 × 1.2 mm. X-nicols.

Euhedral crystals of epidote (white) and actinolite (mottled gray) with albite, chlorite and magnetite (dark) forming the groundmass of typical spilitic basalt of Franciscan Group. 175 meters above steam zone.

PLATE 14.

Amygdule of quartz and chlorite in greenstone, Lakoma Fame No. 19, The Geysers. 622 to 628 meters depth.

Area of view: 1.6 × 1.2 mm. X-nicols.

Originally a vesicle in a pillow basalt, now filled with quartz (white, toward outside) and chlorite (mottled gray, in core), surrounded by matrix of typical Franciscan greenstone (cf. PLATE 13) containing smaller chlorite amygdules. 175 meters above steam zone.

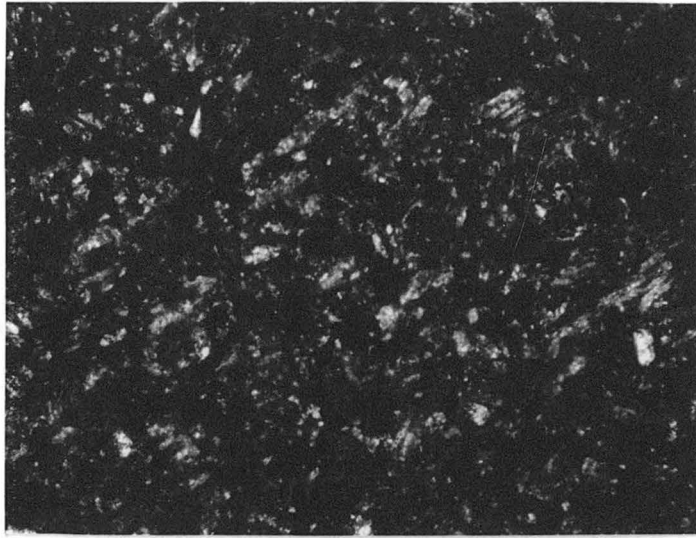


PLATE 13

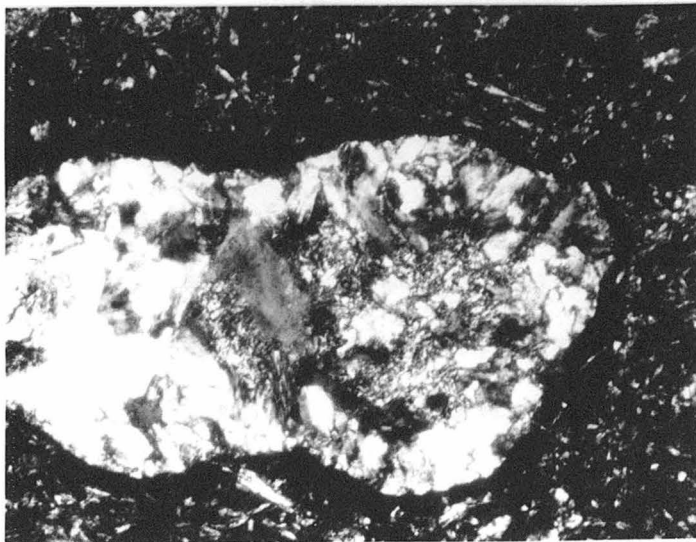


PLATE 14

is fine-grained, yet crystalline (Plate 10). In spite of the petrographic evidence for some hydrothermal alteration, a pervasive regional metamorphism is not apparent.

The metamorphic grade of the Franciscan during the upper zone veining episode seems to have not been high enough to produce the +15‰ quartz of Garlick and Epstein (conditions producing the "biotite zone" in pelitic rocks). It is concluded that the quartz whose $\delta^{18}\text{O}$ is 14 to 15.5‰ quartz has been derived from older rocks. The $\delta^{18}\text{O}$ values of graywacke quartz from the upper zone of LF 15 (Table 6; Figure 13) are still within the range of $\delta^{18}\text{O}$ values for metamorphic quartz.

It was previously shown that most of the graywacke quartz was not in equilibrium with the vein fluid. Furthermore, many of the graywacke quartz samples have the same $\delta^{18}\text{O}$ values as the graywackes from which they came. This relationship is shown in Figure 23. Clearly, by any linear combination of oxygen atoms it is impossible to produce a whole rock $\delta^{18}\text{O}$ the same as that of the quartz, using equilibrium values of its component minerals at any temperature short of infinite. Indeed it is difficult to say which minerals (aside from quartz in the cataclastic graywacke), if any, did isotopically equilibrate with the upper zone vein fluid, or even with each other.

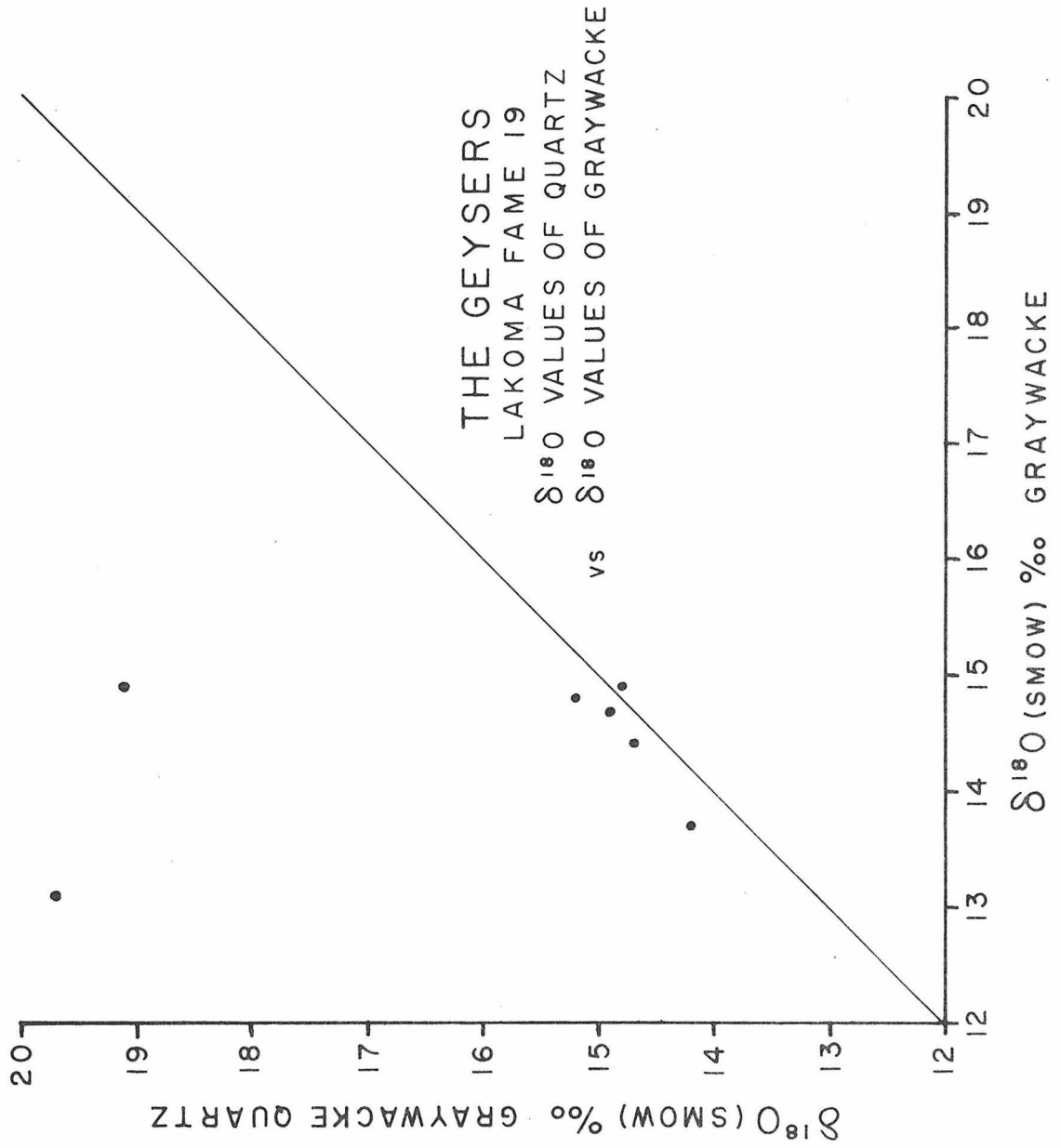
It was usually not possible to obtain from Franciscan rocks at The Geysers clean mineral separates in large enough quantity to be analyzed. The chlorite-rich separates which were obtained had $\delta^{18}\text{O}$ values between 9.3‰ and 11.5‰ (Table 3).

In rocks in the cataclastic zone whose graywackes contained quartz

FIGURE 23

$\delta^{18}\text{O}$ values of upper zone graywacke quartz plotted against the values of graywacke from which they came, Lakoma Fame No. 19, The Geysers.

Most points fall on the 45° line, indicating that the $\delta^{18}\text{O}$ value of graywacke is the same as that of the graywacke, indicating that the quartz is not in isotopic equilibrium with the other minerals in the graywacke. The other two points that are far from the 45° line represent graywacke from the cataclastic zone.



with a $\delta^{18}\text{O}$ value of 19‰, the chlorite $\delta^{18}\text{O}$ is about 11.5‰; the value for 1000 $\ln \alpha$ between quartz and chlorite is about 7.5. For this same fractionation observed in a metamorphic rock, Garlick and Epstein (1967) inferred a metamorphic temperature of about 550°C, which was the temperature calculated from the $\delta^{18}\text{O}$ values of quartz and magnetite in their rock. Since there is no evidence for a temperature higher than about 200°C in the upper zone at The Geysers, the quartz-chlorite fractionation observed in the cataclastic zone is probably non-equilibrium. In actual fact, the 2‰ variation in chlorite $\delta^{18}\text{O}$ values in LF 19 upper zone graywackes indicates that the chlorites probably had not obtained oxygen isotope equilibrium with each other, as would be expected in a muddy sandstone.

3.7.9.2.3 δD of Upper Zone Vein Water, Indicated by δD of Graywacke

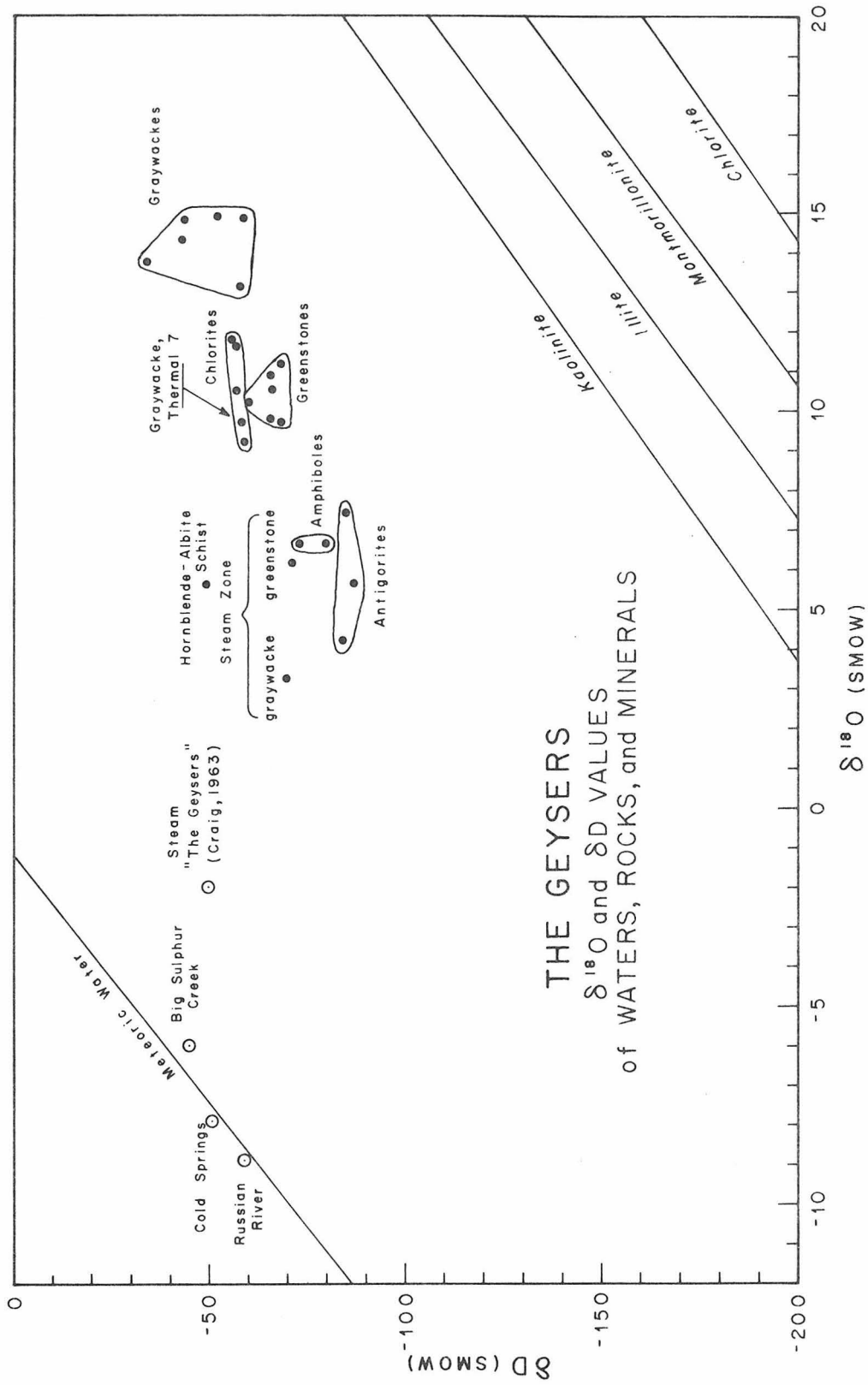
The total hydrogen extracted from upper zone graywackes varies between -35 to -59‰ (Figure 24). Chlorite-rich fractions were prepared from graywackes whose total hydrogen had δD values of -52 to -59‰. The δD values of these chlorite-rich fractions were between -56 and -59‰. Magnetic separation had allowed the removal of most of the other hydrous minerals (micas, epidote, amphiboles, etc.) from the chlorite-rich material, so the range in δD values between -56 and -59‰ probably represents the hydrogen isotopic composition of chlorite alone. Consequently, essentially the only hydrous mineral contained in graywacke whose δD value is between -52 and -59‰ is chlorite.

If the highest temperature the graywacke experienced is that indicated by the isotopic geothermometry of the upper zone veins,

FIGURE 24

δD versus $\delta^{18}O$ for rocks, minerals and waters from The Geysers.

Surface water samples and the steam analysis, as well as the meteoric water line, are taken from Figure 11. Upper zone graywacke and greenstone δD values are suggestive of an interaction of the hydrous minerals of these rocks (chlorite, white mica, actinolite, epidote) with ocean water at about 200°C. δD of antigorite is the same in both upper ($\delta^{18}O = 7\%$) and lower ($\delta^{18}O = 4\%$) zones. Amphibole δD and $\delta^{18}O$ values are characteristic of those from metamorphic rocks. Hydrous minerals from graywacke and greenstone in the steam zone do not appear to be in hydrogen isotope equilibrium with the steam. Lines marked "Kaolinite", "Illite", "Montmorillonite", and "Chlorite" represent isotopic compositions of these minerals which were calculated to be in equilibrium with meteoric waters at surface temperatures (Savin and Epstein, 1970b).



THE GEYSERS
 $\delta^{18}O$ and δD VALUES
of WATERS, ROCKS, and MINERALS

(about 200°C) the δD value of the water, in equilibrium with chlorite whose δD value is -55‰, is 0‰ (according to a low temperature estimate of D/H fractionation between chlorite and water [Taylor, 1974]). In section 3.7.3.2 it was shown that the upper zone vein water could have originated as ocean water, entrapped in the Franciscan sediments, that exchanged oxygen with the minerals in the rock to take on $\delta^{18}O$ values as high as 7‰. The uniform chlorite δD values, all of which are compatible with ocean water at 200°C, suggest that the ocean water determined the final δD value of the chlorite, and that the upper zone vein water had a δD value that was not far from the original δD value of the entrapped ocean water, 0‰.

Some graywackes have total hydrogen δD values as high as -35‰. In such rocks, there is clearly another hydrous mineral present in addition to chlorite. The muscovite-water D/H fractionation at 200°C is smaller than that of chlorite-water. In equilibrium with the same water, muscovite would have a higher δD value than chlorite. It is conceivable that graywackes with total hydrogen δD values higher (less negative) than about -55‰ have a substantial component of muscovite, whose δD is ocean water at 200°C would be -30 to -40‰ (Taylor, 1974).

In actual fact, the "white mica" which occurs in many graywackes, both around feldspar fragments (Plate 9) and in the matrix (Plate 10) cannot be identified positively as to whether it is muscovite, sericite, or illite. The feldspar alteration mineral (Plate 9) is probably sericite, which is mineralogically equivalent to muscovite. The matrix "white mica" could be sericite or illite. According to Eslinger and

Savin (1973a) illite oxygen isotope exchange with water behaves the same as muscovite and water (cf. O'Neil and Taylor, 1969). Since illite is chemically similar to muscovite, its hydrogen isotope exchange properties should be similar to those of muscovite (cf. Suzuoki and Epstein, 1975). In mixtures of varying proportions of the hydrous minerals "white mica" and chlorite, the δD values of total rock hydrogen would be expected to vary from -35 to -59‰. The graywackes with the lowest δD values would have the greatest amount of chlorite. This was actually observed because only graywackes which were initially chlorite-rich allowed chlorite-rich mineral fractions to be prepared from them, as was shown above, and these graywackes had lower δD values. It is important to note that even with an appreciable amount of "white mica," the δD values of the total graywacke hydrogen are still compatible at about 200°C with water whose δD is about 0‰.

3.7.9.2.4 Upper Zone Greenstones

All upper zone greenstones analyzed (Table 3) cover a very narrow range both in $\delta^{18}O$ (9.7 to 11.2‰, Figure 21) and δD (-60 to -69‰, Figure 24). The $\delta^{18}O$ value spread lies well within that of chlorite extracts from graywackes. Whole-rock greenstone δD values are slightly less than those of the chlorites (Figure 24).

Mineralogy of the greenstones resembles that of the graywacke: plagioclase (An_{20} to An_{30} , according to McNitt, 1968), chlorite, sericite (an alteration product of feldspar phenocrysts), augite, epidote, and actinolite. Graywacke contained some of these minerals only as they occurred in lithic fragments. This greenstone contains

quartz only in veins and vein-like segregations.

Because of their mineralogical similarities, the $\delta^{18}\text{O}$ values of these greenstones will be compared with values of submarine greenstones reported by Muehlenbachs and Clayton (1972). Most of their greenstones were between 2.8 and 6.8‰ (mean 5.2‰). The average $\delta^{18}\text{O}$ of 14 greenstones was only slightly lower than that of fresh unmetamorphosed submarine basalt. Fresh basalts from 4 oceanic rises had $\delta^{18}\text{O}$ values between 5.5 and 5.9‰. The highest $\delta^{18}\text{O}$ of weathered basalt reported by Muehlenbachs and Clayton (1971) was 17.6‰, with 7 weight % H_2O (This was an extreme, found in the weathered rind). There was a positive correlation of $\delta^{18}\text{O}$ with weight % total water. Metamorphosed basalts (greenstones) were said to have equilibrated with sea water ($\delta^{18}\text{O} = 0$) at temperatures of 200 to 300°C, with a water to rock ratio of at least 1 to 8.

Metamorphosed basalts of Muehlenbachs and Clayton (1972) contained 2 to 4% water. Greenstones analyzed in this study contained 3.9 to 6.4% H_2O by weight (Table 3). There is no apparent correlation of either δD or $\delta^{18}\text{O}$ with weight % H_2O . Mineralogically, Franciscan greenstones are identical to submarine metamorphosed basalts, since both consist of quartz, albite, chlorite, actinolite and epidote, with relic plagioclase (commonly sericitized) and pyroxene.

In view of the mineralogical similarities between the Franciscan greenstones and those analyzed by Muehlenbachs and Clayton, the difference between the mean $\delta^{18}\text{O}$ value of their greenstones (5.2‰) and the mean $\delta^{18}\text{O}$ value of these (10.2‰) is quite striking. In order to

account for the unusually high $\delta^{18}\text{O}$ of Franciscan greenstones, either (1) the rocks must have interacted with large quantities of water whose $\delta^{18}\text{O}$ value was at least 5‰, or (2) the basalts deposited on the ocean floor during the accumulation of Franciscan rocks incorporated some high- $\delta^{18}\text{O}$ material. It was shown previously (section 3.7.3.2) that water with a $\delta^{18}\text{O}$ value as high as 5‰ can occur in small, but not large amounts. The more likely explanation for the high $\delta^{18}\text{O}$ values of greenstones is that the basalts were mixed with materials deposited in a marine environment, whose $\delta^{18}\text{O}$ values are known to be high (Savin and Epstein, 1973b). Examples of such materials are marine carbonate, radiolarian ooze, zeolites, and authigenic marine clay minerals. If the $\delta^{18}\text{O}$ value of this high- $\delta^{18}\text{O}$ reservoir is about 30‰, a mixture of 20% high $\delta^{18}\text{O}$ materials and 80% basalt would be required to produce a greenstone whose $\delta^{18}\text{O}$ value was 10‰. It seems likely that the greenstones represent such a mixture that has been metamorphosed.

The δD values of whole greenstone hydrogen, -60 to -69‰, are not far removed from those of whole graywacke hydrogen. Such δD values would result from a mixture of hydrous minerals, dominated by chlorite, with lesser amounts of actinolite and epidote, whose δD values would be lower than that of the chlorite with which they were in equilibrium. The δD values of whole greenstone hydrogen are also compatible with the δD value of ocean water, 0‰ at about 200°C. Hydrogen isotope exchange between the entrapped ocean (vein) water and hydrous minerals in upper-zone greenstones and graywackes seems to be more pervasive than oxygen isotope exchange between the vein water and rocks in the same zone.

3.7.9.2.5 Serpentinites

3.7.9.2.5.1 General Features

Serpentinites occur in Lakoma Fame No. 19 from 700 meters depth to the bottom of the hole at 1659 meters depth. The main serpentine mineral in the serpentinite is antigorite, which was identified by X-ray diffraction, using the criteria for the X-ray identification of serpentine minerals given by Whittaker and Zussman (1956). The serpentinite is intensely sheared and recrystallized, and is typical of the sheared antigorite bodies described by Bailey *et al.* (1964). (cf. section 3.4.3 of this work.) In Lakoma Fame No. 19 the upper 100 meters of the serpentinite is included in the upper zone (the carbonate $\delta^{18}\text{O}$ discontinuity, described in section 3.7.3.1, occurs at 800 meters depth), and serpentinite is by far the most abundant host rock type found in the steam zone.

These serpentinites are high in magnesium, but the FeO content varies from 4 to 7% by weight, and Al_2O_3 from 0.5 to 2%. One mineral grain in LF 19-45 (a cuttings fraction containing serpentinite and metamorphic rock, cf. Table 3) was indicated by electron microprobe analysis to be "jadeite." The average of two analyses indicated 12% diopside (CaMg), 8% hedenbergite (CaFe), 8% acmite (NaFe), and 71% jadeite (NaAl) Si_2O_6 in terms of pure end-members. This gives an approximate formula $\text{Ca}_{0.2}\text{Na}_{0.8}(\text{Mg}_{0.1}\text{Fe}_{0.2}\text{Al}_{0.7})(\text{Si}_{1.96}\text{Al}_{0.04})\text{O}_6$. This is to be compared with a jadeite reported by Coleman (1955, 1961) to be "10% diopside, 14% acmite," and formed under conditions of "low temperature and low pressure" according to the mode of occurrence. The

origin of the LF 19-45 "jadeite" is not known, but it may be only a tectonic inclusion in the sheared serpentinite body.

Isotopic analyses of serpentinites from 18 different cuttings fractions from Lakoma Fame No. 19 gave a range in $\delta^{18}\text{O}$ of 4.2 to 7.4‰. The total range in δD for antigorite from both the upper and the steam zone is -84 to -87‰. The antigorite δD and $\delta^{18}\text{O}$ values are plotted in Figure 24. Typical mesh-structure antigorite is shown in Plate 15.

3.7.9.2.5.2 Upper Zone Serpentinite

Three samples of antigorite isolated from serpentinite in the upper zone between 700 and 800 meters depth gave $\delta^{18}\text{O}$ values of 6.5 to 7.5‰. The δD value is -85‰. This δD value is slightly below the range of δD values given by Wenner and Taylor (1971, 1973) for antigorites (-40 to -70‰), but both the δD and $\delta^{18}\text{O}$ values of upper zone antigorite are well within the variation of hydrogen and oxygen isotopic compositions found by Wenner and Taylor in lizardite-chrysolite from ophiolite complexes. The serpentinite body in the Franciscan Group at The Geysers is not demonstrably part of an ophiolite complex, but its low δD value indicates that it has exchanged hydrogen with meteoric water, as other continental antigorites are thought to have done.

Wenner and Taylor (1971) concluded that antigorite serpentinization takes place in the temperature range 220°C to 460°C. The lower limit of this range corresponds to the upper limit of the range of temperatures in upper zone type alteration. The $\delta^{18}\text{O}$ of antigorite, +7‰, is estimated to be in equilibrium at 200 to 300°C with water

whose $\delta^{18}\text{O}$ is +5 to +7‰, according to the estimates of Wenner and Taylor (1971) and Taylor (1974). However, at those same temperatures, the δD of antigorite, -85‰, indicates that equilibrium water had a δD value of -50‰ since $1000 \ln \alpha$ for serpentine-water at 200°C is -35‰ for serpentine-water. Clearly the serpentine δD indicates equilibrium with an isotopically different water than do greenstone and graywacke chlorite δD values. Water with δD of -50‰ is virtually identical to that of present-day local meteoric water.

The veining which took place during the upper-zone type hydrothermal alteration post-dated the emplacement of the serpentinite body. The fact that the serpentinite is sheared might indicate that it was intruded into the Franciscan sediments at low temperatures, not as a dunite but as a serpentinite, before the entrapped ocean water in the sediments interacted with the marine sediments to form veins at 170 to 200°C.

3.7.9.2.5.3 Hydrothermal Alteration of Serpentinite in the Steam Zone

In the steam zone serpentinite has not been completely adjusted in isotopic composition to reflect equilibrium with the steam. Temperatures in the steam zone (200 to 300°C) are the same as those postulated for the formation of the antigorite (section 3.7.9.2.5.2), so the δD values of -84 to -87‰ observed would be coincidental with antigorite values calculated to be in equilibrium with present-day local meteoric water (-50‰). This is because the δD value of local meteoric water happens to coincide with the inferred δD of the serpentinitization water.

The $\delta^{18}\text{O}$ of serpentinite is an indicator of the degree of

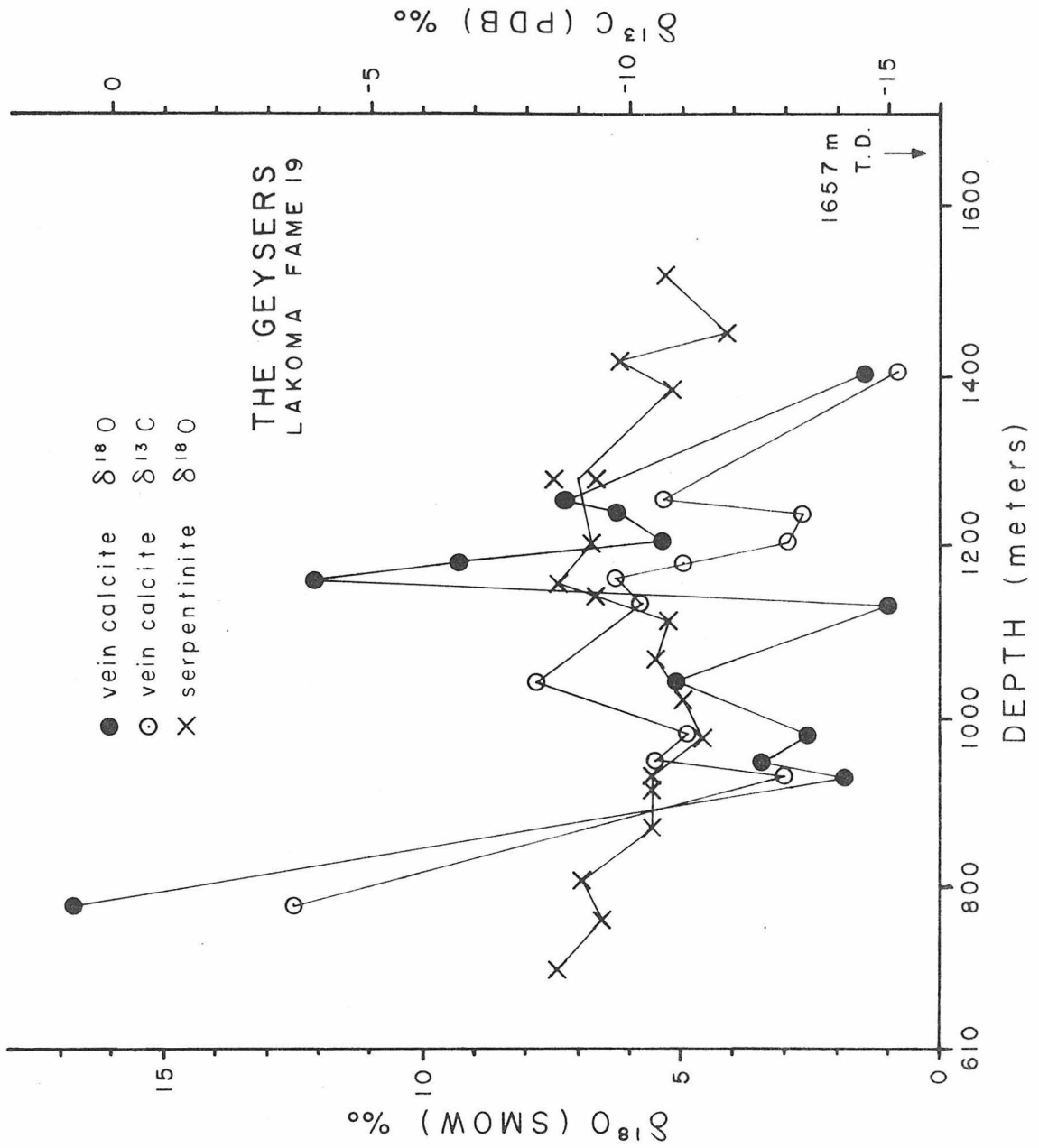
isotopic alteration. In a previous section (3.7.3.8) the maximum oxygen shift experienced by the steam was said to have yielded a $\delta^{18}\text{O}$ as high as -1% for the steam. At 300°C , serpentine and chlorite (according to Taylor, 1974, estimates) should have equilibrium $\delta^{18}\text{O}$ values of -1% in the presence of this steam. The lowest $\delta^{18}\text{O}$ value of serpentinite observed is 4% . Neglecting all components except serpentine and initially-meteoric water, the mass ratio of water to serpentine that interacted to form this value is 0.28, since the meteoric water increased $\delta^{18}\text{O}$ by 7% and the serpentine $\delta^{18}\text{O}$ value was apparently decreased to 4% at about 1425 meters depth (Figure 21) from its upper zone value 7% .

Degree of alteration is not constant throughout the serpentinite body. In Figure 25 the variations with depth of $\delta^{18}\text{O}$ of serpentinite and $\delta^{13}\text{C}$ and $\delta^{18}\text{O}$ of vein carbonate have been superimposed. The last two were found to be very sensitive to variations in fluid temperature and isotopic composition. It can be seen that the cuttings fractions which contain carbonates with the lowest $\delta^{18}\text{O}$ and $\delta^{13}\text{C}$ values also contain the lowest $\delta^{18}\text{O}$ values of serpentinite (4 to 5%). Carbonates having the lowest $\delta^{18}\text{O}$ and $\delta^{13}\text{C}$ values were previously found to have been formed at moderate (160 to 240°C) temperatures with essentially meteoric water having no $\delta^{18}\text{O}$ shift. The cuttings fraction which provided minerals that indicated the highest temperature (1204 m, 320°C) corresponded to restricted fluid circulation (large $\delta^{18}\text{O}$ shift in water, from -8% to -1%) and the serpentinite from that fraction had a normal $\delta^{18}\text{O}$ value of about 7% . Thus significant isotopic

FIGURE 25

Superimposed variations with depth of $\delta^{18}\text{O}$ and $\delta^{13}\text{C}$ of vein calcite and $\delta^{18}\text{O}$ of serpentinite host rock in the lower 800 meters of Lakoma Fame No. 19, The Geysers.

$\delta^{18}\text{O}$ and $\delta^{13}\text{C}$ values indicated at depths less than 800 meters are characteristic of rocks and minerals of the upper zone. Depths of minimum values of $\delta^{13}\text{C}$ and $\delta^{18}\text{O}$ for calcite coincide with depths where $\delta^{18}\text{O}$ values of serpentinite are lower. Note that at the depth at which occurred the highest quartz-calcite isotopic temperature (320°C), the $\delta^{18}\text{O}$ of serpentinite is much like its upper-zone value 7‰. The depth of the lower quartz-calcite isotopic temperature (160°C) yielded a serpentinite whose $\delta^{18}\text{O}$ is 5‰. The degree of isotopic alteration of host rock is therefore more dependent upon the fluid/rock ratio being high than the temperature being high.



alteration of serpentine occurred only near fractures which carried meteoric water. The restricted circulation, even at high temperatures (320°C) at 1200 meters depth in LF 19 did not allow for much alteration of the serpentine by the fluid. Also, the partially-equilibrated calcite near 1160 meters depth is not accompanied by any significant alteration of serpentinite in which it was found.

3.7.9.2.6 Greenstone, Graywacke and "Red Rock" in the Steam Zone

Only one sample each of graywacke, greenstone and red rock (inferred to be red chert) was found in cuttings from the lower zone of LF 19; their $\delta^{18}\text{O}$ values are 6.1‰, 3.2‰, and 4.6‰, respectively, and are included in Figure 21. The δD values of the first two are in Figure 24.

Graywacke (1420 m) has a $\delta^{18}\text{O}$ value of 6‰, 9‰ less than most upper zone graywackes, but its purified quartz $\delta^{18}\text{O}$ is 15‰, which is the same as that of the quartz in upper zone graywacke (section 3.7.9.2.1). The fact that quartz from graywacke found in the steam zone retains a $\delta^{18}\text{O}$ value (15‰) similar to that of upper zone graywacke quartz indicates that the low- $\delta^{18}\text{O}$ hydrothermal fluids in the steam zone have not exchanged oxygen with the steam zone graywacke quartz. The graywacke contains about 50% quartz whose $\delta^{18}\text{O}$ value is 15‰. In order that the whole-rock $\delta^{18}\text{O}$ value of steam zone graywacke be 6‰, material balance requires that all other minerals besides quartz have a bulk $\delta^{18}\text{O}$ value of -3‰. A $\delta^{18}\text{O}$ value so low can come about only by oxygen exchange with meteoric water at moderate (up to 200°C) temperatures. The profound recrystallization and oxygen exchange of

the graywacke minerals chlorite and "white mica" (accompanied by the complete alteration of feldspars to hydrous minerals, Plate 16) seems to have taken place under hydrothermal conditions typical of a hot water system, during the 160 to 180°C thermal event, associated with large amounts of meteoric water.

Greenstone from the LF 19 steam zone (1570 meters depth) similarly shows the effects of at least partial oxygen exchange with hot meteoric water, because its $\delta^{18}\text{O}$ value is only 3‰ compared to 10‰ in the upper zone.

Both graywacke and greenstone in the steam zone have a δD of about -70‰. This value is not significantly different from the δD values of total hydrogen of graywacke and greenstone in the upper zone (-34‰ to -70‰). This is only 20‰ less than the δD value of meteoric water. A 20‰ D/H fractionation between pure muscovite (an important component of the graywacke) and water, for example, occurs at about 500°C (Suzuoki and Epstein, 1975). Clearly this temperature is unreasonably high for the steam zone. The hydrous minerals in the steam zone graywacke and greenstone may have associated with them a complex history of rock-water interaction that culminated in δD values out of hydrogen isotopic equilibrium with the steam.

"Red rock" in the steam zone of LF 19 (1420 meters depth) has a $\delta^{18}\text{O}$ of about +4.5‰ (Table 3), as compared to +13‰ in the upper zone of LF 15 (Table 6). This is probably a result of selective removal of quartz from "red rock" in the steam zone leaving a low $\delta^{18}\text{O}$ hematite (Plate 5).

PLATE 15.

Mesh-structure antigorite, from serpentinite body, Lakoma Fame No. 19, The Geysers. 927 to 923 meters depth.

Area of view: 1.6×1.2 mm. X-nicols.

Antigorite, main constituent of serpentinite bodies which concordantly intrude Franciscan Group at The Geysers. Contains minor iron oxides from steam zone.

PLATE 16.

Hydrothermally-altered graywacke from steam zone, Lakoma Fame No. 19, The Geysers. 1415 to 1421 meters depth.

Area of view: 1.6×1.2 mm. X-nicols.

Quartz clasts (white) have partially dissolved, large plagioclase clast (right) completely sericitized, fine-grained matrix of chlorite and white mica (gray stippled). Cf. PLATE 10.

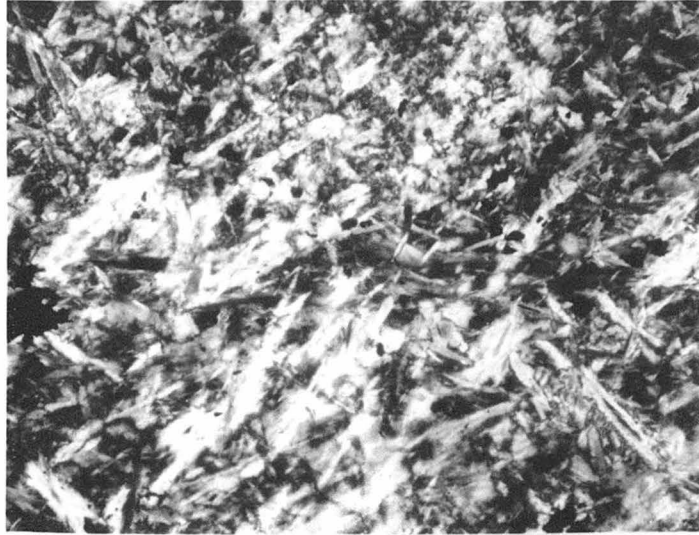


PLATE 15

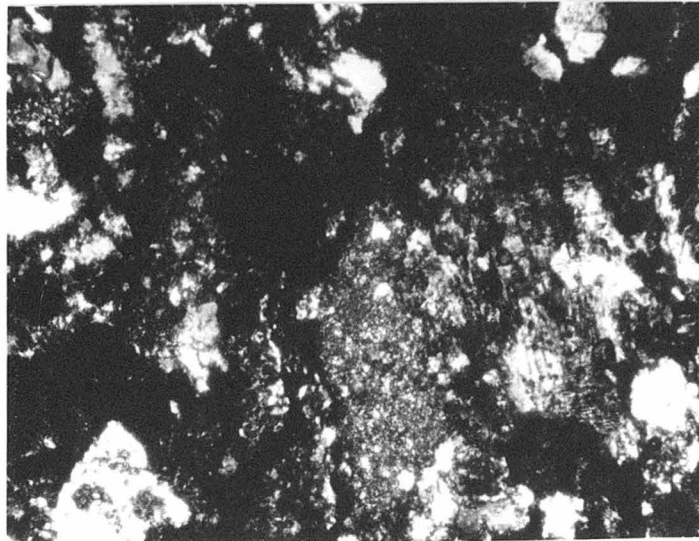


PLATE 16

3.7.9.2.7 "Metamorphic Rocks"

The "blue green hornblende-albite schist" from the LF 8 steam zone (Table 7) also has its δD (-50%) and $\delta^{18}O$ (5.6%) plotted in Figure 24. Its isotopic composition indicates that its isotopic record belongs more to the realm of metamorphism than to hydrothermal alteration, for their $\delta^{18}O$ values are typical of those found in metamorphic rocks (Garlick and Epstein, 1967). Similarly, the $\delta^{18}O$ values of the hornblende and actinolite from sample LF 19-45 (Table 3), both of which are 6.4% , are reminiscent of normal metamorphic values. Their δD values (-73% for hornblende and -80% for actinolite) are also typical metamorphic values (Taylor, 1974).

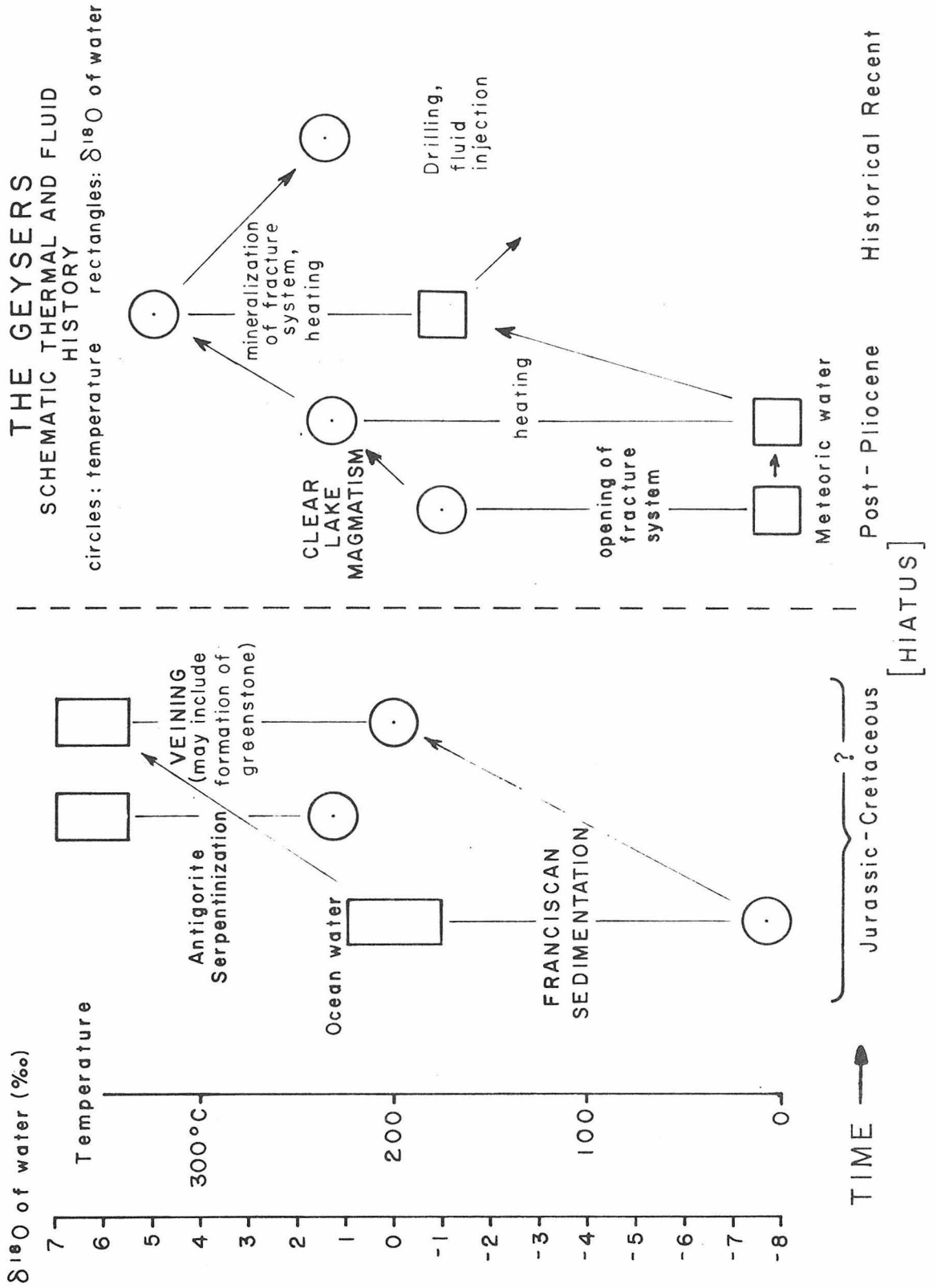
3.8 Summary of Hydrothermal Alteration of Host Rock at the Lakoma Fame Tract of The Geysers

The thermal and fluid history indicated by the isotopic records of rocks and minerals at the Lakoma Fame Tract at The Geysers is shown schematically in Figure 26. The history of hydrothermal alteration recorded in the rocks and minerals can be divided into two distinct periods. The first period, closely associated with the deposition, diagenesis and, possibly, metamorphism of the Franciscan Group, had ocean water as its dominant hydrothermal fluid, with temperatures associated with burial of sediments in a nearly-normal geothermal gradient (section 3.7.3.2). The time covered by this period is the late Jurassic, at which time the deposition of the first Franciscan sediments and lava flows took place, to the Franciscan metamorphism in the late Cretaceous (?). The second period began with the emplacement

FIGURE 26

Schematic thermal and fluid history of hydrothermal activity at The Geysers.

Changes in temperature and $\delta^{18}\text{O}$ of hydrothermal fluid with time are shown. Various events which are thought to have caused the changes are noted. The earlier episode of rock-fluid interaction includes sedimentation on the ocean floor, the formation of antigorite serpentinite from dunite and its subsequent emplacement in Franciscan rocks, and a low-temperature hydrothermal event at about 200°C which might have formed greenstone from basalts and given rise to veining. The episode some 60 million years later involves the evolution of the present hydrothermal system at The Geysers, which may have begun as a hot-water system, heated by the nearby magma chamber, becoming vapor-dominated as the fluid/rock ratio was lowered when circulation was limited and temperatures were raised.



of a magma chamber, which imposed an abnormally-high geothermal gradient on the host rocks, in the Pliocene. Fractures developing in the brittle Franciscan sedimentary rocks allowed heated meteoric water to pass through them, interacting with the host rock and depositing minerals in the fractures (section 3.7.7). This latter period eventually led to the development of the present vapor-dominated hydrothermal system.

Throughout the thermal and fluid history of hydrothermal activity at The Geysers, the interaction between minerals and fluids has been in large part confined to fractures, which later became veins. In the earlier period, the ocean water constituted as much as 40 volume percent of unconsolidated sand-sized detritus. The accumulation of eugeosynclinal sediments entrapped some of this water. As the sediments became buried to depths of a few kilometers (section 3.7.3.2) their temperature increased to 170 to 200°C. Fractures developed and the entrapped ocean water began to migrate toward the fractures, carrying with it silica and carbonate derived from readily soluble marine silica and carbonate. The water interacted only slightly with the oxygen in the detrital minerals in sandstones, but exchanged readily with the hydrogen in the hydrous minerals. Perhaps the heat which caused the rock-water interactions that produced the veining also was responsible for the metamorphism of the spilitic basalts to greenstones. The metamorphism was accompanied by an increase in $\delta^{18}\text{O}$, which was 5‰ for the basalt and 10‰ for the greenstone. Probably during this "metamorphism" neither carbon dioxide (discussed by Ernst, 1972) nor water was available in great quantity. The $\delta^{18}\text{O}$ of the metamorphic fluid

appeared to be primarily determined by the $\delta^{18}\text{O}$ of the original unmetamorphosed sediments. Before the rocks became heated in this period, serpentinite bodies were intruded concordantly between some of the layers of Franciscan sediments and volcanics. The formation of serpentinite from dunite was probably not related to any of the hydrothermal episodes experienced by the other rocks in the area now known as The Geysers, but might have taken place elsewhere (section 3.7.9.2.5).

It is noteworthy that even though the Cretaceous (?) episode of rock-fluid interaction and the recent episode are genetically unrelated and are separated in time by some 60 million years, both episodes took place in the temperature range 160° to 320°C. The difference in the $\delta^{18}\text{O}$ values of the quartz and calcite which best record the isotopic temperatures of the first episode are similar to the same difference in the second episode. The actual $\delta^{18}\text{O}$ values of the minerals found in the two episodes differ by 7 to 20‰. The actual $\delta^{18}\text{O}$ values of the minerals are sensitive to the fluid/mineral ratios, which are obviously very different for the two episodes. The principal differences between the two episodes are (1) the origin of the hydrothermal fluids and (2) the nature of the heat source.

At The Geysers the present hydrothermal system, which appears to be a continuation of the second episode, is supplied with meteoric rather than ocean water. The heat source is presumably a magma chamber at some undetermined depth, whose emplacement set up a locally high geothermal gradient. The second episode probably involved seismic activity which created fractures in otherwise impermeable rock of the

Franciscan Group, allowing meteoric water to penetrate to hot rocks near the magma chamber by way of the fractures and to become heated and rise again in circulation, establishing a hot-water system. Large amounts of meteoric water traveled through the fractures at first, exchanging oxygen and probably hydrogen with the rock and altering its mineralogy. In time, however, the hot water also deposited minerals in the fractures, reducing the permeability of the rocks, causing the host rock temperatures to rise. With the permeability of the rock reduced, the ancestral hot-water system gave way to the vapor-dominated hydrothermal system which is now producing superheated steam at The Geysers. Tapping the steam reservoir by drilling has lowered the reservoir temperature somewhat, but hydrothermal activity remains largely undiminished (section 3.7.7).

It is apparent that the geological history of rocks at The Geysers is exceedingly complex. Evidence of many types of rock-fluid interactions was uncovered, however, through the measurements of stable isotope ratios in the rocks and minerals. The information provided by stable isotope analysis has enabled the various episodes of rock-fluid interactions to be identified and described, whereas many of the effects of these past events might not have been detected by any other analytical technique. The conclusions regarding the thermal and fluid history of The Geysers area are the simplest and most reasonable that can be made on the basis of the isotopic and petrological data, without the invocation of ad hoc explanations of observed phenomena.

4. STUDIES AT VALLES CALDERA, JEMEZ MOUNTAINS, NEW MEXICO

4.1 A Hydrothermal System in a Volcano

The occurrence of fumarolic activity in the base of an old collapsed volcano should be no surprise, especially since "hot springs have long been regarded as the latest phase of volcanism" (Allen and Day, 1935; cf. section 0). The Valles Caldera, a remnant of a volcano which collapsed upon itself in the late Pliocene or early Pleistocene in the northern Jemez Mountains of New Mexico, is a typical caldera. The presence of hot springs on the floor of the Caldera and just outside its rim pays tribute to the existence of a cooling magma chamber which once was the source of many kinds of extrusive rocks in the area, mostly ash-flow tuffs. The Valles Caldera is an excellent place in which to sample rocks from an active hydrothermal system. The occurrence of a heat source directly below the rocks probably represents the closest approach of the actual magma chamber to near-surface ground waters. With the combination of a near-surface heat source and a plentiful supply of water, a hydrothermal system would surely result. The Valles Caldera represents a unique opportunity to investigate the interaction between water driven into circulation by a nearby magma, and the rocks which overlie the magma chamber.

In the past few years the Valles Caldera has become important in terms of its potential as a geothermal energy resource. The Union Oil Company is drilling exploratory holes inside the Caldera, while the Los Alamos Scientific Laboratory has been drilling outside the Caldera in search of hot dry rock. The results reported for this portion of

the present study are very preliminary, but the information provided by the isotopic data from the Valles Caldera permits comparison of the Valles hydrothermal system with other hot-water systems and with The Geysers, which was discussed in detail in the previous chapter. This information should be of interest to the other institutions which are now exploring the Caldera.

4.2 Geological Overview

At the south end of the west branch of the southern Rocky Mountains in New Mexico lie the Jemez Mountains. The east branch of the Rockies contains the Sangre de Cristo and the Cimarron Ranges. The "Jemez Uplift" is the term applied to the structural feature whose physiographic expression is the Jemez Mountains. The most prominent landforms in the Jemez Mountains are Valles Candera and Toledo Caldera, on the northeast edge of Valles. Both of these features are products of Pleistocene volcanism.

The Jemez Uplift of northern New Mexico is on the west side of a structural depression called the Rio Grande Trough (Kelley and Silver, 1952). The Jemez Mountains culminate topographically in Redondo Peak, 11,254 feet (3431. m) above sea level, and level off toward Los Alamos on the Pajarito Plateau, 9 kilometers to the east, and in the Jemez Plateau to the west. The Rio Grande River runs in the Trough to the east of the Pajarito Plateau.

A geologic map of the Jemez Mountains was compiled by Smith, Bailey and Ross (1970) from field work done between 1946 and 1967. Information for this map was taken from works on the Tertiary geology

of the Abiquiu quadrangle (Smith, 1938), an exhumed erosion surface in the Jemez Mountains (Church and Hack, 1939), the Santa Fe Formation (Denny, 1940), the Galisteo Formation (Stearns, 1943), the Nacimiento Mountains and San Pedro Mountain (Wood and Northrop, 1946), the Caballo Mountains (Kelley and Silver, 1952), the tectonics of the Rio Grande area (Kelley, 1954), the geology of the Santa Fe area (Spiegel and Baldwin, 1963), and the Zia Sand Formation (Galusha, 1966), all of which were directly concerned with the geologic history of the Rio Grande River Valley.

Rocks in the Jemez Mountains area include Tertiary deposits of terrigenous material, with associated volcanics, and Quaternary volcanics on the inside, rim and flanks of Valles Caldera, laid down both before and after the collapse of Valles Caldera. To the west Precambrian, Paleozoic, and Mesozoic rocks are exposed which are overlain by the Tertiary and Quaternary rocks in the Jemez Mountains. The individual rock types will be described below.

The first large volcanic ash-producing eruption in the Jemez Mountains took place 1.4 million years ago (Kolstad et al., 1975), resulting in a ring of domes on the inferred ring fracture of Valles Caldera.

Thermal activity at the surface abounds in Valles Caldera, giving rise to such features as Sulphur Creek, Sulphur Springs, Sulphur Point, San Antonio Hot Spring, and numerous hot springs without names, as may be discovered from a perusal of the Jemez Springs 15-minute quadrangle topographic map.

4.3 Rock Types Encountered in Cuttings from the Wells

4.3.1 The Sources of Samples

Samples isotopically analyzed in this part of the study were almost entirely selected from cuttings from two wells drilled during the exploration for geothermal steam by the Union Oil Company of California. Those two are part of a series of 10 wells (as of spring, 1973) drilled into the floor of Valles Caldera on a land grand called Baca Location No. 1. Rock types will be described according to their occurrences in the cuttings. The names of these sampled wells are Baca No. 4 (near the center of the Caldera) and Baca No. 7 (just inside the northwest rim), Figure 27 is a map of Valles Caldera, showing the outline of the Caldera, the ring of rhyolite domes, extent of the Bandelier Tuff (an important steam reservoir rock) on the Caldera floor, the locations of Baca No. 4 and Baca No. 7, and Los Alamos as a landmark.

Rock types below listed are in stratigraphic sequence from youngest to oldest, and the descriptions follow those of Smith, Bailey and Ross (1970) and Spiegel and Baldwin (1963). Those descriptions are supplemented by observations on cuttings made by Richard Dondanville, R. L. Smith, and the present author.

4.3.2 Quaternary Rocks

Redondo Creek Member, Valles Rhyolite

The Valles Rhyolite is the first unit encountered in Baca No. 7. It is widespread in the area encompassed by Valles Caldera. The Redondo

FIGURE 27

Map of Valles Caldera and vicinity, New Mexico.

The Valles Caldera is shown with its ring of rhyolite domes. The locations of steam wells Baca No. 4 and Baca No. 7 are given. The distribution of Bandelier Tuff, an important hot-water reservoir rock, inside the caldera is shown. The location of the city of Los Alamos is given for reference.

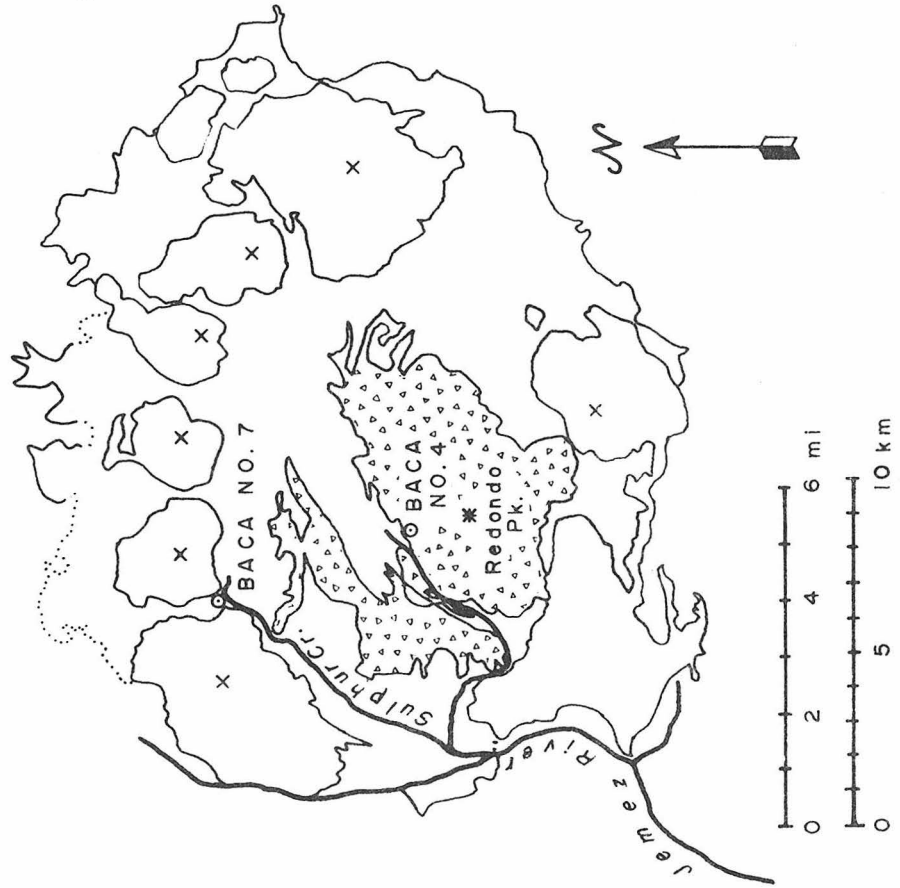
VALLES CALDERA

after SMITH, BAILEY, and ROSS
1970



Los Alamos

- WELL LOCATION
- × RHYOLITE DOME
-  SURFACE OUTCROPS OF BANDELIER TUFF IN VALLES CALDERA



Creek member, which is the only part of the Valles Rhyolite found in Baca No. 7, is confined almost totally to the region inside the inferred ring fracture (Figure 32), and consists of interlayered tuffs, containing no quartz, but characterized by phenocrysts of plagioclase mantled with sanidine. Also biotite and pyroxene phenocrysts are present.

Caldera Fill

The Caldera Fill is the most lithologically heterogeneous unit encountered in the cuttings from Baca No. 7. It includes breccia, sand, gravel, and silt, and covers portions of the floor of Valles Caldera. This unit is mostly volcanic detritus (including some pyroclastics of the Valles Rhyolite-type) and landslide deposits from Caldera walls. The unit also contains some early-formed sediments deposited by a caldera lake, including carbonates.

Detrital material from 470 meters depth in Baca No. 7 contains 8% carbonate by weight based on calcite. The $\delta^{18}\text{O}$ and the $\delta^{13}\text{C}$ were determined for both calcite and dolomite, the carbonate minerals in the detrital material (Epstein, Graf and Degens, 1964). The $\delta^{18}\text{O}$ value of the calcite fractions was 21.5‰. The $\delta^{18}\text{O}$ value of the dolomite fraction was 29.6‰. These results are comparable to those obtained for calcite and dolomite from Deep Springs Lake (California) sediments by Clayton, Jones and Berner (1968). The $\delta^{18}\text{O}$ values for their calcite was 24‰, and for their dolomite 33‰. The results of Clayton *et al.* are 2 to 3‰ higher for both calcite and dolomite than the values given here but the $\delta^{18}\text{O}$ values of the carbonates in the Valles Caldera Fill indicate that the carbonates were deposited in an environment similar

to that found in a fresh-water lake. The significance of the $\delta^{18}\text{O}$ values of these carbonates (and of their $\delta^{13}\text{C}$ values) will be discussed in greater detail below.

If calcite from 470 meters depth in Baca No. 7 formed in an intermittent caldera lake, the $\delta^{18}\text{O}$ value of the calcite should reveal some information about the lake. Assuming that the mean water temperature in the lake was no higher than about 20°C, water in equilibrium with calcite whose $\delta^{18}\text{O}$ value is 21.5‰ has a $\delta^{18}\text{O}$ value no greater than -7‰. This number is reasonable, since the lake was probably formed from meteoric water (whose present $\delta^{18}\text{O}$ value is estimated at -12‰) and evaporated, during which the $\delta^{18}\text{O}$ of the water increased. The difference in $\delta^{18}\text{O}$ between the Caldera lake water (indicated by the carbonate) and the present-day meteoric water may also be a reflection of a different climate in the area at the time the lake was formed.

Bandelier Tuff

The Bandelier Tuff is composed of non-welded to densely-welded deposits of rhyolite, ash and pumice. It contains bipyramidal quartz and chatoyant ("like a cat's eye") sanidine crystals.

The Tschirege (upper) member of the Bandelier Tuff contains inclusions of hornblende-rich quartz-lattice pumice and accidental lithic inclusions of varied lithology. The Tsankawi pumice bed is the basal unit of the Tschirege, consisting of 1 to 4 meters of bedded, air-fall material.

The Otowi member contains abundant accidental lithic inclusions. The basal Guaje bed is an accumulation of bedded air-fall pumice, up

to 10 meters thick.

4.3.3 Pre-Volcanic (Tertiary and Older) Rocks

Santa Fe Formation

The Tertiary Santa Fe Formation has widespread exposure in the Rio Grande Trough, but is covered by Quaternary rocks in the Jemez Mountains. It is a poorly-consolidated accumulation of buff, red, and gray arkosic sandstone, siltstone, clay and pebbles, with minor thin white and green ash beds.

Abiquiu Tuff

A lithologically heterogeneous unit associated with the Santa Fe Formation is the Tertiary Abiquiu Tuff, white to light-gray tuffaceous sandstone and conglomerate, with a 20 to 100 meter thick basal gravel member containing Precambrian crystalline rocks. This unit includes tuffaceous sediments and the 2 to 8 meter thick Pedernal chert member.

Permian Rocks

Rocks of the Permian system were not divided by Smith, Bailey and Ross (1970). They include red, gray, and green sandstone, siltstone and shale of the Glorieta, Yeso, Abo, and Cutler Formations.

Carboniferous Rocks

Rocks designated as undivided Carboniferous include the Madera Limestone and the Sandia Sandstone (Pennsylvanian) and miscellaneous Mississippian rocks.

Precambrian Crystalline Rocks

The Precambrian basement encountered in Baca No. 7 is a pink

microcline-muscovite granite, hydrothermally altered so that it contains chlorite, epidote and pyrite. This unit corresponds mineralogically to the "gneissoid granite" of Spiegel and Baldwin (1963).

4.4 Estimation of the Isotopic Composition of Local Meteoric Water

The $\delta^{18}\text{O}$ value of local meteoric water could not be measured because of lack of samples of hot-spring discharge and local precipitation. However, δD values of waters were measured for four surface waters from the Jemez Mountains by Friedman, Redfield, Schoen and Harris (1964). Their data as well as elevations and locations, both in latitude and longitude, and with respect to Redondo Peak (Figure 27), of these water samples are given in Table 8. The mean elevation is 2237 meters, and the mean δD is -86.5% . The minimum elevation inside the Caldera is 2440 meters. In view of the well known relationship of generally decreasing δD value of precipitation with increasing elevation, a reasonable estimate for δD of local precipitation in the Jemez Mountains is -90% . Using this δD value and the meteoric water relationship $\delta\text{D} = 8\delta^{18}\text{O} + 5$ the estimated $\delta^{18}\text{O}$ value of local precipitation in the Jemez Mountains is approximated to be -12% . This meteoric water is a potentially important source for the hydrothermal fluid at Valles Caldera.

4.5 The Wells

4.5.1 General Statements

Liquid water is the principal fluid flowing from the geothermal wells at Baca Location No. 1. The hot water flashes into steam when

TABLE 8
 SURFACE WATER SAMPLES FROM THE JEMEZ MOUNTAINS, NEW MEXICO

<u>Source</u>	<u>Location</u>	<u>Elevation (meters)</u>	<u>δD (SMOW)</u>
Rio Del Oso	36°02' N; 106°18' W* 30 km NE of Redondo Peak	2216	- 87 ‰
Sulfur Spring	35°55' N; 106°37' W 7 km NW of Redondo Peak	2506	- 76 ‰
Soda Dam	35°48' N; 106°41' W 13 km SW of Redondo Peak	1921	- 93 ‰
Well, Bland	35°48' N; 106°28' W 16 km SE of Redondo Peak	2305	- 90 ‰
	mean 2237 m S.D. 243 m		mean - 86.5 ‰ S.D. 7.4 ‰

*Given incorrectly as 32°50' N; 107°55' W by Friedman, et al. (1964).

lithostatic pressure is released as reservoir cap rock is penetrated. This behavior is characteristic of a hot-water system.

The approximate surface area of the Valles Caldera floor is 300 square kilometers. The two wells from which samples were recovered (Baca 4 and 7) are 6 kilometers apart (one-third the Caldera diameter, if the ring of rhyolite domes is taken as the boundary). The depth of Baca No. 4 is not known, but samples of hot-water reservoir rock were recovered from depths as great as 1539 meters. Baca 7 ends in hot rock at 1687 meters depth. These dimensions suggest that the potential volume of hydrothermally-altered rock is huge.

Calcite is the mineral most sensitive to isotopic exchange with a fluid at Valles Caldera. Even with such a great variety of rock types at Baca, a considerable amount of isotopic homogenization has taken place, even to the extent that different formations have similar isotopic compositions.

All isotopic and mineralogical alteration in the rocks from Baca 4 and 7 is attributable to the action of meteoric water, whose $\delta^{18}\text{O}$ is estimated at -12% . The presence of appreciable amounts of magmatic and/or metamorphic water in the hydrothermal fluid is not indicated by isotopic compositions of hydrothermally-altered material. Temperatures are somewhat lower than those at The Geysers. 229°C was logged at the bottom of Baca No. 7. In Baca 4 a rock temperature of 232°C was recorded at 969 meters, and 278°C at 1539 meters. This gives an apparent gradient of 89°C per kilometer in the zone between those measurements. It will be recalled that an isotopic equilibrium

temperature and a temperature measured shortly after drilling at The Geysers were 300°C at 1200 meters depth or less.

The maximum permeability at Baca exists in the weakly welded pumice layers in the Bandelier Tuff (700 to 930 meters depth). The Bandelier is the most copious producer of hot water that can be flashed to steam at Baca (R. F. Dondanville, personal communication). Densely welded zones in the Bandelier Tuff have negligible inherent permeability, but have been altered to the same degree as more porous materials in the section

Minerals formed by the hydrothermal alteration of the host rocks occur in pore space in the rock or have formed by replacement. No widespread veining has developed during hydrothermal alteration of rocks at Valles Caldera, in contrast to the extensive veining at The Geysers, where the effects of hydrothermal alteration were mostly confined to fractures and veins. Except in densely welded zones in tuffs, volcanic tuffs and tertiary sandstones have high permeability, and should readily allow the passage of fluid through them. The hydrothermal alteration, however, is pervasive. In the hot water zone all the rock was altered isotopically and petrographically to the same degree. Rocks that were originally less permeable are still isotopically as altered as any other rocks.

$\delta^{18}\text{O}$ values of carbonates and feldspars were found to be sensitive indicators of hydrothermal alteration in the active hot water zone at Valles Caldera. Oxygen isotopic compositions of these minerals respond to changes in temperature and $\delta^{18}\text{O}$ of water with which they

they interacted.

The maximum measured temperature in Baca No. 7 on the edge of the Caldera, 229°C, corresponds closely with the temperature calculated from the $\delta^{18}\text{O}$ values of calcite and water. The measured temperature in Baca No. 4 near the center of the Caldera is 278°C.

4.5.2 Isotopic Analyses of Materials from Baca No. 7

4.5.2.1 General Statements

The $\delta^{18}\text{O}$, δD and $\delta^{13}\text{C}$ values of rocks and minerals selected from the cuttings of Baca No. 7 are given in Table 9. The table also gives depths of origin and descriptions of materials, as well as other pertinent information regarding special treatments, etc. The $\delta^{18}\text{O}$ values of the rocks and minerals of Baca No. 7 are plotted against depth of origin in Figures 28 and 29. Also, these figures contain a brief outline of the stratigraphic sequence penetrated by Baca No. 7. Each major rock type will be discussed individually in terms of its variations in isotopic composition.

4.5.2.2 Unaltered or Little-Altered Rock in Baca No. 7 (surface to 500 meters depth).

4.5.2.2.1 Redondo Creek Member, Valles Rhyolite

The Redondo Creek Member of the Valles Rhyolite contains no quartz, and is characterized by phenocrysts of plagioclase mantled with sanidine. This rock would more correctly be called a pyroxene-biotite trachyte. Pyroxene crystals show signs of resorption, and the biotite appears weathered.

TABLE 9

DESCRIPTIONS AND ISOTOPIC COMPOSITIONS OF ROCKS AND MINERALS
FROM BACA NO. 7, VALLES CALDERA, NEW MEXICO

See "General Remarks", Table 3

<u>Well and Number</u>	<u>Depth, meters</u>	<u>Sample Description</u>	$\delta^{18}\text{O} \text{ ‰}$	$\delta^{13}\text{C} \text{ ‰}$	$\delta\text{D} \text{ ‰}$	<u>Remarks</u>
B 7 - 2	152 - 183	Redondo Cr. Member	+ 7.10		-77.9	trachyte, 0.4 wt. % H ₂ O
B 7 - 4	213 - 244	Redondo Cr. Member	+ 4.45		-83.9	trachyte, 0.6 wt. % H ₂ O
B 7 - 6	274 - 305	Redondo Cr. Member	+ 5.68			trachyte
B 7 - 8	335 - 366	Redondo Cr. Member	+ 6.81			trachyte
B 7 - 10	396 - 427	Redondo Cr. Member	+ 5.46			trachyte
B 7 - 12 a	457 - 488	volcanic detritus	+ 7.92			formic acid treated
b		carbonate from same	+21.45	- 3.02		calcite fraction
		carbonate from same				dolomite fraction
B 7 - 14	518 - 549	volcanic detritus	+ 6.68		-86.2	0.9 wt. % H ₂ O
B 7 - 16	579 - 610	volcanic detritus	+ 4.64			
		carbonate, from same	+ 6.31	- 3.34		
B 7 - 19	671 - 701	volcanic detritus	+ 6.75			
B 7 - 20	701 - 732	a	+ 2.56			} 2.40 ± 0.23
		b	+ 2.23			
		c				
		d	+10.38		-97.6	1.1 wt. % H ₂ O
		e	+ 8.22			-100 mesh, HF-HCl treated HF-HCl treated

TABLE 9: BACA NO. 7, CONTINUED

<u>Well and Number</u>	<u>Depth, meters</u>	<u>Sample Description</u>	$\delta^{18}\text{O} \text{ ‰}$	$\delta^{13}\text{C} \text{ ‰}$	$\delta\text{D} \text{ ‰}$	<u>Remarks</u>
B 7 - 20 f		carbonate	- 0.66	- 5.54		
B 7 - 22 a	762 - 793	Bandelier Tuff, altered quartz, groundmass	+ 2.43			-100 mesh, HF-HCl treated
			+10.16			
B 7 - 24 a	823 - 854	Bandelier Tuff, altered quartz, mixture	+ 2.45			HF-HCl treated, phenocryst-groundmass mixture
			+ 8.94			
B 7 - 26 a	884 - 933	Bandelier Tuff, altered quartz, groundmass	+ 1.85			-100 mesh, HF-HCl treated
			+ 9.76			HF-HCl treated
		quartz, phenocryst	+ 8.53			
		quartz, phenocryst	+ 8.40			
B 7 - 28 a	976 - 1006	red tuffaceous sandstone	+ 3.18			Santa Fe Formation, arkosic
		quartz, crystals	+10.90			cleaned with HF-HCl
		quartz, crystals	+11.19			cleaned with HF-HCl
B 7 - 30 a	1037 - 1067	red tuffaceous sandstone	+ 2.18			cleaned with HF-HCl
		quartz, crystals	+10.41			
		calcite, w/quartz crystals	- 1.87	- 6.01		
B 7 - 32 a	1098 - 1128	red tuffaceous sandstone	+ 1.10			cleaned with HF-HCl
		quartz, crystals	+ 9.75			
B 7 - 34	1159 - 1189	buff sandstone	+ 3.90			Permian; arkosic

TABLE 9: BACA NO. 7, CONTINUED

<u>Well and Number</u>	<u>Depth, meters</u>	<u>Sample Description</u>	$\delta^{18}\text{O} \text{ ‰}$	$\delta^{13}\text{C} \text{ ‰}$	$\delta\text{D} \text{ ‰}$	<u>Remarks</u>
B 7 - 44 a	1463 - 1494	quartz, with wairakite	+ 9.74			} cleaned with HF-HCl } 9.60 ± 0.20 } from gray, silicified lime- } stone
b		quartz, with wairakite	+ 9.46			
c		calcite	- 2.32	- 3.14		
B 7 - 45 a	1494 - 1524	calcite	- 1.48	- 3.27		from white, silicified lime- stone
b		calcite	- 4.26	- 0.64		} from gray, silicified } limestone
c		calcite	- 4.33	- 0.29		
B 7 - 51 a	1677 - 1687	milky quartz	+ 8.37			} HF-HCl treated, from } granite } 8.18 ± 0.02 } 1.34 ± 0.02 } -91.7 0.5 wt. % H ₂ O
b		milky quartz	+ 7.99			
c		milky quartz	+ 8.17			
d		k-feldspar	+ 1.35			
e		k-feldspar	+ 1.32			
f		granite				

FIGURE 28

$\delta^{18}\text{O}$ values of calcite and whole-rocks from various depths, Baca No. 7, Valles Caldera.

A stratigraphic column, in which the rock types penetrated by the well are described, appears along the left side of the figure. Isotopically-estimated temperatures of formation of calcite are noted next to calcite $\delta^{18}\text{O}$ values. Included are $\delta^{18}\text{O}$ values of little-altered volcanic rocks from depths less than 700 meters, surface samples of Bandelier Tuff, and hydrothermally-altered tuff and tuffaceous sandstone in the well. The uppermost occurrences of the hydrothermally-formed minerals epidote, pyrite and wairakite are indicated.

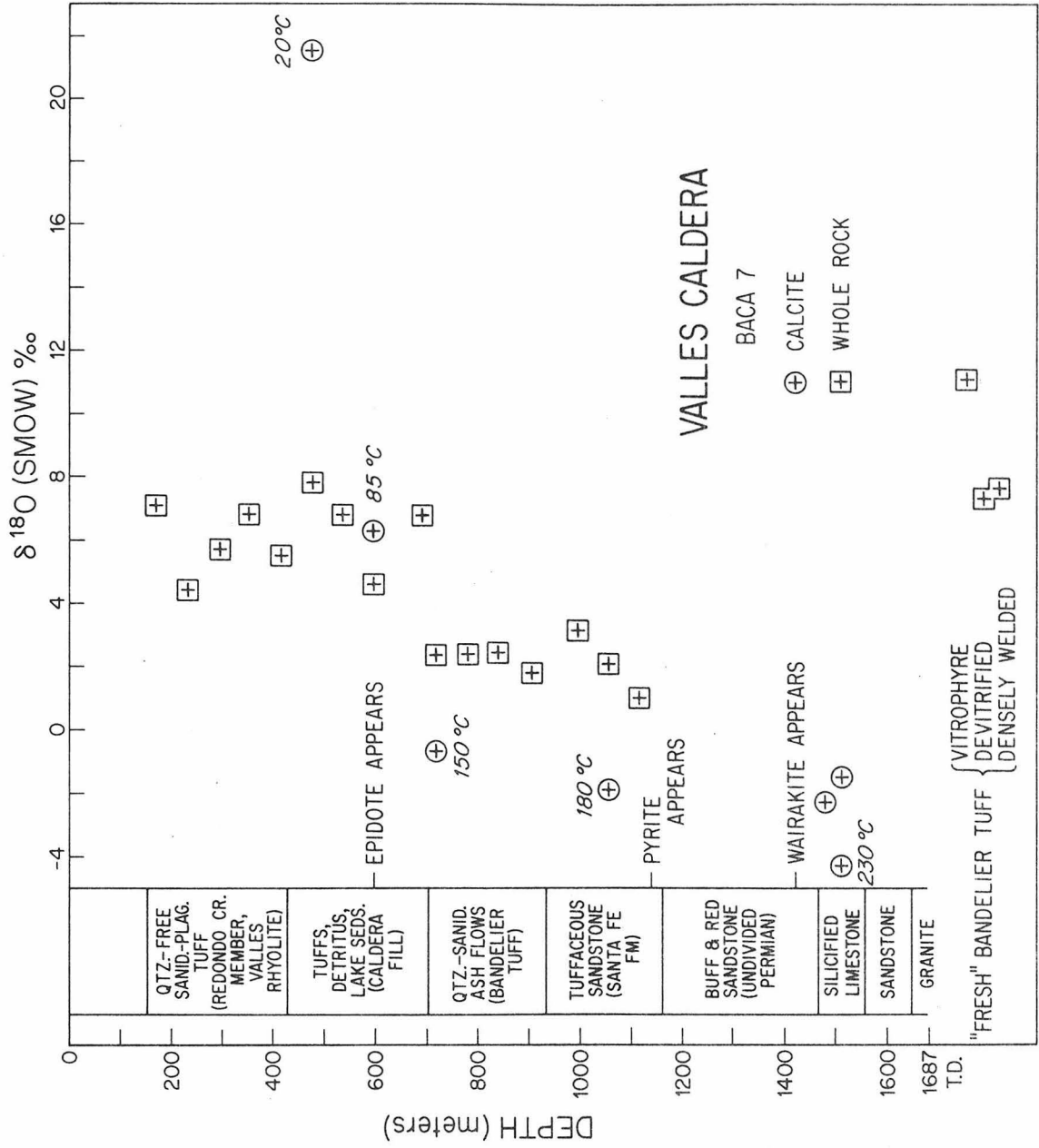
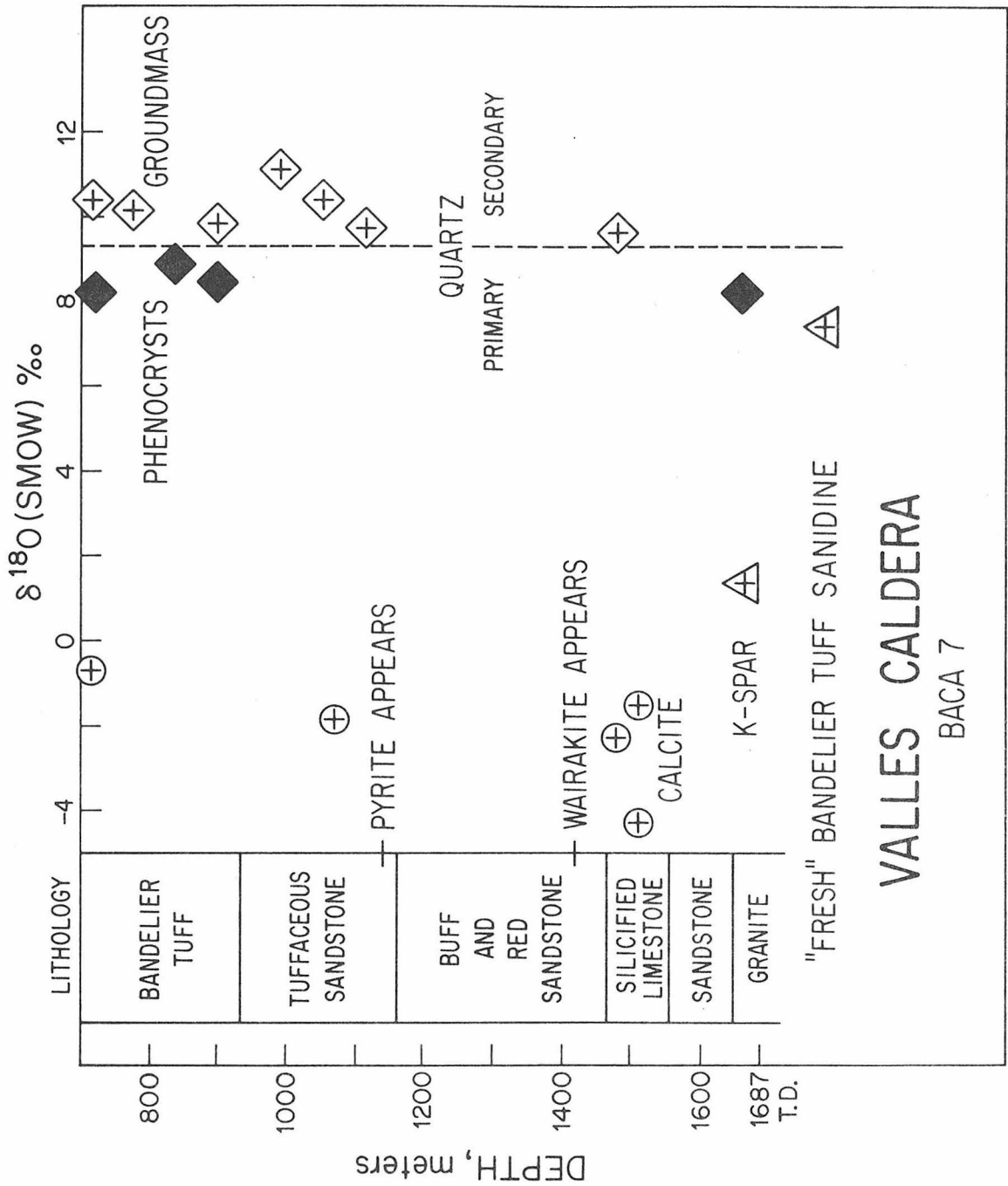


FIGURE 29

$\delta^{18}\text{O}$ values of minerals from various depths in the hot-water zone, Baca No. 7, Valles Caldera.

Part of the stratigraphic column which appeared in Figure 28 is repeated here, as are $\delta^{18}\text{O}$ values of calcite and the uppermost occurrences of pyrite and wairakite. The figure shows that quartz from the volcanic rock groundmass that crystallized from glass has higher $\delta^{18}\text{O}$ values than primary (phenocryst) quartz. This suggests the possibility that the groundmass crystallized at low-temperature hydrothermal conditions (around 100°C) in the presence of meteorically-derived fluid. Quartz from the granite is also shown, as well as its feldspar, whose $\delta^{18}\text{O}$ is lower by 6‰ relative to Bandelier Tuff sanidine which is not hydrothermally altered.



The $\delta^{18}\text{O}$ of the analyzed samples of Redondo Creek Member ranges in value between 4 and 7‰, as compared to the range from 6 to 8‰ for trachytes analyzed by Taylor (1974). Most of the plagioclase-rich cores of the feldspar phenocrysts have been sericitized, and the groundmass has been slightly devitrified. The petrographic features and the $\delta^{18}\text{O}$ values lower than the typical values for trachytes are evidence of some sort of hydrothermal alteration involving the addition of ^{16}O .

Hydrous minerals have been formed in the Redondo Creek member as a result of feldspar sericitization and groundmass devitrification. The rock contains 0.4 to 0.6 weight % H_2O , and the δD value is between -78 and -84‰, the most positive whole-rock δD values in Baca No. 7.

4.5.2.2.2 Caldera Fill

The whole-rock $\delta^{18}\text{O}$ of detrital material in Caldera Fill is similar to that of the Valles Rhyolite which might be the main source of the Fill (Figure 28). The range in $\delta^{18}\text{O}$ values of Caldera Fill (4.5 to 8‰) corresponds closely to the range of Redondo Creek Member (4 to 7.5‰). The δD value of whole-rock volcanic detritus, -86‰, is comparable to that of the Redondo Creek Member (-78 to -86‰), but the H_2O content has increased substantially, from 0.4 to 0.6% by weight in the Redondo Creek Member to 0.9% by weight in Caldera Fill (Table 9).

4.5.2.2.3 Determination of the Upper Boundary of the Hot-Water Zone in Baca No. 7

Down to this point in the well carbonate $\delta^{18}\text{O}$ values were near 20‰. Attention is here given to the intermediate $\delta^{18}\text{O}$ value of calcite, 6.3‰, which occurs at 595 meters depth, 125 meters below the

fresh-water, low temperature (high $\delta^{18}\text{O}$) carbonates. Under the assumption that the $\delta^{18}\text{O}$ of the fluid was -12% , the calculated isotopic temperature of formation of the calcite, whose $\delta^{18}\text{O}$ is 6.3% is 85°C . Consequently, the closest that the hot water (at least as hot as 85°C) approached the surface at Baca No. 7 was somewhere between 470 and 595 meters depth. The drastic change of the $\delta^{18}\text{O}$ value of the carbonate from 20% to 6% represents an unmistakable indicator of hydrothermal alteration between 470 and 595 meters depth

4.5.2.3 Physical Evidence for Hydrothermal Alteration of Host Rock in Baca No. 7

4.5.2.3.1 Authigenic Minerals

The uppermost occurrences in the stratigraphic section at Valles Caldera of certain minerals commonly associated with hydrothermal alteration are indicated in Figure 28. The minerals are epidote, pyrite, and wairakite (the calcium-analogue of analcite). Wairakite was first described in an occurrence at Wairakei, New Zealand (Steiner, 1955). A short time later, wairakite was found at The Geysers (Steiner, 1958). In the cuttings from Baca No. 7, wairakite is well developed near the top of the silicified limestone (Figure 28) as a matrix between authigenic quartz crystals. Its highest occurrence is 1400 meters below the surface in the "buff and red sandstone." Wairakite was identified by X-ray diffraction. The mineral is thought to form from solution only under conditions of supersaturation with respect to silica (Coombs, Ellis, Fyfe and Taylor, 1959).

Pyrite occurs as euhedral crystals with brightly-reflective

faces, less than 1/2 mm wide in any direction. The fact that it is so well preserved at depths greater than 1140 meters indicates that the pyrite and the hydrothermal fluid were at the time of drilling, in chemical equilibrium, for pyrite becomes etched readily when the pH, oxygen partial pressure, or total dissolved sulfur changes in the solution.

Epidote's highest occurrence coincides with the appearance of calcite whose $\delta^{18}\text{O}$ value is 6.3‰ (595 meters) whose formation could have taken place in the presence of a hydrothermal fluid at 85°C. It occurs as yellow-green prismatic crystals, commonly replacing other iron and magnesium silicate minerals in igneous rocks. Epidote and chlorite replace the original hornblende and biotite of the pink granite in the bottom of the well (1680 meters deep).

4.5.2.3.2 Changes in Rock Textures

All surface samples of Bandelier Tuff (Plate 17) have a glassy groundmass. The principal difference between fresh Bandelier Tuff and that from the well cuttings is that hydrothermal alteration of the well samples has crystallized the groundmass to a mixture of quartz, clay and/or mica minerals and carbonates (Plate 18). Also sanidine phenocrysts in hydrothermally-altered volcanics contain clay and/or mica minerals and carbonates, especially along fractures (Plate 19).

4.5.2.4 Isotopic Changes Accompanying Hydrothermal Alteration of Rock

In order to determine the changes in isotopic composition that accompany the hydrothermal alteration of rock, it is desirable to

PLATE 17.

Fresh Bandelier Tuff, Los Alamos, New Mexico.

Area of view: 1.6×1.2 mm. X-nicols.

Phenocrysts of sanidine (lower left), quartz (left center) and hornblende (lower right) in a groundmass of glass which is only slightly devitrified. A surface sample.

PLATE 18.

Hydrothermally altered Bandelier Tuff, Baca No. 7, Valles Caldera.
701 to 732 meters depth.

Area of view: 1.6×1.2 mm. X-nicols.

Phenocrysts of sanidine (white) partially sericitized and replaced with calcite (light gray), in crystalline groundmass (mottled) of quartz, carbonate and white mica. From the hot-water zone.

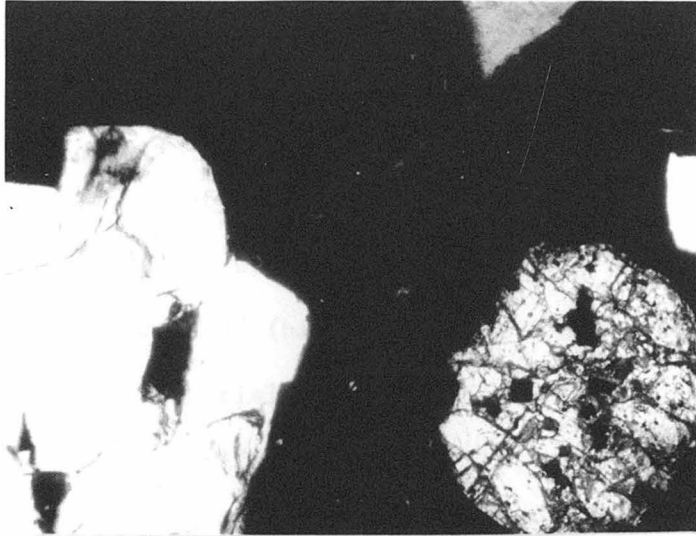


PLATE 17

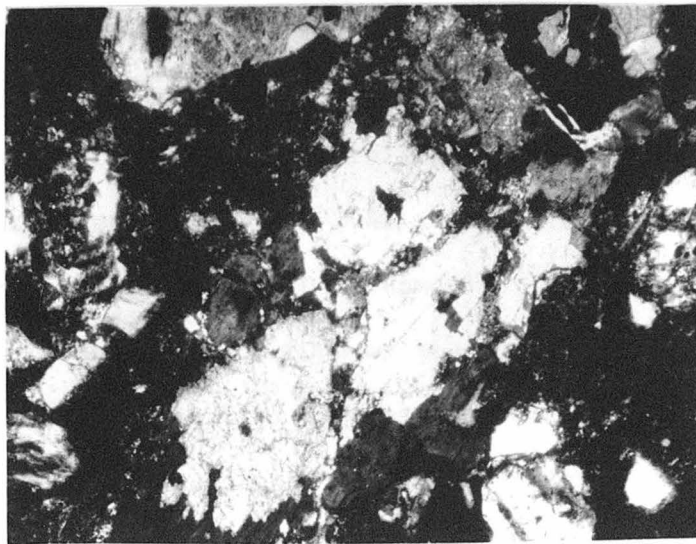


PLATE 18

know the isotopic composition of the unaltered as well as the altered rock. Samples of altered and unaltered Bandelier Tuff were available from Valles Caldera, and allow a comparison of their $\delta^{18}\text{O}$ values to be made.

Surface samples of Bandelier Tuff collected by R. F. Dondanville near Los Alamos consisted of three varieties: "vitrophyre," "devitrified," and "densely welded" (his terms). The isotopic compositions of some samples of this material are given in Table 10. $\delta^{18}\text{O}$ values of densely welded and devitrified Bandelier Tuff are around 7.5‰, but the vitrophyre $\delta^{18}\text{O}$ value is 11.2‰. The vitrophyre value, higher than the others, is in agreement with $\delta^{18}\text{O}$ values of volcanic rocks rich in hydrated glass shards, analyzed and discussed by Taylor (1968). The sanidine $\delta^{18}\text{O}$ value from the "densely welded" sample is about 7‰, similar to the feldspars from Taylor's glassy ash-flow tuffs (7 to 9.8‰).

Bandelier Tuff with a crystalline groundmass (Plate 18; Plate 19) has $\delta^{18}\text{O}$ values between 1.8 and 2.4‰, indicating that hydrothermal alteration has lowered the $\delta^{18}\text{O}$ of Bandelier Tuff about 5.5‰ from its normal value of about 7.5‰. One of the obvious reasons for this change is the crystallization of the glass in the groundmass in the presence of the aforementioned hydrothermal fluid.

The rock unit stratigraphically below Bandelier Tuff consists of tuffaceous and arkosic sandstones of the Tertiary Santa Fe Formation. Whole-rock $\delta^{18}\text{O}$ values of the Santa Fe Formation are similar to those of the Bandelier Tuff, 1.1 to 3.2‰ (Table 9 and Figure 28).

TABLE 10

ISOTOPIIC COMPOSITION OF SURFACE SAMPLES
OF BANDELLIER TUFF, LOS ALAMOS, NEW MEXICO

See "General Remarks", Table 3

<u>Sample Name</u>	<u>Depth, meters</u>	<u>Sample Description</u>	<u>$\delta^{18}O$ ‰</u>	<u>Remarks</u>
Qb - a	surface	Bandelier Tuff sandine	+ 7.63 + 7.27	densely welded hand-picked from rock
Qb - b	surface	Bandelier Tuff	+ 7.26	incipiently devitrified
Qb - c	surface	Bandelier Tuff Bandelier Tuff	+11.10 +11.17	} vitrophyre, fresh 11.14 ± 0.05

Stratigraphically just below the Santa Fe, buff sandstone from the undivided Permian unit has a $\delta^{18}\text{O}$ of 3.9‰. The Bandelier and the Santa Fe are sufficiently similar mineralogically, that the isotopic similarity is not surprising. The Bandelier, Santa Fe and Permian sandstone represent a stratigraphic thickness of 700 meters.

4.5.2.5 Isotopic Changes in Individual Minerals in the Hot-Water Zone of Baca No. 7 (Depths greater than 700 meters).

Essential to an understanding of the isotopic alteration of rock is a study of isotopic changes in minerals. Few of the minerals in rocks of the Baca No. 7 cuttings could be purified for analysis, so the following discussion is restricted to those minerals whose isotopic compositions could be measured directly or determined indirectly by difference or by material balance.

4.5.2.5.1 $\delta^{18}\text{O}$ Values of Carbonates

The lowest $\delta^{18}\text{O}$ value of a calcite found in Baca No. 7 is -4.3‰, one of the lowest $\delta^{18}\text{O}$ values known for a naturally occurring calcite. This calcite appears in a gray silicified limestone from 1510 meters depth in Baca No. 7. The highest temperature logged in Baca No. 7 is 229°C near the bottom of the well. If the calcite in equilibrium with water at 230°C had a $\delta^{18}\text{O}$ value of -4.3, equation (G-3) requires that the $\delta^{18}\text{O}$ of the water be -11.8‰, corresponding almost exactly to the average $\delta^{18}\text{O}$ value of meteoric water in the Jemez Mountains, suggesting that the $\text{H}_2\text{O}/\text{calcite}$ ratio was very much greater than one.

From the same cuttings fraction which yielded the low- $\delta^{18}\text{O}$ calcite from gray limestone, another limestone (white) was found to

contain calcite with a $\delta^{18}\text{O}$ value of -1.5‰ . In a gray silicified limestone occurring at 1480 meters depth, calcite was found with a $\delta^{18}\text{O}$ value of -2.3‰ . At about 1050 meters depth calcite occurred as a cement holding together some detrital quartz grains of the Santa Fe Formation. Its $\delta^{18}\text{O}$ value is -1.9‰ . These similar $\delta^{18}\text{O}$ values of calcite between -1.5‰ and -2.3‰ all suggest that the three calcites were crystallized under similar conditions of temperature and $\delta^{18}\text{O}$ of water. If the water was essentially meteoric ($\delta^{18}\text{O} = -12\text{‰}$) and the three calcites formed in equilibrium with the water, the temperature range they record is 170°C (for the -1.5‰ calcite) to 190°C (for the -2.3‰ calcite). Alternatively, all three might have formed at the same temperature with varying values of the water/calcite ratio.

Calcite in the topmost part of the Bandelier Tuff at 720 meters depth has a $\delta^{18}\text{O}$ value of -0.7‰ . If this calcite also formed in equilibrium with the meteoric water ($\delta^{18}\text{O} = -12\text{‰}$) then its calculated isotopic temperature of formation is about 160°C . The estimated temperature of the Bandelier Tuff in Baca No. 7 is 150 to 200°C (R. F. Dondanville, personal communication). Again, the calculated isotopic temperature based on an assumption regarding the water $\delta^{18}\text{O}$ is in good agreement with an approximate measured temperature.

All of the above temperature estimates are based on a hydrothermal fluid $\delta^{18}\text{O}$ value of -12‰ , which implies that in each case the water/calcite ratio was much greater than one. Actually this cannot be far from the truth. If the $\delta^{18}\text{O}$ value of the hydrothermal fluid were less negative than -12‰ , the isotopic temperature inferred from

the calcite $\delta^{18}\text{O}$ values would be unreasonably higher than logged temperatures.

If the difference in the $\delta^{18}\text{O}$ value between the gray and white limestone (-4.3‰ vs. -1.5‰) is real, then the calcite recorded at least two different hydrothermal events, the higher temperature one being most similar to the present-day activity (about 230°C) as indicated by the logged temperature. This suggests that the temperatures of the rocks in Valles Caldera may still be rising.

4.5.2.5.2 Quartz $\delta^{18}\text{O}$ Values

Quartz was isolated from samples of altered Bandelier Tuff by the HF-HCl treatment described previously. The purification of quartz resulted in two physically-distinct fractions: primary, vitreous phenocryst quartz and second, milky groundmass quartz, which ends up finer than 100 mesh after the HF-HCl treatment. Phenocryst quartz from well samples had $\delta^{18}\text{O}$ values between 8.2 and 8.9‰ (Table 9). Milky fine-grained quartz from the crystalline groundmass had $\delta^{18}\text{O}$ values between 9.8‰ and 10.4‰.

Besides the vitreous quartz and milky groundmass quartz in the Bandelier Tuff there are other occurrences of quartz in the cuttings of Baca No. 7. The quartz in the pink granite at the bottom of the well (1687 meters depth) has a $\delta^{18}\text{O}$ value of 8.2‰, which is a typical value for igneous quartz. Authigenic quartz from the tuffaceous sandstones (Santa Fe Formation) has a range in $\delta^{18}\text{O}$ of 9.8 to 11‰.

All the $\delta^{18}\text{O}$ values of individual minerals (calcite, quartz and feldspar) as well as the depths of their locations are plotted in

Figure 29. The diagram covers only the active hot-water zone (700 to 1687 meters depth). The stratigraphic column is included as it was in Figure 28, and the highest occurrences of pyrite and wairakite are marked.

A dividing line is drawn in Figure 29 at $\delta^{18}\text{O} = 9.2\text{‰}$. On the lower $\delta^{18}\text{O}$ -side of the line, the $\delta^{18}\text{O}$ values are those of phenocrysts and granite quartz. On the high- $\delta^{18}\text{O}$ side the quartz is authigenic. All the quartz values are typical of igneous rocks (Taylor, 1968) and the dividing line at $\delta^{18}\text{O} = 9.2\text{‰}$ has no particular numerical significance, other than to indicate that ranges of $\delta^{18}\text{O}$ values of primary and hydrothermal authigenic quartz in these rocks do not overlap. The significance of the dividing line is to illustrate primarily that $\delta^{18}\text{O}$ of secondary (groundmass) quartz in the Bandelier Tuff is 1 to 2‰ higher than that of primary (phenocryst) quartz.

The $\delta^{18}\text{O}$ value of quartz formed by a meteorically-derived hydrothermal fluid cannot be greater than the $\delta^{18}\text{O}$ of igneous quartz unless its temperature of formation were low.

In those cuttings fractions whose rock material contained both secondary quartz and calcite, the Δ_{QC} is in all cases about 12‰. Clearly the quartz and calcite are not in isotopic equilibrium for even at 0°C, the Δ_{QC} predicted by the low-temperature extrapolation of the quartz-calcite geothermometer, Equation (G-1), is about 8‰. It was shown that the minimum temperature of formation isotopically recorded by calcite was 150°C in the hot-water zone, in the presence of water whose $\delta^{18}\text{O}$ was -12‰. If the same fluid was responsible for the

crystallization of volcanic glass in the groundmass to a mixture of quartz and other minerals, the quartz $\delta^{18}\text{O}$ value indicates a very large Δ_{QW} , about 22‰. Using the extrapolated quartz-water isotopic geothermometer, the approximate temperature of formation of groundmass quartz, in equilibrium with meteoric water, is about 90°C. The quartz evidently formed at temperatures lower than those indicated by the $\delta^{18}\text{O}$ values of calcite in the hot-water zone, but once the quartz was formed, it was resistant to subsequent isotopic exchange with the fluid even at temperatures greater than 90°C.

The temperature of formation suggested by the $\delta^{18}\text{O}$ value of the crystalline groundmass quartz from the Bandelier Tuff is almost identical with the temperature that was suggested by the $\delta^{18}\text{O}$ of recrystallized calcite in the detritus at 595 meters depth. The thermal events which resulted in the formation of the groundmass quartz and the recrystallized calcite may very well have been contemporaneous during the early stages of the hydrothermal system, if the water/mineral ratios were very large.

The fluids in the hot-water zone were probably rich in dissolved silica. This is indicated by the presence of wairakite and by the development of authigenic quartz in the tuffaceous sandstone.

The total amount of quartz in altered Bandelier Tuff is as high as 40%. All the quartz has been shown to have $\delta^{18}\text{O}$ values at least as high as 8‰. There must be other low- $\delta^{18}\text{O}$ minerals in the altered Bandelier Tuff to account for a whole-rock $\delta^{18}\text{O}$ value of 2‰. The lowest- $\delta^{18}\text{O}$ mineral found in the Bandelier Tuff is calcite (-1‰), but

the tuff contains only 2% calcite by weight. The isotopic compositions of other minerals, the clays, micas and feldspars, must be very important in determining the $\delta^{18}\text{O}$ values of Bandelier Tuff.

4.5.2.5.3 Feldspar

The only primary feldspar analyzed from the unaltered Bandelier Tuff surface samples was hand-picked from disaggregated "devitrified" tuff. Its $\delta^{18}\text{O}$ value was 7.3‰, a normal igneous value (Table 10).

The $\delta^{18}\text{O}$ value of a pink feldspar hand-picked from the granite at the bottom of Baca No. 7 was 1.3‰ (Table 9). This is far outside the normal igneous range for alkali feldspars (7 to 10‰; Taylor, 1968). The granite quartz, however, has retained its igneous $\delta^{18}\text{O}$ value, 8.2‰. Clearly, the feldspar in the granite has interacted with meteoric water, which resulted in a lowering of the $\delta^{18}\text{O}$ value of the feldspar.

There is some evidence that the water/feldspar ratio is not very large in the granite. The $\Delta_{\text{feldspar-water}}$, using the $\delta^{18}\text{O}$ values of granite feldspar and meteoric water, is 13.3‰. By low-temperature extrapolation of the relationship between α and temperature for feldspar and water (O'Neil and Taylor, 1967), the calculated temperature is 144°C, considerably lower than the temperature logged at the bottom of the well, 229°C. At 229°C, the $\delta^{18}\text{O}$ value of water in equilibrium with the granite feldspar is about -7‰, not -12‰. This apparent oxygen isotope shift in the meteorically-derived hydrothermal fluid may be indicative of less water circulation in the granite than in the tuffs and tuffaceous sandstone.

At 180°C, the maximum logged temperature of the Bandelier Tuff,

estimated from the calcite $\delta^{18}\text{O}$ value, feldspar in equilibrium with the meteoric water would have a $\delta^{18}\text{O}$ value of -12% . Petrographic evidence indicates that the sanidine phenocrysts in the Bandelier Tuff of Baca No. 7 have been hydrothermally altered (Plate 18; Plate 19). It is reasonable that oxygen exchange between feldspar and fluid has taken place during the hydrothermal alteration of feldspar in Bandelier Tuff. The lowering of the $\delta^{18}\text{O}$ of feldspar from igneous values would be reflected in a lowering of $\delta^{18}\text{O}$ of Bandelier Tuff from its normal igneous values.

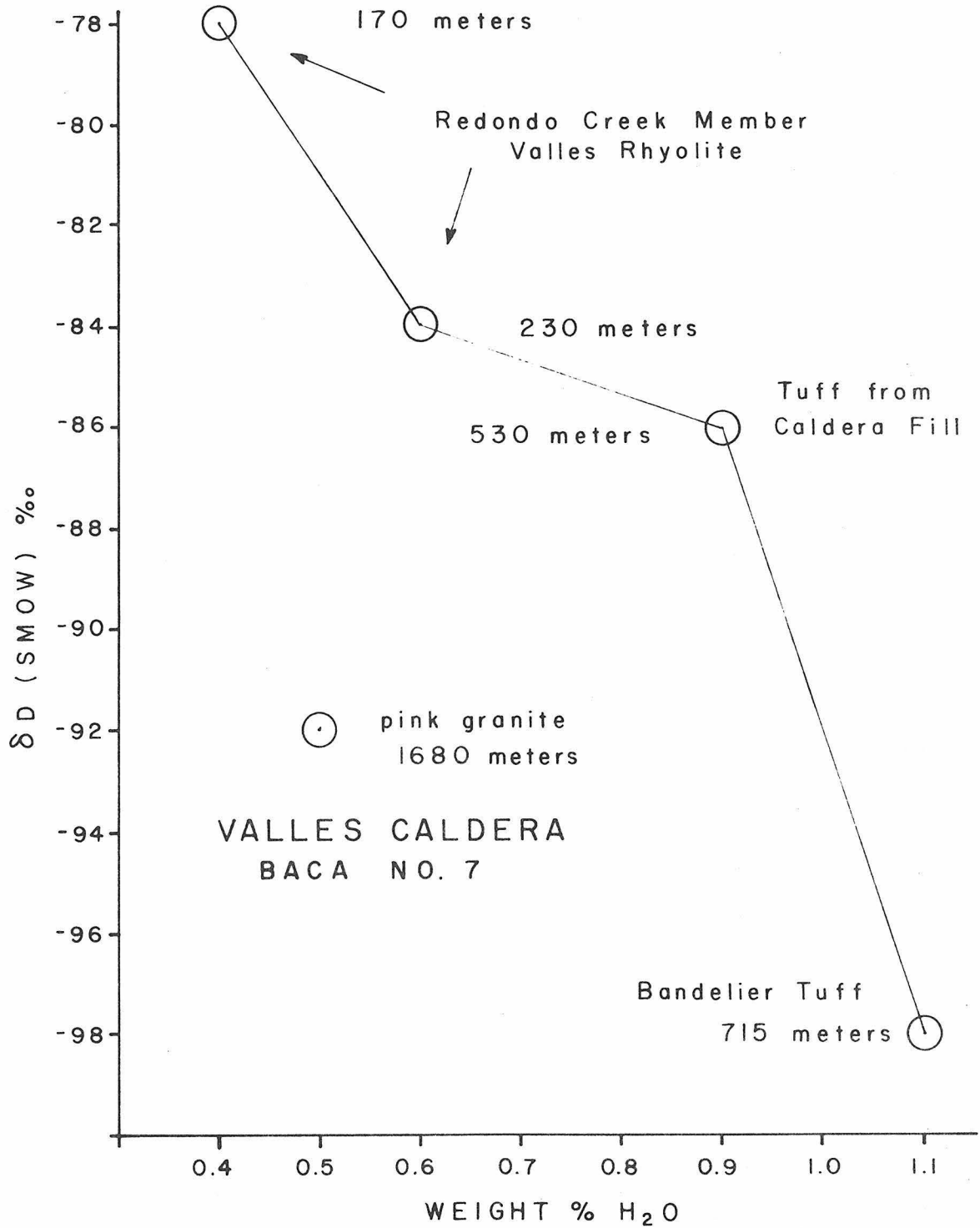
4.5.2.5.4 Hydrous Minerals (Clays and Micas)

Although the $\delta^{18}\text{O}$ values of clays and micas which occur in hydrothermally-altered Bandelier Tuff were not directly determined, their values contribute to the whole-rock $\delta^{18}\text{O}$ value of the Bandelier Tuff. Clays and micas (probably illite and sericite) have formed from the hydrothermal alteration of sanidine in the Bandelier Tuff. Since sericite (muscovite) and illite are chemically similar, their $\delta^{18}\text{O}$ value could be approximated using the relationship of O'Neil and Taylor (1969) for the oxygen isotope fractionation between muscovite and water. If the sericite and illite formed in equilibrium with the meteoric water at Valles Caldera at 180°C (the isotopic temperature of calcite deposition in the Bandelier Tuff), the $\delta^{18}\text{O}$ value of sericite and illite in the Bandelier Tuff would be -5% . Thus the formation of clays and micas, constituting as much as 40 weight % of the rock could certainly contribute to the lowering of the $\delta^{18}\text{O}$ value of Bandelier Tuff to 2% .

FIGURE 30

δD values of hydrothermally altered volcanic rocks plotted against water content in weight percent, Baca No. 7, Valles Caldera.

The figure shows that as hydrothermal alteration proceeds as the water content of volcanic rocks increases, the water that is added is low in deuterium.



4.5.2.5.5. δD Variations in Rocks of Baca No. 7

Hydrous minerals were not separated from rocks of Valles Caldera, so δD measurements were made on the whole rocks. Besides the alteration products, such as clays and micas, the only minerals in the cuttings fractions that contain water are traces of biotite (Redondo Creek Member), hornblende (Bandelier Tuff), chlorite (pink granite) and epidote (found throughout the section at depths greater than 515 meters), aside from the secondary micas and clays which were discussed above. The δD values of the whole rocks are given in Table 9.

The range in δD values of whole rocks from Baca No. 7, -78 to -98‰, happens to overlap the range for "normal" igneous rocks, -50 to -85‰ (Taylor, 1974). Two of the rocks have δD values that fall outside the normal igneous range: Bandelier Tuff (-98‰) and pink granite (-92‰).

Figure 30 shows a plot of δD values of various whole-rock types as a function of the weight percent of water they contained. Aside from the pink granite, the tuffs show decreasing δD value with increasing water content. Samples of the Redondo Creek Member have the highest δD values, -78 and -84‰, which are within the "normal" igneous δD range. The H_2O -rich sample (0.6% by weight) has the lower δD (-84‰). The sample poorer in H_2O (0.4% by weight) has a δD value of -78‰. The diagram shows that as hydrothermal alteration of tuffaceous rock proceeds, the water that is progressively added to the rock during the formation of hydrous minerals is low in deuterium. The δD value of the H_2O in the Bandelier Tuff is -98‰, outside the igneous range, while

the H₂O content is as high as 1% by weight

4.5.2.5.6 $\delta^{13}\text{C}$ Variations in Carbonates

$\delta^{13}\text{C}$ values of calcites range from 0.3‰ to -6‰. At 1510 meters depth the calcite from the marine limestone has a typical marine $\delta^{13}\text{C}$ value, 0.5‰, but calcite from white limestone has a $\delta^{13}\text{C}$ value of -3.3‰. Even within the range of $\delta^{13}\text{C}$ values of carbonates at Valles Caldera (which is narrow compared to the 16‰ spread in calcite $\delta^{13}\text{C}$ values at The Geysers) there is some variation. The carbonates in the cuttings of Baca No. 7 have $\delta^{13}\text{C}$ values that are characteristic of both marine and fresh-water carbonates, even though their $\delta^{18}\text{O}$ values are in some cases drastically different from those of marine and fresh-water carbonates.

The ^{13}C values of hydrothermal carbonate at Valles Caldera are evidently the same as those of non-hydrothermal carbonates from which they were locally derived.

4.5.3 Isotopic Data from Baca No. 4

4.5.3.1 Introduction

The chief significance of the Baca No. 4 samples is that the well is located near the center of the Caldera. Temperatures logged in Baca No. 4 are slightly higher than those of Baca No. 7. The rock type available for analysis from Baca No. 4 is Bandelier Tuff, which has been previously described.

Two samples of Bandelier Tuff from Baca No. 4 became available when a hot-water zone was encountered by the drill bit and material was

blown out. Some fragments came from 969 meters depth, the others from 1494 to 1539 meters depth. The similarity of the two samples taken at least 525 meters apart indicate that the thickness of the Bandelier Tuff is greater at the center of Valles Caldera, near Baca No. 4, than it was at the northern edge of the Caldera. At Baca No. 7 it was only 200 meters thick. The logged rock temperatures at Baca No. 4 were also greater: 232°C at 969 m and 278°C at 494 to 1539 m as compared to the maximum rock temperature in Baca No. 7 of 229°C. Petrographically the rocks from Baca No. 4 are very similar to the Bandelier Tuff in Baca No. 7, and show the same types of hydrothermal alteration discussed previously (Plate 20). The isotopic data for Baca No. 4, depths of origin of the samples, and descriptions of samples are given in Table 11.

4.5.3.2 Results

The calcite content in the 969 m sample was 1.3% by weight. Its $\delta^{18}\text{O}$ value is -2.83% and its $\delta^{13}\text{C}$ is -4.16% . If the calcite was in isotopic equilibrium with the hydrothermal water at the logged 232°C, then the $\delta^{18}\text{O}$ value of the water is -10.3% , which is only marginally different from the estimated meteoric value -12% . Using the $\delta^{18}\text{O}$ of calcite and the estimated meteoric water value, the calculated isotopic temperature is 196°C. It is conceivable that this represents the correct temperature of formation of the calcite. Thus the calcite could be a relic of a former temperature regime. It was also suggested that there were relic $\delta^{18}\text{O}$ values of calcite in Baca No. 7 that indicated lower calcite crystallization temperatures at 1510 meters depth than those logged. It is more likely, however, that because the

PLATE 19.

Hydrothermally altered Bandelier Tuff, with sanidine phenocryst, Baca No. 7, Valles Caldera. 701 to 732 meters depth.

Area of view: 1.6×1.2 mm. X-nicols.

Sanidine phenocryst partially hydrothermally altered to white mica (white spots in phenocryst). Note unaltered quartz (upper right) in crystalline groundmass of quartz, carbonate and white mica. From the hot-water zone.

PLATE 20.

Hydrothermally altered Bandelier Tuff, Baca No. 4, Valles Caldera. 969 meters depth.

Area of view: 1.6×1.2 mm. X-nicols.

Note that quartz phenocrysts are unaltered (upper left), but sanidine (lower right) is partially replaced by carbonate and white mica. Plagioclase in center is partially resorbed. From the hot-water zone.

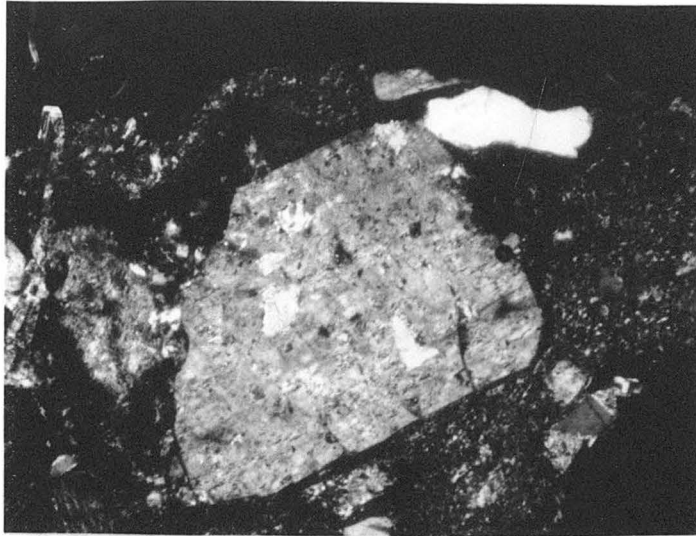


PLATE 19

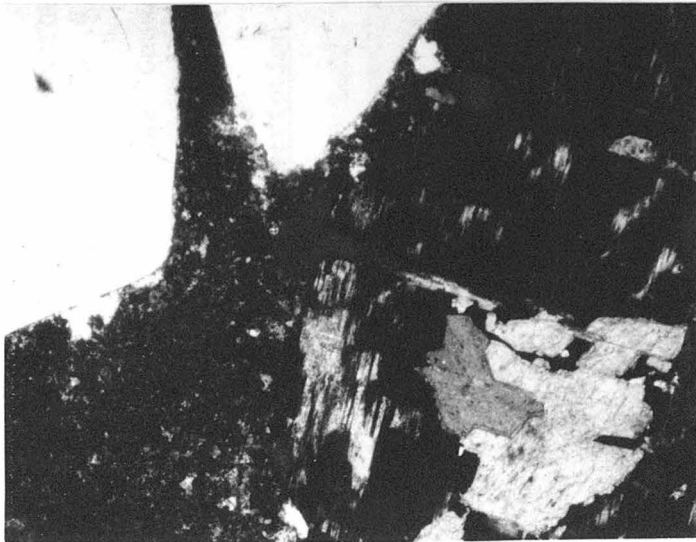


PLATE 20

TABLE 11

DESCRIPTIONS AND ISOTOPIC ANALYSES OF ROCKS AND MINERALS
FROM BACA NO. 4, VALLES CALDERA, NEW MEXICO

See "General Remarks", Table 3

<u>Well and Number</u>	<u>Depth, meters</u>	<u>Sample Description</u>	<u>$\delta^{18}O$ ‰</u>	<u>$\delta^{13}C$ ‰</u>	<u>Remarks</u>
B 4 - 1 a	969	Bandelier Tuff, altered	+0.92		blown-out fragments
b		quartz, phenocryst	+8.38		HF-HCl treated
c		quartz, phenocryst	+8.54		} 8.39 ± 0.15
d		quartz, phenocryst	+8.24		
e		carbonate	-2.83	- 4.16	
B 4 - 2 a	1494 -1539	Bandelier Tuff, altered	+0.18		blown-out fragments
b		quartz, phenocryst	+8.38		} HF-HCl treated
c		quartz, phenocryst	+8.20		
d		quartz, phenocryst	+8.13		

969 m Baca No. 4 samples came from a permeable zone containing hot water, the calcite has responded isotopically to the present hot water and is in equilibrium with the fluid. If this is the case, then there has been a true oxygen isotope shift from -12% in meteoric water to -10.3% in hydrothermal water. It is not really possible to be certain of which interpretation is correct, on the basis of these few data. Nevertheless, in principle such questions can be resolved by isotope data.

The Bandelier Tuff from Baca No. 4 is replete with evidence of hydrothermal alteration just as was the rock from Baca No. 7. The groundmass was fine-grained crystalline quartz, for the most part. Calcite is also present in significant amounts; hydrous minerals, however, are not conspicuous even in the vicinity of former sanidine crystals, but are dispersed in the groundmass. The only phenocrysts which have withstood alteration are quartz (Plate 20). In addition, the rock contains partially-assimilated accidental inclusions of pyritiferous sandstone. In many cases, all that remains of these inclusions are local concentrations of pyrite and recrystallized quartz.

Values of $\delta^{18}\text{O}$ for the whole rocks of Baca No. 4 are 0.9% for the 969 meter sample and 0.2% for the 1494 to 1539 sample. These values are to be compared with the $\delta^{18}\text{O}$ range of altered Bandelier Tuff from Baca No. 7: 1.9 to 2.6% . If the isotopic composition of fluid were the same in Baca No. 4 as in Baca No. 7, $\delta^{18}\text{O}$ values of Baca No. 4 Bandelier Tuff, which are 1 to 2% lower than their counterparts in Baca No. 7, are indicative of higher temperatures of

alteration than those which prevailed in Baca No. 7.

The mean $\delta^{18}\text{O}$ value of 6 quartz samples independently prepared by the HF-HCl treatment (3 each from both rocks from Baca No. 4) was 8.3‰. The standard deviation was 0.15‰. All of these samples were composed entirely of milky groundmass quartz and contained no phenocrysts, yet the mean $\delta^{18}\text{O}$ value, 8.3‰, is virtually identical with that of phenocryst quartz in Baca No. 7. Even though the $\delta^{18}\text{O}$ value is typical of igneous quartz, the quartz is definitely not igneous in origin, and could still have formed by crystallization from a glassy groundmass in ash-flow tuff at temperatures in the neighborhood of 120°C. The true test, however, of the formation of low-temperature quartz in Baca No. 4 would be authigenic quartz with a $\delta^{18}\text{O}$ value 8.3‰ in a non-igneous rock. Without such data, the occurrence of milky groundmass quartz with a $\delta^{18}\text{O}$ value of 8.3‰ in an igneous rock is not conclusive.

4.6 Summary: Rock-Fluid Interactions at Valles Caldera

It has been shown that a hydrothermal fluid whose isotopic composition is close to that of local meteoric water was responsible for most of the hydrothermal alteration of rocks in two wells in the Valles Caldera of New Mexico. Furthermore, only a small oxygen isotope shift in the fluid had taken place, suggesting that the effective fluid/rock ratio was very large. This tremendous quantity of water in relation to the volume of rock attests to a high permeability of the host rocks of the hydrothermal system, which are mostly volcanically derived materials. It would appear that if large-scale isotopic

interaction between rocks and meteoric water is to take place, there must be a heat source, some of the rocks must be permeable, and the system must be near the earth's surface. Volcanic terrains, and calderas in particular, satisfy all three requirements. The heat source is the cooling magma chamber, the surrounding and overlying volcanic rocks are commonly vesicular and have porosity, and calderas are near-surface features, so meteoric water can readily gain access to the heat source.

Even with only the few isotopic data that have been obtained from Valles Caldera, the results have allowed the determination of the effects of a number of variables that govern hydrothermal alteration. Isotopic analyses have again provided the basis for making estimates of temperatures at which hydrothermal alteration took place. The results have suggested that hydrothermal activity at Valles Caldera is episodic, and that these may have been separate thermal events whose temperatures were 90°C, 160°C and 230°C. The temperature seems to have increased with time.

The isotopic results have given some indication of the areal and depth distribution of temperatures. The upper boundary of hydrothermal alteration was determined in the northern part of the caldera to be about 600 meters below the surface. Slightly higher temperatures were found to be associated with the center of the Valles Caldera than the edge. This is not a surprising result, if water enters the system at its cooler margins and becomes heated most strongly nearest the heat source. The oxygen isotope shift in the fluid at the center of the

system (if indeed there is only one spatially-continuous hydrothermal system in the entire Caldera) is slightly larger than at the margin, perhaps because there is more water available in the system at the margins. If the hydrothermal system at Valles Caldera is spatially continuous, as is indicated in the isotopic similarities between rocks at the center and at the margin, the system is huge indeed, because the surface area of the Caldera is 300 square kilometers and recent hydrothermal alteration has been found as deep as 1600 meters.

The isotopic results from Valles Caldera give some insight into what sorts of isotopic variations might be expected to occur in fossil hydrothermal systems, such as those in the San Juan Mountains, Western Scotland, and perhaps the Western Cascades (Taylor, 1974). For example, the quartz in the granite in Valles Caldera has retained its igneous $\delta^{18}\text{O}$ value, whereas the feldspar $\delta^{18}\text{O}$ has been lowered by interaction with the hydrothermal fluid, which was meteorically derived. Similar relationships have been observed in fossil systems. The obvious advantage of working with an active hydrothermal system is the availability of information regarding temperatures and isotopic compositions of fluids, whereas in fossil systems these parameters must be deduced. Even though a substantial amount of information was available about the Valles Caldera, however, the isotopic results were not without complication. The possibility of the variability of the mineral/water ratio has in many instances in this chapter rendered a unique interpretation of the isotopic results impossible. This complication would probably be encountered during the study of fossil systems also, and

in the absence of such information as logged temperatures and isotopic compositions of source waters would make the interpretations of some of the fossil system data even more difficult.

5. STUDIES AT THE HEBER GEOTHERMAL ANOMALY,
IMPERIAL VALLEY, CALIFORNIA

5.1 General Statements Concerning the Imperial Valley and Heber Samples

The Imperial Valley in southern California is the northern part of a structural and topographic depression called the Salton Trough, which is considered to be an extension of the Gulf of California (Elders et al., 1972). Since 1961 the Imperial Valley has been the site of extensive exploration drilling for geothermal steam. The drilling has been concentrated around areas of high heat flow, in which the geothermal gradient at the surface is 20°C per 100 meters or greater, as compared to the normal 3°C per 100 meters. These areas, none of which are more than about 10 kilometers across, are called geothermal anomalies. At present, only one, the Cerro Prieto anomaly in Mexico, is being exploited to generate electricity.

The Standard Oil Company of California has drilled some exploration holes into the Heber geothermal anomaly, which underlies a tract of private land midway between Calexico and El Centro, California. The Chevron Oil Field Research Company has made available for study some core plugs from J. D. Jackson Well No. 1, located on Standard's lease on the Heber geothermal anomaly. Standard has not made available the exact location of the well, temperatures measured in the well, or the total depth of the well. The well penetrates at least 1843 meters of sand and mud which are for the most part unconsolidated, except for some minor degrees of cementation by hydrothermal mineral deposition in pore spaces. The porosity of these sediments is quite high, particularly in

the sands, as might be expected. According to reports by Standard Oil, the wells which have been drilled discharge large quantities of nearly neutral, chloride-rich water. Total dissolved solids amount to less than 1.5% by weight, which is substantially less than the maximum which has been observed in thermal water in the Imperial Valley, 26% by weight in the Imperial Irrigation District Well No. 1 (Skinner *et al.*, 1967). It is clear that the Heber geothermal anomaly satisfies the criteria for a hot-water system.

Samples which were made available for isotopic analyses were weakly consolidated cylindrical cuts of sandstone, upon which density, porosity and permeability measurements were made by Standard Oil. There were four sets of samples: three from 975 to 977 meters depth, two from 979 to 980 meters depth, three from 1410 to 1412 meters depth, and two from 1837 to 1843 meters depth.

5.2 Variations in Carbonate $\delta^{18}\text{O}$ and $\delta^{13}\text{C}$

All sandstone samples from J. D. Jackson No. 1 were analyzed for calcite and dolomite by the 100% phosphoric acid treatment. The reaction was complete overnight in all cases, indicating the absence of dolomite. Calcite content varied from 0.5% by weight to 7.5% by weight. The $\delta^{13}\text{C}$ and $\delta^{18}\text{O}$ values of carbonates together with their percentages of the rock by weight, are given in Table 12, and the $\delta^{18}\text{O}$ values are plotted against depth in Figure 31.

The range in $\delta^{18}\text{O}$ values for carbonates from J. D. Jackson No. 1 is 1.3 to 8.3‰. There is no correlation between the $\delta^{18}\text{O}$ and depth or with carbonate content of the rock. The range in $\delta^{18}\text{O}$ values corresponds

TABLE 12

DESCRIPTIONS AND ISOTOPIC ANALYSES OF ROCKS AND MINERALS
FROM J. D. JACKSON NO. 1, HEBER, CALIFORNIA

See "General Remarks", Table 3

<u>Well and Number</u>	<u>Depth, meters</u>	<u>Sample Description</u>	$\delta^{18}\text{O}$ ‰	$\delta^{13}\text{C}$ ‰	δD ‰	<u>Remarks</u>
JDJ - 3199•0	975.30	carbonate	+ 2.47	- 3.22		All are sandstones 0.5 wt. % CaCO_3
JDJ - 3200•5 a	975.74	carbonate	+ 3.05	- 3.33		3.6 wt. % CaCO_3
b		sandstone	+ 9.56		-74.9	chloritic, formic acid treated, 0.5 wt. % H_2O
c		quartz	+10.50			HF-HCl treated; detrital, with euhedral overgrowths
JDJ - 3204•6	976.98	carbonate	+ 3.16	- 3.47		2.75 wt. % CaCO_3
JDJ - 3213•2 a	979.62	carbonate	+ 8.31	- 1.51		2.4 wt. % CaCO_3
b		sandstone	+10.64			formic acid treated
c		quartz	+11.62			HF-HCl treated, detrital, -200 mesh
JDJ - 3214•8	980.08	carbonate	+ 8.05	- 2.11		1.5 wt. % CaCO_3
JDJ - 4626•4	1410.47	carbonate	+ 2.31	- 1.59		1 wt % CaCO_3
JDJ - 4628•1	1411.00	carbonate	+ 2.37	- 2.61		2.5 wt. % CaCO_3
JDJ - 4630•6	1411.74	carbonate	+ 1.27	- 2.49		1.5 wt. % CaCO_3

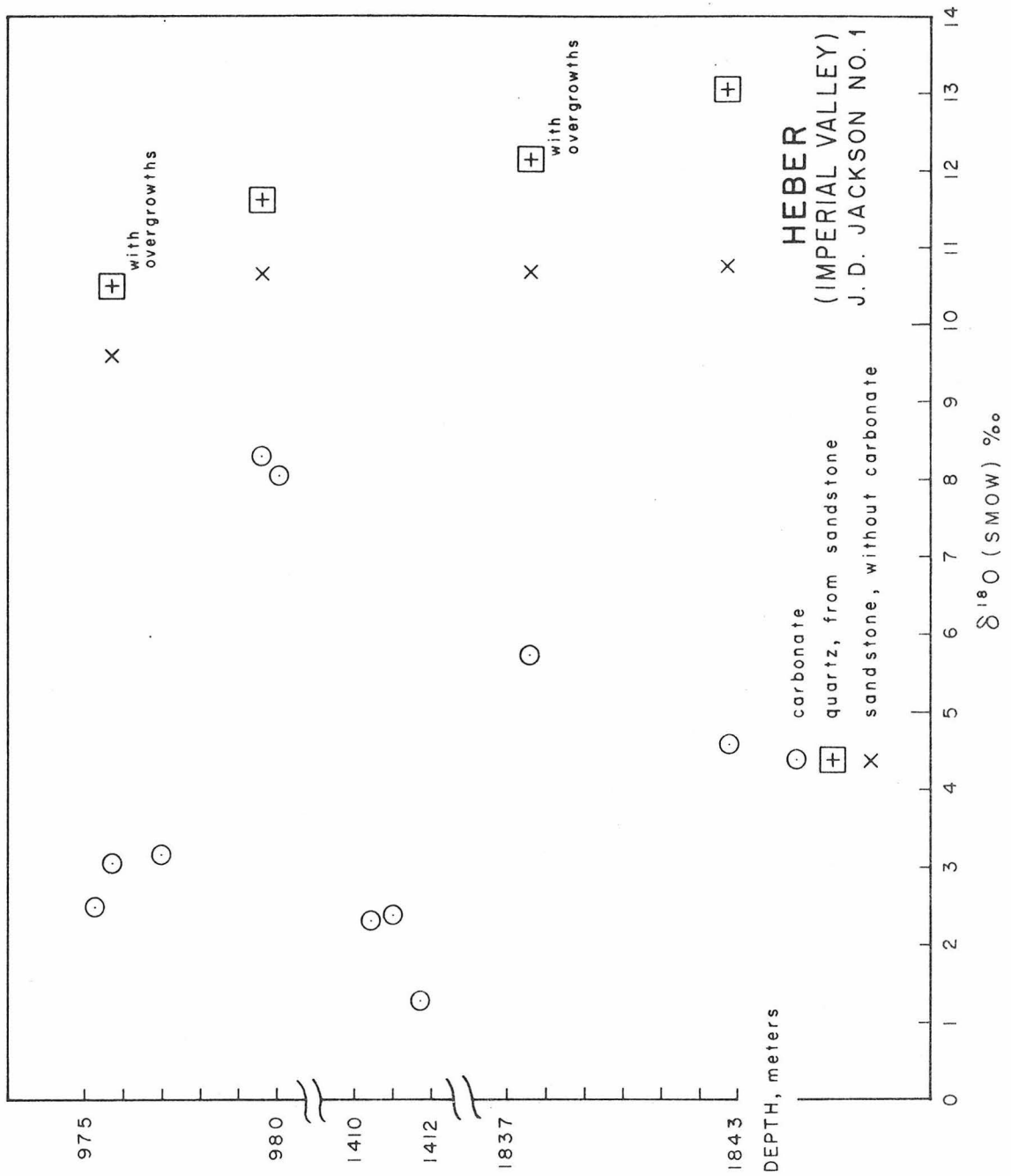
TABLE 12: J. D. JACKSON NO. 1, CONTINUED

<u>Well and Number</u>	<u>Depth, meters</u>	<u>Sample Description</u>	<u>$\delta^{18}O$ ‰</u>	<u>$\delta^{13}C$ ‰</u>	<u>δD ‰</u>	<u>Remarks</u>
JDJ - 6027.5 a	1837.63	carbonate sandstone quartz	+ 5.73	- 3.02		3.8 wt. % $CaCO_3$ formic acid treated HF-HCl treated, detrital, with euhedral overgrowths
b	+10.67					
c	+12.12					
JDJ - 6044.5 a	1842.81	carbonate sandstone quartz	+ 4.56	- 2.57		7.5 wt. % $CaCO_3$ formic acid treated HF-HCl treated, detrital
b	+10.76					
c	+13.05					

FIGURE 31

$\delta^{18}\text{O}$ values of calcite, sandstone quartz and whole rocks from various depths, J.D. Jackson No. 1, Imperial Valley.

Variations in $\delta^{18}\text{O}$ values of calcite (as large as 5‰ over a distance of 4 meters) indicated that the hot-water bearing sandstones are very effectively isolated from each other by the impermeable shale beds that separate them. Thus, the fluid/mineral ratios may be different in all the aquifers, even though their temperatures might be similar. There is little variation in the whole-rock $\delta^{18}\text{O}$ values. Note also that the presence of euhedral quartz overgrowths on detrital quartz grains seems to contribute to only a minor degree to the $\delta^{18}\text{O}$ value of quartz from the sandstone.



closely to the range in calcite $\delta^{18}\text{O}$ found deposited by presently active hydrothermal fluids at The Geysers and Valles Caldera. The $\delta^{18}\text{O}$ value of detrital carbonate reported in surface samples of recent Colorado River deltaic sediments is around 24‰ (Clayton *et al.*, 1968). The considerably lower $\delta^{18}\text{O}$ values of carbonate from J. D. Jackson No. 1 indicates that they have formed in the presence of hot, low- $\delta^{18}\text{O}$ fluid.

Since temperatures in J. D. Jackson No. 1 were not made available, they might be estimated on the basis of the isotopic data. A water sample was not available from the well, either, so the isotopic composition of the water must be estimated. The ground water in Imperial Valley is largely derived from Colorado River water which has evaporated to various degrees; the Imperial Valley is an irrigated, otherwise arid desert. The δD and $\delta^{18}\text{O}$ values of water from a spring at the base of the Chocolate Mountains, northeast of Imperial Valley, should be typical of the ground water. These values are -78‰ and -9.5‰, respectively (Craig, 1963; the filled circle in the "Niland" line in Figure 11). First, if it is assumed that the water in J. D. Jackson No. 1 has undergone no oxygen isotope shift, the minimum isotopic temperature indicated by the calcite with the lowest $\delta^{18}\text{O}$ value, 1.3‰ at 1412 meters, is 170°C (Equation G-3). If there has been an oxygen isotope shift in the water to a higher $\delta^{18}\text{O}$ value than -9.5‰, the calcite isotopic temperature would be higher. All of the calcites whose $\delta^{18}\text{O}$ values are higher than 1.3‰ indicate lower temperatures of equilibration with water whose $\delta^{18}\text{O}$ is -9.5‰ at 170°C. If the waters which deposited the other calcites had an oxygen isotope shift, then nothing conclusive can

be said about the temperatures of calcite deposition, for each calcite might have been deposited by a water with a different $\delta^{18}\text{O}$ value.

The distribution of calcite $\delta^{18}\text{O}$ values indicates that certain horizons are isotopically and perhaps thermally isolated from each other. For example, the cluster of calcite $\delta^{18}\text{O}$ values between 975 and 977 meters depth are about 5‰ lower than the calcite $\delta^{18}\text{O}$ values at 979 to 980 meters depth. There has been little fluid transfer between these two sandstone horizons, which are separated only by two meters. However, it is important to note that these two sandstone horizons are separated by an impermeable clay bed, which makes a very effective barrier to fluid flow. The confinement of clusters of $\delta^{18}\text{O}$ values of calcite to certain horizons is also demonstrated in the intervals 1410 to 1412 meters, and 1837 to 1843 meters, although these two are separated by over 400 meters of stratigraphic section.

With no oxygen isotope shift in the water assumed, the minimum calcite-water isotopic temperature, indicated by the calcite at 979 to 980 meters ($\delta^{18}\text{O} = 8‰$) is about 100°C. Thus, the hot water reservoir at the Heber geothermal anomaly seems to be distributed as a set of horizontal aquifers of sandstone separated by less permeable layers of claystone. If the $\delta^{18}\text{O}$ values of carbonates are a consequence only of temperature, then the hotter parts of the sampled reservoir are at 976 meters and 1411 meters depth (150 to 170°C), and cooler regions are found at 980 meters and 1840 meters depth (90 to 120°C). The calcite $\delta^{18}\text{O}$ values must be results of differences in $\delta^{18}\text{O}$ values of water as well, because a gradient of 30°C between 976 and 980 meters is

unreasonably high. The calcite $\delta^{18}\text{O}$ values are plotted against $\delta^{13}\text{C}$ values in Figure 32. The variation in $\delta^{13}\text{C}$ values in carbonates of J. D. Jackson No. 1 is between -1.5% to -3.5% , a difference of only 2% . This is considerably less than the 6% variation in $\delta^{13}\text{C}$ observed in the hot-water system at Valles Caldera. The mean $\delta^{13}\text{C}$ value of detrital carbonate in Imperial Valley surface sediments is -2.2% (Clayton et al., 1968), and is indicated in Figure 32. This figure emphasizes the nonuniformity of $\delta^{18}\text{O}$ values of calcite, and the tendency of these values to "cluster" at certain depth horizons. In striking contrast, the $\delta^{13}\text{C}$ values show no such "clustering" tendency, but all are within 1.3% of the surface carbonate $\delta^{13}\text{C}$ value, -2.2% . Either the hydrothermal carbonate recrystallized in place with little change in $\delta^{13}\text{C}$, or the carbon introduced into the calcite from the hydrothermal fluid during recrystallization was the same as that of the original carbonate. Plans have been made by Standard Oil to determine the amount and isotopic composition of gases in the Heber fluid, but at the present time this has not been done. The problem of the origin of $\delta^{13}\text{C}$ values in hot-water system carbonates is discussed near the end of this section.

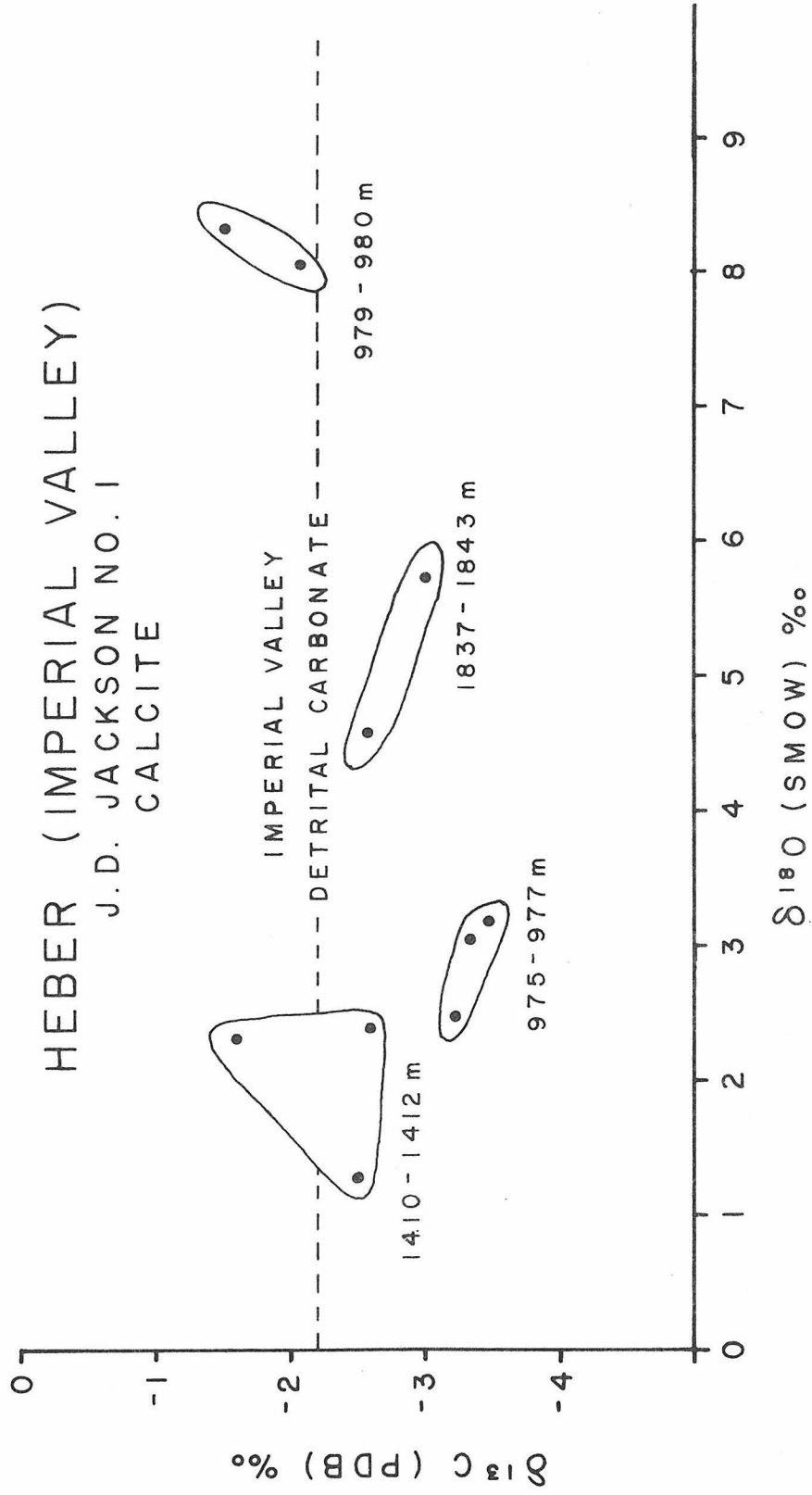
5.3 Variations in $\delta^{18}\text{O}$ Values of Sandstones and Quartz

Table 12 and Figure 31 contain the $\delta^{18}\text{O}$ values of sandstones (acidified with formic acid to remove carbonate) and quartz isolated from sandstones by the HF-HCl treatment. These sandstones consist mostly of quartz (60 to 80%), and feldspar (as much as 30%), with minor percentages of oxides, kaolinite, illite and chlorite, as reported from the Standard Oil x-ray diffraction analyses. Thin sections were not

FIGURE 32

$\delta^{13}\text{C}$ values plotted against $\delta^{18}\text{O}$ values of calcite, J.D. Jackson No. 1, Imperial Valley.

Note that all the $\delta^{13}\text{C}$ values of calcite are very close to that of detrital carbonate in Imperial Valley detrital material (measured by Clayton et al., 1968). This indicates that the $\delta^{13}\text{C}$ value of hydrothermal carbonates is controlled by local sources of carbonate and not the hydrothermal fluid.



made available. The occurrence of epidote, a hydrothermal alteration mineral which was commonly found in the cuttings from River Ranch No. 1 (Calyton et al., 1968) was not reported by Standard Oil in their mineralogical analyses of J. D. Jackson No. 1 rocks, but with careful study might be found. The two points in Figure 31 marked "with overgrowths" denote the presence of euhedral prismatic crystals of quartz attached to rounded detrital quartz grains. The points which are not so marked are analyses of rounded grains only.

All of the quartz $\delta^{18}\text{O}$ values fall between 10.5 and 13‰, well within the range of values of igneous and metamorphic quartz, 8 to 16‰. There is little variation in the $\delta^{18}\text{O}$ values of the quartz, and the presence of overgrowths on the detrital quartz has had only a minor effect on the $\delta^{18}\text{O}$ value of quartz (Figure 31). Virtually all that can be said is that the contribution of hydrothermally deposited quartz is as yet small, in relation to the amount of detrital quartz present. At 170°C (see above) the $\delta^{18}\text{O}$ value of quartz in isotopic equilibrium with water (whose $\delta^{18}\text{O}$ value is -9.5‰) should be about 7‰. The lowest $\delta^{18}\text{O}$ of quartz is 10.5‰. The rock pore space has not been filled by the deposition of minerals (self-sealing), nor were any of these sandstones well cemented. In the sandstone horizons investigated, the deposition of silica has not been extensive, according to the $\delta^{18}\text{O}$ analyses of quartz.

The acidified whole-rock $\delta^{18}\text{O}$ values in Table 12 and Figure 31 are also quite uniform. The lowest- $\delta^{18}\text{O}$ rock contains calcite of 3‰, and quartz (with overgrowths) of 10.5‰. The rock itself (9.5‰) is

only slightly depleted in ^{18}O with respect to rocks containing higher $\delta^{18}\text{O}$ calcite. The values of the other rocks are all 10.7‰.

The rock with the lowest $\delta^{18}\text{O}$ value is greenish in color, and contains chlorite. By all appearances this is the most intensely hydrothermally altered rock in the well. The $\delta^{18}\text{O}$ value of this rock is only 1‰ lower than that of the other rocks (Figure 31), and does not indicate that an appreciable degree of interaction between the minerals of the rock and the hydrothermal fluid has taken place.

Water was extracted from the rock and analyzed for D/H. The rock contained 0.5% by weight water and the δD value was -75‰ (Table 12, JDJ - 3200.5). This δD value is virtually the same as the δD value of the local water, which is shown for the Imperial Valley at Niland in Figure 11. The water in the rock is probably contained in both detrital and authigenic minerals.

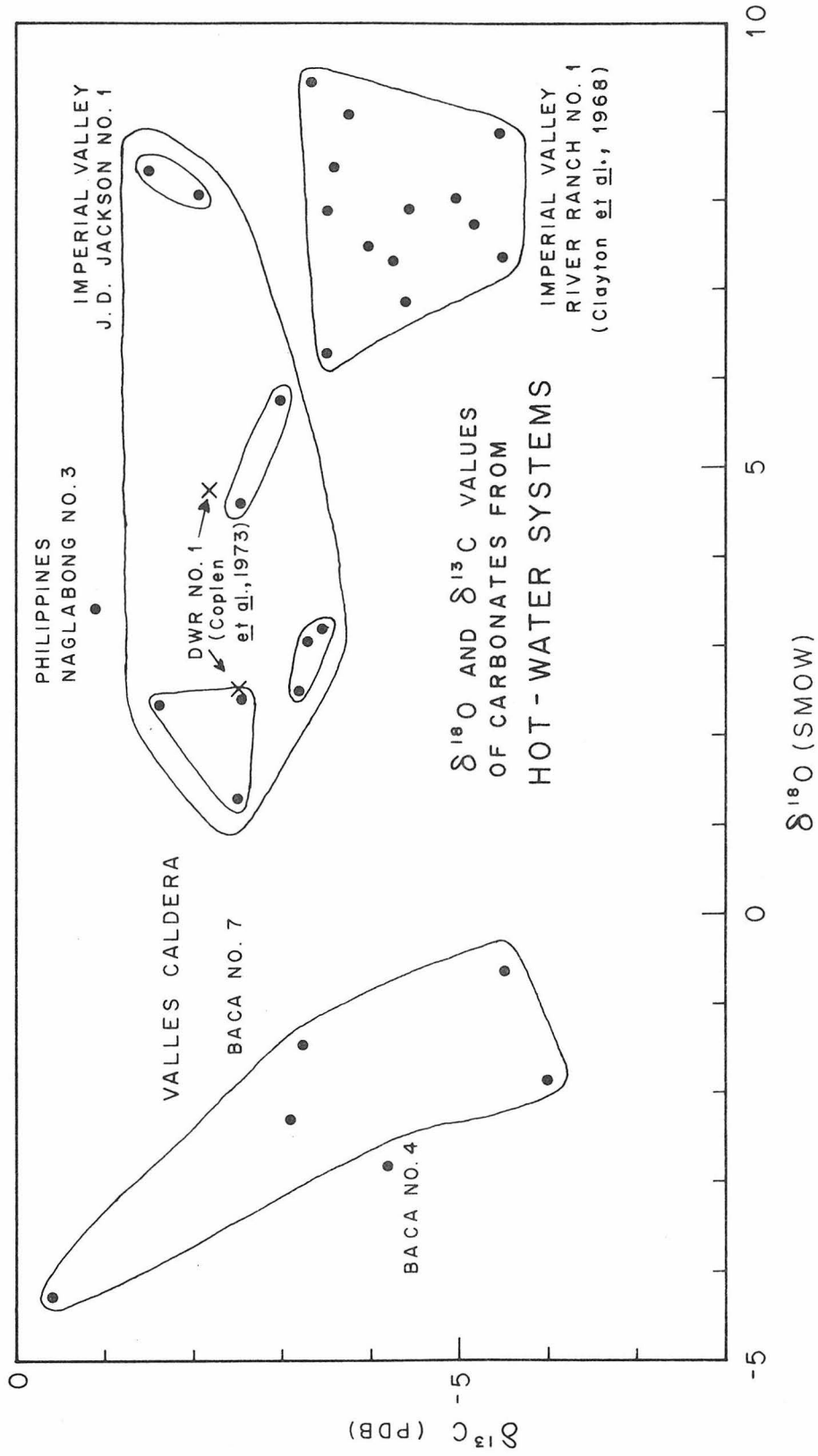
5.4 Relationships between Results from J. D. Jackson No. 1 and Studies of Other Imperial Valley Wells

The largest body of isotopic data in the literature for any Imperial Valley well consists of carbonate $\delta^{13}\text{C}$ and $\delta^{18}\text{O}$ values. They are therefore the best basis for comparison of the work of different laboratories which dealt with different sampling localities. Figure 33 shows a plot of $\delta^{13}\text{C}$ vs. $\delta^{18}\text{O}$ for carbonates from various wells: J. D. Jackson No. 1, River Ranch No. 1 (Clayton et al., 1968) and DWR No. 1 (Coplen et al., 1973). Isotope data for the Valles Caldera carbonates as well as those from a well in the Philippines, Naglabong No. 3, are included. All of these, except for Naglabong, whose status is unknown,

FIGURE 33

$\delta^{13}\text{C}$ values plotted against $\delta^{18}\text{O}$ values of calcite from various hot-water systems.

In spite of the large variation in calcite $\delta^{18}\text{O}$ values shown from Valles Caldera, Philippines, and Imperial Valley (including River Ranch No. 1 and DWR No. 1 as well as J.D. Jackson No. 1), the $\delta^{13}\text{C}$ values are all within the range of marine and fresh-water carbonate $\delta^{13}\text{C}$ values, indicating that hydrothermal carbonate carbon is locally-derived from pre-existing marine and fresh-water carbonates, which are found in all the areas mentioned in this figure.



are known to be parts of hot-water systems. Note that the $\delta^{13}\text{C}$ values are all confined to the range 0 to -6% . The range $\delta^{13}\text{C}$ for steam zone carbonates at The Geysers was -8 to -15% . The two ranges are mutually exclusive. $\delta^{13}\text{C}$ values of calcite at The Geysers seemed to be controlled by the $\delta^{13}\text{C}$ value of CO_2 (-11 to -12%). The CO_2 constituted a significant portion of the fluid in The Geysers steam system and could have served as a reservoir of exchangeable carbon during calcite crystallization. The $\delta^{13}\text{C}$ value of calcite in hot water systems seems to be determined by the local $\delta^{13}\text{C}$ value of the original carbonate that was crystallized by the hydrothermal fluid.

Calcite from River Ranch No. 1 (Clayton et al., 1968) had $\delta^{13}\text{C}$ values that were roughly correlative with calcite content of rock; the less calcite, the smaller the $\delta^{13}\text{C}$. This effect was attributed to the preferential release of higher- $\delta^{13}\text{C}$ CO_2 during decarbonation reactions which formed epidote from calcite and other minerals, at temperatures between 240 and 350°C. If this controls the variation in $\delta^{13}\text{C}$, rather than $\delta^{13}\text{C}$ of carbon introduced by the fluid, then it is not surprising that higher $\delta^{13}\text{C}$ values are found in DWR No. 1 and J. D. Jackson No. 1, whose temperatures are less than 200°C and exhibit no decarbonation products. The Valles Caldera calcite whose $\delta^{13}\text{C}$ was -6% could have evolved as a result of preferential decarbonation, for epidote is common at Valles Caldera, and might be in part derived from calcite.

5.5 Summary of Hydrothermal Activity at Heber

Hot water at Heber in the Imperial Valley occurs in poorly consolidated sandstone layers 1000 to 1500 meters below the surface. The

isotopically estimated temperatures are a maximum of 170°C. The permeable sandstone aquifers are separated by less permeable beds of claystone, effectively isolating bodies of hot water from each other. Differences in $\delta^{18}\text{O}$ values of calcite from adjacent sandstones separated by clay horizons indicate that not all the sandstones contain the same amounts of water, or that rates of circulation of water are not the same in all sandstones.

Authigenic quartz has been deposited as overgrowths on detrital quartz grains in some, but not all, sandstone bodies. The amount of this hydrothermally deposited quartz is very minor. The sandstones analyzed contain at most 4% calcite by weight. Deposition of hydrothermal minerals has not been in sufficient amount either to completely cement the sandstone or to significantly reduce the permeability of the sandstone aquifers by self-sealing. The hydrothermal activity at the Heber geothermal anomaly seems to be quite recent, since hydrothermal alteration of rock has taken place only to a minor degree.

6. A BRIEF INVESTIGATION OF A SAMPLE FROM NAGLABONG WELL NO. 3,PHILIPPINE ISLANDS

A cuttings fraction from 1293 to 1300 meters depth was made available by the Union Oil Company, from a well drilled in a hot-water(?) system in the Philippine Islands, Naglabong No. 3 in the Tiwi area of Becol Peninsula of southeast Luzon. No temperature data were made available, nor even a well location. The rock type is a plagioclase-rich volcanic rock, hydrothermally altered almost beyond recognition. The only unaltered phenocrysts seem to be magnetite. Plagioclase phenocrysts are still recognizable as such, but the felted, fine-grained groundmass contains abundant chlorite, calcite and hydrous minerals (illite?). Plate 21 is a photograph of this rock.

The rock from Naglabong No. 3 contains 2.2% by weight calcite, whose $\delta^{13}\text{C}$ is -1.0% and $\delta^{18}\text{O}$ is $+3.3\%$. The whole-rock $\delta^{18}\text{O}$ value is 4.0% , and the δD is -62.4% . The water content is 1.3 weight %.

The seasonal variation in $\delta^{18}\text{O}$ of rainfall in the Philippines is between 0 and -10% (Dansgaard, 1964). Since the area is tropical, the weighted average $\delta^{18}\text{O}$ of precipitation is probably no less than the mean of the extremes, -5% . Assuming no oxygen isotope shift, the minimum temperature of formation, using the calcite $\delta^{18}\text{O}$ value above, is 220°C , a respectably high temperature for a hot-water system. The $\delta^{18}\text{O}$ of the calcite is indicative of interaction between rock and hot meteoric water. The $\delta^{18}\text{O}$ value of the rock, 4% , is lower than that of most volcanics, so the feldspar in the rock has probably exchanged oxygen with low- ^{18}O water also.

PLATE 21.

Hydrothermally altered volcanic rock, Naglabong No. 3, Philippines.
1290 meters depth.

Area of view: 1.6 × 1.2 mm. X-nicols.

Plagioclase-rich volcanic rock, highly sericitized. Contains carbonate (small white spots) and chlorite (mottled gray, near center). Note relict zoning of plagioclase to right of center. From the hot-water zone.



PLATE 21

If the δD value of local meteoric Philippines water is $8 \cdot \delta^{18}O + 5 = -35\%$, the difference between water and rock δD values is 27% . The δD value of the rock is not sufficiently removed from the δD range in unaltered igneous rocks to allow for the evaluation of the contribution of water to the rock by hydrothermal alteration.

No conclusions can be drawn from $\delta^{13}C$ of the carbonate, other than the fact that it is -1.0% , which is within the range of marine carbonates. The origin of carbon in the Naglabong hydrothermal system would bear further study.

7. CONCLUSION: ISOTOPIC RECORDS IN VAPOR-DOMINATED
HYDROTHERMAL SYSTEMS AND HOT-WATER SYSTEMS

Summaries of the conclusions drawn from isotopic investigations of individual hydrothermal systems in this study have been given in sections 3.8 (The Geysers), 4.6 (Valles Caldera), 5.5 (Heber), and 6 (Philippines). The Geysers was given the most attention because it represented a vapor-dominated hydrothermal system, a type which had never before been isotopically studied in detail, and because it was studied in greater detail than any of the others. The other three are hot-water systems, examples of which are presently more numerous than vapor-dominated systems. There are important isotopic differences between the vapor-dominated and the hot-water dominated systems. These differences may prove to be critical in understanding the origins and histories of hydrothermal systems as a whole.

The isotopic compositions of the products of hydrothermal alteration in each of the three hot-water systems give evidence that a single episode of interaction between hot water and rock brought about the hydrothermal alteration. However, the temperature of this interaction may have been rising during the life of the hydrothermal system. All of the host rocks of the hot-water system are young, probably no older than Pleistocene, and their geologic histories have been rather simple. The thermal and fluid history of rock-water interaction at the Geysers, however, included a number of episodes during which the rock/water ratio and the source of the water changed as well as the temperature. Host rocks at The Geysers are as old as Jurassic, and have a

more complex geologic history, in which rock-fluid interaction was taking place probably as early as the Cretaceous during the diagenesis and metamorphism of the Franciscan. There is evidence of an ancestral hot-water system at The Geysers that might later have evolved into the present-day vapor-dominated system.

Two factors apparently determine whether hot rock and water will combine to form a vapor-dominated or a hot-water system. These factors are temperature (which can be isotopically determined from differences in $\delta^{18}\text{O}$ value between two cogenetic minerals) and permeability (which can be determined isotopically by calculating the mineral fluid ratio, a qualitative measure of rates of fluid circulation). The vapor-dominated hydrothermal system shows little host rock alteration by steam, indicating an overall small fluid/rock ratio.

Even though both types of hydrothermal system are supplied by meteoric water in the locale of the system, the degree of hydrothermal alteration of host rocks in the hot-water system indicated by their changes in isotopic composition could be relatively large, resulting in a fluid/rock ratio that is much greater than unity. Aside from systems which have large concentrations of solutes in their fluids (as high as 26 weight % in some Imperial Valley wells; Skinner *et al.*, 1967) higher temperatures are associated with vapor-dominated systems than with hot-water systems. Higher temperatures in steam systems may be the result of lower rates of fluid circulation, which minimizes the rate of cooling of the heat source by meteoric water. Aside from the high-temperature concentrated brines, temperatures in hot-water

systems are probably no higher than about 280°C (cf. section 4.5.1), whereas vapor dominated-hydrothermal systems can have steam-zone temperatures of at least 300°C and perhaps higher, without the assistance of a highly-concentrated brine, which has never been found at the expected depths of The Geysers.

Essentially the same authigenic minerals occur in both types of systems. $\delta^{18}\text{O}$ values of minerals tend to be lower if the fluid/mineral ratio is large. This is particularly true of calcite, whose $\delta^{18}\text{O}$ values were lowest in the Valles Caldera hot-water system (-4.3‰) and highest in the post-Cretaceous hydrothermal event at The Geysers (17‰) in which the fluid/rock ratio was less than unity. Even in the steam-system episode at The Geysers the $\delta^{18}\text{O}$ value of hydrothermal calcite was as high as 5‰, which at 320°C suggested a fluid/mineral ratio not greater than unity.

The $\delta^{13}\text{C}$ values of carbonates in hot-water systems seem to be determined by the $\delta^{13}\text{C}$ values of the carbonate in the pre-hydrothermal host rocks. Hot water cannot carry in solution large amounts of carbon species (as HCO_3^- , $\text{CO}_3^{=}$, etc.), so hot-water system calcite is simply precipitated from the solution which picked up carbonate elsewhere, the $\delta^{13}\text{C}$ remaining almost unchanged by the dissolution-reprecipitation. In a vapor-dominated system CO_2 can coexist with water in the vapor, and may account for several weight percent of the vapor. During the formation of hydrothermal carbonate in the steam zone, the CO_2 provides a large reservoir of exchangeable carbon that can appreciably affect the $\delta^{13}\text{C}$ of the carbonate, which seems to have been the case at The

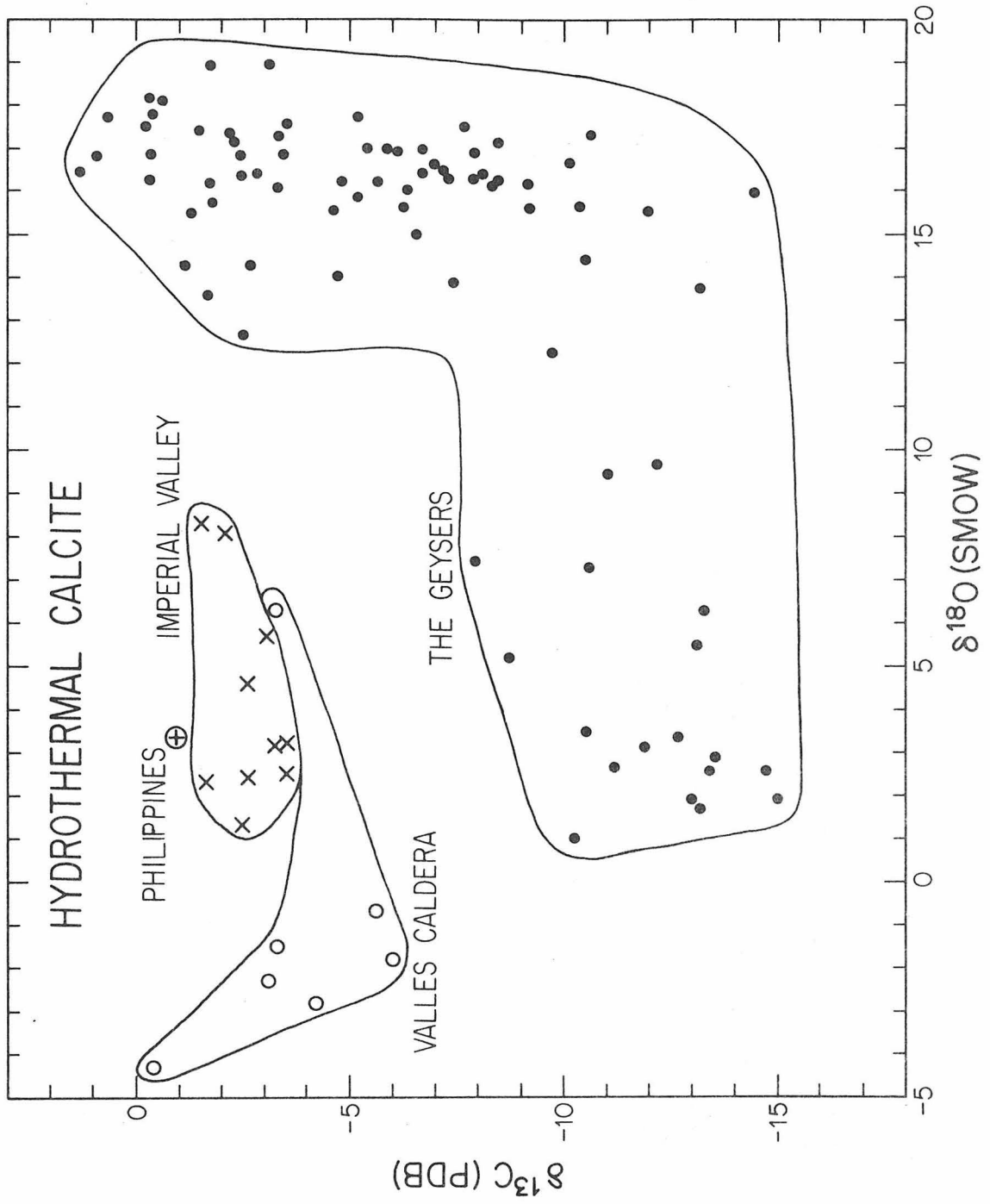
Geysers. The $\delta^{13}\text{C}$ of the carbonates in The Geysers steam zone are in the neighborhood of -12‰ , suggesting that this CO_2 may have come from organic matter. As a summary, the $\delta^{13}\text{C}$ values of all hydrothermal calcites analyzed in this study appear in Figure 34, plotted against their $\delta^{18}\text{O}$ values. As mentioned previously, the hot-water system carbonates lie within the $\delta^{13}\text{C}$ range of marine and fresh-water low-temperature carbonates while the $\delta^{13}\text{C}$ values of steam-zone calcites from The Geysers resemble the measured $\delta^{13}\text{C}$ values of the CO_2 (-11 to -12‰).

Finally, the effect of the $\delta^{18}\text{O}$ value of meteoric water on the isotopic compositions of the hydrothermal minerals can be evaluated because hydrothermal samples from various locations were available. If the isotopically estimated temperatures of calcite formation are available for a number of calcites from various hot-water systems, and the fluid/mineral ratios are similarly large, the $\delta^{18}\text{O}$ values of the calcites could be used to determine the $\delta^{18}\text{O}$ values of the hydrothermal fluids. The $\delta^{18}\text{O}$ values of calcites estimated to have formed at about 160 to 170°C from Valles Caldera, Heber, and the Philippines are -2‰ , 1.3‰ , and 3.3‰ , respectively. The corresponding $\delta^{18}\text{O}$ values of meteoric waters that supply these hydrothermal systems are approximately -12‰ , 9.5‰ and -5‰ . Thus, the higher-elevation, lower- $\delta^{18}\text{O}$ precipitation at Valles Caldera produces a lower- $\delta^{18}\text{O}$ hydrothermal calcite (-2‰) while the less negative $\delta^{18}\text{O}$ value of semi-tropical rain in the Philippines leads to a higher $\delta^{18}\text{O}$ calcite (3.3‰). There appears to be at least a qualitative sensitivity of the $\delta^{18}\text{O}$ values of the

FIGURE 34

$\delta^{13}\text{C}$ values *versus* $\delta^{18}\text{O}$ values of all hydrothermal calcites analyzed in this study.

The fields of $\delta^{18}\text{O}$ and $\delta^{13}\text{C}$ values of hot-water systems (Valles Caldera, Philippines and Imperial Valley) do not overlap. The large variation in $\delta^{13}\text{C}$ values of calcites from The Geysers (-15 to -12‰) suggests that calcite carbon may contain an organically-derived component. In the steam zone the $\delta^{13}\text{C}$ of abundant CO_2 appears to control the $\delta^{13}\text{C}$ of calcite. This CO_2 may itself be organically derived. $\delta^{13}\text{C}$ values of hot-water system calcites indicate that they are derived from other marine and/or fresh water carbonates which occur abundantly in those areas, but not at The Geysers.



hydrothermal minerals to geographic location.

The isotopic investigations of a variety of hydrothermal systems have been used to describe a number of types of rock-fluid interactions. The thermal histories as well as the natures of the different waters of hydrothermal systems have been deduced from isotopic compositions and paragenetic relationships of minerals. The isotopic record of the magnitude and spatial extent of hydrothermal alteration was determined for those systems which had been sampled over a wide area to appreciable depths. The ability to determine the magnitude and spatial extent of hydrothermal alteration is of utmost economic importance in evaluating the potential of a geothermal energy resource. The isotopic investigations of active hydrothermal systems are geologically important because they are fundamental to an understanding of isotopic evidence for rock-fluid interaction in the past, a process associated with many geological processes of interest and importance to man.

APPENDIX I

TERMINOLOGY

Potentially ambiguous terms used in this report are defined in this appendix. Definitions are drawn from common usage by many investigators over the years, but this glossary will help to put these terms into the context of this report, making distinctions between terms which might otherwise differ only subtly.

Terms

Magmatism: The generation, development, movement, emplacement, cooling, crystallization, and differentiation of a natural silicate melt in the earth. The term can be extended to include volcanism if the earth's surface is involved. The term in this work does not imply a consideration of secondary effects: heat transfer out of a cooling magma is part of magmatism, but the effects of the heat released into other rocks are not.

Metamorphism: Physico-chemical changes in a rock resulting in the formation of new mineral assemblages in response to those changes. The new phases will be those stable under the new conditions brought about by the changes, but might be unstable (or metastable) under any others. The fact that some minerals temporarily show good preservation under ambient earth surface conditions does not imply stability at those conditions. The term "metamorphism" is usually applied to changes in heat and/or pressure. The cause of the changes might be unspecified.

Metasomatism (replacement): "The simultaneous capillary solution and

deposition by which a new mineral of partly or wholly differing chemical composition may grow in the body of an old mineral or mineral aggregate" (Lindgren, 1933). Metasomatism occurs in metamorphism when the bulk rock composition changes. The term implies the presence of a fluid phase. Metasomatism may occur at temperatures and pressures greater than at the surface. The time scale involved may be geological, rather than historical.

Metamorphism usually indicates a complete change of mineral assemblage such that chemical equilibrium prevails. It is also commonly associated with a loss of volatiles (H_2O , CO_2) in rocks rich in them, and uptake of volatiles in rocks poor in them. Metasomatism is the effects of volatiles and the chemical species they might carry along with them. The term does not necessarily imply complete chemical re-equilibration among all phases accessible to the volatiles.

Diagenesis: Changes occurring in a sediment after accumulation and leading to complete lithification. These changes include consolidation, cementation, recrystallization, actions of organisms, and permeation by ground water. The processes in diagenesis are usually confined to depths less than 1 km (Turner, 1968), but may involve metasomatism.

Hydrothermal alteration: Partial or complete metasomatism of pre-existing solid phases enacted by water-rich fluids at temperatures above those of the earth's surface. The process implies the existence of a subterranean heat source. Mineralogical, chemical and isotopic equilibrium typically has not been obtained among all phases. There

are commonly mineralogical and textural remnants to indicate the nature of the original material. Hydrothermal alteration could be an incomplete metamorphism, or a metamorphism of limited spatial extent. Temperatures and pressures are in the lower part of the metamorphic regime. The time scale may be historical.

Hydrothermal phenomena: Anything related to hot water. The term applies to magmatic emanations containing much water, other waters heated by these emanations or by any other source, alteration products of these waters, and hot springs which are surface manifestations of such activity. Many kinds of veined ore deposits are called magmatic-hydrothermal, indicating the source of the energy that heated the water which concentrated and deposited minerals of economic interests. A hydrothermal system is a localized collection of hydrothermal phenomena. A geothermal system is a localized body of hot rock with or without water.

Weathering: Processes at the surface of the earth in which rocks, exposed to chemical action of ocean water, rain, the atmosphere, organisms, and temperature and mechanical perturbations, are altered to ultimately form soil. Surface alteration by hot-spring activity is hydrothermal alteration and not weathering. Products of such alteration, however, can be further weathered. For example, the Grand Canyon of the Yellowstone below Lower Falls was originally the site of a geyser basin. The hydrothermal alteration made the host rocks more susceptible to both weathering and erosion. The alteration

was also responsible for the colors that gave the river and the region the name (Hague, 1892a; Chittenden, 1895).

APPENDIX II

THE THEORETICAL BASIS FOR ISOTOPIC
EQUILIBRIUM FRACTIONATION

II.1 Introduction

The ensuing section of this work has a threefold purpose:

1. To provide the writer with experience in theoretical calculations, which allow a better understanding of all the parameters determining isotopic fractionation factors.

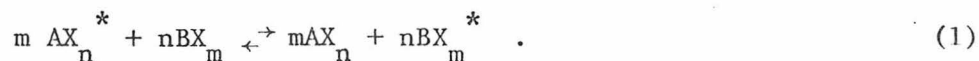
2. To provide the background necessary for evaluating the correctness of theoretical calculations of isotopic fractionation factors which have appeared in the literature.

3. To illuminate certain concepts which have not been treated in sufficient detail by authors of theoretical papers. Such concepts are fundamental to many of these previously-published works.

For those whose interest lies strictly with the mechanics of these calculations, the author recommends sections II.9 through II.14. Elementary theoretical considerations of thermodynamics and statistical mechanics, including some simple partition functions, are treated in sections II.2 through II.7. Section II.8 is recommended only to those who have an interest in the anharmonicity of molecular motion.

II.2 Thermodynamic Considerations

A generalized isotopic exchange reaction can be written:



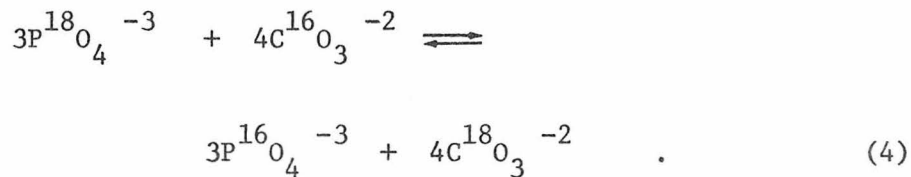
The expression for the equilibrium constant is

$$K = \frac{[AX_n]^m [BX_m^*]^n}{[AX_n^*]^m [BX_m]^n} \quad (2)$$

The standard free energy for this reaction is related to K as follows:

$$\Delta G^0 = -RT \ln K \quad (3)$$

In the present discussion X and X* are isotopes of an atom. A specific example of the generalized reaction (1) would be:



The quantity α , the fractionation factor for oxygen in the $CO_3^{-2} - PO_4^{-3}$ system, is defined as follows:

$$\alpha = \frac{\frac{Y}{Y'}}{\frac{X}{X'}} = \frac{\left(\frac{[^{18}O]}{[^{16}O]}\right)_{\text{carbonate}}}{\left(\frac{[^{18}O]}{[^{16}O]}\right)_{\text{phosphate}}} \quad (5)$$

where Y = the abundance of ^{18}O in carbonate
 Y' = the abundance of ^{16}O in carbonate
 X = the abundance of ^{18}O in phosphate
 X' = the abundance of ^{16}O in phosphate

Let us now suppose that the various isotopic species (involving only oxygen) of CO_3^{-2} and PO_3^{-3} can be formed from random combinations of monoisotopic C and P with ^{18}O and ^{16}O . Considering all the resulting molecular species ($\text{C}^{16}\text{O}^{16}\text{O}^{18}\text{O}$, $\text{C}^{16}\text{O}^{18}\text{O}^{18}\text{O}$, etc.), it has been shown by Epstein (1959) that

$$\alpha = K^{1/mn} \quad (6)$$

where m and n are defined in equation (1). For example, the α at 25°C for $\text{CO}_2\text{-H}_2\text{O}$ oxygen isotope exchange is 1.041. $K = 1.0837$ and $\Delta G^\circ = -47.6$ calories. This last number is of the same order as the magnitudes of errors obtained even with the best calorimetric techniques. In general, isotopic exchange is accompanied by relatively small changes in the values of thermodynamic functions. One precise method of calculating α 's is based on statistical mechanics.

II.3 The Statistical Mechanical Free Energy

It is known that for any particle (i.e., molecular) system,

$$G_T^\circ - G_0^\circ = -N_0 kT \ln \frac{Q^\circ}{N} \quad (7)$$

describes the free energy change in terms of Avogadro's number N_0 , Boltzmann's constant, k, the absolute temperature T, the number of molecules in the system, N and a function designated Q. Combining N_0 and k produces the more familiar form utilizing the standard free energy of formation:

$$\Delta G_f^\circ = -RT \ln \frac{Q^\circ}{N} \quad (8)$$

(Davidson, 1962). Q° is the standard state partition function for the canonical ensemble that is the system being considered. In a reaction, such as (1),

$$\Delta G_{\text{rxn}}^\circ = -RT \ln k = -RT \ln \frac{\prod Q_{\text{products}}}{\prod Q_{\text{reactants}}} \quad (9)$$

so that

$$k = \frac{\left(\frac{Q_{AX_n}}{N}\right)^m \left(\frac{Q_{BX_m}^*}{N}\right)^n}{\left(\frac{Q_{AX_n}^*}{N}\right)^m \left(\frac{Q_{BX_m}}{N}\right)^n} = \frac{\left(\frac{Q_{BX_m}^*}{Q_{BX_m}}\right)^n}{\left(\frac{Q_{AX_n}^*}{Q_{AX_n}}\right)^m}$$

which is the same as equation 1 of Urey (1947).

II.4 The Canonical Partition Function, Q

In a molecular system all the modes of motion must be included, because each mode can have a capacity for an appreciable fraction of the total energy. In a molecule or a crystal, there may be several vibrational (and/or rotational and/or translational) modes. Some of these modes can be degenerate, i.e., different kinds of relative atomic motion can have the same energy.

A partition function for a collection of atoms or molecules (or groups thereof, such as gases, liquids and crystals) must take into account all the states of all the modes, including degeneracy. Such

a collection of atomic and/or molecular systems is called a canonical ensemble.

The form of Q is:

$$Q = \sum_{ijk\dots} e^{-E_{ijk\dots}/kT} \quad (11)$$

where i , j , and k index the energy levels of three different modes, such that $E_{ijk\dots} = \epsilon_i + \epsilon_j + \epsilon_k + \dots$

Now

$$Q = q_i q_j q_k \dots \quad (12)$$

where q_j is the molecular partition function ("sum over states") for the j^{th} mode of motion (vibration, rotation, etc.). The degeneracies are all one in the above equations for simplicity. If a mode is n -fold degenerate, its Q is simply q^n . The expression for Q which will be used here is

$$Q = \prod_j (q_j)^{d_j} \quad (13)$$

where d_j is the degeneracy of the j^{th} mode.

Three general types of modes of molecular motion must be considered: (1) translational, (2) vibrational, (3) rotational. The potential energy boundaries that limit these motions are also of interest. If the total energy of a molecular system is

$$E_{\text{total}} = E_{\text{electronic}} = E_{\text{vibrational}} + E_{\text{rotational}} \\ + E_{\text{translational}}$$

then by the properties of exponentials,

$$Q_{\text{total}} = Q_{\text{electronic}} Q_{\text{vibrational}} Q_{\text{rotational}} Q_{\text{translational}}$$

Unless the contribution to the internuclear potential of gravitational nucleus-electron interactions is considered, $Q_{\text{electronic}}$ is the same for all isotopic species of a molecule, and does not contribute to isotopic fractionation. Isotope effects are, however, entirely dependent upon masses of nuclei, and $Q_{\text{electronic}}$ is usually developed entirely from a consideration of the electrostatic interaction of nucleus and electron. In practice the electron effect is not considered to be important, except in the case of hydrogen isotopes. Urey (1947) mentions the example of a deuterium-hydrogen-bearing system, in which the difference in energy arising from the electron effect can be as much as 30 cm^{-1} .

II.5 The Molecular Partition Function, q

The discussion will be confined to a treatment of partition functions as applied to an understanding of isotope effects. Most of this treatment of partition functions follows that of Davidson (1962).

Certain quantum phenomena must be considered. The canonical partition function Q is a product of molecular partition functions, q . Energy at the molecular level is quantized, and a complete description of the energy in a system is built up from descriptions of molecular motion. Isotope fractionation effects are entirely due to the quantized nature of molecular energy. The molecular partition function,

q , is defined as follows:

$$q = \sum_i g_i e^{-\epsilon_i/kT} , \quad (14)$$

where i refers to an energy level (or state), ϵ_i is the energy of the i^{th} state, and g_i is the degeneracy of the i^{th} state. All the states in q belong to the same principal mode of motion, and q is often called "the sum over states."

It is at this point useful to obtain the q expressions for some simple systems. All of the following treatments will make use of the Schrödinger equation:

$$H \Psi - \epsilon \Psi = 0 \quad (15)$$

II.6 The One-Dimensional Harmonic Oscillator

The harmonic oscillator is applicable as an approximate description of many kinds of molecular vibrations. It has a potential energy $V = \frac{1}{2} k_2 (x-x_0)^2$; x is the displacement from a parabola vertex at $x = x_0$, and k_2 is the Hook's Law spring-type force constant. For the harmonic oscillator the Hamiltonian is

$$H = -\frac{\hbar^2}{2m} \frac{\partial^2}{\partial x^2} + \frac{1}{2} k_2 x^2 \quad (16)$$

for $x_0 = 0$. When (16) is substituted into (15), the equation becomes

$$-\frac{\hbar^2}{2m} \frac{\partial^2}{\partial x^2} \Psi + \frac{1}{2} k_2 x^2 \Psi = \epsilon \Psi$$

$\hbar = \frac{h}{2\pi}$, h = Planck's constant, m is the mass of the particle. With a two-particle system the center-of-mass system convention is adopted, and m becomes μ , the reduced mass, which is equal to $\frac{m_1 m_2}{m_1 + m_2}$. In general, $m_1 \neq m_2$.

The wave function Ψ is not of interest here, but the eigenvalue ϵ (the energy) is of interest:

$$\epsilon_n = \left(n + \frac{1}{2}\right) h\nu \quad n = 0, 1, 2, \dots \quad (17)$$

$$\nu = \frac{1}{2\pi} \left(\frac{k_2}{\mu}\right)^{\frac{1}{2}}, \text{ vibrational frequency in sec}^{-1}.$$

An important consequence of (17) is that even at $n = 0$, some energy remains, the "zero-point energy," $\frac{1}{2} h\nu$ (in ergs) above the point of lowest potential energy.

At this point a shorthand is developed:

$$u = \frac{h\nu}{kT}. \quad (18)$$

The partition function, q , for a harmonic oscillator, according to (14) is

$$q_{\text{vib}} = \sum_{n=0}^{\infty} e^{-u(n+\frac{1}{2})} \quad (19)$$

The state $n=0$ is included in the summation because (1) zero-point energies are different for isotopic species of the same molecule, (2) spacings (i.e., u 's) are different for isotopic species of the same

molecule and (3) consequently when taking energy differences, all energies must be referred to the same state (the minimum of the potential curve).

Equation (19) is a geometric series for which the sum is well known:

$$q_{\text{vib}} = \frac{e^{-u/2}}{1 - e^{-u}} \quad (20)$$

II.7 A Free Particle in a Three-Dimensional Box

The next problem is applicable to the determination of translational q 's, and its Schrödinger equation is

$$-\frac{\hbar^2}{2m} \left(\frac{\partial^2}{\partial x^2} + \frac{\partial^2}{\partial y^2} + \frac{\partial^2}{\partial z^2} \right) \Psi + U(x, y, z) \Psi = \epsilon \Psi \quad (21)$$

where

$U = \infty$ outside the box of dimensions X, Y, Z

$U = 0$ inside the box.

Again, Ψ is not of interest here, but the energy expression is of interest:

$$\epsilon_{S_X, S_Y, S_Z} = \frac{h^2}{8m} \left(\frac{S_X^2}{X^2} + \frac{S_Y^2}{Y^2} + \frac{S_Z^2}{Z^2} \right) \quad (22)$$

$$S_X, S_Y, S_Z = 1, 2, 3, \dots$$

Using (19), the q_x is

$$q_x = \sum_{s_x=1}^{\infty} e^{-\frac{h^2 s_x^2}{8mkTX^2}} \quad (23)$$

If $\frac{h^2 s_x^2}{8mkTX^2} \ll 1$, q_x is approximated by the integral, which will converge. The treatment becomes classical because the energies are so close together as to be almost a continuum:

$$q_x = \int_{s_x=0}^{\infty} e^{-\frac{h^2 s_x^2}{8mkTX^2}} ds_x = \left(\frac{2\pi mkT}{h^2}\right)^{\frac{1}{2}} X \quad (24)$$

The same is true for the y and z components so that the three-dimensional q is:

$$q_{\text{trans}} = q_x q_y q_z = \left(\frac{2\pi mkT}{h^2}\right)^{3/2} XYZ \quad (25)$$

and if XYZ is the volume, V,

$$q_{\text{trans}} = \left(\frac{2\pi mkT}{h^2}\right)^{3/2} V \quad (26)$$

II.8 The Cubic-Quartic Anharmonic Oscillator

II.8.1 The Morse Potential

Most molecular potentials are not that of a simple coil-spring, $\frac{1}{2} k_2 x^2$. For the purpose of illustration in this discussion, the potential of P. M. Morse (1929) will be used. This potential has been widely used to facilitate the interpretation of molecular spectra:

$$V(r) = D_e e^{-2\beta(r-r_0)} - 2D_e e^{-\beta(r-r_0)} \quad (27)$$

where r is the internuclear separation distance

β is related to the width of the "well"

D_e is the depth of the "well" (energy separation between $V(r = r_0)$ and $V(r = \infty)$).

r_0 is the separation distance at which $V(r)$ is minimum

A graph of the Morse potential is shown in Figure II-1, following the convention of Schiff (1968), such that $\beta = \frac{2}{r_0}$.

The solution of the Schrödinger equation using the Morse potential is best done by approximating $V(r)$ by a power series and applying non-degenerate double perturbation theory. For this undertaking, the origin is shifted so that the new potential expression becomes

$$V(x) = D_e e^{-2\beta x} - 2D_e e^{-\beta x} \quad (28)$$

The power series by which the Morse potential will be approximated is the potential of the cubic-quartic anharmonic oscillator.

II.8.2 · The Perturbation Theory Solution

Much of the following discussion is taken from a manuscript by W. A. Goddard III and T. H. Dunning, Jr. (1971), and the use of the Morse potential was an exercise suggested by them.

The H for the cubic-quartic one-dimensional anharmonic oscillator is

$$H = -\frac{\hbar^2}{2\mu} \frac{d^2}{dx^2} + \frac{1}{2} k_2 x^2 + k_3 x^3 + k_4 x^4 \quad (29)$$

FIGURE II-1

The Morse potential

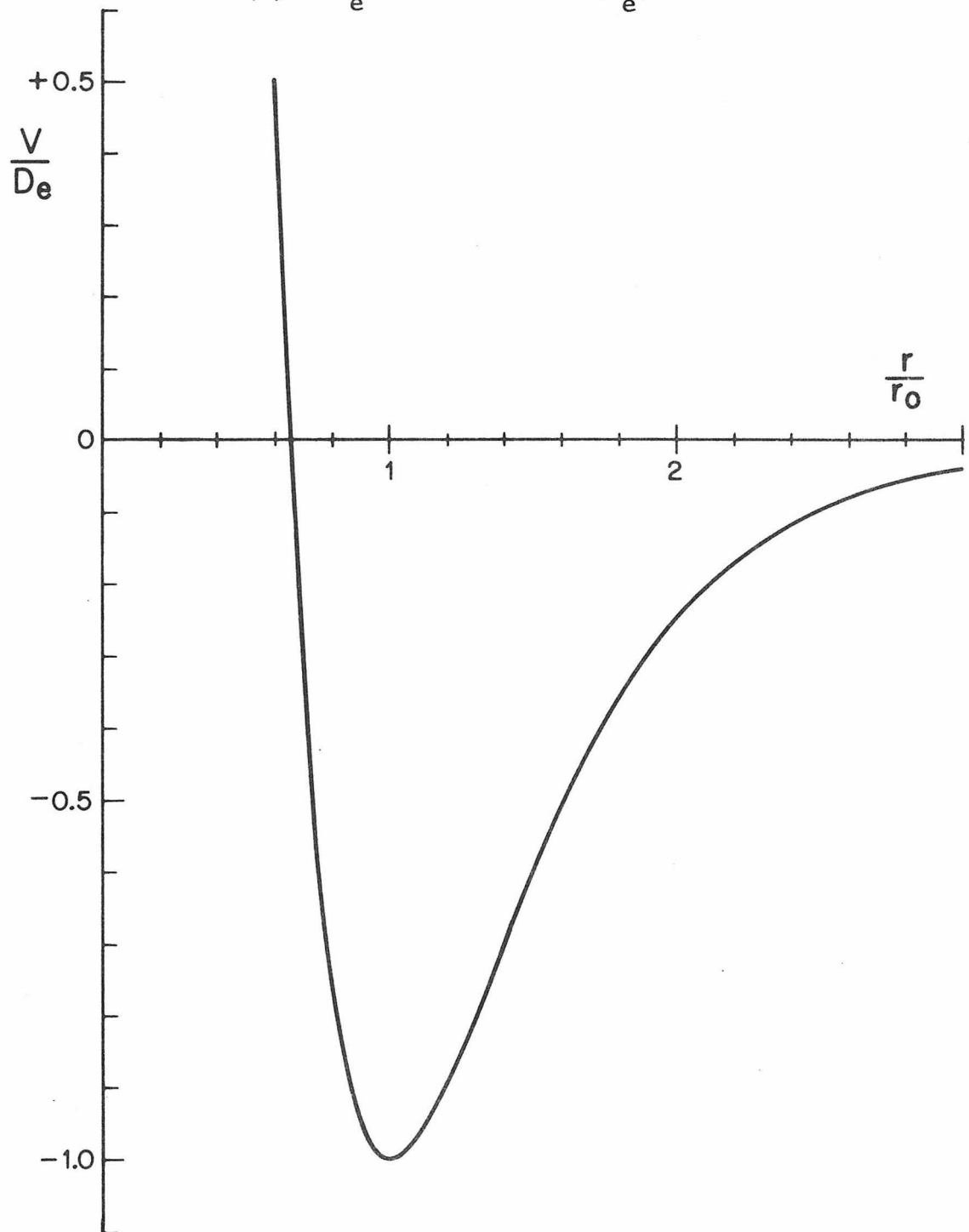
The equation of this potential energy function is

$$V(r) = D_e e^{-2\beta(r-r_0)} - 2D_e e^{-\beta(r-r_0)}$$

in which r is the separation distance between two atoms, r_0 is the separation distance at which the potential energy is minimum, D_e and β are constants. The potential has been widely used to interpret some kinds of molecular vibrations. For convenience, $\beta = 2/r_0$.

MORSE POTENTIAL

$$V(r) = D_e e^{-2\beta(r - r_o)} - 2D_e e^{-\beta(r - r_o)}$$



k_2 , k_3 and k_4 will be evaluated in a later section. The unperturbed Hamiltonian, $H^{(0,0)}$ is

$$H^{(0,0)} = -\frac{\hbar^2}{2\mu} \frac{d^2}{dx^2} + \frac{1}{2} k_2 x^2 . \quad (30)$$

The cubic and quartic perturbations are

$$H^{(1,0)} = k_3 x^3 \quad (31a)$$

$$H^{(0,1)} = k_4 x^4 \quad (31b)$$

The first-order correction to the energy levels, E_n , by the first perturbation, $H^{(1,0)}$, is given by

$$E^{(1,0)} = \langle \psi_n^{(0,0)} | H^{(1,0)} | \psi_n^{(0,0)} \rangle \quad (32)$$

which is bracket notation for

$$E^{(1,0)} = \int \psi_n^{(0,0)*} H^{(1,0)} \psi_n^{(0,0)} d\tau \quad (\text{Levine, 1970}).$$

Equation (32) says that $H^{(1,0)}$ is operating on $\psi_n^{(0,0)}$, and the result is multiplied by $\psi_n^{(0,0)*}$, the complex conjugate of $\psi_n^{(0,0)}$. This product is integrated over all space, as signified by $d\tau$.

For the harmonic oscillator, the unperturbed wave functions $\psi_n^{(0,0)}$ are orthogonal, i.e.,

$$\int \psi_m^{(0)*} \psi_n^{(0)} d\tau = \langle \psi_m^{(0)} | \psi_n^{(0)} \rangle = 0 \quad \text{if } m \neq n \quad (33)$$

and normalized:

$$\langle \psi_m^{(0)} | \psi_n^{(0)} \rangle = 1 \quad \text{if } m = n \quad (34)$$

When wavefunctions exhibit both of these properties, they are said to be orthonormal. $\psi_n^{(0)}$, $n = 0, 1, 2, 3, \dots$, are the orthonormal wavefunctions of the harmonic oscillator. Their precise forms are not important here.

II.8.3 Application of Ladder Operators

It is convenient at this point to introduce operators with special properties:

$$a^+ = \frac{1}{(2\mu)^{1/2}} [p_x + 2\pi i\mu\nu x] \quad (35a)$$

$$a^- = \frac{1}{(2\mu)^{1/2}} [p_x - 2\pi i\mu\nu x] \quad (35b)$$

in which p_x is the x-direction momentum operator, $-i\hbar \frac{d}{dx}$ ($i = \sqrt{-1}$).

The properties of these operators can be seen when they are applied to the $\psi_n^{(0)}$'s.

$$a^+ \psi_n^{(0)} = \sqrt{(n+1)h\nu} \psi_{n+1}^{(0)} \quad (36a)$$

$$a^- \psi_n^{(0)} = \sqrt{nh\nu} \psi_{n-1}^{(0)} \quad (36b)$$

Because application of a^+ to $\psi_n^{(0)}$ raises the quantum number n by 1, a^+ is called the raising operator. a^- is the lowering operator.

Together they are the ladder operators:

$$a^+ a^- = H(0,0) - \frac{1}{2} h\nu . \quad (37)$$

The operator x is

$$\frac{1}{i\sqrt{2k_2}} (a^+ - a^-) ,$$

so x^3 is

$$\begin{aligned} x^3 = & \frac{1}{i^3\sqrt{8k_2^3}} (a^+ a^+ a^+ - a^- a^+ a^+ - a^+ a^- a^+ \\ & + a^- a^- a^+ - a^+ a^+ a^- + a^- a^+ a^- \\ & + a^+ a^- a^- - a^- a^- a^-) . \end{aligned} \quad (38)$$

The application of equation (31a) to $\psi^{(0,0)}$ gives

$$\begin{aligned} k_3 s^3 \psi_n^{(0,0)} = & \frac{k_3 \sqrt{h^3 \nu^3}}{i^3 \sqrt{8k_2^3}} \left[\sqrt{(n-1)(n-2)(n-3)} \psi_{n+3}^{(0,0)} \right. \\ & \left. - 3\sqrt{(n+1)^3} \psi_{n+1}^{(0,0)} + 3\sqrt{n^3} \psi_{n-1}^{(0,0)} - \sqrt{n(n-1)(n-2)} \psi_{n-3}^{(0)} \right] . \end{aligned} \quad (39)$$

Substituting (39) into (33) makes all the terms vanish, since the $\psi_n^{(0,0)}$'s are orthonormal, ($n-3, n-1, n+1$ and $n+3$ are all different from n). Therefore, $E_n^{(1,0)} = 0$.

The second-order correction to E_n is given thusly:

$$\begin{aligned}
 E_n^{(2,0)} &= \langle \psi_n^{(0,0)} | H^{(1,0)} | \psi_n^{(1,0)} \rangle \\
 &= \langle \psi_n^{(0,0)} | k_3 x^3 | \psi_n^{(1,0)} \rangle \\
 &= \langle k_3 x^3 \psi_n^{(0,0)} | \psi_n^{(1,0)} \rangle
 \end{aligned} \tag{40}$$

This last transformation is possible because the operator x is "Hermitian" (Levine, 1970). It is seen that $\psi_n^{(1,0)}$, the first-order corrected wavefunctions, are now needed. These wavefunctions will be solutions to the equation

$$\begin{aligned}
 &\left[-\frac{\hbar}{2\mu} \frac{d}{dx} + \frac{1}{2} k_2 x^2 - (n + \frac{1}{2}) \hbar \nu \right] \psi_n^{(1,0)} \\
 &+ k_3 x^3 \psi_n^{(0,0)} = 0
 \end{aligned} \tag{41}$$

By applying (37) and (39) to (41), the following is obtained:

$$\begin{aligned}
 &(a^+ a^- - n \hbar \nu) \psi_n^{(1,0)} + \frac{k_3}{i^3} \sqrt{\frac{\hbar^3 \nu^3}{8k_2^3}} \left[\sqrt{(n+1)(n+2)(n+3)} \psi_{n+3}^{(0,0)} \right. \\
 &\left. - 3 \sqrt{(n+1)^3} \psi_{n+1}^{(0,0)} + 3 \sqrt{n^3} \psi_{n-1}^{(0,0)} - \sqrt{n(n-1)(n-2)} \psi_{n-3}^{(0,0)} \right] = 0
 \end{aligned} \tag{42}$$

Since $a^+ a^- \psi_n^{(0,0)} = n h \nu \psi_n^{(0,0)}$, it is seen from (42) that $\psi_n^{(1,0)}$ is

$$\begin{aligned} \psi_n^{(1,0)} &= C_{n+3} \psi_{n+3}^{(0,0)} + C_{n+1} \psi_{n+1}^{(0,0)} \\ &\quad + C_{n-1} \psi_{n-1}^{(0,0)} + C_{n-3} \psi_{n-3}^{(0,0)} \end{aligned} \quad (43)$$

and each term in (42) must vanish. Therefore, the C's may be evaluated:

$$C_{n+3} = -\frac{k_3}{3i^3} \sqrt{\frac{h\nu}{8k_2^3}} (n+1)(n+2)(n+3)$$

$$C_{n+1} = +\frac{3k_3}{i^3} \sqrt{\frac{h\nu}{8k_2^3}} (n+1)^3$$

$$C_{n-1} = +\frac{3k_3}{i^3} \sqrt{\frac{h\nu}{8k_2^3}} n^3$$

$$C_{n-3} = -\frac{k_3}{3i^3} \sqrt{\frac{h\nu}{8k_2^3}} (n)(-1)(n-2)$$

So, $E_n^{(2,0)}$ may be evaluated:

$$\begin{aligned} E_n^{(2,0)} &= \frac{k_3^2}{24k_2^3} h^2 \nu^2 \left\langle \sqrt{(n+1)(n+2)(n+3)} \psi_{n+2}^{(0,0)} \right. \\ &\quad - 3 \sqrt{(n+1)^3} \psi_{n+1}^{(0,0)} + 3 \sqrt{n^3} \psi_{n-1}^{(0,0)} \\ &\quad - \sqrt{n(n-1)(n-2)} \psi_{n-3}^{(0,0)} \left| \sqrt{(n+1)(n+2)(n+3)} \psi_{n+3}^{(0,0)} \right. \\ &\quad - 9 \sqrt{(n+1)^3} \psi_{n+1}^{(0,0)} - 9 \sqrt{n^3} \psi_{n-1}^{(0,0)} \\ &\quad \left. + \sqrt{n(n-1)(n-2)} \psi_{n-3}^{(0,0)} \right\rangle \end{aligned} \quad (44)$$

Once again, orthonormality is invoked, and only the products of $\psi^{(0,0)}$'s having the same subscripts survive, giving $E_n^{(2,0)}$:

$$E_n^{(2,0)} = - \frac{k_3^2 h^2 v^2}{8k_2^3} [30n^2 + 3n + 11] \quad (45)$$

The third-order correction to the energy, $E_n^{(3,0)}$, $k_3 \langle \psi_n^{(1,0)} | x^3 | \psi_n^{(1,0)} \rangle$ will be zero. The subscripts of $\psi_n^{(1,0)}$ produced by x^3 acting upon it will be chosen from among the group (+6, +4, +2, 0, -2, -4, -6), all of which are different from (+3, +1, -1, -3). By orthonormality all terms in $E_n^{(3,0)}$ will vanish.

The perturbation due to equation (31b) can be treated in much the same way as the $H^{(1,0)}$ perturbation was. The first-order energy correction is

$$E_n^{(0,1)} = k_4 \langle \psi_n^{(0,0)} | x^4 | \psi_n^{(0,0)} \rangle \quad (46)$$

The operator x^4 is

$$x^4 = \frac{1}{i^4 \sqrt{16k_2^4}} \begin{aligned} & (a^+ a^+ a^+ a^+ - a^- a^+ a^+ a^+ \\ & - a^+ a^- a^- a^+ + a^- a^- a^+ a^+ \\ & - a^+ a^+ a^- a^+ + a^- a^+ a^- a^+ \\ & + a^+ a^- a^- a^+ - a^- a^- a^- a^+ \\ & - a^+ a^+ a^+ a^- + a^- a^+ a^+ a^- \\ & + a^+ a^- a^+ a^- - a^- a^- a^+ a^- \\ & + a^+ a^+ a^- a^- - a^- a^+ a^- a^- \\ & - a^+ a^- a^- a^- + a^- a^- a^- a^-) \end{aligned} \quad (47)$$

Applying Equation (47) to $\psi_n^{(0,0)}$ leads to

$$\begin{aligned}
 x^4 \psi_n^{(0,0)} &= \frac{\sqrt{h^4 v^4}}{i^4 \sqrt{16k_2^4}} \left\{ \sqrt{(n-1)(n-2)(n-3)(n-4)} \psi_{n+4}^{(0,0)} \right. \\
 &- [4n + 6] \sqrt{(n+1)(n+2)} \psi_{n+2}^{(0,0)} \\
 &- [4n - 2] \sqrt{n(n-1)} \psi_{n-2}^{(0,0)} \\
 &\left. + [6n + 6n + 3] \psi_n^{(0)} + \sqrt{n(n-1)(n-2)(n-3)} \psi_{n-4}^{(0)} \right\}. \quad (48)
 \end{aligned}$$

So $E_n^{(0,1)}$ is readily obtained:

$$E_n^{(0,1)} = \frac{3k_4 h^2 v^2}{4k_2^2} [2n^2 + 2n + 1] \quad (49)$$

The correction to the energy that is first-order in both perturbations is

$$\begin{aligned}
 E_n^{(1,1)} &= \langle \psi_n^{(0,0)} | H^{(1,0)} | \psi_n^{(0,1)} \rangle \\
 &+ \langle \psi_n^{(0,0)} | H^{(0,1)} | \psi_n^{(1,0)} \rangle \quad (50)
 \end{aligned}$$

At this point the first-order corrections to the wavefunctions for $H^{(0,1)}$ are yet to be determined, but are not necessary if Dalgarno's interchange theorem is applied:

$$\begin{aligned}
& \langle \Psi_n^{(1,0)} | H^{(0,1)} | \Psi_n^{(0,0)} \rangle \\
& = \langle \Psi_n^{(0,1)} | H^{(1,0)} | \Psi_n^{(0,0)} \rangle .
\end{aligned} \tag{51}$$

Furthermore, x is Hermitian, so

$$\begin{aligned}
& \langle \Psi_n^{(0,0)} | H^{(1,0)} | \Psi_n^{(0,1)} \rangle \\
& = \langle \Psi_n^{(1,0)} | H^{(0,1)} | \Psi_n^{(0,0)} \rangle
\end{aligned} \tag{52}$$

Then

$$E_n^{(1,1)} = 2k_4 \langle \Psi_n^{(1,0)} | x^4 | \Psi_n^{(0,0)} \rangle = 0 \tag{53}$$

This is the highest order of perturbation that will be considered in this example. The energy of the n^{th} level of the cubic-quartic anharmonic oscillator is

$$\begin{aligned}
E_n & \approx \left(n + \frac{1}{2}\right) h\nu - \frac{k_3^2 h^2 \nu^2}{8k_2^3} (30n^2 + 30n + 11) \\
& + \frac{3k_4^2 \nu^2}{4k_2^2} (2n^2 + 2n + 1) .
\end{aligned} \tag{54}$$

II.8.4 The Relationship between Energy Level Spacings and an Anharmonic Potential

It is instructive to consider the effects of anharmonicity in a system of two particles of different mass as a guide to the

understanding of more complex systems. The constants k_2 , k_3 , and k_4 must now be evaluated.

The Morse potential, Equation (28), can be expanded in terms of a power series:

$$\begin{aligned}
 V(x) = & V(0) + V'_x(0)x + \frac{1}{2} V''_x(0)x^2 \\
 & + \frac{1}{6} V'''_x(0)x^3 + \frac{1}{24} V''''_x(0)x^4 + \dots
 \end{aligned} \tag{55}$$

where the number of primes indicates the order of the derivative of V with respect to x .

It can be seen that

$$\begin{aligned}
 V(0) &= -D_e \\
 V'_x(0) &= 0 \\
 V''_x(0) &= 2D_e \beta^2 \\
 V'''_x(0) &= -6D_e \beta^3 \\
 V''''_x(0) &= 14D_e \beta^4
 \end{aligned}$$

When the above substitutions are made in Equation (55), the constants in Equation (29) are

$$\begin{aligned}
 k_2 &= 2D_e \beta^2 \\
 k_3 &= -D_e \beta^3 \\
 k_4 &= \frac{7}{12} D_e \beta^4
 \end{aligned}$$

When the above substitutions are made in Equation (54), the E_n expression becomes

$$E_n \approx (n + \frac{1}{2})h\nu - \frac{h^2\nu^2}{64D_e} (30n^2 + 30n + 11) + \frac{7}{64} \frac{h^2\nu^2}{D_e} (2n^2 + 2n + 1) \quad (56)$$

Equation (56) will now be expressed as a power series in $(n + \frac{1}{2})$:

$$d(n + \frac{1}{2}) = dn$$

$$\frac{dE}{dn} = h\nu - \frac{h^2\nu^2}{64D_e} (60n + 30) + \frac{7}{64} \frac{h^2\nu^2}{D_e} (4n + 2) \quad (57)$$

$$\frac{d^2E}{dn^2} = - \frac{h^2\nu^2}{64D_e} (60) + \frac{7}{16} \frac{h^2\nu^2}{D_e} (4) \quad (58)$$

These two equations are evaluated at $n = -\frac{1}{2}$, since $n + \frac{1}{2} = 0$:

$$E_n(-\frac{1}{2}) = 0$$

$$E'_n(-\frac{1}{2}) = h\nu$$

$$E''_n(-\frac{1}{2}) = -\frac{1}{2} \frac{h^2\nu^2}{D_e}$$

The new approximation for the energy levels of the cubic-quartic one-dimensional anharmonic oscillator is:

$$E(n + \frac{1}{2}) = h\nu(n + \frac{1}{2}) - \frac{1}{4} \frac{h^2\nu^2}{D_e} (n + \frac{1}{2})^2 \quad (59)$$

Some texts give an expression equivalent to Equation (59) in a slightly different form:

$$\epsilon_n = hc\omega_e \left(n + \frac{1}{2}\right) - h\omega_e x_e \left(n + \frac{1}{2}\right)^2 \quad (60)$$

The similarity between Equations (59) and (60) is readily seen; in Equation (60) ω is measured in cm^{-1} . c is the velocity of light. The factor x_e in (60) is equivalent to

$$\frac{1}{4} \frac{hv}{D_e}$$

and is commonly called the anharmonicity constant. (Davidson, 1962). Others (Herzberg, 1945; Urey, 1947) may include the minus sign in the constant.

II.8.5 The Precision of Approximations to the Morse Potential

By using the values of k_2 , k_3 , and k_4 , adopting a co-ordinate system in terms of D_e and r_0 , and shifting the origin to (1, -1), comparisons can be made among the shapes of the Morse, harmonic, cubic-anharmonic, cubic-quartic-anharmonic potential curves, illustrating how well they approximate the Morse curve. Such curves for the $\frac{1}{2}k_2x^2$, $\frac{1}{2}k_2x^2+k_3x^3$ and $\frac{1}{2}k_2x^2+k_3x^3+k_4x^4$ potentials appear in Figures II-2, II-3 and II-4, respectively. The convention $\beta = 2/r_0$ of Schiff (1968) was used for this comparison. Equation (27) was used to determine the Morse curve.

Table II-1 gives the deviations from the Morse potential of the harmonic, cubic-anharmonic, and cubic-quartic anharmonic potentials. The deviations are plotted in Figure II-5.

FIGURE II-2

The harmonic potential.

This is the potential energy function used in the solution of the harmonic oscillator problem. The potential energy varies as the square of the displacement from the equilibrium separation distance of two atoms, r_0 .

313
HARMONIC POTENTIAL

$$V(r) = 4 \frac{D_e}{r_0} (r - r_0)^2$$

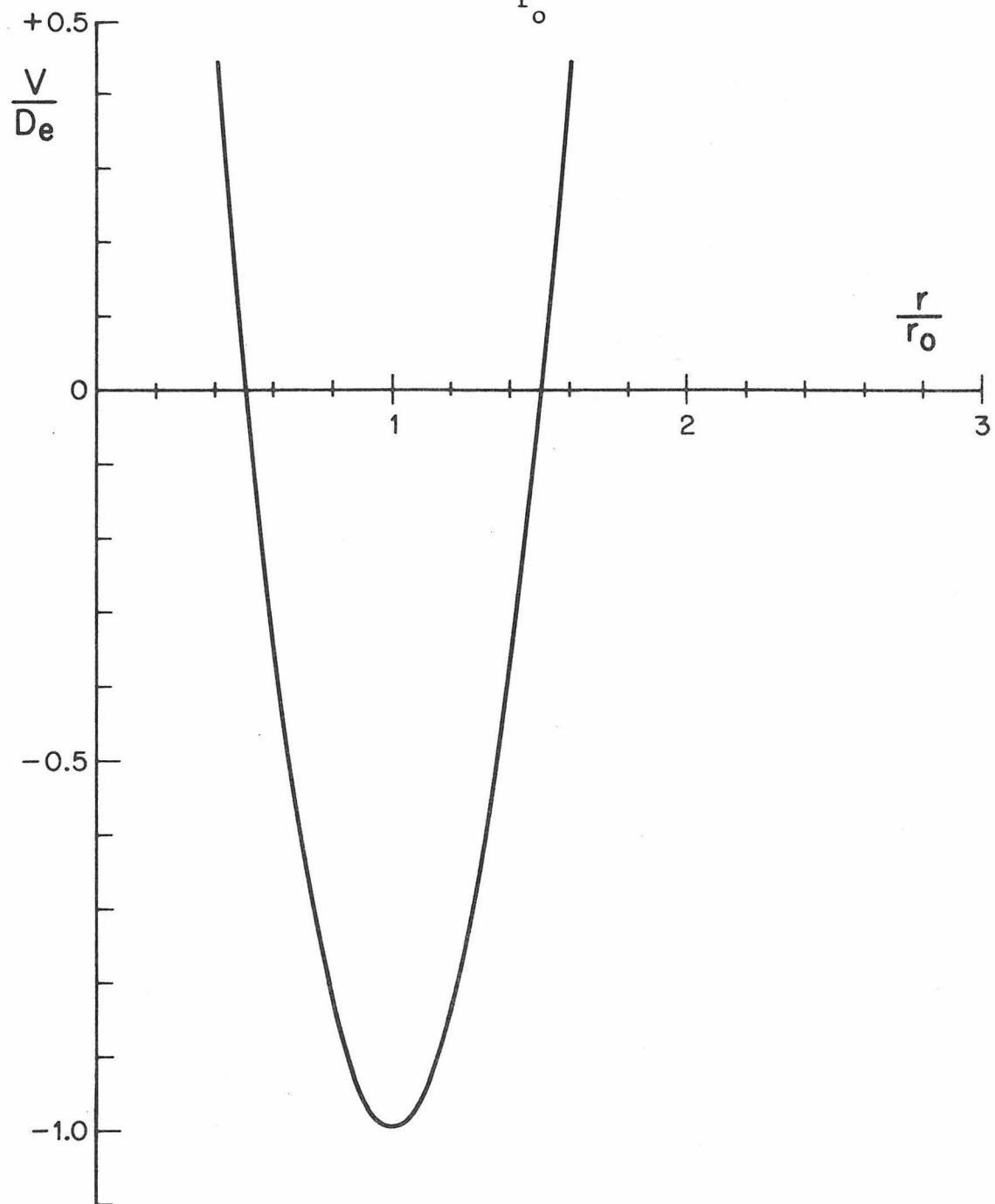


FIGURE II-3

The cubic-anharmonic potential.

This potential energy function results when a term that is third-order in displacement is added to the harmonic potential (Figure II-2).

315
CUBIC-ANHARMONIC POTENTIAL

$$V(r) = 4 \frac{D_e}{r_o^2} (r - r_o)^2 - 8 \frac{D_e}{r_o^3} (r - r_o)^3$$

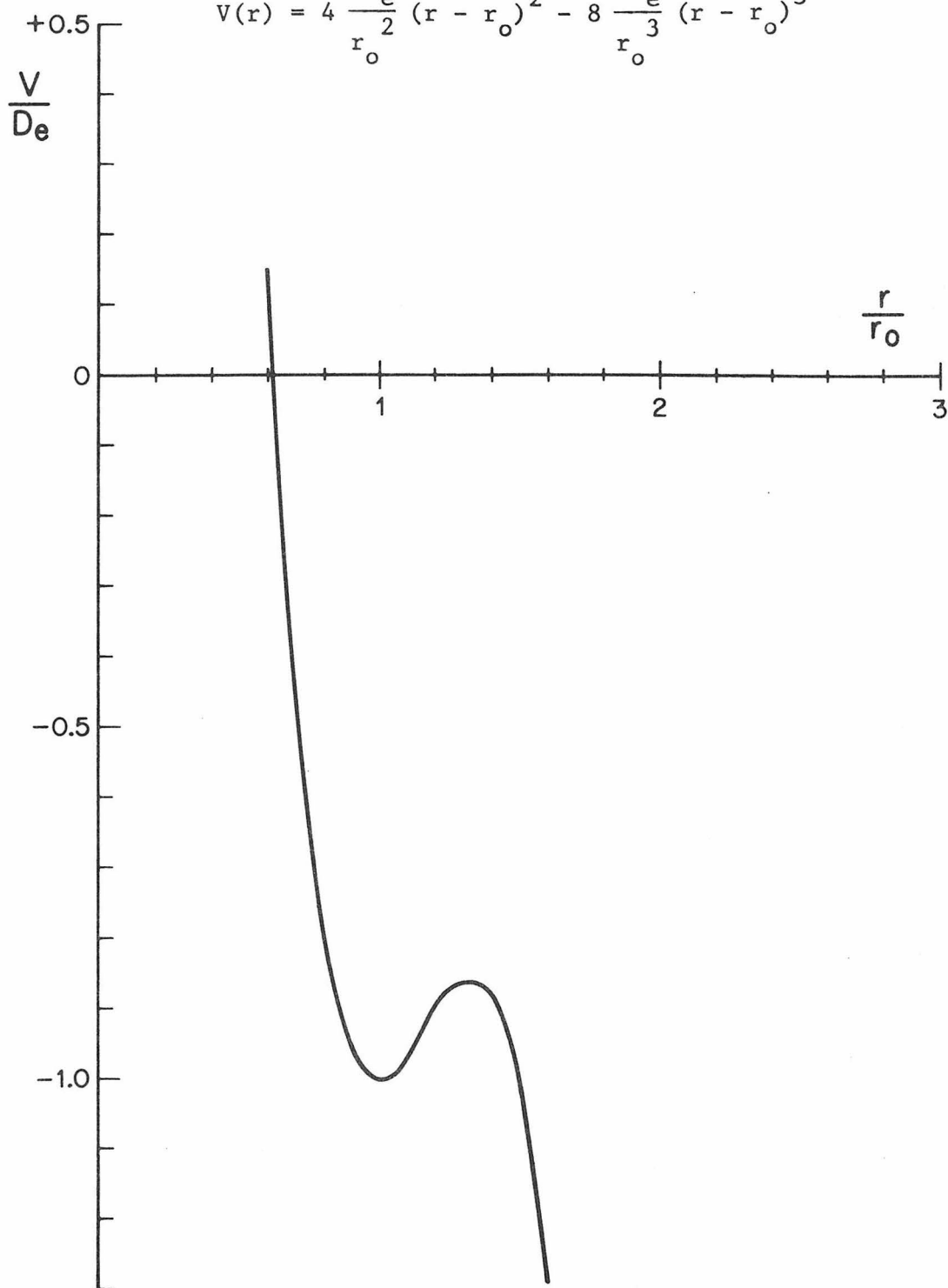


FIGURE II-4

The cubic-quartic-anharmonic potential.

This potential is used to approximate the Morse potential and to derive the form of the anharmonicity constant. As the name implies, the potential energy contains terms that are third- and fourth-order in displacement from the equilibrium separation, r_0 , as well as a second-order term.

CUBIC-QUARTIC-ANHARMONIC POTENTIAL

$$V(r) = 4 \frac{D_e}{r_0} (r - r_0)^2 - 8 \frac{D_e}{r_0^3} (r - r_0)^3 + \frac{7D_e}{12r_0^4} (r - r_0)^4$$

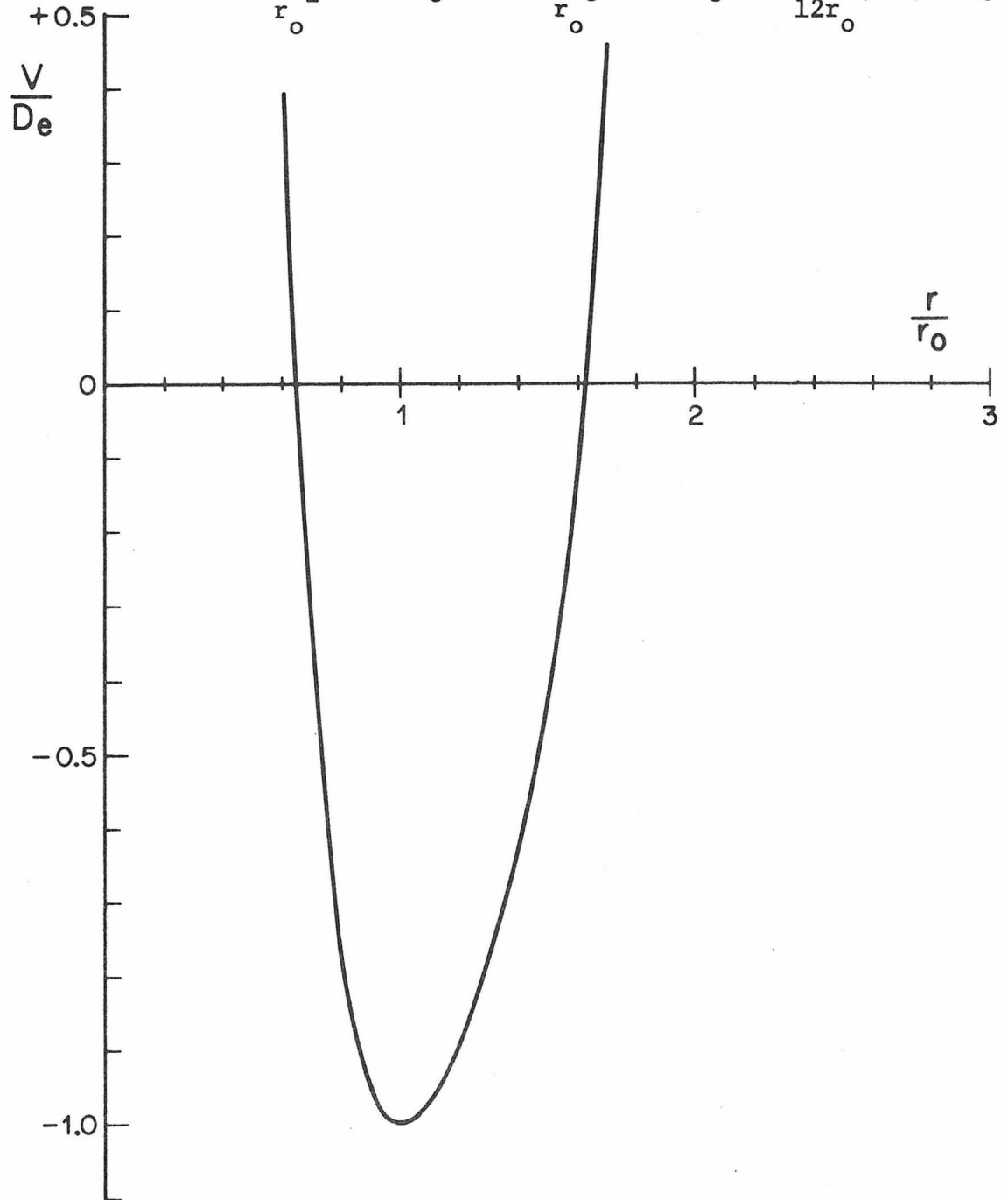


Table II-1

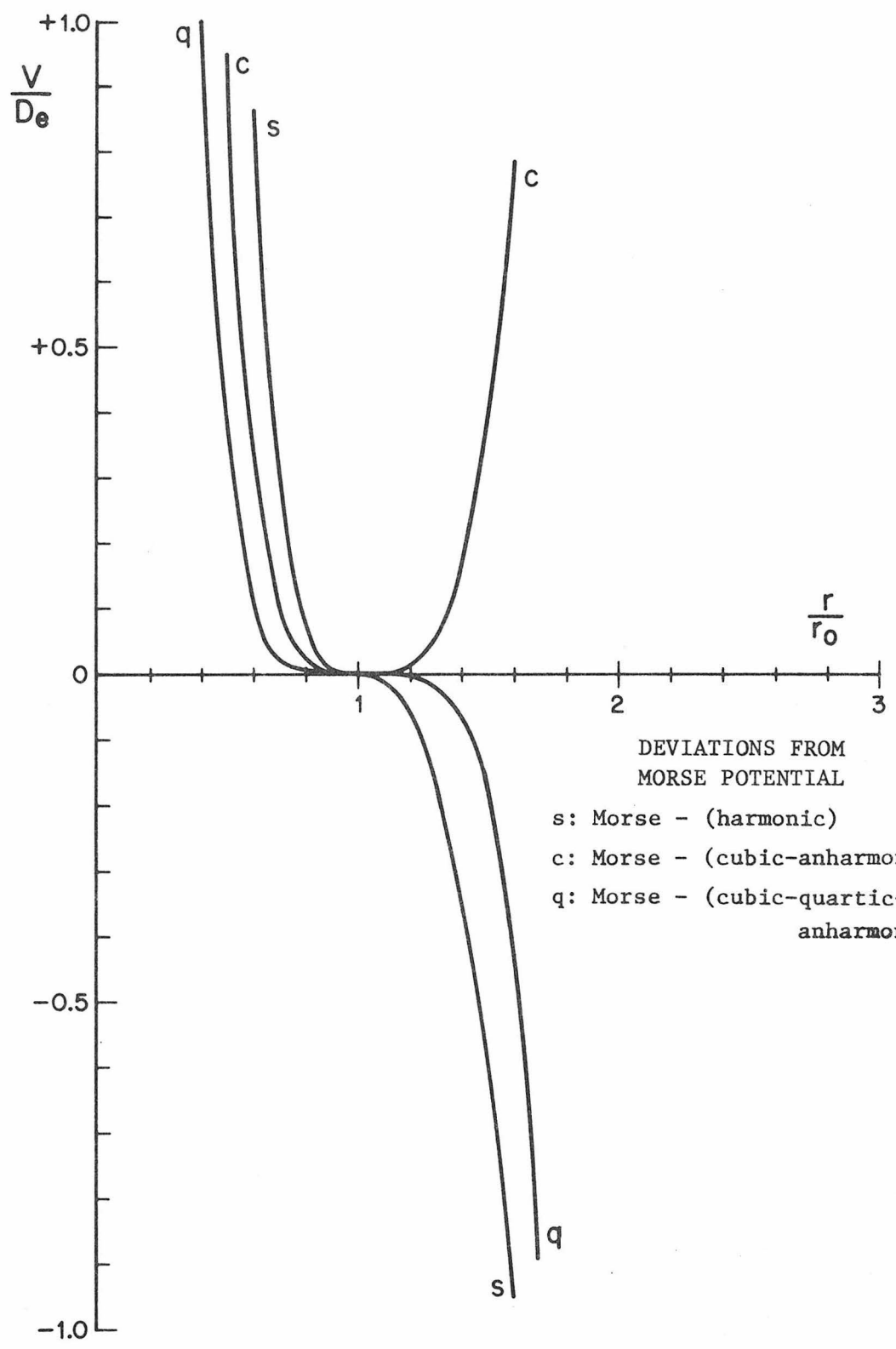
Deviations from Morse Potential
of Harmonic, Cubic-Anharmonic and
Cubic-Quartic-Anharmonic Potentials

<u>r</u>	<u>M-(harm)</u>	<u>M-(cu-anh)</u>	<u>M-(cu-q-anh)</u>
0.4r _o	3.94D _e	2.21D _e	1.00D _e
0.5r _o	1.95D _e	0.95D _e	0.37D _e
0.6r _o	0.86D _e	0.35D _e	0.11D _e
0.7r _o	+0.32D _e	+0.10D _e	+0.02D _e
0.75r _o	+0.17D _e	+0.05D _e	+0.01D _e
0.8r _o	+0.08D _e	+0.02D _e	+0.01D _e
0.9r _o	+0.01D _e	0	0
r _o	0	0	0
1.1r _o	-0.01D _e	0	0
1.2r _o	-0.05D _e	+0.01D _e	0
1.3r _o	-0.16D _e	+0.06D _e	-0.02D _e
1.4r _o	-0.34D _e	+0.17D _e	-0.07D _e
1.5r _o	-0.60D _e	+0.40D _e	-0.18D _e
1.6r _o	-0.95D _e	+0.78D _e	-0.43D _e
1.7r _o	-1.39D _e	+1.35D _e	-0.89D _e
1.8r _o	-1.92D _e	+2.18D _e	-1.64D _e

FIGURE II-5

Deviations from the Morse potential of the harmonic, cubic-anharmonic, and cubic-quartic anharmonic potentials.

This figure is a plot of all the values in Table II-1, which gives for various values of r the differences between the Morse potential and each of the other three. It is apparent that the cubic-quartic-anharmonic potential is a reasonable approximation to the Morse potential in the range of r values of interest.



DEVIATIONS FROM
MORSE POTENTIAL

- s: Morse - (harmonic)
- c: Morse - (cubic-anharmonic)
- q: Morse - (cubic-quartic-anharmonic)

The width of the potential well at any level determines the $E(n + \frac{1}{2})$ spacing. The harmonic potential produced equal spacing. When perturbations to the potential produced deviations from the harmonic, toward a "distorted" well, the spacings became non-uniform. The higher the n , the more significant the contribution of $\frac{1}{4} \frac{h^2 v^2}{D_e} (n + \frac{1}{2})$ to E_n (Equation 59). Thus, the spacing between any pair of adjacent levels will be smaller than the spacing of the pair immediately below. Figure II-5 indicates that the cubic-quartic potential is the best, the cubic next best and the harmonic worst of those approximations considered. Over the range in r/r_0 of 0.7 to 1.3, the deviation of the cubic-quartic from the Morse is 2% or less. In Figure II-1 it is seen that this interval of r/r_0 contains that portion of the Morse curve below $V/D_e = 0.8$. As long as all the E_n 's of interest are in the region below $-0.8D_e$ in Figure II-4, the cubic-quartic curve coincides with the Morse curve reasonably well.

The partitioning of energy among the E_n states is described by the partition function. By setting Equation (59) equal to $0.2 D_e$ (the minimum in the potential curve corresponds to $E=0$), and solving for $n + \frac{1}{2}$, $n + \frac{1}{2}$ is $0.22 D_e/hv$. Similarly, for $E(n + \frac{1}{2}) = D_e$, $n + \frac{1}{2}$ is $2D_e/hv$, using the cubic-quartic potential.

A simple example will be used to illustrate the partitioning of energy. D_e for the $^1\Sigma$ state of CO is given by Morse as $\sim 92000 \text{ cm}^{-1}$ or 1.8×10^{-11} ergs. Urey (1947) gives ω_0 for $^{12}\text{C}^{16}\text{O}$ as 2167.4 cm^{-1} , or $6.5 \times 10^{13} \text{ sec}^{-1}$. Therefore, at $E_n = 0.2 D_e$, $n \approx 84$, according to the cubic-quartic treatment. The ratio of the number of molecules in

the first nine energy levels to the number of molecules in all energy levels is the ratio of the q 's:

$$\frac{N_{0-9}}{N_{0-84}} = \frac{q_{0-9}}{q_{0-84}} \quad (61)$$

The expression for q , using Equations (61) and (11) is

$$q = \sum_{n=0}^{\infty} e^{-\frac{h\nu(n+\frac{1}{2})}{kT}} + \frac{1}{4} \frac{h^2\nu^2}{D_e kT} (n+\frac{1}{2})^2 . \quad (62)$$

Equation (62) is quite unwieldy, so the harmonic approximation will be made now, and justified later.

At 500°K (227°C), a typical temperature encountered in hydrothermal systems, the q 's according to (14) are:

$$\begin{aligned} q(n=0 \text{ to } 9) &= 4.46268 \times 10^{-2} \\ q(n=0 \text{ to } 84) &= 4.46268 \times 10^{-2} \end{aligned}$$

The astonishing result is that virtually all of the CO molecules are still within the first 9 levels at 500°K. In fact, 99.81% of the particles will be found at levels no higher than that of $n = 1$, in the harmonic approximation. The discrete sums, using Equation (62), are

$$\begin{aligned} q(n=0) &= 4.45333 \times 10^{-2} \\ q(n=1) &= 4.46266 \times 10^{-2} \\ q(n=2) &= 4.46268 \times 10^{-2} \\ q(n=3) &= 4.46268 \times 10^{-2} \end{aligned}$$

The anharmonic q converges much faster than the harmonic, and 99.9996% of the CO molecules will be in states 0 or 1 according to the anharmonic approximation. It is concluded that all particles will have energies in the region for which the anharmonic approximation is extremely good (with less than 1% deviation from the Morse potential).

II.9 Q Ratio for a Perfect Gas

The first isotopic case to be treated has its foundation in the harmonic oscillator - rigid asymmetric rotor model (after Davidson, 1962). Let the gas be contained in a finite volume, V . The translational motion is given by Equation (25), with m replaced by M , the molecular weight:

$$q_{\text{trans}} = \left(\frac{2\pi M k T}{h^2} \right)^{3/2} V . \quad (63)$$

For rotational motion, the q for the rigid asymmetric rotor will be given without derivation:

$$q_{\text{rot}} = \frac{\pi^{1/2}}{\sigma} \left(\frac{8\pi^2 k T}{h^2} \right)^{3/2} (I_x I_y I_z)^{1/2} . \quad (64)$$

σ is the symmetry number, "defined as the number of different values of the rotational co-ordinates which all correspond to one orientation of the molecule, remembering that the identical atoms are indistinguishable" (Mayer and Mayer, 1940). I_x , I_y , and I_z are the principal moments of inertia, and will be dealt with shortly.

The value of q for one degree of freedom of harmonic vibration is

given by Equation (20). For all j of the modes, the q becomes:

$$q_{\text{vib}} = \prod_{j=1}^{3N-6} \frac{e^{-u_j/2}}{1-e^{-u_j}} \quad (65)$$

where u is as before. The upper limit of the product, $3N-6$, arises as follows: there would ordinarily be $3N$ (N is the number of "vibrators" in the molecule) integral degrees of freedom; six (three translational and three rotational degrees of freedom) are already accounted for.

The q thus far is

$$\begin{aligned} q_{\text{total}} &= q_{\text{trans}} q_{\text{rot}} q_{\text{vib}} \\ &= \left(\frac{2\pi M k T}{h^2} \right)^{3/2} V \frac{\pi^{1/2}}{\sigma} \left(\frac{8\pi^2 k T}{h^2} \right)^{3/2} (I_x I_y I_z) \\ &\quad \cdot \prod_{j=1}^{3N-6} \frac{e^{-u_j/2}}{1-e^{-u_j}} \end{aligned} \quad (66)$$

From this point onward, every term with "*" attached pertains to a heavier isotopic species. The desired ratio, q^*/q is

$$\begin{aligned} \frac{q^*}{q} &= \left(\frac{M^*}{M} \right)^{3/2} \frac{\sigma}{\sigma^*} \left(\frac{I_x^* I_y^* I_z^*}{I_x I_y I_z} \right)^{1/2} \\ &\quad \cdot \prod_{j=1}^{3N-6} e^{(u_j - u_j^*)/2} \left(\frac{1-e^{-u_j}}{1-e^{-u_j^*}} \right) \end{aligned} \quad (67)$$

The Teller-Redlich Product Rule will be stated without proof (Redlich, 1935):

$$\prod_{j=1}^{3N-6} \frac{v_j^*}{v_j} \left[\prod_{i=1}^n \left(\frac{m_i}{m_i^*} \right)^{3/2} \right] \left(\frac{M^*}{M} \right)^{3/2} \left(\frac{I_x^* I_y^* I_z^*}{I_x I_y I_z} \right)^{1/2} \quad (68)$$

When (68) is rearranged, it becomes

$$\left(\frac{M^*}{M} \right)^{3/2} \left(\frac{I_x^* I_y^* I_z^*}{I_x I_y I_z} \right)^{1/2} = \prod_{j=1}^{3N-6} \frac{v_j^*}{v_j} \prod_{i=1}^n \left(\frac{m_i^*}{m_i} \right)^{3/2} \quad (69)$$

When (69) is substituted into (67), some unwieldy terms disappear:

$$\frac{q^*}{q} = \frac{\sigma}{\sigma^*} \prod_{i=1}^n \left(\frac{m_i^*}{m_i} \right)^{3/2} \prod_{j=1}^{3N-6} \frac{u_j^*}{u_j} e^{(u_j - u_j^*)/2} \cdot \frac{(1 - e^{-u_j})}{(1 - e^{-u_j^*})} \quad (70)$$

m^* and m are the atomic weights of the two isotopic species of the exchanging atom. In each molecule there are n atoms. The canonical partition function ratio for the molecule must include the degeneracy of each vibrational mode:

$$\frac{Q^*}{Q} = \frac{\sigma}{\sigma^*} \left(\frac{m^*}{m} \right)^{3n/2} \prod_j \left(\frac{u_j^*}{u_j} e^{(u_j - u_j^*)/2} \frac{(1 - e^{-u_j})}{(1 - e^{-u_j^*})} \right)^{d_j} \quad (71)$$

where d_j is the degeneracy of the j^{th} mode. The ratio is often written in terms of natural logarithms:

$$\begin{aligned} \ell_n \frac{Q^*}{Q} &= \ell_n \frac{\sigma}{\sigma^*} + \frac{3n}{2} \ell_n \left(\frac{m^*}{m} \right) \\ &+ \ell_n \left[\prod_j \frac{u_j^*}{u_j} e^{(u_j - u_j^*)/2} \frac{(1 - e^{-u_j})}{(1 - e^{-u_j^*})} \right]^{d_j} \end{aligned} \quad (72)$$

The above equation is similar to Equation (4') of Urey (1947). Note that the first two terms in (72) are the vestiges of q_{rot} and q_{trans} .

II.10 The Effects of Anharmonicity on Perfect Gas Q's

The initial part of this discussion follows Herzberg (1945).

In a multidimensional, generalized anharmonic oscillator, the energy is obtained rigorously from the following expression:

$$\begin{aligned} E(n_1, n_2, n_3, \dots) &= h\nu_1(n_1 + \frac{1}{2}) = h\nu_2(n_2 + \frac{1}{2}) + h\nu_3(n_3 + \frac{1}{2}) + \dots \\ &+ hx_{11}(n_1 + \frac{1}{2})^2 + hx_{22}(n_2 + \frac{1}{2})^2 + hx_{33}(n_3 + \frac{1}{2})^2 + \dots \\ &+ hx_{12}(n_1 + \frac{1}{2})(n_2 + \frac{1}{2}) + hx_{13}(n_1 + \frac{1}{2})(n_3 + \frac{1}{2}) \\ &+ hx_{23}(n_2 + \frac{1}{2})(n_3 + \frac{1}{2}) + \dots \end{aligned} \quad (73)$$

x_{ii} is the same as $\omega_e x_e$ in (60). The vibrational modes are no longer independent of one another, so the energy expression contains cross terms x_{ij} ($i \neq j$) to account for the interactions between the modes. Each vibrating system of, say, two atoms, will have its own anharmonicity. Each system is further influenced by interactions with vibrations in other modes, if all the atoms in the molecule (containing more than two atoms) are connected together. These inter-mode interactions will contribute additional anharmonicity, as indicated by the x_{ij} terms.

The correction to the zero-point energy ($n_1=0, n_2=0, n_3=0, \dots$) for any interaction between modes i and j , taking into account degeneracy, will be:

$$\frac{1}{4} h x_{ij} d_i d_j$$

When the * notation is applied, denoting the heavy isotopic species, the Q-ratio correction, due to the anharmonic effects on the zero-point energy, is

$$\ln \left(\frac{Q^*}{Q} \right)_{\text{correction}} = \frac{1}{4} \frac{h}{kT} \sum_i \sum_j (x_{ij} - x_{ij}^*) d_i d_j. \quad (74)$$

The general expression for the anharmonic oscillator transition energies ($E_n - E_0$) is given by Herzberg and is stated here without derivation:

$$E = h \left\{ \sum_i \omega_i n_i + \sum_i \sum_k x_{ik} [n_i n_k + (d_i n_k + d_k n_i)] \right\} \quad (75)$$

Equations (74) and (75) are only approximations, and should contain third- and higher-order interactions involving $x_{ijk} \dots$, in order to be perfectly rigorous. The higher-order terms have a physical significance in that "certain energy levels that coincide in the harmonic oscillator approximation split into a number of levels when anharmonicity is taken into account" (Herzberg, 1945).

By using a Mellin integral transform, Vojta (1961) derived an expression for the Q of this system:

$$Q = \prod_j \frac{1}{(1-e^{-u_j})^{d_j}} \left\{ 1 - \sum_i d_i (d_i+1) \frac{h x_{ii}}{kT} \frac{e^{-u_i}}{(1-e^{-u_i})^2} \right. \\ \left. - \frac{1}{2} \frac{h}{kT} \sum_{i < j} d_i d_j \frac{x_{ij} (e^{-u_i} - e^{-u_j})}{(1-e^{-u_i})(1-e^{-u_j})} \right\} \\ + \text{higher-order terms in } x \quad (76)$$

The x 's are measured in sec^{-1} .

This expression accounts for energies above the zero-point energy, and includes the harmonic factor,

$$\frac{1}{(1-e^{-u_j})^{d_j}}$$

which has already been dealt with in the Q^*/Q ratio. The last correction to be made to the Q^*/Q ratio for perfect gases is that for the anharmonicity of states above the zero-point energy, a correction provided by Equation (76). In $*$ notation the Q ratio becomes:

$$\ln \frac{Q^*}{Q} = \ln \frac{\sigma}{\sigma^*} + \frac{3n}{2} \ln \left(\frac{m^*}{m} \right) + \sum_j \left[\ln \frac{u_j^*}{u_j} + \frac{u_j - u_j^*}{2} + \ln \frac{(1-e^{-u_j})}{(1-e^{-u_j^*})} \right] d_j \\ + \frac{1}{4} \frac{h}{kT} \sum_{i \leq j} (x_{ij} - x_{ij}^*) d_i d_j + \ln \left\{ 1 - \frac{h}{kT} \sum_i d_i (d_i - 1) \left[x_{ii}^* \frac{e^{u_i^*}}{(e^{u_i^*} - 1)^2} \right] \right. \\ \left. - \frac{1}{2} \frac{h}{kT} \sum_{i < j} d_i d_j x_{ij}^* \frac{e^{-u_i^*} + e^{-u_j^*}}{(1-e^{-u_i^*})(1-e^{-u_j^*})} \right\} \\ - \ln \left\{ 1 - \frac{h}{kT} \sum_i d_i (d_i + 1) \left[x_{ii} \frac{e^{u_i}}{(e^{u_i} - 1)^2} \right] \right. \\ \left. - \frac{1}{2} \frac{h}{kT} \sum_{i < j} d_i d_j x_{ij} \frac{e^{-u_i} + e^{-u_j}}{(1-e^{-u_i})(1-e^{-u_j})} \right\} \quad (77)$$

The unwieldy Equation (77) can be simplified slightly by noting that the arguments of some logarithms are of the form:

$$(1 + \text{"some number"})$$

The limits of "some number" will now be evaluated. At 300°K, $h/kT = 1.59 \times 10^{-13}$. Up to this point, all ν 's were in units of sec^{-1} . For the purpose of consistency with other workers (Davidson, Urey, Bottinga) ν will be replaced by ω , such that $c\omega = \nu$. ω is measured in cm^{-1} . Thus, $hc/kT = 4.77 \times 10^{-3}$, a small number with respect to 1. A typical maximum value of x_{ij} is 20 cm^{-1} , except in hydrogenous substances (Urey, 1947) and d is a small interger (usually 1, 2, or 3).

The u term in the expression

$$\frac{e^u}{e^{2u} - 2e^{u+1}}$$

typically lies between 0.5 ($\omega = 100 \text{ cm}^{-1}$) and 20 ($\omega = 4000 \text{ cm}^{-1}$). The corresponding range in the above expression containing the exponentials is -1 to 2×10^{-9} . In the extreme cases mentioned the approximation:

$$\ln(1 + \text{"some number"}) \approx \text{"some number"} \quad (78)$$

(if "some number" is small compared to 1), is just beginning to break down. In systems with large anharmonicity constants, high degeneracy and/or small ω 's, Equation (77) must be used as is.

If the approximation (78) is made and applied to (77), the final form of the perfect gas Q ratio becomes

$$\begin{aligned}
 \ln \frac{Q^*}{Q} = & \ln \frac{\sigma}{\sigma^*} + \frac{3n}{2} \ln \left(\frac{m^*}{m} \right) \\
 & + \sum_j \left[\ln \frac{u_j^*}{u_j} + \frac{u_j - u_j^*}{2} + \ln \frac{(1-e^{-u_j})}{(1-e^{-u_j^*})} \right] d_j \\
 & + \frac{1}{4} \frac{hc}{kT} \sum_i \sum_{i \leq j} (x_{ij} - x_{ij}^*) d_i d_j \\
 & + \ln \left\{ 1 + \frac{hc}{kT} \sum_i [d_i (d_i + 1)] \left[\frac{x_{ii} e^{u_i}}{(e^{u_i} - 1)^2} - \frac{x_{ii}^* e^{u_i^*}}{(e^{u_i^*} - 1)^2} \right] \right. \\
 & \left. + \frac{1}{2} \frac{hc}{kT} \sum_i < \sum_j d_i d_j \left[\frac{x_{ij} (e^{u_i} + e^{u_j})}{(e^{u_i} - 1)(e^{u_j} - 1)} - \frac{x_{ij}^* (e^{u_i^*} + e^{u_j^*})}{(e^{u_i^*} - 1)(e^{u_j^*} - 1)} \right] \right\} \quad (79)
 \end{aligned}$$

Equation (79) is the same as Bottinga's Equation (5) (1968), with an exception: his term s^*/s should be s/s^* for the correct treatment of symmetry numbers.

II.11 Q Ratios for Crystals

Just as all states of all modes of motion were needed to characterize a perfect gas, the same is true of crystals. If a crystal can be considered a large molecule, translational modes are absent (a special kind of translation will be discussed later).

The atomic groups in a crystal lattice are not spinning around as rigid asymmetrical rotors, but some hindered rotation in a potential

$$v = v_0 \frac{(1 - \cos n)}{2} \quad (80)$$

is taking place. Stockmayer (1957) showed that the Q ratio used in calculating isotopic effects due to hindered rotation in a crystal is the same as the Q ratio for the harmonic oscillator, with a characteristic ω . Hindered rotations are often called librations.

Internal vibrations are present, as before, and are dealt with accordingly: these are the atomic-level interactions, taking place in a localized environment of groups of atoms (commonly ions) within the crystal lattice (Example: vibrational modes of $(\text{SO}_2)^{-2}$ in anhydrite). Information regarding anharmonicity of internal vibrations in a crystal (i.e., the x-values) is commonly not available.

The optical modes of vibration involve unit cells in the crystal lattice vibrating against each other. In an ionic crystal the modes are the same as internal vibrations. Optical modes need not be active in visible light; most appear in the infrared. Acoustic modes of vibration involve the propagation of continuous waves through the crystal lattice, with a resultant, instantaneous displacement of atoms at lattice sites. In spite of the name "acoustic," the frequencies of these vibrations are not necessarily audible. The name refers to the fact that the method of propagation is the same as that of sound waves. In most crystals there is a longitudinal mode and a doubly-degenerate transverse (i.e., shear) mode of acoustic vibration.

All of this energy must be accounted for in order to evaluate the differences in the Q's for isotopic species. Motion which results in a

change in the dipole moment somewhere in the crystal arises from interaction of the unperturbed dipole moment with the electric field. Such modes will be infrared active.

Some species have no dipole moment in an unperturbed state, but an electric field can rearrange the charge distribution to induce a dipole moment. The extent to which this dipole moment can be induced is called the polarizability and changes during the course of vibrations that are Raman active (and in some cases, infrared active also, depending on the symmetry of the vibration).

Finally, there is the acoustic vibrational mode, which involves motion of several unit cells (or groups of atoms) in phase with each other in the lattice. Most of these modes will not be infrared active, but may be Raman active, depending on the exact mechanism of elastic deformation of the lattice in a given mode.

All the modes of vibration except the acoustic can be treated with the anharmonic oscillator model developed here (Equation 77), because they are quantum-mechanical. Acoustic (lattice) vibrations occur at a continuum of frequencies (within limits) and must be treated somewhat differently. In this treatment use is commonly made of the Debye theory of the solid state (Rice, 1967).

The Debye theory considers the crystal as a large molecule with $3N$ normal modes of vibration, N of them in each principal direction. Q for such a molecule is

$$Q = \prod_{j=1}^{3N} \frac{e^{-\frac{h\nu_j}{2kT}} e^{-\frac{h\nu_j}{kT}}}{e^{\frac{h\nu_j}{kT}} - 1} e^{-\frac{E_0}{kT}} \quad (81)$$

Since each ν_j is the zero-point frequency of an individual quantized mode, and the ν_j 's are very close together, the expression for $\ln Q$ can be approximated by the integral:

$$\ln Q = \int_0^{\nu_D} \left(\ln \frac{e^{-\frac{h\nu}{2kT}} e^{-\frac{h\nu}{kT}}}{e^{\frac{h\nu}{kT}} - 1} \right) g(\nu) d\nu - \frac{V_0}{kT} \quad (82)$$

In the above expression $g(\nu)d\nu$ is the number of ν_j 's between ν and $\nu + d\nu$. The last term V_0/kT is the contribution of the potential energy, which will be dealt with later.

It can be shown that, for vibration in one of the principal directions:

$$g(\nu)d\nu = \frac{4\pi V}{c^3} \nu^2 d\nu \quad (83)$$

in which V is the volume of the crystal and c is the propagation velocity for standing waves in the specified direction (Davidson, 1962).

This treatment of a set of vibrational modes differs from the previous treatments because:

1. Debye theory treats a continuum of vibrational frequencies while Einstein functions (q 's for harmonic oscillators)

are derived from summations of discrete (quantum) energies.

2. There exists an upper cutoff frequency, ν_D , corresponding to the highest energy in the continuum of acoustic vibrations. In previous treatments ν was a zero point (lower cutoff) frequency of vibration.

It is easy to see that the graph of $g(\nu)$ will be one-half of a parabola whose vertex is at the origin. $g(\nu) = 0$ for all $\nu > \nu_D$. It is required that the total number of vibrations in one direction be N , the number of unit cells:

$$\int_0^{\nu_D} g(\nu) d\nu = N \quad (84)$$

Consequently, $g(\nu)d\nu$ is obtained in terms of ν_D :

$$g(\nu)d\nu = \frac{3N}{\nu_D^3} \nu^2 d\nu \quad (85)$$

Substitution of (85) into (82), and the further substitution $\nu^2 d\nu = \frac{kT}{h} u^2 du$ leads to:

$$\ln Q = \frac{3N}{u_D} \int_0^{u_D} \left[-\frac{1}{2} u - \ln(1 - e^{-u}) \right] u du - \frac{E_0}{kT} \quad (86)$$

in which $u_D = \frac{h\nu_D}{kT}$. Integration gives

$$\ln Q = -\frac{3}{8} N u_D - \frac{3N}{u_D} \int_0^{u_D} u^2 \ln(1 - e^{-u}) du - \frac{E_0}{kT} \quad (87)$$

The second term of (92) can be integrated by parts to give

$$\left\{ \frac{N}{u_D^3} [u^3 \ln(1-e^{-u})]_0^{u_D} - \frac{N}{u_D^3} \int_0^{u_D} \frac{u^3}{e^u - 1} du \right\}.$$

The first term of the above expression, when u approaches 0, vanishes.

Therefore for N unit cells of crystal lattice, the result is

$$\ln Q = -\frac{3}{8} N u_D - N \ln(1 - e^{-u_D}) + N D_e(u_D) - \frac{E_0}{kT} \quad (88)$$

in which

$$D_e(u_D) = \frac{1}{3} \int_0^{u_D} \frac{u^3}{e^u - 1} du, \quad \text{or}$$

for one unit cell,

$$\ln Q = -\frac{3}{8} u_D - \ln(1 - e^{-u_D}) + D_e(u_D) - \frac{E_0}{NkT}. \quad (89)$$

The $\ln \frac{Q^*}{Q}$ for a crystal then becomes

$$\begin{aligned} \ln \frac{Q^*}{Q} = \sum_i \left\{ \frac{3}{8} (u_i - u_i^*) + \ln \frac{(1 - e^{-u_i})}{(1 - e^{-u_i^*})} \right. \\ \left. + D_e(u_i^*) - D_e(u_i) \right\} d_i. \quad (90) \end{aligned}$$

Note that the potential energy term, the same for both isotopic species, has vanished. Equation (90) is the same as the acoustic term in Equation (6) of Bottlinga (1968). The integral D_e is the Debye

energy integral and must be evaluated numerically.

II.12 Sources of Data for Calculations

Most spectroscopic data are reported as energies of transition between states of given modes. Interpretation of spectra and assignment of resonant absorption and/or emission peaks to various states and modes is commonly not a trivial task. The data are usually the energies of the fundamental transitions between the ground state (zero-point-energy) and the first excited state. It has been stated by Herzberg (1945) that the fundamental transition in any spectrum is the most probable one to be observed.

In the consideration of isotopic species of a substance, the potentials can be taken as virtually the same for all species. The differences between the bottom of the potential curve and the lowest vibrational state ($n = 0$, the one having the zero-point energy) are not the same for all species. The respective spacings between the higher levels are not the same for all isotopic species, either. If they were, there would be no isotopic fractionation at all. The energy separation between the bottom of the curve and the zero point energy level is small. It is so small that often an approximation is made:

$$\omega - \omega^* \approx \nu(n=1) - \nu^*(n=1)$$

or, the difference in zero-point-energies for two isotopic species is approximately the difference in fundamental vibration energies. The approximation is particularly useful when information about

anharmonicity is lacking. As was demonstrated in a previous section, the anharmonic constant(s) can in principle be evaluated from the $E(n + \frac{1}{2})$ values (Equation 60), and from such data the ω 's could be calculated more accurately. The approximation works well for low frequencies ($\sim 1500 \text{ cm}^{-1}$ or less), but anharmonic effects are significant in systems involving hydrogen (Herzberg, 1945).

If spectroscopic data are not available for some of the isotopic species, they must be estimated or calculated. In the course of such calculations, each substance must be considered individually; each will present unique problems regarding the form of the potential, nearest-neighbor (and more distant) interactions, the anharmonicities resulting from differences in mass, electronic structure, vibrational-rotational coupling with other modes, etc. It should be readily obvious that $(\text{CO}_3)^{-2}$ must be treated differently from CO_2 ; H_2O is another entirely unique system. Bottinga (1968) relied upon the models proposed by Heath and Linnett (1947), Giulotto and Loinger (1951) and Janz and Mikawa (1960) in order to calculate the Q ratios for calcite.

Some vibrations, particularly those of the acoustic mode, are difficult to observe, and require advanced techniques for their detection, specifically, inelastic scattering of slow neutrons. Because of the technical problems involved, this type of analysis is rarely performed. Furthermore, the results obtained in such experiments cannot be interpreted unambiguously. Safford et al. (1963) tentatively assigned the brucite absorption band peaked at 130 cm^{-1} to an acoustic-mode lattice vibration, but they also indicated that their understanding

of brucite, $\text{Mg}(\text{OH})_2$, did not at that point permit unique assignments of neutron spectra peaks to particular modes. The values of ν_D for calcite obtained by Giulotto and Loinger (1951) are calculated; the modes are only surmised and have not been observed, but fit the heat capacity data for calcite.

Because differences in Q^*/Q ratios between different substances are small, and because these differences determine the values of the fractionation factor, α , the values of q and consequently u and v must be known very precisely if α is to have a precision of 0.1‰. Many of the data (i.e., u -values) are only estimated or calculated for some isotopic species, and large discrepancies between α 's can result, using u 's that differ by only a few cm^{-1} .

II.13 Liquids

Nobody knows how to calculate partition function ratios for liquids, because a satisfactory model of a liquid does not exist. Urey (1947) broached this problem in his discussion of boron fractionation. Many boron compounds are liquids at ambient room temperatures, and errors in predicting the isotopic behavior of boron can arise in the approximation of liquid partition functions by gas partition functions.

II.14 Example Calculation:

Calcite-water oxygen isotope fractionation at 0°C (273°K) and 527°C (800°K)

This calculation was originally done by McCrea (1950). The data used in this section are those used by Bottinga (1968) in his

calculations. Values of h , k , and c are taken from Davidson (1962). Table II-2 contains the data used in Equation (95) for calcite. Table II-3 contains some values of $D_e(u_D)$, evaluated according to the series approximation:

$$x^{1/3} \int_0^x \frac{t^3 dt}{e^t - 1} = \left[\frac{1}{3} - \frac{x}{2(3+1)} + \sum_{k=1}^{\infty} \frac{B_{2k} x^{2k}}{(2k+3)(2k)!} \right] \quad (91)$$

in which B_n are the Bernoulli numbers, $B_0 = 1$, $B_1 = -\frac{1}{2}$, $B_2 = \frac{1}{6}$, $B_3 = -\frac{1}{30}$, $B_4 = \frac{1}{210}$, ... (Handbook of Mathematical Functions, NBS, 1964).

Table II-4 contains a summary of contributions to the Q ratio for calcite. The individual values are compared with Bottinga's, and the total reduced partition function ratios are compared with those of Bottinga and Shiro and Sakai (1972) and O'Neil, Clayton and Mayeda (1969). The reduced partition function ratio, $(Q^*/Q)_r$ is equal to $(Q^*/Q)(16/18)^{9/2}$ for oxygen. Anharmonicity effects are not considered, in view of the absence of x -values for calcite, so except for acoustic vibrations, Equation (20) was used to calculate q 's. Examples of the relative contributions to the total Q^*/Q ratios arising from anharmonicity of the ground-state and excited-states are given by Bottinga (1968) for H_2O and CO_2 , for which anharmonicity data (x -values) were available.

In Table II-4, the optical and rotational and acoustic components were divided by two to account for the fact that the calcite unit cell contains two formula units. The multiplier $1/3$ adjusts the

Table II-2

Vibrational Frequency Data for Calcite

* denotes $\text{CaC}^{18}\text{O}_3$ no * denotes $\text{CaC}^{16}\text{O}_3$ all ω -values in cm^{-1}

T = 273°K

	j	ω_j	ω_j^*	u_j	u_j^*	d_j
Internal vibrations of $\text{CO}_3^{=}$	1	1070	1008.67	5.63941	5.31617	1
	2	881	871.13	4.64329	4.59127	1
	3	1460	1436.15	7.69490	7.56919	2
	4	712	674.69	3.75258	3.55594	2
Optical & rotational vibrations (per unit cell)	1	282.2	266	1.48733	1.40195	2
	2	155.1	147	0.81745	0.77476	2
	3	397.2	388	2.09343	2.04494	1
	4	106.1	100	0.55920	0.52705	1
	5	345.3	334	1.81990	1.76034	2
	6	110.9	111	0.58450	0.58497	2
	7	256.5	249	1.35188	1.31235	2
	8	269.1	255	1.41829	1.34397	1
	9	99.1	94	0.52230	0.49542	1
	10	294.6	295	1.55268	1.55479	1
	i	ω_i	ω_i^*	u_i	u_i^*	d_i
Acoustic vibrations (per unit cell)	1	104.3	101	0.54971	0.53232	2
	2	142.1	137	0.74893	0.72206	1

Table II-2, continued

T = 800°K

	j	ω_j	ω_j^*	u_j	u_j^*	d_j
Internal vibrations of $\text{CO}_3^{=}$	1	1070	1008.67	1.92573	1.81535	1
	2	881	871.13	1.58557	1.56781	1
	3	1460	1436.15	2.62763	2.58470	2
	4	712	674.69	1.28142	1.21427	2
Optical & rotational vibrations (per unit cell)	1	282.2	266	0.50861	0.47873	2
	2	155.1	147	0.27914	0.26456	2
	3	397.2	388	0.71486	0.69830	1
	4	106.1	100	0.19095	0.17997	1
	5	345.3	334	0.62145	0.60111	2
	6	110.9	111	0.19959	0.19977	2
	7	256.5	249	0.46163	0.44814	2
	8	269.1	255	0.48431	0.45893	1
	9	99.1	94	0.17835	0.16918	1
	10	294.6	295	0.53020	0.53092	1
	i	ω_i	ω_i^*	u_i	u_i^*	d_i
Acoustic vibrations (per unit cell)	1	104.3	101	0.18759	0.18165	2
	2	142.1	137	0.25557	0.24640	1

Table II-3

Values of the Debye Energy Function

u	$D_e(u)$
0.18165	0.31118
0.18759	0.31047
0.24640	0.30355
0.25557	0.30248
0.53232	0.27152
0.54971	0.26966
0.72206	0.25177
0.74893	0.24907

Table II-4

Contributions to Calcite Partition Function Ratios
for $^{18}\text{O}/^{16}\text{O}$

	<u>273°K</u>		<u>800°K</u>	
	Bottinga(1968)	This work	Bottinga(1968)	This work
Optical & Rotational	0.30318	0.30352	0.27282	0.27339
Acoustic	0.04810	0.05136	0.04730	0.05057
Internal vibration	0.52209	0.52245	0.25973	0.25986

$\frac{1}{3} \ln$ (Reduced partition function ratios)

	<u>273°K</u>	<u>800°K</u>
Bottinga (1968)	0.14404	0.01628
O'Neil, Clayton & Mayeda (1969)	0.11348	0.01860 (773°K)
Shiro & Sakai (1972) using Bottinga's data	0.11547	0.01862 (773°K)
Shiro & Sakai (1972) their data, their equations	0.11250	0.01826 (773°K)
This work	0.11577	0.01793

reduced partition function ratios to the basis of one oxygen (instead of three).

Shiro and Sakai (1972) remarked that their "Bottinga's values" are approximately 1.5‰ larger than his at all temperatures, and that the reason was not clear. It is quite clear to this author that while Bottinga's Q expressions are the best available, his calculations are in error. The numbers determined in this work were obtained quite independently of any knowledge of Shiro and Sakai. This is not to say, however, that the results of Shiro and Sakai are entirely correct. Their expression for the acoustic vibration contribution to the Q ratio,

$$\ln f_{\text{acoust}} = \frac{3}{40} (\Theta^2 - \Theta^*{}^2)/T^2 ,$$

which is their Equation (11), is itself only an approximation based on an approximation by Bigeleisen and Mayer (1947). Furthermore, their fractionation factor, from their data, is too low by 1‰, with respect to the measured value of Epstein et al. (1953) which is 1.0344. The Q ratio for water vapor at 0°C was calculated by this author to be 0.0752 (compare with Bottinga's 0.06822). The resulting CaCO₃-water fractionation, using the $\ln \alpha$ (liquid-vapor) of Shiro and Sakai, 0.01119, is $1000 \ln \alpha = 34.06$.

Shiro and Sakai pointed out the possible sources of discrepancy between theory and measurement. Overwhelming considerations were thought by them to be the non-ideality involved in the water liquid-vapor fractionation, and the non-ideal behavior of H₂O in the

supercritical region. Also, they pointed out that Bottinga did not treat the splitting of the 1467 cm^{-1} vibration into 1434 cm^{-1} and 1484 cm^{-1} , which arises due to interaction of carbonate ions. There is substantial disagreement between the two determinations of vibrational frequencies. The Q-ratios of Shiro and Sakai, using their data, and the Q-expressions derived here, have not been evaluated. The calculated results of O'Neil, Clayton and Mayeda (1969) are based on yet other data and other approximations.

It should be noted that the temperature of no fractionation (the "crossover") according to the measurements of O'Neil et al. (1969) is near 700°C . Bottinga's work predicted a crossover at 450°C , and the Shiro and Sakai "recalculation," the Shiro and Sakai complete redetermination and this work all indicate a crossover at about 550°C . It should be obvious that until better data, including anharmonicity constants, for minerals become available, theoretical and measured isotopic equilibrium fractionations will be imperfectly reconciled.

APPENDIX III

CORRECTIONS AND CONVERSIONS PERFORMEDON MASS SPECTROMETRIC MEASUREMENTSIII. 1 Introduction

Corrections and conversions must always be performed on measurements of $^{18}\text{O}/^{16}\text{O}$, $^{13}\text{C}/^{12}\text{C}$ and D/H ratios made with modified Nier-type mass spectrometers. Those which were performed in the course of this study are briefly reviewed here. More detailed explanations of these corrections and conversions have been given by Knauth (1973).

III. 2 Background and Port Leakage

The first correction performed upon all measurements of δ -values was that which accounts for the imperfect vacuum in the mass spectrometer (background), and the imperfect sealing provided by the ground-glass sample intake valves (port leakage). Both these effects are taken into account in a factor by which all δ values must be multiplied:

$$1 + \frac{b}{I}$$

in which b typically varies from 30 to 70. The value of I is 2520 for the CO_2 mass spectrometer and 2500 for the hydrogen instrument. The resulting range of values of the background and port leakage correction factor is between 1.0119 and 1.0278.

III. 3 Corrections for CO_2 Analyses

In $^{18}\text{O}/^{16}\text{O}$ analyses the mass spectrometer measures differences in the intensities of ion beams whose mass/charge ratios are

46 ($^{12}\text{C}^{16}\text{O}^{18}\text{O}$) and 44 ($^{12}\text{C}^{16}\text{O}^{16}\text{O}$). For $^{13}\text{C}/^{12}\text{C}$ the mass/charge 45 ($^{13}\text{C}^{16}\text{O}^{16}\text{O}$) and 44 beams are compared. The desired ratios are $^{18}\text{O}/^{16}\text{O}$ and $^{13}\text{C}/^{12}\text{C}$, so a set of corrections must be applied in order to offset the ion-beam contributions of species of CO_2 formed from ^{13}C , ^{12}C , ^{16}O , ^{17}O and ^{18}O other than those listed above. The forms and derivations of these correction expressions are given by Craig (1957). The values of the constants in these expressions are characteristic of the machine reference sample (CO_2 extracted from Harding Iceland Spar, in this work). The expressions used were:

$$\delta^{18}\text{O corrected} = 1.0014 \delta^{18}\text{O} + 0.009 \delta^{13}\text{C}$$

$$\delta^{13}\text{C corrected} = 1.0673 \delta^{13}\text{C} - 0.0323 \delta^{18}\text{O}$$

The $\delta^{18}\text{O}$ and $\delta^{13}\text{C}$ on the right-hand side of the equations have been corrected for the background and port leakage. In the case of CO_2 derived from silicates, $\delta^{13}\text{C}$ was that of the carbon rod, an average of -20‰ relative to Harding Iceland Spar.

III. 4 Conversion of $\delta^{18}\text{O}$ and $\delta^{13}\text{C}$ to the PDB Standard

Periodically, the $\delta^{18}\text{O}$ and $\delta^{13}\text{C}$ values of the reference sample (Harding Iceland Spar) are measured against a secondary standard, whose isotopic composition relative to the Chicago Peedee Belemnite is known. The average $\delta^{18}\text{O}$ and $\delta^{13}\text{C}$ values of H.I.S. relative to PDB during this study were -4.56‰ and -18.58‰, respectively. The expressions used to relate δ values to PDB are:

$$\begin{aligned} \delta \text{ (PDB) sample} &= \delta \text{ (H.I.S.) sample} + \delta \text{ (PDB) H.I.S.} \\ &+ \frac{1}{1000} \cdot \delta \text{ (H.I.S.) sample} \cdot \delta \text{ (PDB) H.I.S.} \end{aligned}$$

III. 5 Conversion of δD to the SMOW Standard

The reference sample in the D/H instrument has a δD value 7.31% relative to Standard Mean Ocean Water. Conversion of δD values from machine reference to SMOW standard involves the use of an expression analogous to that given in Section III. 4, but δD is usually obtained in %:

$$\begin{aligned} \delta \text{ (SMOW) sample} &= \delta \text{ (reference) sample} + \delta \text{ (SMOW) reference} \\ &+ \frac{1}{100} \cdot \delta \text{ (reference) sample} \cdot \delta \text{ (SMOW) reference} \end{aligned}$$

III. 6 Measurement of $^{18}O/^{16}O$ Ratios of Total Oxygen in Carbonates

The treatment of carbonates with 100% H_3PO_4 liberates only two-thirds of the oxygen in the carbonates as CO_2 . Kinetic fractionation factors for this reaction have been measured by Sharma and Clayton (1965) for the H_3PO_4 reaction at 25.4°C. These fractionation factors have the following values:

$$\alpha_{CO_2-CO_3} = 1.01008 \text{ for calcite}$$

$$\alpha_{CO_2-CO_3} = 1.01090 \text{ for dolomite}$$

Then the expression:

$$\delta^{18}O \text{ total oxygen} = \frac{\delta^{18}O \text{ CO}_2 + 1000}{\alpha_{CO_2-CO_3}} - 1000$$

gives the $\delta^{18}O$ value for total carbonate oxygen.

III. 7 Conversion of $\delta^{18}O$ (PDB) Measurements to $\delta^{18}O$ (SMOW)

From a combination of the $\delta^{18}O$ value of PDB CO_2 relative to the CO_2 equilibrated with SMOW (about 0.1‰) and the $\alpha_{CO_2-H_2O}$ at 25.4°C (1.0410 according to unpublished results of O'Neil and Epstein), the

$\delta^{18}\text{O}$ value of PDB CO_2 relative to the oxygen in SMOW is 41.1‰. The conversion of δ values on the PDB scale to δ values on the SMOW scale can then be made using an equation similar to that in III.4.

III. 8 Correction for $\delta^{18}\text{O}$ Analyses of Water Samples

Since the $\text{CO}_2\text{-H}_2\text{O}$ equilibration method of Epstein and Mayeda (1953) was used to determine the $\delta^{18}\text{O}$ values of water samples, a correction to the $\delta^{18}\text{O}$ obtained for the CO_2 was applied, to account for the isotopic exchange between the water and the CO_2 . The correction expression involves the $\text{CO}_2/\text{H}_2\text{O}$ ratio, the $\text{CO}_2\text{-H}_2\text{O}$, and the original $\delta^{18}\text{O}$ value of the tank CO_2 that was used in the equilibration. The expression used for this correction was:

$$\delta^{18}\text{O CO}_2 \text{ eq} = 1.00670 \delta^{18}\text{O CO}_2 - 0.00670 \delta^{18}\text{O tank}$$

in which $\delta^{18}\text{O tank}$ is the original $\delta^{18}\text{O}$ value of tank CO_2 , $\delta^{18}\text{O CO}_2$ is the measured value of the CO_2 after equilibration with water, the corrections described in Sections III.2 and III.3 having been applied and $\delta^{18}\text{O CO}_2 \text{ eq}$ is the $\delta^{18}\text{O}$ value of CO_2 whose $^{18}\text{O}/^{16}\text{O}$ ratio differs from that of the original water by the factor $\alpha_{\text{CO}_2\text{-H}_2\text{O}}$. The $\alpha_{\text{CO}_2\text{-H}_2\text{O}}$ is applied to the value $\delta^{18}\text{O CO}_2 \text{ eq}$ to obtain the $\delta^{18}\text{O}$ value of the water being measured.

III. 9 Correction for Contaminant Oxygen in the Fluorine

The commercial fluorine cylinder contained oxygen as an impurity which was mixed with the oxygen liberated from fluorinated silicates. By material balance, the $\delta^{18}\text{O}$ value of the silicate, corrected for the

reagent impurity, is given by:

$$\delta^{18}\text{O}_{\text{silicate}} = \frac{\delta^{18}\text{O}_{\text{gas}} - \frac{ni}{y} \delta_i}{1 - \frac{ni}{y}}$$

in which $\delta^{18}\text{O}_{\text{gas}}$ is the measured value of oxygen from sample and impurity, corrected according to Sections III.2 and III.3, y is the oxygen yield of the sample plus the impurity (in micromoles), ni is the number of micromoles of oxygen impurity introduced with the fluorine into each reaction vessel, and δ_i is the $\delta^{18}\text{O}$ value of the oxygen impurity. The value of ni was 4.3 moles for all silicate analyses, and the value of δ_i was determined to be -14.4‰ relative to Harding Iceland Spar.

III.10 Conversion of Silicate $\delta^{18}\text{O}$ Values to the SMOW Scale Using a Reference Sample of Known Isotopic Composition

As described in Section 2.3.3.4, one out of every six silicate samples analyzed was an aliquot of Ramona Rose Quartz. The ^{18}O value of Ramona Rose Quartz is 8.43‰ relative to SMOW. The ^{18}O values of silicates can be reduced to the SMOW scale from the H.I.S. scale if the ^{18}O value of RRQ relative to H.I.S. is determined, together with the other five ^{18}O values (relative to H.I.S.) in each group of six. The expression which allows this reduction is:

$$\begin{aligned} \delta^{18}\text{O (SMOW) sample} &= \delta^{18}\text{O (SMOW) RRQ} \\ &+ \left[1 + 10^{-3} (\delta^{18}\text{O (SMOW) H.I.S.}) \right] \left[\delta^{18}\text{O (H.I.S.) sample} \right. \\ &\quad \left. - \delta^{18}\text{O (H.I.S.) RRQ} \right] \end{aligned}$$

$\delta^{18}\text{O (SMOW) RRQ} = 8.43\%$, $\delta^{18}\text{O (SMOW) H.I.S.} = 21.6\%$, and $\delta^{18}\text{O (H.I.S.) sample}$ and $\delta^{18}\text{O (H.I.S.) RRQ}$ are the mass spectrometric measurements corrected according to Sections III.2, III.3, and III.9.

BIBLIOGRAPHY

- Agricola, Georgius, 1556, De Re Metallica; translated by Herbert and Lou Henry Hoover. New York, Dover Publications, Inc., 1950.
- Allen, E. T., and Day, Arthur L., 1927, Steam wells and other thermal activity at "The Geysers," California: Carnegie Inst. of Wash. Publ. 378.
- _____ 1935, The hot springs of the Yellowstone National Park: Carnegie Inst. of Wash. Publ. 466.
- Averiev, V. V., 1967, Hydrothermal process in volcanic areas and its relations to magmatic activity: Bull. Volcanologique, v. 30, p. 51-62.
- Baertschi, Peter, and Silverman, S. R., 1951, The determination of the relative abundance of the oxygen isotopes in silicate rocks: Geochim. et Cosmochim. Acta, v. 1, p. 317-328.
- Bailey, E. H., Irwin, W. P., and Jones, D. L., 1964, Franciscan and related rocks and their significance in the geology of western California: California Div. Mines and Geology Bull. 183.
- Barrow, G., 1893, On an intrusion of biotite-muscovite gneiss in the south-east Highlands of Scotland and its accompanying metamorphism: Geol. Soc. London Quart. Jour., v. 49, p. 330-358.
- Benseman, R. F., 1965, The components of a geyser: New Zealand Jour. Science, v. 8, p. 24-44.
- Bigeleisen, J., and Mayer, M. G., 1947, Calculation of equilibrium constants for isotopic exchange reactions: Jour. Chem. Physics, v. 15, p. 261-267.
- Bigeleisen, J., Perlman, M. L., and Prosser, H. C., 1952, Conversion of hydrogenic materials to hydrogen for isotopic analysis: Anal. Chem., v. 24, p. 1356-1357.
- Bottlinga, Y., 1968, Calculation of fractionation factors for carbon and oxygen isotopic exchange in the system calcite-carbon dioxide-water: Jour. Phys. Chem., v. 72, p. 800-808.
- Brice, G., 1953, Geology of Lower Lake quadrangle, California: California Div. Mines and Geology Bull. 166.
- Brown, E. H., 1967, The greenschist facies in part of eastern Otago, New Zealand: Contrib. Mineralogy Petrology, v. 4, p. 259-292.

- Bunsen, Robert, 1847, *in* Liebig's Annalen, v. 62, p. 1 ff: cited in Allen and Day, 1935.
- Chittenden, Hiram Martin, 1895, The Yellowstone National Park: Historical and Descriptive: Cincinnati, Stewart and Kidd Company.
- Choquette, P. W., 1968, Marine diagenesis of shallow-marine lime-mud sediments: Insights from $\delta^{18}\text{O}$ and $\delta^{13}\text{C}$ data: Science, v. 161, p. 1130-1132.
- Church, F. S., and Hack, T. J., 1939, An exhumed erosion surface in the Jemez Mountains, New Mexico: Jour. Geology, v. 47, p. 613-629.
- Clayton, R. N., and Epstein, S., 1958, Relationship between $^{18}\text{O}/^{16}\text{O}$ ratios in coexisting quartz, carbonate and iron oxides from various geological deposits: Jour. Geology, v. 66, p. 352-373.
- Clayton, R. N., Jones, B. F., and Barner, R. A., 1968, Isotope studies of dolomite formation under sedimentary conditions: Geochim. et Cosmochim. Acta, v. 32, p. 415-432.
- Clayton, Robert N., Muffler, L. J. P., and White, Donald E., 1968, Oxygen isotope study of calcite and silicates of the River Ranch No. 1 well, Salton Sea Geothermal Field, California: Am. Jour. Science, v. 266, p. 968-979.
- Clayton, R. N., O'Neil, J. R., and Mayeda, T. K., 1972, Oxygen isotope exchange between quartz and water: Jour. Geophys. Research, v. 77, p. 3057-3067.
- Coleman, R. G., 1955, Optical and chemical study of jadeite from California (abstr.): Am. Mineralogist, v. 40, p. 312.
- _____, 1961, Jadeite deposits of the Clear Creek area, New Idria district, San Benito County, California: Jour. Petrology, v. 2, p. 209-247.
- Coombs, D. S., Ellis, A. D., Fyfe, W. S., and Taylor, A. M., 1959, The zeolite facies, with comments on the interpretation of hydrothermal syntheses: Geochim. et Cosmochim. Acta, v. 17, p. 53-107.
- Coplen, T. B., Combs, J., Elders, W. A., Rex, R. W., Burckhalter, G., and Laird, R., 1973, Preliminary findings of an investigation of the Dunes Geothermal Anomaly, Imperial Valley, California: Riverside, California, Institute of Geophysics and Planetary Physics, University of California.
- Craig, Harmon, 1953, The geochemistry of the stable carbon isotopes: Geochim. et Cosmochim. Acta, v. 3, p. 53-92.

- _____. 1957, Isotopic standards for carbon and oxygen and correction factors for mass-spectrometric analysis of carbon dioxide: *Geochim. et Cosmochim. Acta*, v. 12, p. 133-149.
- _____. 1961a, Isotopic variations in meteoric waters: *Science*, v. 133, p. 1702-1703.
- _____. 1961b, Standard for reporting concentrations of deuterium and oxygen-18 in natural waters: *Science*, v. 133, p. 1833-1834.
- _____. 1966, Isotopic composition and origin of the Red Sea and Salton geothermal brines: *Science*, v. 154, p. 1544-1548.
- _____. Boato, G., and White, D. E., 1956, The isotopic geochemistry of thermal waters: National Research Council Nuclear Science Series, Report No. 19: Nuclear Processes in Geologic Settings, p. 29-44.
- Dansgaard, W., 1964, Stable isotopes in precipitation: *Tellus*, v. 16, p. 436-468.
- Davidson, Norman, 1962, *Statistical Mechanics*: New York, McGraw-Hill Book Company.
- Day, A. L., and Allen, E. T., 1925, The volcanic activity and hot springs of Lassen Peak: *Carnegie Inst. Wash. Publ.* 360.
- de Beaumont, Élie, 1847, Des émanations volcaniques et métallifères: *Bull. Soc. Geol. de France*, v. 4, pt. 2, p. 1249 ff, cited in Allen and Day, 1935.
- Denny, S., 1940, Santa Fe Formation in the Espanola Valley, New Mexico: *Geol. Soc. America Bull.*, v. 51, p. 677-694.
- Deville, Sainte-Claire, 1857, Sur les émanations volcaniques: *Bull. Soc. Geol. de France*, v. 14, pt. 2, p. 254 ff, cited in Allen and Day, 1935.
- Elders, W. A., Rex, R. W., Meidav, R., Robinson, P. T., and Biehler, S., 1972, Crustal spreading in Southern California: *Science*, v. 178, p. 15-24.
- Engel, A. E. J., Clayton, R. N., and Epstein, S., 1958, Variations in isotopic composition of oxygen and carbon in Leadville Limestone (Mississippian, Colorado) and its hydrothermal and metamorphic phases: *Jour. Geology*, v. 66, p. 374-390.
- Epstein, Samuel, 1959, The variations of the $^{18}\text{O}/^{16}\text{O}$ ratio in nature and some geologic implications, *in* Abelson, P. H., ed., *Researches in Geochemistry*, vol. 1: New York, John Wiley and Sons, Inc.

- ____ Buchsbaum, Ralph, Lowenstam, H. A., and Urey, H. C., 1951, Carbonate-water isotopic temperature scale: Geol. Soc. America Bull., v. 62, p. 417-426.
- ____ 1953, Revised carbonate-water isotopic temperature scale: Geol. Soc. America Bull., v. 64, p. 1315-1326.
- Epstein, Samuel, Graf, Donald L., and Degens, Egon T., 1963, Oxygen isotope studies of the origin of dolomites, *in* Craig, H., Miller, S. L., and Wasserburg, G. J., eds., *Isotopic and Cosmic Chemistry*: Amsterdam, North-Holland Pub. Co.
- Epstein, S., and Mayeda, T., 1953, Variation of O^{18} content of waters from natural sources: *Geochim. et Cosmochim. Acta*, v. 4, p. 213-224.
- Epstein, S., Sharp, R. P., and Gow, A. J., 1965, Six-year record of oxygen and hydrogen isotope variations in South Pole firn: *Jour. Geophys. Research*, v. 70, p. 1809-1814.
- ____ 1970, Antarctic ice sheet: Stable isotope analyses of Byrd station cores and interhemispheric climatic implications: *Science*, v. 168, p. 1570-1572.
- Epstein, S., and Taylor, H. P., Jr., 1970, The concentration and isotopic composition of hydrogen, carbon and silicon in Apollo 11 lunar rocks and minerals: *Proc. Apollo Lunar Sci. Conf.*, v. 2, p. 1085-1096.
- Ernst, W. G., 1972, CO_2 -poor composition of the fluid attending Franciscan and Sanbagawa low-grade metamorphism: *Geochim. et Cosmochim. Acta*, v. 36, p. 497-504.
- Eslinger, E. V., and Savin, S. M., 1973a, Mineralogy and oxygen isotope geochemistry of the hydrothermally altered rocks of the Ohaki-Broadlands, New Zealand, geothermal area: *Am. Jour. Sci.*, v. 273, p. 240-267.
- ____ 1973b, Oxygen isotope geothermometry of the burial metamorphic rocks of the Precambrian Belt Supergroup, Glacier National Park, Montana: *Geol. Soc. America Bull.*, v. 84, p. 2549-2560.
- Facca, G., and Tonani, F., 1967, The self-sealing geothermal field: *Bull. Volcanologique*, v. 30, p. 271-273.
- Forrester, J. D., and Thune, H. W., 1942, A model geyser: *Science*, v. 95, p. 204-206.
- Friedman, Irving, 1953, Deuterium content of natural waters and other substances: *Geochim. et Cosmochim. Acta*, v. 4, p. 89-103.

- ____ Redfield, Alfred C., Schoen, Beatrice, and Harris, Joseph, 1964, The variation of the deuterium content of natural waters in the hydrologic cycle: *Rev. of Geophysics*, v. 2, p. 177-224.
- Friedman, I., and Smith, R. L., 1958, The deuterium content of water in some volcanic glasses: *Geochim. et Cosmochim. Acta*, v. 15, p. 218-228.
- Galusha, Ted, 1966, The Zia Sand Formation, new early to medial Miocene beds in New Mexico: *Am. Mus. Novitates*, No. 2271, p. 1-12.
- Garlick, G. Donald, and Epstein, Samuel, 1966, The isotopic composition of oxygen and carbon in hydrothermal minerals at Butte, Montana: *Econ. Geology*, v. 61, p. 1325-1335.
- ____ 1967, Oxygen isotope ratios in coexisting minerals of regionally metamorphosed rocks: *Geochim. et Cosmochim. Acta*, v. 31, p. 181-214.
- Garrison, L. E., 1972, Geothermal steam in The Geysers-Clear Lake region, California: *Geol. Soc. America Bull.*, v. 83, p. 1449-1468.
- Giulotto, L. and Loinger, A., 1951, Oscillazioni esterne e calore specifico della calcite: *Nuovo Cimento*, v. 8, p. 475-486.
- Goddard, W. A., III, and Dunning, Thomas H., Jr., 1971, Elements of Quantum Chemistry, manuscript, California Institute of Technology, Pasadena, California.
- Godfrey, J. D., 1962, The deuterium content of hydrous minerals from the east-central Sierra Nevada and Yosemite National Park: *Geochim. et Cosmochim. Acta*, v. 26, p. 1215-1245.
- Gross, M. G., 1964, Variations in the O^{18}/O^{16} and C^{13}/C^{12} ratios of diagenetically altered limestones in the Bermuda Islands: *Jour. Geology*, v. 72, p. 170-194.
- Hague, Arnold, 1892a, Geological history of the Yellowstone National Park: *U. S. Smithsonian Inst. Ann. Rept.*, p. 133-152.
- ____ 1892b, Soaping geysers: *U. S. Smithsonian Inst. Ann. Rept.*, p. 153-161.
- Hallock, Wm. H., 1884, Physics of Geysers: unpublished manuscript, cited in Allen and Day, 1935.
- Heath, D. F., and Linnett, J. W., 1948, Molecular force fields, Part III -- The vibration frequencies of some planar XY_3 molecules: *Trans. Faraday Soc.*, v. 44, p. 873-878.

- Herzberg, Gerhard, 1945, Molecular Spectra and Molecular Structure. II. Infrared and Raman Spectra of Polyatomic Molecules: New York, Van Nostrand Reinhold Company.
- Hills, T. M., and Warthin, A. S., Jr., 1942, Experiments in geyser action: *Am. Jour. Science*, v. 240, p. 512-517.
- Hudson, J. D., 1975, Carbon isotopes and limestone cement: *Geology*, v. 3, p. 19-22.
- Janz, G. J. and Mikawa, Yukio, 1960, The evaluation of Urey-Bradley force constants in planar XY₃ type molecules: *Jour. Molec. Spectroscopy*, v. 5, p. 92-100.
- Keith, M. L., and Weber, J. N., 1964, Carbon and oxygen isotopic composition of selected limestones and fossils: *Geochim. et Cosmochim. Acta*, v. 28, p. 1787-1816.
- Kelley, V. C., 1954, Tectonic map of a part of the Rio Grande area, New Mexico: U. S. Geol. Survey Oil and Gas Investigation Map OM-157.
- Kelley, V. C., and Silver, Caswell, 1952, Geology of the Caballo Mountains: New Mexico Univ. Publ. Geol. No. 4.
- Knauth, Leroy Paul, 1973, Oxygen and hydrogen isotope ratios in cherts and related rocks (Ph.D. thesis): Pasadena, California, California Institute of Technology.
- Knauth, L. P., and Epstein, S., 1975, Hydrogen and oxygen isotope ratios in silica from the Joides deep sea drilling project: *Earth Planet. Sci. Letters*, v. 25, p. 1-10.
- Kolodny, Yehoshua, and Gross, Shulamit, 1974, Thermal metamorphism by combustion of organic matter: Isotopic and petrological evidence: *Jour. Geology*, v. 82, p. 489-506.
- Kolstad, C., Albright, J., and McGetchin, T., 1975, Numerical studies of the thermal evolution of intrusions in relationship to observed temperatures in GT-2 (abstr.): *EOS*, v. 56, p. 461.
- Landis, Gary P., and Rye, Robert O., 1974, Geologic, fluid inclusion, and stable isotope studies of the Pasto Bueno tungsten-base metal ore deposit, Northern Peru: *Econ. Geology*, v. 69, p. 1025-1059.
- Lange, A. L., and Westphal, W. H., 1969, Microearthquakes near The Geysers, Sonoma County, California: *Jour. Geophys. Research*, v. 74, p. 4377-4378.

- Levine, Ira N., 1970, Quantum Chemistry, Volume I: Quantum Mechanics and Molecular Electronic Structure: Boston, Allyn and Bacon.
- Lindgren, Waldemar, 1933, Mineral Deposits: New York, McGraw-Hill Book Company, Inc.
- Mackenzie, Sir George, 1811, Voyage to the Island of Iceland in the Summer of 1810: Edinburgh.
- Matthews, Wm. H., III, 1968, A Guide to the National Parks: The Landscape and Geology Volume I. The Western Parks: Garden City, NY, The Natural History Press.
- Mayer, J. E., and Mayer, M. G., 1940, Statistical Mechanics: New York, Wiley.
- McCrea, J. M., 1950, On the isotopic chemistry of carbonates and a paleotemperature scale: Jour. Chem. Physics, v. 18, p. 849-857.
- McKinney, C. R., McCrea, J. M., Epstein, S., Allen, H., and Urey, H. C., 1950, Improvements in mass spectrometers for the measurement of small differences in isotope abundance ratios: Rev. Scientific Instruments, v. 21, p. 724-730.
- McNitt, J. R., 1963, Exploration and development of geothermal power in California: California Div. Mines and Geology Special Report 75, p. 1-44.
- _____ 1968, Geology of the Kelseyville Quadrangle, Sonoma, Lake, and Mendocino Counties, California: California Div. Mines and Geology Map Sheet 9.
- Morse, Philip M., 1929, Diatomic molecules according to the wave mechanics II. Vibrational levels: Phys. Rev., v. 34, p. 57-64
- Muehlenbachs, K., and Clayton, R. N., 1972, Oxygen isotope geochemistry of submarine greenstones: Canadian Jour. Earth Sci., v. 9, p. 471-478.
- Murata, K. J., Friedman, I., and Madsen, B. M., 1969, Isotopic composition of diagenetic carbonates in marine Miocene formations of California and Oregon: U. S. Geol. Survey Prof. Paper 614-B, p. 1-24.
- Nier, Alfred O., 1947, A mass spectrometer for isotope and gas analysis: Rev. Scientific Instruments, v. 18, p. 398-411.
- _____ and Gulbransen, Earl A., 1939, Variations in the relative abundance of the carbon isotopes: Jour. Am. Chem. Soc., v. 61, p. 697-698.

- O'Neil, J. R., Clayton, R. N., and Mayeda, Toshiko K., 1969, Oxygen isotope fractionation in divalent metal carbonates: *Jour. Chem. Physics*, v. 51, p. 5547-5558.
- O'Neil, James R., and Taylor, Hugh P., Jr., 1967, The oxygen isotope and cation exchange chemistry of feldspars: *Am. Mineralogist*, v. 52, p. 1414-1437.
- _____ 1969, Oxygen isotope equilibrium between muscovite and water: *Jour. Geophys. Research*, v. 74, p. 6012-6022.
- Otte, Carel, and Dondanville, R. F., 1968, Geothermal developments in The Geysers area, California (abstr.): *Am. Assoc. Petroleum Geologists Bull.*, v. 52, p. 565.
- Peale, A. C., 1883, Yellowstone National Park: Section II. Thermal Springs: Twelfth Annual Report of the U. S. Geological and Geographical Survey of the Territories (Hayden Survey): Washington, D. C., U. S. Gov't Printing Office, p. 65-454.
- Redlich, Otto, 1935, Eine allgemeine Beziehung zwischen den Schwingungsfrequenzen isotoper Molekeln: *Z. physikal. Chem.*, v. 28, p. 371-382.
- Rice, Oscar Knefler, 1967, *Statistical Mechanics, Thermodynamics and Kinetics*: San Francisco, W. H. Freeman and Company.
- Rye, R. O., and O'Neil, J. R., 1968, The ^{18}O content of water in primary fluid inclusions from Providencia, North-Central Mexico: *Econ. Geology*, v. 63, p. 232-238.
- Safford, G., Brajovic, V., and Boutin, H., 1963, An investigation of the energy levels in alkaline earth hydroxides by inelastic scattering of slow neutrons: *Jour. Phys. Chem. Solids*, v. 24, p. 771-777.
- Savin, Samuel M., and Epstein, Samuel, 1970a, The oxygen and hydrogen isotope geochemistry of clay minerals: *Geochim. et Cosmochim. Acta*, v. 34, p. 25-42.
- _____ 1970b, The oxygen and hydrogen isotope geochemistry of ocean sediments and shales: *Geochim. et Cosmochim. Acta*, v. 34, p. 43-63.
- _____ 1970c, The oxygen isotope compositions of coarse-grained sedimentary rocks and minerals: *Geochim. et Cosmochim. Acta*, v. 34, p. 323-329.
- Schiff, Leonard I., 1968, *Quantum Mechanics*: New York, McGraw-Hill Book Company.

- Sharma, Taleshwar, and Clayton, R. N., 1965, Measurement of O^{18}/O^{16} ratios of total oxygen of carbonates: *Geochim. et Cosmochim. Acta*, v. 29, p. 1347-1353.
- Shieh, Y. N., and Taylor, H. P., Jr., 1969, Oxygen and carbon isotopes studies of contact metamorphism of carbonate rocks: *Jour. Petrology*, v. 10, p. 307-331.
- Shiro, Yuji, and Sakai, Hitoshi, 1972, Calculation of the reduced partition function ratios of α -, β -quartzes and calcite: *Bull. Chem. Soc. Japan*, v. 45, p. 2355-2359.
- Skinner, Brian J., White, D. E., Rose, H. J., and Mays, R. E., 1967, Sulfides associated with the Salton Sea geothermal brine: *Econ. Geology*, v. 62, p. 316-330.
- Smith, H.T.U., 1938, Tertiary geology of the Abiquiu quadrangle, New Mexico: *Jour. Geology*, v. 46, p. 933-965.
- Smith, R. L., Bailey, R. A., and Ross, C. S., 1970, Geologic map of the Jemez Mountains, New Mexico: U. S. Geol. Survey Misc. Geol. Investigations Map I-571.
- Spiegel, Zane, and Baldwin, Brewster, W., 1963, Geology and water resources of the Santa Fe area, New Mexico: U. S. Geol. Survey Water Supply Paper 1525.
- Stearns, C. E., 1943, The Galisteo Formation of north-central New Mexico: *Jour. Geology*, v. 51, p. 301-319.
- Steiner, A., 1955, Wairakite; the calcium analogue of analcime, a new zeolite mineral: *Mineralogical Magazine*, v. 20, p. 691-698.
- Steiner, A., 1958, Occurrence of wairakite at The Geysers, California: *Am. Mineralogist*, v. 43, p. 781.
- Stockmayer, W. H., 1957, Isotope effects on thermodynamic functions of hindered rotators: *Jour. Chem. Physics*, v. 27, p. 321-322.
- Suzuoki, Tetsuro, and Epstein, Samuel, 1975, Hydrogen isotope fractionation between OH-bearing minerals and water: *Geochim. et Cosmochim. Acta*, in preparation.
- Swe, W., and Dickinson, W. R., 1970, Sedimentation and thrusting of late Mesozoic rocks in the Coast Ranges near Clear Lake, California: *Geol. Soc. America Bull.*, v. 81, p. 165-188.
- Taylor, Hugh P., Jr., 1968, The oxygen isotope geochemistry of igneous rocks: *Contrib. Mineralogy Petrology*, v. 19, p. 1-71.

- _____ 1973, O^{18}/O^{16} evidence for meteoric-hydrothermal alteration and ore deposition in the Tonopah, Comstock Lode, and Goldfield mining districts, Nevada: *Econ. Geology*, v. 68, p. 747-764.
- _____ 1974, The application of oxygen and hydrogen isotope studies to problems of hydrothermal alteration and ore deposition: *Econ. Geology*, v. 69, p. 843-883.
- Taylor, Hugh P., Jr., Albee, Arden L., and Epstein, Samuel, 1963, O^{18}/O^{16} ratios of coexisting minerals in three assemblages of kyanite-zone pelitic schist: *Jour. Geology*, v. 71, p. 513-522.
- Taylor, Hugh P., Jr., and Epstein, Samuel, 1962a, Relationship between O^{18}/O^{16} ratios in coexisting minerals of igneous and metamorphic rocks, Part 1: Principles and experimental procedures: *Geol. Soc. America Bull.*, v. 73, p. 461-480.
- _____ 1962b, Relationship between O^{18}/O^{16} ratios in coexisting minerals of igneous and metamorphic rocks, Part 2: Application of petrologic problems: *Geol. Soc. America Bull.*, v. 73, p. 675-694.
- _____ 1963, O^{18}/O^{16} ratios in rocks and coexisting minerals of the Skaergaard intrusion, East Greenland: *Jour. Petrology*, v. 4, p. 51-74.
- Taylor, Hugh P., Jr., and Forester, R. W., 1971, Low- O^{18} igneous rocks from the intrusive complexes of Skye, Mull and Ardnamurchan, Western Scotland: *Jour. Petrology*, v. 12, p. 465-497.
- _____ 1973, An oxygen and hydrogen isotope study of the Skaergaard intrusion and its country rocks (abstr.): *EOS*, v. 54, p. 500.
- Thoroddsen, Th., 1925, *Die Geschichte der islandischen Vulkane*: Copenhagen.
- Tilden, Freeman, 1956, *The National Parks: What They Mean to You and Me*: New York, Alfred A. Knopf.
- Turi, Bruno, and Taylor, Hugh P., Jr., 1971, An oxygen and hydrogen isotope study of a granodioritic pluton from the Southern California Batholith: *Geochim. et Cosmochim. Acta*, v. 35, p. 383-406.
- Urey, H. C., 1947, The thermodynamic properties of isotopic substances: *Jour. Chem. Soc.*, p. 562-581.
- _____ Lowenstam, H. A., Epstein, S., and McKinney, C. R., 1951, Measurement of paleotemperatures and temperatures of the Cretaceous of England, Denmark and the Southeastern United States: *Geol. Soc. America Bull.*, v. 62, p. 399-416.

- Urey, Harold C. and Rittenberg, D., 1933, Some thermodynamic properties of the HD and D₂ molecules and compounds containing the D atom: Chem. Phys. Jour., v. 1, p. 137-143.
- Vojta, G., 1961, Berechnung der Schwingungszustandsumme entarteter anharmonischer Oszillatoren mit Hilfe der Mellinschen Integraltransformation: Ann. Physik., v. 7, p. 397-402.
- von Nidda, Krug, 1836, Karsten's Archiv., v. IX, p. 247 ff: cited in Allen and Day, 1935.
- Wenner, D. B., and Taylor, Hugh P., Jr., 1971, Temperatures of serpentinization of ultramafic rocks based on O¹⁸/O¹⁶ fractionation between coexisting serpentine and magnetite: Contrib. Mineralogy Petrology, v. 32, p. 165-185.
- _____ 1973, Oxygen and hydrogen isotope studies of the serpentinization of ultramafic rocks in oceanic environments and continental ophiolite complexes: Am. Jour. Science, v. 273, p. 207-239.
- White, D. E., 1967, Some principles of geyser activity, mainly from Steamboat Springs, Nevada: Am. Jour. Science, v. 265, p. 641-648.
- _____ Hem, J. D., and Waring, G. A., 1963, Chemical compositions of subsurface waters *in* Data of Geochemistry: U. S. Geol. Survey Prof. Paper 440-F, p. 1-67.
- White, D. E., Muffler, L.J.P., and Truesdell, A. H., 1971, Vapor-dominated hydrothermal systems compared with hot-water systems: Econ. Geology, v. 66, p. 75-97.
- Whittaker, E.J.W., and Zussman, J., 1956, The characterization of serpentine minerals by X-ray diffraction: Mineralogical Magazine, v. 31, p. 107-126.
- Wood, G. H., Jr., and Northrop, S. A., 1946, Geology of Nacimiento Mountains, San Pedro Mountain, and adjacent plateaus in parts of Sandoval and Rio Arriba Counties, New Mexico: U. S. Geol. Survey Oil and Gas Investigation Preliminary Map. 57.
- Yeager, Dorr, 1959, National Parks in California: Menlo Park, California, Lane Publishing Co.
- Yeh, Hsueh-Wen, and Savin, S. M., 1974, Quartz-clay isotope geothermometer applied to shales (abstr.): Geol. Soc. America Annual Meeting, Abstracts with Programs, v. 6, no. 7, p. 1011-1012.
- Zartman, R. E., Wasserburg, G. J., and Reynolds, J. H., 1961, Helium, argon and carbon in some natural gases: Jour. Geophys. Research, v. 66, p. 277-306.